Long-term Capacity Expansion Planning with Variable Renewable Energies

-

Enhancement of the REMix Energy System Modelling Framework

Von der Fakultät für Energie-, Verfahrens- und Biotechnik der Universität Stuttgart
zur Erlangung der Würde eines Doktor-Ingenieurs (Dr.-Ing.)
genehmigte Abhandlung

Vorgelegt von

Tobias Fichter

aus Waiblingen

Hauptberichter: Prof. Dr. André Thess
Mitberichter: Prof. Dr. Christian Breyer

Tag der mündlichen Prüfung: 22. August 2017

Institut für Energiespeicherung
Universität Stuttgart

2017

Erklärung über die Eigenständigkeit der Dissertation

Ich versichere, dass ich die vorliegende Arbeit mit dem Titel

”Long-term Capacity Expansion Planning with Variable Renewable Energies - Enhancement of the REMix Energy System Modelling Framework”

selbständig verfasst und keine anderen als die angegebenen Quellen und Hilfsmittel benutzt habe. Aus fremden Quellen entnommene Passagen und Gedanken sind als solche gekennzeichnet.

Declaration of authorship

I hereby declare that the dissertation entitled

”Long-term Capacity Expansion Planning with Variable Renewable Energies - Enhancement of the REMix Energy System Modelling Framework”

is entirely based on my own work except where stated otherwise. Passages and ideas from other sources have been clearly indicated.

Stuttgart, den 28. März 2017 Tobias Fichter

Acknowledgement

The preparation of this thesis was only possible due to the continuous support of outstanding people. This makes me feel deeply grateful. In particular I would like to thank:

- My wife Daniela for supporting me from the very beginning of this work and for accepting so many times my probably most popular saying during this time: “I just want to check something quickly!”
- My parents Claudia and Rolf as well as my entire family who have always believed in me and supported me in everything I have been trying in my life.
- Prof. Dr. Hans Müller-Steinhagen for giving me the opportunity to work at the Department of Systems Analysis and Technology Assessment of the German Aerospace Center after graduating from University and for accepting my research proposal.
- Prof. Dr. André Thess for taking over the supervision of my thesis after Prof. Dr. Müller-Steinhagen became the Rector of the Technical University of Dresden, and for offering me continuous and prompt support despite a full timetable.
- Prof. Dr. Christian Breyer for acting as co-examiner and for the fruitful discussions during the THERMVOLT project.
- Dr. Franz Trieb who agreed to take over the daily supervision of my thesis. The controversial and fruitful discussions with Franz have contributed to this work enormously. Especially during the beginning of my thesis, he encouraged me to think critically and not to follow something just because it is currently the mainstream trend in the field of energy systems analysis.
- My close colleagues and roommates Jürgen Kern and Dr. Massimo Moser. Together with Jürgen, I spend many days in Morocco during the MOREMix project. The discussions with him and his support during the project helped me considerably to sharpen the developed capacity expansion optimization model within this thesis. Massimo supported me incredibly with his profound knowledge about the concentrating solar power technology.
- Dr. Yvonne Scholz and Dr. Diego Luca de Tena Costales for their great work on the REMix energy system modelling framework on which I could build on.

In addition, I would like to thank everyone I met along the way who either helped me with fruitful discussions or had a valuable impact on me in any other way.

Abstract

The large-scale integration of variable renewable energies (VRE) like Photovoltaics and wind power into the power system is crucial for the transition towards a sustainable electricity supply. However, due to the inherent characteristics of VRE, i.e. the site-specific, highly variable, and unreliable power generation, as well as their low variable generation costs, the large-scale deployment of VRE causes adequacy-, grid-related, and balancing-impacts for the residual system. These impacts and the related costs need to be considered for a concerted capacity expansion planning with VRE in order to identify cost-efficient and reliable transition pathways. Traditionally applied capacity expansion planning models have limitations to consider the value of energy at its time of the delivery of VRE and their impacts on the system due to the applied low system-operational detail. Hence, new planning methods are required to ensure a successful transition towards a sustainable electricity supply.

This work enhances the REMix energy system modelling framework to allow for a concerted long-term capacity expansion planning with VRE. The outcome of this is the REMix-Capacity Expansion Model (REMix-CEM). The optimization model bridges the gap between traditional long-term capacity expansion planning and short-term power system operation models. This enables the model to consider the value and the impacts of a large-scale integration of VRE into the power system accurately within capacity expansion planning. This thesis describes the challenges of long-term capacity expansion planning with VRE and presents the developed model in detail. This includes a principle description of how REMix-CEM is typically applied by DLR for a science-based consultancy of planning authorities in developing and emerging countries. To demonstrate its capabilities, the flexible formulation of the model is used to investigate two important issues within a model-based long-term capacity expansion planning with VRE - the model foresight and the applied system-operational detail. Both issues can have a significant influence on results and computational effort of the model. These correlations are investigated within two case studies for a fictitious but representative power system of a developing country.

Results of the first case study indicate that the type of model foresight (single-year myopic, multi-annual rolling horizon, or perfect foresight) has a strong influence when some of the input parameters change suddenly at one point of the planning time frame, while its influence is less pronounced when parameters changes rather continuously over the period of study. Only a large model foresight enables the model to anticipate future occurrences well in advance and to adopt its investment strategies accordingly. Furthermore, the analysis shows that the larger the model foresight the higher is the competitiveness of VRE and dispatchable RE, because their advantage to produce electricity at stable costs over the lifetime can be captured more precisely. However, it is also demonstrated that a larger model foresight means also a higher computational effort to solve the capacity expansion optimization problem. In addition, a large model foresight with perfect information over the planning time frame might not fully capture the decision frame-work of real-life decision makers.

To keep computational effort manageable for long-term capacity expansion planning with VRE, investment decisions are typically based on a limited number of representative dispatch periods. These dispatch periods have the aim to represent the temporal variability of load and RE resources over the year as accurate as possible. Within the second case study it is shown that the average day method, which uses average values to assign values for RE resource availability to the utilized dispatch periods, is inappropriate for capacity expansion planning with VRE. The value of energy at its time of the delivery of VRE is modeled inaccurately and system flexibility requirements, caused by the integration of VRE, are underestimated systematically. The representative day method, which uses a sample of “real” historical days instead of average values, is significantly more suitable because extreme values are not averaged. This leads to a better approximation of VRE electricity generation, which allows a more accurate consideration of the value of energy at its time of the delivery of VRE and system flexibility requirements.

System flexibility requirements can be captured within capacity expansion optimization especially by considering unit commitment constraints (UCCs) of thermal generators. However, this requires a large number of integer decision variables that describes the unit commitment status. This leads to high computational complexity. Hence, UCCs are typically neglected during capacity expansion optimization. Within the second case study it is however demonstrated that neglecting UCCs within capacity expansion planning with VRE leads to an overestimation of the competitiveness of VRE and an underestimation of the need for flexible generation and storage technologies. This work shows that by a linear relaxation for UCCs system flexibility restrictions can be captured accurately during long-term capacity expansion optimization with comparably low additional computational effort.

Zusammenfassung

Die großtechnische Integration variabler regenerativer Energien (VRE) wie Photovoltaik und Windkraft in das Stromversorgungssystem ist für die Transformation hin zu einer nachhaltigen Stromversorgung von entscheidender Bedeutung. Aufgrund der spezifischen Eigenschaften von VRE, wie die standortspezifische, stark fluktuierende und unsichere Stromproduktion, sowie geringe variable Erzeugungskosten, hat die Integration von VRE jedoch Auswirkungen auf die Versorgungsicherheit, die Stromnetze und den Systembetrieb. Diese Auswirkungen und die damit einhergehenden Kosten müssen für eine ausgewogene Ausbauplanung mit VRE berücksichtigt werden. Traditionell angewendete Ausbauplanungsmodelle können aufgrund ihres geringen Detailierungsgrades hinsichtlich der Modellierung des Systembetriebs nur begrenzt die Wertigkeit der zeitlichen Einspeisung von VRE und die Auswirkungen der Integration von VRE auf das residuale Versorgungsystem abbilden. Für eine erfolgreiche Transformation hin zu einer nachhaltigen Stromversorgung bedarf es deshalb neuer Methoden.

Diese Arbeit entwickelt das Energiesystemmodell REMix weiter um eine ausgewogene Ausbauplanung mit VRE zu ermöglichen. Das Resultat dieser Weiterentwicklung ist das Optimierungsmodel REMix-CEM. Das entwickelte Model schlägt die Brücke zwischen traditionellen langfristigen Ausbau- und kurzfristigen Kraftwerkseinsatzoptimierungsmodellen, um die Wertigkeit und die Auswirkungen der Integration von VRE während der Ausbauplanung möglichst akkurat zu berücksichtigen. Die Arbeit thematisiert die Herausforderungen der Ausbauplanung mit VRE und beschreibt das entwickelte Optimierungsmodell im Detail. Zudem wird aufgezeigt, in welcher Form REMix-CEM typischerweise für die wissenschaftsbasierte Beratung von Energieplanungsbehörden in Entwicklungs- und Schwellenländern durch das DLR eingesetzt wird. Um die Fähigkeiten des Modells zu demonstrieren, wird dessen flexible Formulierung dazu genutzt, um zwei wichtige Faktoren der modellgestützten langfristigen Ausbauplanung mit VRE zu untersuchen - die angenommene Modellvoraussicht über den Planungszeitraum und der angewandte Detaillierungsgrad bzgl. der Modellierung des Systembetriebs. Beide Faktoren können einen wesentlichen Einfluss auf die Ergebnisse und den zeitlichen Rechenaufwand des Optimierungsmodells haben. Diese Zusammenhänge werden im Rahmen zweier Fallstudien untersucht.

Ergebnisse der ersten Fallstudie zeigen, dass die Modellvoraussicht (einjährig-myopisch, mehrjährig-rollierend, oder perfekte Voraussicht) einen starken Einfluss auf die Modellergebnisse hat, wenn sich Inputparameter des Modells an einem Punkt des Planungszeitraums unvermittelt ändern. Dahingegen ist der Einfluss moderat, wenn sich die Inputparameter kontinuierlich entwickeln. Nur eine große Voraussicht erlaubt es dem Modell zukünftige Ereignisse zu antizipieren und Investitionsentscheidungen frühzeitig anzupassen. Die Analyse zeigt zudem, dass die Konkurrenzfähigkeit von VRE und regelbarer RE mit der Größe der Modellvoraussicht zunimmt, da deren Vorteil einer kostenstabilen Stromerzeugung über die betriebliche Lebensdauer akkurater erfasst werden kann. Jedoch geht eine große Modellvoraussicht mit perfekter Voraussicht mit einem erhöhten zeitlichen Rechenaufwand einher und spiegelt nur unzureichend den realen Entscheidungsrahmen in der Energiewirtschaft wieder.

Um den zeitlichen Rechenaufwand in Grenzen zu halten, werden bei der Ausbauplanung mit VRE normalerweise wenige repräsentative Zeitschritte herangezogen, um die zeitliche Schwankung der Last und der Verfügbarkeit von regenerativen Ressourcen abzubilden. In der zweiten Fallstudie wird aufgezeigt, dass die „average day method“, welche Durchschnittswerte für die zeitliche Verfügbarkeit von regenerativen Ressourcen nutzt, ungeeignet für die Ausbauplanung mit VRE ist. Die Wertigkeit der zeitlichen Stromerzeugung durch VRE kann nur ungenau abgebildet werden und die Anforderungen an die Systemflexibilität werden systematisch unterschätzt. Die „representative day method“, welche anstatt Durchschnittswerte „reale“ repräsentative Tage nutz, ist wesentlich geeigneter, da eine Mittelung der zeitlichen Einspeisung von VRE vermieden wird. Dies führt zu einer akkurateren Erfassung der Wertigkeit von VRE und der Flexibilitätsanforderungen für das residuale Versorgungssystem.

Flexibilitätsrestriktionen des Versorgungssystems können innerhalb der modellgestützten Ausbauplanung vor allem durch die Berücksichtigung von Kraftwerkseinsatzrestriktionen für thermische Kraftwerke abgebildet werden. Da dies eine hohe Anzahl an ganzzahligen Entscheidungsvariablen für den diskreten Kraftwerkseinsatz benötigt, wird innerhalb der Ausbauplanung aufgrund der hohen Rechenkomplexität aber typischerweise darauf verzichtet. Innerhalb der zweiten Fallstudie wird jedoch gezeigt, dass dies zu einer Überschätzung der Konkurrenzfähigkeit von VRE und einer gleichzeitigen Unterschätzung des Bedarfs an flexiblen Stromerzeugungs- und Speichertechnologien führt. Die Arbeit zeigt, dass mit Hilfe einer Relaxation für die ganzzahligen Kraftwerkseinsatzentscheidungsvariablen dieser Problematik mit vertretbarem Rechenmehraufwand begegnet werden kann.

Table of content

List of figures

List of tables

List of abbreviations

BB	Back-up burner
BIO	Biomass steam power plant
CAPEX	Capital expenditures
CCGT	Combined-cycle gas turbine
CCS	Carbon capture with storage
CEM	Capacity expansion model
CO_2	Carbon dioxide
CSP	Concentrating solar thermal power
DLR	Deutsches Zentrum für Luft- und Raumfahrt/German Aerospace Center
DLR-SYS	Department of Systems Analysis and Technology Assessment of DLR
DNI	Direct normal irradiation
DRE	Dispatchable renewable energies
EDM	Economic dispatch model
EPA	Energy system planning authority
Flh	Full load hours
GEP	Generation expansion planning
GHG	Greenhouse gas
GHI	Global horizontal irradiation
GIS	Geographical information system
GIZ	Deutsche Gesellschaft für Internationale Zusammenarbeit
GT	Open-cycle gas turbine
HVAC	High voltage alternating current
HYDRO-RES	Reservoir hydro power
HYDRO-ROR	Run of the river hydro power
ICE	Internal combustion engine (motors)
ICI	International cooperation institution
IEA	International Energy Agency
IPP	Independent power producer
kUSD	1000 United States Dollars
LCOE	Levelized cost of electricity
LDC	Load duration curve
LEAP	Long-range Energy Alternatives Planning
LHV	Lower heating value
LP	Linear programming
LRMC	Long-run marginal costs
MEMEE	Ministry of Energy, Mines, Water and Environment of Morocco
MENA	Middle East and North Africa

MESSAGE	Model for Energy Supply Strategy Alternatives and their General Environmental Impact
MILP	Mixed integer linear programming
MMEWR	Ministry of Minerals, Energy and Water Resources of Botswana
NOx	Nitrogen oxide
NPV	Net present value
NTC	Net transfer capacity
O&M	Operation and maintenance
OPEX	Operational expenditures
OPFM	Optimal power flow model
PB	Power block
PCM	Production cost model
PFM	Power flow model
$PM_{2.5}$	Particulate matter
PV	Photovoltaics
RE	Renewable energy
REMix	Renewable Energy Mix (Energy system modelling framework)
REMix-CEM	REMix-Capacity Expansion Model
REMix-EnDAT	REMix-Energy Data Analysis Tool
REMix-OptiMo	REMix-Optimization Model
REMix-PCM	REMix-Production Cost Model
RES-E	Renewable energy sources for electricity generation
SA	Scientific advisor
SF	Solar field
SM	Solar Multiple
SO_2	Sulfur dioxide
SRMC	Short-run marginal costs
TEP	Transmission expansion planning
TES	Thermal energy storage
TIMES	The Integrated MARKAL-EFOM System
TL	Transmission line
UCC	Unit commitment constraints
UCM	Unit commitment model
USD	United States Dollar
VRE	Variable renewable energies
WACC	Weighted average cost of capital
WASP	Wien Automatic System Planning Package
WD	Working day
WE	Weekend day

List of symbols

The diurnal temporal resolution of the optimization model is denoted by the time step Δt, in hours.

Table 1: Utilized sets within presented modules of REMix-CEM

Sets	Description
B	Set of blocks of piecewise linear fuel consumption curve
$CP \in P$	Set of candidate projects
$CSP \in G$	Set of CSP generators
$CTG \in G$	Set of conventional thermal generators
D	Set of representative days/weeks of a season
$DG \in G$	Set of dispatchable generators
$FSG \in G$	Set of thermal generators with fast start-up capabilities
FT	First dispatch period of representative day/week of season
G	Set of existing and candidate generators and storage facilities
LPY	Last year of planning horizon
LT	Last dispatch period of representative day/week of season
N	Set of model nodes of system
P	Set of all existing and candidate generation, storage, and transmission projects
R	Set of model regions of system (balancing areas)
S	Set of seasons of a year
$STO \in G$	Set of storage facilities
T	Set of dispatch periods of a representative day/week
$VRE \in G$	Set of VRE generators
Y	Set of milestone years

Table 2: Variables of module System Planner & Operator

Variables	Description	Unit	Type
CAP	Installed gross capacity at generator	[MW]	Positive
$CAPEX$	Annual capital expenditures	[kUSD/y]	Positive
C^{Invest}	Overnight investment costs	[kUSD]	Positive
$EXPORT$	Export to other nodes of the system	[MW]	Positive
$IMPORT$	Imports from other nodes of the system	[MW]	Positive
NPV^{System}	Net present value of total system costs (objective variable)	[kUSD]	Positive
OFF	Indicates the number of offline units at the generator	[-]	Positive
$OPEX$	Annual operational expenditures	[kUSD/y]	Positive
OR^{Spin-}	Negative spinning reserve capacity	[MW]	Positive
OR^{Spin+}	Positive spinning reserve capacity	[MW]	Positive
P^{Charge}	Charging of storage	[MW]	Positive
$P^{Grid,Aux}$	Grid consumption to cover auxiliaries	[MW]	Positive
P^{Net}	Net power generation	[MW]	Positive

Table 3: Parameters of module System Planner & Operator

Parameter	Description	Unit
$\overline{p}$	Gross capacity of single unit	[MW]
$Ec.life$	Economic life-time	[y]
a	Availability factor	[%]
af	Annuity factor	[%]
aux	Auxiliary power expressed as percentage of installed capacity	[%]
cc	Capacity credit expressed as percentage of installed gross capacity	[%]
cf^p	Correction factor for available capacity according to ambient temperature	[%]
ct	Construction time of generator	[y]
d^{MY}	Duration of period represented by milestone year	[y]
df	System discount factor (discounts values to basis year of the analysis)	[%]
for	Forced outage rate	[%]
idc	Factor for interest during construction	[%]
$load$	Temporal load	[MW]
orc^{10min-}	Negative spinning reserve which must be available within 10 minutes	[MW]
orc^{10min+}	Positive spinning reserve that must be available within 10 minutes	[MW]
orc^{60min+}	Positive standing reserve capacity that must be available within 60 minutes	[MW]
rm	Adequacy reserve margin	[%]
$wacc$	Weighted average cost of capital	[%]
mor	Maintenance outage rate	[%]

Table 4: Variables of module Conventional Thermal Generators

Variables	Description	Unit	Type
$BUILD$	Number of units installed at generator	[-]	Integer
$BUILD^{Cum}$	Cumulative number of installed units at generator	[-]	Positive
CAP	Cumulative installed gross capacity at generator	[MW]	Positive
C^{Invest}	Overnight investment costs	[kUSD]	Positive
C^R	Ramping costs	[Δt kUSD/h]	Positive
C^{SD}	Shut-down costs	[Δt kUSD/h]	Positive
C^{SRMC}	Short-run marginal cost	[Δt kUSD/h]	Positive
C^{SU}	Start-up costs	[Δt kUSD/h]	Positive
FC	Fuel consumption	[Δt MW_{th}/h]	Positive
OFF	Indicates the number of offline units at the generator	[-]	Positive
ON	Indicates the number of online units at the generator	[-]	Integer
$OPEX$	Annual operational expenditures	[kUSD/y]	Positive
OR^{Spare-}	Negative spare capacity	[MW]	Positive
OR^{Spare+}	Positive spare capacity	[MW]	Positive
OR^{Spin-}	Negative spinning reserve capacity	[MW]	Positive
OR^{Spin+}	Positive spinning reserve capacity	[MW]	Positive
P	Power generation above minimum generation level	[MW]	Positive
P^{Net}	Net power generation	[MW]	Positive
SD	Indicates a shut-down of a unit	[-]	Integer
SU	Indicates a start-up of a unit	[-]	Integer
δ	Generation in block b of piecewise linear production curve	[MW]	Positive

Table 5: Parameters of module Conventional Thermal Generators

Parameter	Description	Unit
$\overline{p}$	Gross capacity of single unit	[MW]
$\underline{p}$	Minimum generation of single unit	[MW]
$\bar{r}$	Maximum ramping per dispatch period	[MW/Δt]
$\bar{u}$	Maximum installable units at generator	[-]
$\underline{\eta}$	Gross efficiency at minimum generation level	[%]
Δ	Maximum generation within the block of the piecewise linear fuel consumption curve	[MW]
a	Availability factor	[%]
at	Ambient temperature	[°C]
aux	Auxiliary power expressed as percentage of installed capacity	[%]
c^E	Specific emission costs (e.g. for CO_2)	[kUSD/t]
c^{FOM}	Fixed O&M costs expressed as percentage of investment costs	[%]
c^{Fuel}	Primary fuel cost	[Δt kUSD/MWh_{th}]
c^{Invest}	Specific overnight investment costs	[kUSD/MW]
c^R	Specific ramping costs	[kUSD/MW]
c^{SD}	Costs for a unit shut-down	[kUSD]
c^{SU}	Costs for a unit start-up (fuel and CO_2 emission costs excluded)	[kUSD]
c^{VOM}	Variable O&M costs	[Δt kUSD/MWh]
cf^p	Correction factor for available capacity according to ambient temperature	[%]
cf^η	Correction factor for efficiency according to ambient temperature	[%]
d^{DP}	Weighting factor for dispatch period	[-]
e	Emission intensity of fuel (e.g. CO_2)	[Δt t/MWh_{th}]
$fuel^{SU}$	Fuel usage per unit start-up	[MWh_{th}]
fy	First possible year of operation	[-]
ly	Last possible year of operation	[-]
m	Slope of piecewise linear fuel consumption curve	[Δt MW_{th}/MWh]
mdt	Minimum down time of single unit	[Δt]
mut	Minimum up time of single unit	[Δt]
p^{SD}	Shut-down capability of unit	[MW/ Δt]
p^{SU}	Start-up capability of unit	[MW/ Δt]
r^{Max}	Maximum ramping per minute expressed as percentage of installed capacity	[%/min]
$tc^{p,01-10}$	Coefficients for piecewise linear approach for impact of ambient temperature on power generation	[-]
$tc^{\eta,01-10}$	Coefficients for piecewise linear approach for impact of ambient temperature on efficiency	[-]

Table 6: Variables of module Concentrating Solar Power

Variables	Description	Unit	Type
$AUX^{SF,TES}$	Auxiliary power for solar field and thermal storage operation	[MW]	Positive
$BUILD^{BB}$	Installed back-up burner capacity expressed as percentage of installed gross capacity of the generator	[%]	Positive
$BUILD^{Cum,PB}$	Cumulative number of installed power blocks at generator	[-]	Positive
$BUILD^{PB}$	Number of installed power blocks at generator	[-]	Integer
$BUILD^{SF}$	Number of installed SM 1 solar fields at generator	[-]	Positive
$BUILD^{TES}$	Installed thermal energy storage capacity expressed in hours to operate the generator with full capacity	[h]	Positive
CAP	Cumulative installed gross capacity of generator	[MW]	Positive
CAP^{BB}	Total back-up burner capacity expressed as percentage of installed gross capacity of a single power block	[%]	Positive
CAP^{TES}	Total thermal energy storage capacity expressed in hours to operate a single power block with full capacity	[h]	Positive
C^{Invest}	Overnight investment costs	[kUSD]	Positive
C^{R}	Ramping costs	[Δt kUSD/h]	Positive
C^{SD}	Shut-down costs	[Δt kUSD/h]	Positive
C^{SU}	Start-up costs	[Δt kUSD/h]	Positive
FC	Thermal energy consumption	[Δt MW_{th}/h]	Positive
L^{TES}	Maximum fill level of thermal energy storage	[MWh_{th}]	Positive
ON	Indicates the number of online units at the generator	[-]	Integer
$OPEX$	Annual operational expenditures	[kUSD/y]	Positive
P	Power generation above minimum generation level	[MW]	Positive
$P^{Grid,Aux}$	Grid consumption to cover auxiliaries of the generator	[MW]	Positive
P^{Net}	Net power generation	[MW]	Positive
Q^{BB}	Thermal power generation of back-up burner	[MW_{th}]	Positive
$Q^{C,TES}$	Charging of thermal energy storage	[MW_{th}]	Positive
$Q^{Curtail}$	Curtailment of thermal energy	[MW_{th}]	Positive
$Q^{D,TES}$	Discharging of thermal energy storage	[MW_{th}]	Positive
Q^{SF}	Thermal power generation of solar field	[MW_{th}]	Positive
SM^{SF}	Total solar field size expressed as SM (related to the thermal capacity of one single power block)	[-]	Positive
SU	Indicates a start-up of a unit	[-]	Integer

Table 7: Parameters of module Concentrating Solar Power

Parameter	Description	Unit
$\underline{bb}$	Minimum back-up burner capacity expressed as percentage of gross capacity of a single power block	[%]
$\overline{bb}$	Maximum back-up burner capacity expressed as percentage of gross capacity of a single power block	[%]
$\overline{p}$	Gross capacity of single power block	[MW]
$\underline{p}$	Minimum generation of single power block	[MW]
$\overline{q}^{PB}$	Thermal capacity of single power block	[MW_{th}]
$\underline{sm}$	Minimum solar multiple	[-]
$\overline{sm}$	Maximum solar multiple	[-]
$\underline{tes}$	Minimum thermal energy storage capacity expressed in hours to operate a single power block with full capacity	[h]
$\overline{tes}$	Maximum thermal energy storage capacity expressed in hours to operate a single power block with full capacity	[h]
a	Availability factor	[%]
aux	Auxiliary power of a single power block expressed as percentage of power block capacity	[%]
aux^{SF}	Auxiliaries for SM1 solar field at design point	[MW/SM]
aux^{TES}	Specific auxiliaries for thermal energy storage operation	[MW/MW_{th}]
c^{BB}	Specific investment costs of back-up burner	[$kUSD/MW_{th}$]
c^{E}	Specific emission costs (e.g. for CO_2)	[kUSD/t]
c^{FOM}	Fixed O&M costs expressed as percentage of investment costs	[%]
c^{Fuel}	Fuel cost of back-up burner	[Δt $kUSD/MWh_{th}$]
c^{PB}	Specific investment costs of power block	[kUSD/MW]
c^{SM1}	Specific investment costs of solar field	[kUSD/SM]
c^{TES}	Specific investment costs of thermal energy storage	[$kUSD/MWh_{th}$]
c^{VOM}	Variable O&M costs	[Δt kUSD/MWh]
cf^{p}	Correction factor for available capacity according to ambient temperature	[-]
d^{DP}	Weighting factor for dispatch period	[-]
e	Emission intensity of fuel (e.g. CO_2)	[Δt t/MWh_{th}]
$fuel^{SU}$	Fuel usage per unit start-up	[MWh_{th}]
fy	First possible year of operation	[-]
ly	Last possible year of operation	[-]
max^{BB}	Maximum thermal energy generation from the back-up burner expressed as percentage of annual thermal energy generation from the solar field	[%]
$\overline{pb}$	Maximum number of installable power blocks at generator	[-]
$q^{norm,SF}$	Normalized generation of solar field (capacity factor of solar field in dispatch period)	[%]
$\eta^{Self,TES}$	Losses of thermal energy storage due to self-discharge	[%/Δt]
$\eta^{c,TES}$	Thermal energy storage charging efficiency	[%]
$\eta^{d,TES}$	Thermal energy storage discharging efficiency	[%]

1 Introduction

This chapter describes the background of this work (Section 1.1) and highlights the objective and the structure of this PhD thesis (Section 1.2).

1.1 Background

The Paris Agreement, which was negotiated during the 2015 United Nations Climate Change conference (COP 21), entered into force on 4 November 2016. The signing parties agreed on the target of limiting global warming to less than two degrees Celsius above pre-industrial levels [1]. This requires a significant reduction of global anthropogenic greenhouse gas (GHG) emissions. One key-factor to achieve this ambitious goal is the transition of the mainly fossil fuel dominated power systems of today towards a sustainable electricity supply [2]. Levelized cost of electricity (LCOE) of Photovoltaics (PV) and wind power has decreased to a very competitive level, making them an attractive investment option from a single investor and also from an entire system planning perspective [123]. There is no doubt that PV and wind power will play a major role for the transition of power systems worldwide towards a sustainable electricity supply and large shares of future electricity demand will be covered by these low-cost power generation technologies [116]. However, due to the inherent characteristics of PV and wind power, i.e. the site-specific, highly variable, and unreliable power generation, as well as low variable generation costs, a large-scale integration of these variable renewable energy (VRE) technologies has significant impacts on the power system and creates challenges on different timescales [37], [39]. A large-scale deployment of VRE causes adequacy-impacts and related costs for the system due to required back-up capacity and reduced utilization of dispatchable generators. Grid-related impacts and associated costs occur due to required extensions and reinforcements of the transmission grid to balance continuously demand and supply and avoid extensive curtailment of VRE. The large-scale integration of VRE leads to a higher variability of the residual load. This causes balancing impacts and related costs because larger amounts of operating reserve capacity and a more flexible operation of dispatchable generators is required to balance out unreliable and fluctuating power generation from VRE [38], [40], [47], [72]. These impacts and the related integration costs caused by VRE need to be considered by planning authorities when designing the transition towards a sustainable electricity supply.

Several flexibility options are available to back-up and balance out fluctuating power generation from low-cost PV and wind power and therefore support grid integration of VRE. Flexibility options comprise dispatchable conventional thermal generators, energy storage facilities, electricity exchange via transmission lines, sector-coupling, demand side management, and dispatchable renewable energy (DRE) technologies, such as biomass, geothermal, reservoir hydro power, and concentrating solar thermal power (CSP) generators. Besides increasing the share of electricity generation from renewable energy sources (RES - E) itself without increasing flexibility requirements of the system, DRE can ideally complement the integration of VRE due to their capability to deliver firm and flexible generation capacity on demand [3], [4].

By 2040, the power systems of the Middle East and North Africa (MENA), Southern Africa, Latin America, China, and India will consume more than 50% of global electricity demand due to the strongly increasing electricity demand in these world regions [116]. Besides high demand growth rates, these developing and emerging economies have in common that they have access to excellent and abundant solar resources [5–10]. This makes the CSP technology a promising option for the transition of power systems towards a sustainable electricity supply and to support grid integration of VRE. Due to the application of a thermal energy storage and a fossil or bio fuel fired back-up burner, CSP generators can not only produce large quantities of electricity from solar resources but can also provide firm and dispatchable capacity to back-up fluctuating power generation from VRE. Especially for the MENA and Southern Africa region, the CSP technology could be one of the key-factors for a successful transition towards a sustainable electricity supply because resource potentials for other DRE technologies, such as reservoir hydro power or biomass, are very limited. But also for the power systems of India, China, and Latin America, CSP could be a valuable option to complement other DRE for which further deployment often experiences difficulties because of environmental concerns and low public acceptance [10], [62], [86], [87].

In order to design reliable, economically efficient, and environmentally friendly power systems, planning authorities rely on long-term capacity expansion planning models that are able to consider the value of VRE for the system but also the impacts caused by a large-scale integration of VRE. Furthermore, long-term capacity expansion planning models must be able to identify

suitable flexibility options to support grid integration of VRE. Widely used models, such as e.g. WASP, LEAP, or MESSAGE, have proven their value for designing hydro-thermal dominated power systems [11–13]. However, most of this type of planning models have been developed during times when global warming was of less concern and VRE, such as PV and wind power, were far away from economic competitiveness. As a consequence, an adequate modelling approach for VRE and their impacts on the power system as well as for flexibility options, such as CSP or energy storage, is often missing in these traditionally applied models [96]. However, for a successful transition towards a sustainable electricity supply, planning authorities require adequate planning tools which allow for a concerted and reliable capacity expansion planning with VRE. The outcome of this is the need for new methods in the field of power system capacity expansion planning.

1.2 Objective and structure of this work

The objective of this work is the enhancement of the REMix energy system modelling framework to allow long-term capacity expansion optimization over a multi-annual planning time frame for identifying cost-efficient and reliable transition pathways towards a sustainable electricity supply. During capacity expansion optimization the value of energy at its time of the delivery and the impacts of a large-scale integration of VRE into the power system shall be taken into consideration in order to identify concerted and cost-efficient capacity expansion pathways for VRE, dispatchable power plants and other flexibility options, such as e.g. energy storage.

The Renewable Energy Mix (REMix) modelling framework has been developed within several PhD theses at the Department of Systems Analysis and Technology Assessment of the German Aerospace Center (DLR-SYS) [15–17], [67], [69], [70]. The enhancements of the modelling framework during this work led to the Capacity Expansion Model REMix-CEM (see Figure 1). Besides the newly developed model, the REMix modelling framework consists of the Energy Data Analysis Tool REMix-EnDAT and the Optimization Model REMix-OptiMo. REMix-EnDAT can be used to calculate global potentials and temporal resource availability of RES-E technologies. REMix-OptiMo is a linear programming (LP) optimization model with focus on large interconnected energy systems dominated by RES-E. Based on high temporal and spatial resolution, the model is rather used to validate long-term energy supply scenarios by modelling

system operation over one year (e.g. the final year of the proposed scenario) on an aggregated technology level and to investigate economic competiveness of additional flexibility options, such as energy storage, transmission grid expansion, or sector-coupling. In contrast, the newly developed REMix-CEM is a mixed integer linear programming (MILP) optimization model which has the aim to identify concerted transition pathways for national power systems over a multi-annual planning time frame, while considering the impacts of a large-scale integration of VRE into the power system in detail. The model identifies discrete cost-efficient investment options and can apply a high system-operational detail by modelling on a single unit level instead of an aggregated technology level. However, one of the drawbacks of a higher modelling detail is higher computational complexity. Therefore, systems analyzed by REMix-CEM have typically a smaller size than those analyzed by REMix-OptiMo.[1]

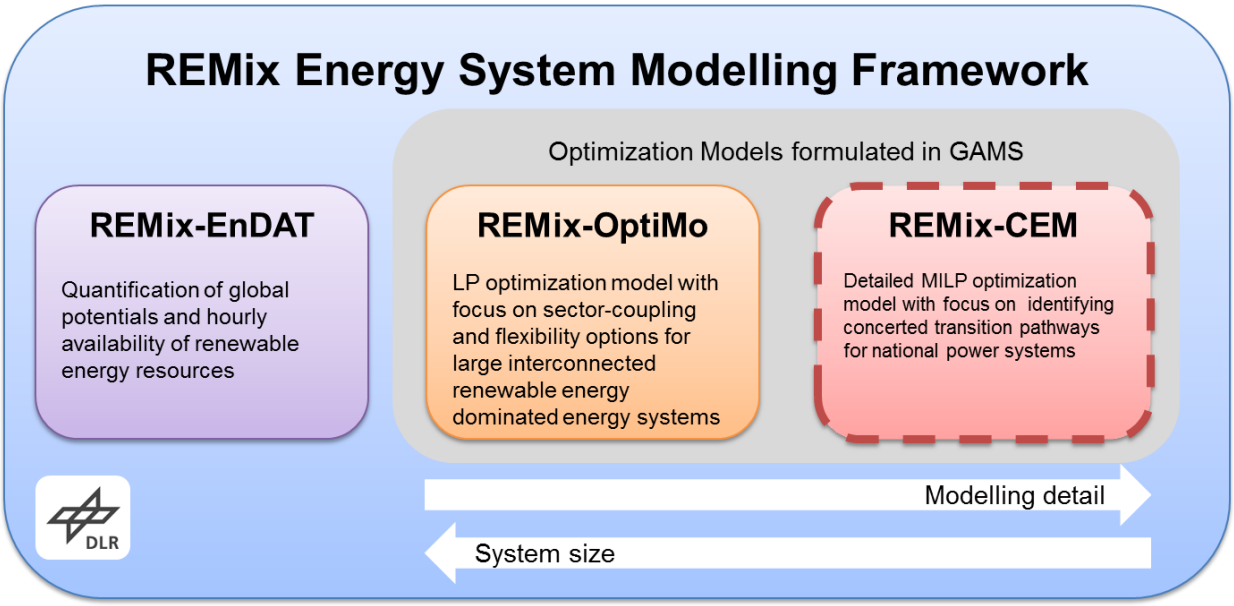

Figure 1: Overview of the REMix energy system modelling framework

REMix-CEM is used by DLR-SYS mainly for supporting national planning authorities of especially developing and emerging countries in the process of determining cost-efficient, reliable, and robust transition pathways for their power systems [99], [127]. Typically, this science-based

[1] The formulation of REMix-CEM allows a flexible application of various constraints on system and single unit level. Computational effort of the model can be reduced significantly by neglecting certain constraints. Hence, the model can be applied also for very large systems when compromises in terms of model fidelity are made.

advisory process is carried out in close collaboration with international cooperation institutions. In this process REMix-CEM is used as decision support tool to answer the key questions of long-term capacity expansion planning with VRE (see Figure 2). Which technologies should be installed when, where, and how much of it in order to meet future electricity demand in the most cost-efficient way, while ensuring applied reliability standards and defined strategic targets for the system? To answer these general planning questions when VRE are included in the analysis, the value of energy at its time of the delivery for different supply options and the impacts of a large-scale deployment of VRE must be analyzed and competitive flexibility options to back-up and balance-out unreliable and fluctuating power generation from VRE must be identified.

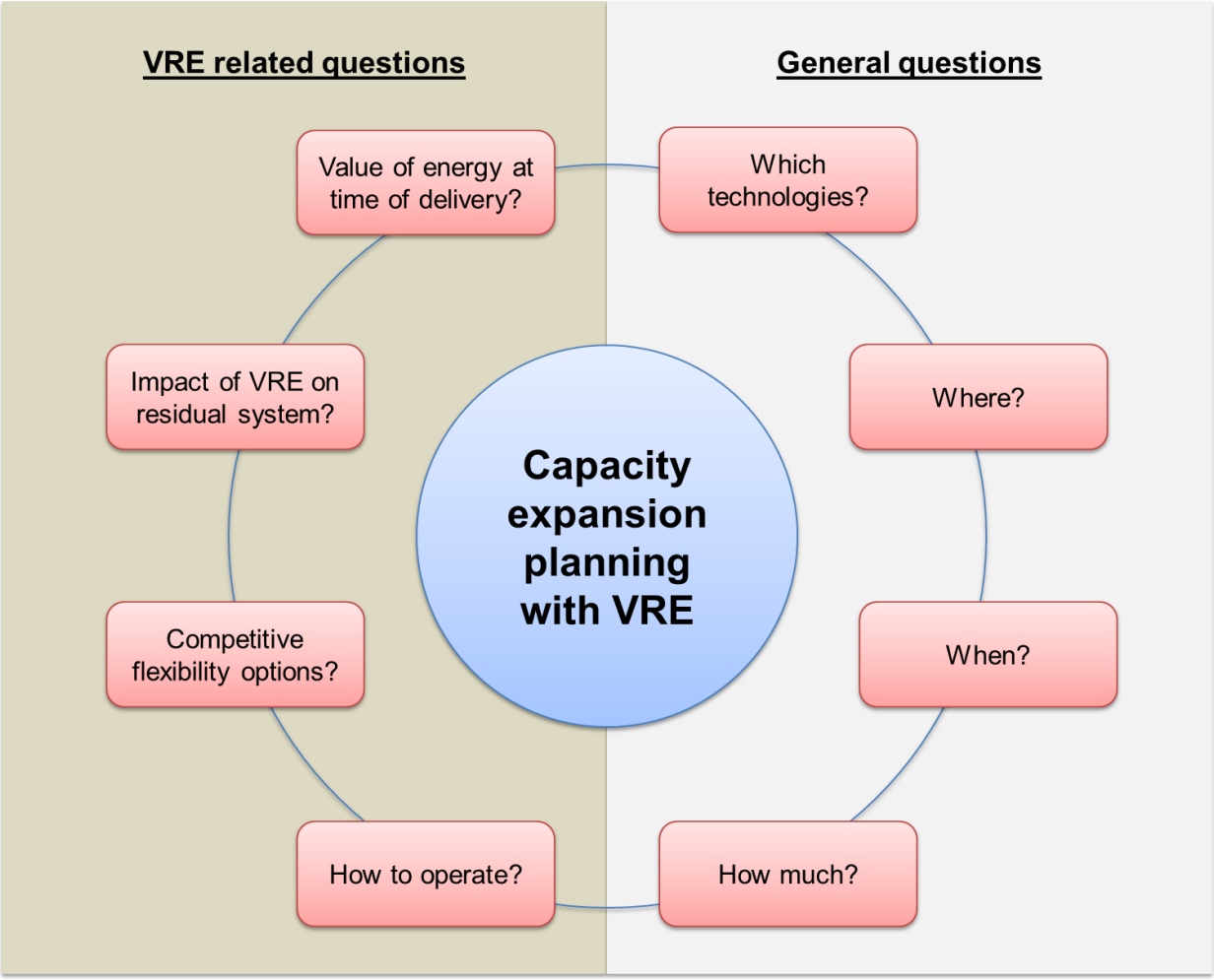

Figure 2: Key questions for capacity expansion planning with VRE

This work comprises a detailed description of the enhancement of the REMix energy system modelling framework and demonstrates the application of the newly developed model REMix-CEM for a fictitious power system.[2] The flexible formulation of the enhanced modelling framework allows performing capacity expansion optimization under myopic, rolling horizon, and perfect foresight approaches as well as considering different system-operational detail levels. The utilized foresight approach determines how possible future occurrences, such as a large-scale integration of VRE or increasing fuel and CO_2 emission costs, can be anticipated by the model in advance and investment decisions can be adopted accordingly. The applied system-operational detail determines how accurate the value of energy at its time of the delivery and the flexibility challenge for the residual system caused by a large-scale integration of VRE is considered during capacity expansion optimization. While performing long-term capacity expansion optimization for the fictitious power system the impact of the applied foresight approach and the applied system-operational detail on model results and computational effort is investigated. Results of this systematic analysis will help to identify the optimal trade-off between required model fidelity and computational effort for a meaningful long-term capacity expansion planning with VRE.

Figure 3 presents the structure of this work. Chapter 1 provides a brief introduction to the REMix energy system modelling framework and describes the enhancements made within this work in a qualitative way. Principles of capacity expansion planning with VRE are discussed in Chapter 3. The chapter contains an overview of power system model types that are applied for different timescales by power system planners and operators. Furthermore, the impacts of a large-scale integration of VRE into the power system are described. The chapter ends with an overview about current developments in model-based capacity expansion planning with VRE. Chapter 4 describes the developed optimization model REMix-CEM in detail and presents the mathematical formulation of the major enhancements of the REMix modelling framework made within this work. Chapter 5 contains the systematic analysis of the impact of the assumed model foresight and the applied system-operational detail on results and computational effort for

[2] Please note that results from real-life model applications during projects e.g. for the World Bank (Botswana) and the GIZ (Morocco) cannot be presented in this PhD thesis due to secrecy clauses that are currently in place.

capacity expansion optimization. Chapter 6 describes how REMix-CEM is typically applied as decision support tool for science-based consultancy of national planning authorities of developing and emerging countries in collaboration with international cooperation institutions. Chapter 7 concludes and discusses the results of this work and highlights further research requirements.

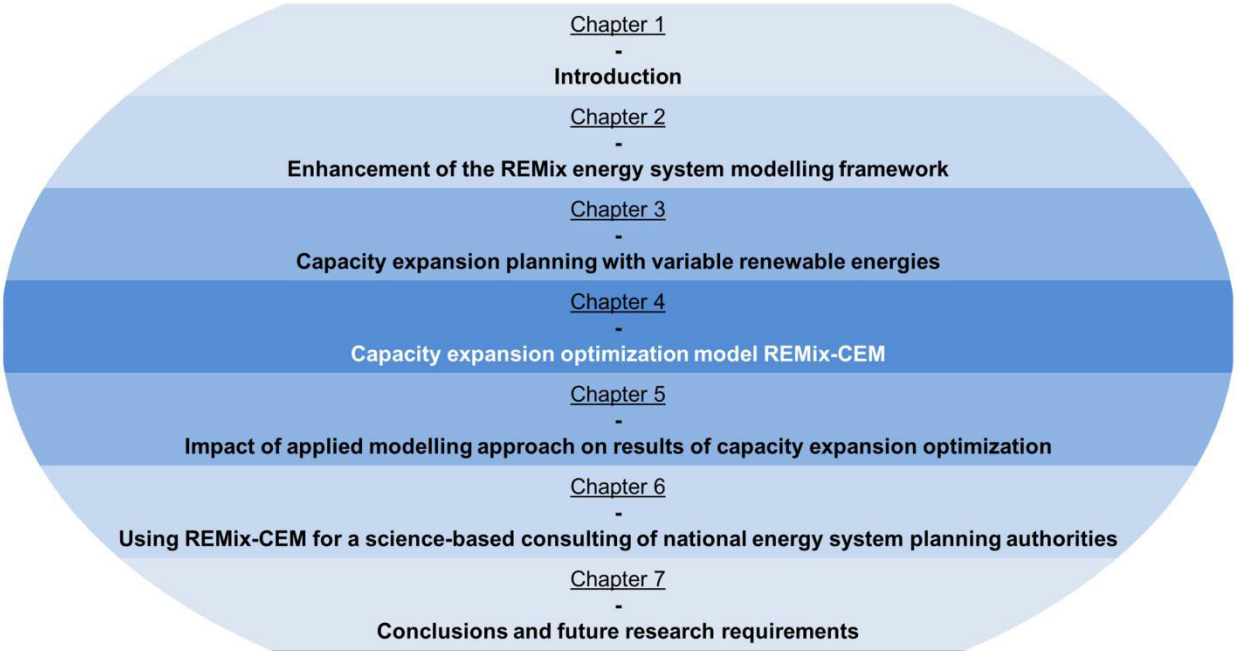

Figure 3: Structure of this work

2 Enhancements of the REMix energy system modelling framework

Section 2.1 introduces briefly the REMix energy system modelling framework which was developed within several PhD theses during the last ten years. The contribution of this work to the modelling framework is described in Section 2.2 in a qualitative way.

2.1 Brief introduction to the REMix energy system modelling framework

The REMix energy system modelling framework consists of two main elements: the Energy Data Analysis Tool REMix-EnDAT and the Optimization Model REMix-OptiMo (see Figure 4). Both elements of the modeling framework were initially developed by Scholz [70]. REMix-EnDAT contains a global data base for RES-E potentials in high spatial and temporal resolution. The model is written in C++ and uses geospatial data as well as renewable energy (RE) resource time series and other climate data to calculate hourly generation profiles and maximum technical potentials for various RES-E technologies. In addition, the model can be used to calculate hourly electricity and heat demand profiles with a flexible spatial resolution [17], [67], [70]. Maximum potentials and normalized generation patterns of RES-E technologies, as well as demand profiles and techno-economic scenario data, serve as input for the energy system model REMix-OptiMo.

REMix-OptiMo is a deterministic bottom-up LP optimization model with a modular structure written in GAMS[3]. REMix-OptiMo is used as a validation tool for energy supply scenarios with high shares of RES-E rather than as a long-term capacity expansion planning model that provides economically efficient multi-annual expansion pathways to meet future demand. The model calculates the economic dispatch on an aggregated technology level of a proposed generation fleet of a certain target year (e.g. 2050) with high temporal and spatial resolution and thereby validates if demand and supply can be balanced in each hour of the year [17]. Additional sectors, such as the heat or transport sector, can be included in the analysis [67], [69]. Taking into account annuities for investment costs, REMix-OptiMo is also able to optimize capacity expansion from a least-cost system approach. Typically, the model is used to optimize for large interconnected systems the deployment of flexibility options, such as energy storage

[3] General Algebraic Modeling System, www.gams.com

systems, transmission grid expansion, or demand side measurement, in addition to the proposed generation fleet of the scenario [15], [16], [67]. However, investment decisions are based only on the performance of the system in the investigated year irrespective of the previous or subsequent years. This approach is often referred to as static capacity expansion planning [14], [33]. Although static capacity expansion planning provides some useful information for the investigated year, it leads to impractical results as the solution for a single year cannot be independent from the preceding or subsequent years.

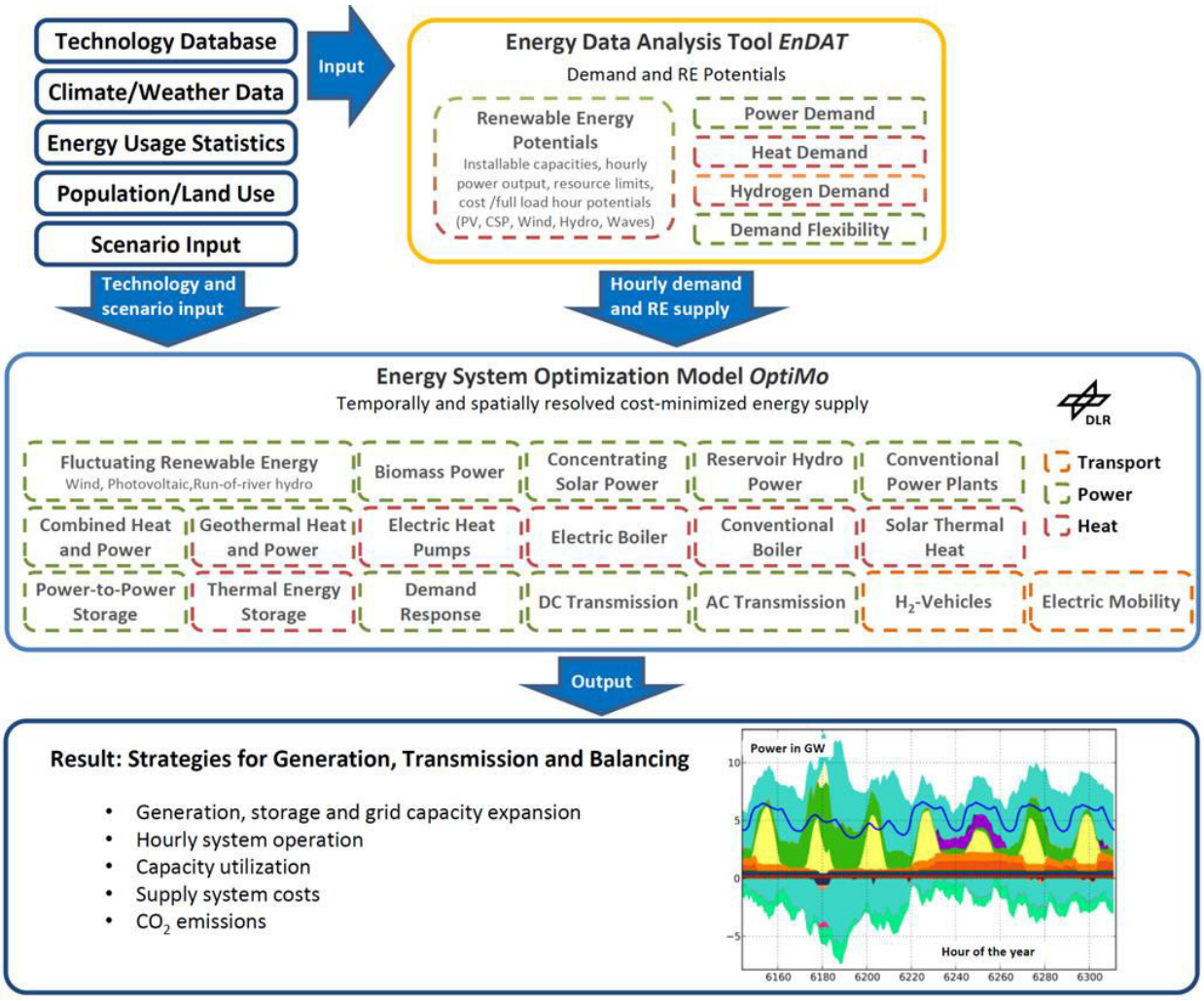

Figure 4: Overview REMix-EnDAT and REMix-OptiMo, extracted from [67]

2.2 Enhancements within this work

The REMix energy system modelling framework is continuously enhanced within projects and especially within various PhD theses at DLR-SYS [15–17], [67], [69], [70]. Figure 5 provides an overview about the different contributions through PhD theses so far. Also this work contributes to the enhancements of the modelling framework. It clearly focuses on the enhancement of the optimization procedure of the modelling framework. The starting point of this work was the initial REMix-OptiMo version developed by Scholz [70]. The enhancements of this work lead to the optimization model REMix-CEM. The objective and characteristics of the newly developed model differ in a certain extent from the model version that was used as a starting point, even though many similarities exist (see Table 8). Instead of focusing on scenario validation for large interconnected system, REMix-CEM aims to identify reliable, concerted, and cost-efficient transition pathways for national power systems.

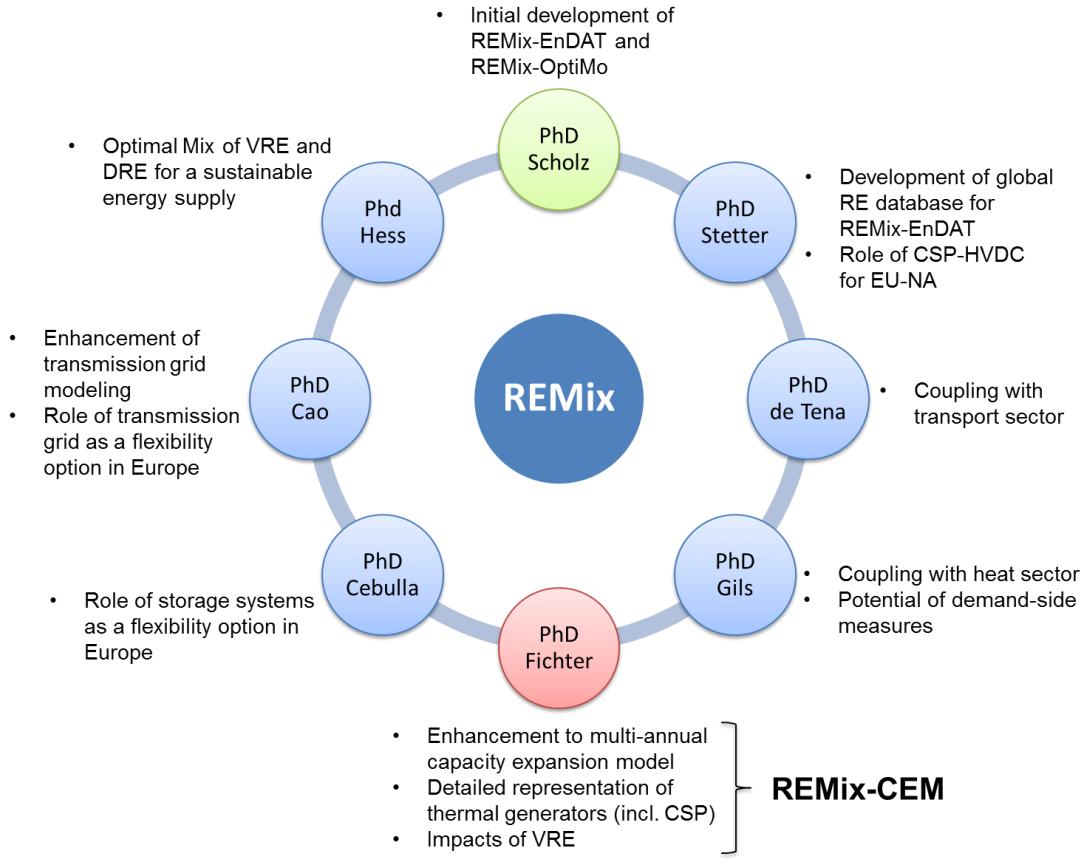

Figure 5: Contribution of different PhD theses to the REMix modelling framework

The major enhancements compared to the REMix-OptiMo version that was used as a starting point (PhD Scholz) can be summarized as follow:

1. Conversion from a scenario validation tool to a dynamic, long-term capacity expansion planning model that allows path-optimization over the planning time frame

The original optimization model is converted from a scenario validation tool, which can be used to perform static capacity expansion optimization for a single year, to a dynamic long-term capacity expansion optimization model with a multi-annual planning time frame. This enhancement allows for computing the least-cost capacity expansion pathway for the power system over a defined planning time frame for a given set of input parameters and model restrictions. The enhanced modelling framework can be used to identify cost-efficient transition pathways for power systems towards a sustainable electricity supply. The path-optimization over the planning time frame allows for considering the risk of a technology lock-in within capacity expansion planning and for identifying strategies to achieve defined targets for the planning time frame with highest economic efficiency. With this enhancement, the modelling framework can be used as the central tool for developing long-term scenarios for a sustainable electricity supply. The optimization model can be used to develop innovative, explorative, or normative scenarios, in order to investigate the impact of innovative technologies in future power systems (e.g. the role of CSP or Lithium-ion batteries), to identify optimal strategies to achieve specific targets (e.g. GHG mitigation), or to analyze the consequence of policy decisions (e.g. quotas for RES-E) respectively.

Capacity expansion for the system can be optimized under the assumption of a single-year myopic, a multi-annual rolling horizon, or a perfect foresight over the planning time frame. While under the single-year myopic foresight approach each considered year of the planning time frame is optimized successively by the model, the perfect foresight approach optimizes all years simultaneously with perfect information over the period of study. The multi-annual rolling horizon foresight approach is a compromise between the myopic and perfect foresight approach, as capacity expansion is optimized for several years of the planning time frame simultaneously, before the model foresight rolls forward and capacity expansion is optimized for the next group of years. The suitability of the foresight approach depends on the objective of the analysis, and the applied approach can have a significant impact on results and on computational effort for capacity expansion optimization. The impact of the applied model foresight within long-term capacity expansion planning with VRE is investigated in Section 5.2.

In order to reduce computational effort, long-term capacity expansion optimization within the enhanced modelling framework is typically based on a sample of representative days or weeks with a high number of diurnal dispatch periods. The impact of the method to assign values for load and RE resource availability to the considered representative dispatch periods on results for capacity expansion optimization is investigated in Section 5.3.

2. Increased modelling detail for conventional thermal generators

An appropriate modelling approach to represent the interaction between conventional thermal power plants and VRE generators is of major importance when designing concerted and reliable transition pathways towards a sustainable electricity supply. Increased flexibility requirements for the system, which come along with a large-scale deployment of VRE, should be considered already within capacity expansion planning [55], [56], [77]. To consider flexibility constraints of conventional thermal generators, so called unit commitment constraints (UCCs) are introduced into the model (minimum generation levels, minimum on- and offline times, part-load performance, start-up and ramping costs). In this context, the mathematical approach of the optimization model is converted from LP to MILP. Considering UCCs ensures a more detailed representation of techno-economic operational characteristics of conventional thermal generators within capacity expansion planning. Generators are dispatched not only according to their position in the merit order but also according to their capability to meet the variable (residual) load. However, considering UCCs means also an increased computational effort due to the large number of integer decision variables, which describe the unit commitment status in each dispatch period. Therefore, single UCCs can be included in a flexible way and a linear relaxation for integer unit commitment decision variables can be applied. This allows the user to identify the model setup which provides the best compromise between computational effort and model accuracy required for the respective analysis. The impact of considering UCCs of thermal generators within capacity expansion planning with VRE is investigated in Section 5.3.

A positive side effect of the enhanced modelling detail for conventional thermal generators is the possibility to apply the optimization model also as detailed production cost model (REMix-PCM), which can be used to model system operation of a given asset fleet in detail. Within annual production cost modelling, a high spatial and temporal resolution (typically 8760 h) and

the full set of UCCs of thermal generators are applied. Annual production cost modelling for a given asset fleet can support capacity expansion planning by providing further details about the annual operation of the proposed system or to investigate the role of a specific technology within the system in detail.

Countries with high solar resource potentials have also high average ambient temperatures. High ambient temperatures have however a significant impact on the performance of thermal generators. This is especially the case for gas turbines and air-cooled Rankine-Cycles [83–85]. The influence of ambient temperature on generator performance is introduced into the model and is considered with the same temporal resolution as other operational aspects.

3. Increased focus on a reliable system design

A reliability system design, despite high shares of VRE on total annual electricity supply, is a prerequisite of a successful transition towards a sustainable electricity supply. Future power systems with high shares of VRE must ensure adequacy of the system by holding available enough firm generation capacity to guarantee that peak load periods can be met by the asset fleet reliably. In addition, enough operating reserve capacity must be hold available to perform frequency stabilization action in the case of an imbalance between demand and supply. To ensure that computed capacity expansion pathways allow a reliable system operation, several restrictions are introduced into the model, which ensure that computed solutions contain sufficient adequacy and operating reserve capacities over the planning time frame.

4. Enhanced modelling approach for CSP

CSP has the potential to play an important role for the transition towards RES-E dominated power systems for countries with high solar resource potentials. An accurate modelling approach that considers technical characteristics of the technology is mandatory when aiming to investigate the potential role of this DRE technology. Enhancements of the modelling approach for CSP comprise a more detailed representation of the thermal power block (similar to the approach for conventional thermal generators) and solar field performance, as well as considering the capability of CSP to provide several system services, such as the provision of firm capacity and different kind of operating reserves, within capacity expansion optimization.

Table 8: Comparison of REMix-CEM and initial REMix-OptiMo version developed by Scholz

	REMix-CEM	**Starting Point Version of REMix-OptiMo** [70]
Type	Bottom-up optimization model	Bottom-up optimization model
Modeling language	GAMS	GAMS
Mathematical approach	Deterministic mixed integer linear programming (MILP)	Deterministic linear programming (LP)
Scope	Minimizing total system costs over multi-annual planning time frame	Minimizing total system costs over one year
Perspective	Central planning authority	Central planning authority
Focus	Identification of transition pathways for national power systems	Validation of long-term electricity supply scenarios
Capacity expansion planning approach	Dynamic (perfect foresight) or semi-dynamic (rolling horizon, myopic foresight)	Static (single year)
Planning time frame	Multi-annual	Single year
Dispatch periods	Flexible, typically hourly for representative days/weeks of a year	Flexible, typically hourly for entire year (8760 dispatch periods)
Sector coverage	Power sector	Power sector
Geographical coverage	Flexible, typically at national level	Flexible, typically at multi-national level
Aggregation level	Single unit level	Technology level (aggregated units)
Dispatch strategy	Flexible, merit order or unit commitment optimization	Merit order optimization
Unit commitment constraints	Yes (optional)	No
Reliability restrictions	Demand and supply balance, adequacy and operating reserves	Demand and supply balance

3 Capacity expansion planning with variable renewable energies

In this chapter an overview about different types of power system models utilized by system planners, policy makers, and engineers is provided (Section 3.1). Models are categorized according to the timescale of the study from very short-term system operation to long-term system planning models. Furthermore, the impacts of a large-scale integration of VRE into the power system are described (in Section 3.2) and an overview about recent developments in capacity expansion planning with VRE is provided (Section 3.3).

3.1 Timescales of power system models

Power system models can be subdivided into planning and operation models. Power system models are applied by system planners, policy makers, and engineers to manage, operate, and plan power systems over timescales from milliseconds to several decades [18], [30], [31]. Figure 6 shows different timescales and issues covered by various power system models. In general, the engineering detail (model fidelity) and temporal resolution of applied models decreases with increasing duration of the investigated time frame due to computational limitations. In contrast, uncertainty regarding input parameters and results increases with the duration of the study period.

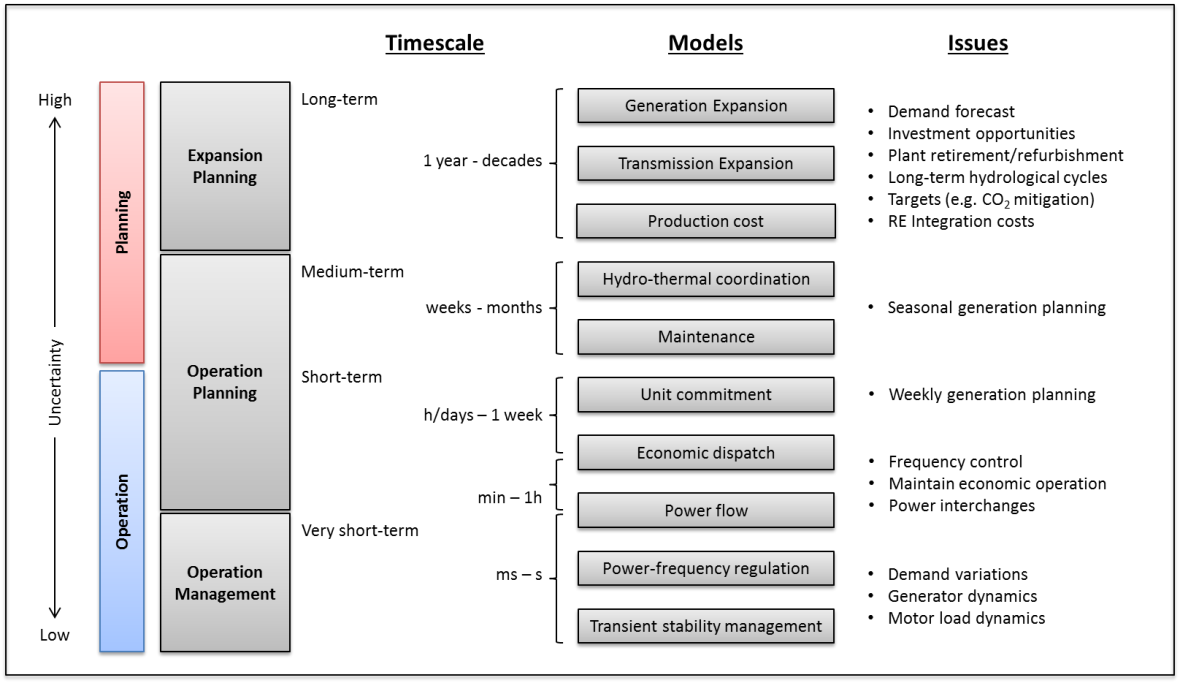

Figure 6: Timescales of power system models (own illustration based on [18], [30], [31]**)**

Very short-term models for transient stability management and power-frequency regulation cover time frames of milliseconds to seconds and are applied to model power system dynamics and transients and to manage a reliable system operation during regular operation and system disturbances [19].

Power flow models (PFMs), economic dispatch models (EDMs), optimal power flow models (OPFMs), and unit commitment models (UCMs) are considered as short-term power system operation planning models. PFMs are used to examine whether the instantaneous balance of generation and supply is ensured by the assessed power system and how power flows according to Kirchhoff's and Ohm's law [20]. EDMs are applied to plan the optimized generation level of online generators to meet temporal load of the system with maximum economic efficiency. OPFMs combine calculations of EDMs with PFMs and plan the least cost dispatch of online generators considering transmission constraints and losses [21]. UCMs are applied for weekly generation planning. Within unit commitment optimization, flexibility constraints of thermal generators (UCCs), such as minimum online and offline times as well as start-up times and ramping limits with their associated costs, are considered. UCMs have typically a temporal resolution of 5 - 60 minutes for the dispatch periods in which demand and supply must be balanced and operating reserve requirements be met by the existing asset fleet [22].

Models for maintenance scheduling and coordination of seasonal power generation of hydro power and conventional thermal units (hydro-thermal coordination) are considered as medium-term power system planning models. Such models cover typically time frames of few weeks to several months [23], [24]. Compared to short-term system operation models, the temporal resolution of these medium-term models is typically significantly lower and load chronology is neglected in most cases. Instead of chronological load curves, load duration curves (LDC)[4] with a relative low number of load levels are applied to match seasonal generation with demand while considering restrictions of fossil fuel and hydro resource availability.

[4] A LDC is constructed from the original chronological load curve by reorganizing values from the highest load values to the lowest ones. The resulting LDC is divided into some dispatch periods (often also called time-slices) in order to represent the different load levels over a period of time (e.g. a season or a year).

Production cost models (PCMs) are used to support long-term capacity expansion planning by calculating annual operation costs of a proposed generation fleet in detail with high temporal resolution (typically hourly). PCMs take into account short-term considerations of EDMs and UCMs as well as medium-term issues addressed by hydro-thermal coordination and maintenance scheduling. Recently, PCMs have been extensively applied in a large number of wind power and PV integration studies to investigate impacts of a large-scale integration of VRE into the power system (wind power, e.g. [41–43], [47] and PV, e.g. [44–46], [75]). PCMs have also been used to analyze the value of CSP and electricity-storage technologies from a system perspective [25], [26], [86]. PCMs are typically computationally demanding due to the high temporal resolution (number of dispatch periods) and the high modelling detail for thermal generators (UCCs) [27].

Generation expansion planning (GEP) and transmission expansion planning (TEP) models are used by power system planners, regulators, and policy makers to identify cost-efficient capacity expansion plans to meet future electricity demand while ensuring a reliable system design and meet other boundary constraints (e.g. CO_2 mitigation or RES-E deployment). GEP and TEP are considered as long-term planning models as investigated time frames cover typically several years or even decades. Within GEP and TEP bottom-up power system models are applied that use optimization, simulation, or equilibration methodologies based on mathematical approaches such as linear programming, integer programming, and dynamic programming [28–31], [57].

Solutions for generation and transmission expansion are often substitutes as loads can be met either by local generators or power transmission from remote sites. However, historically in most cases GEP and TEP were kept separate and treated as two independent expansion planning problems due to computational complexity. Established practice has been that TEP follows GEP. The problem of GEP consists of deciding the type (which?), the quantity (how much?), the timing (when?), and the location (where?) of new generation capacity to meet future demand in the most economic manner. Within TEP, the optimal transmission expansion plan to accompany the previous defined generation expansion plan is determined. This decoupled approach is justified by the fact that transmission costs of current fossil fuel fired

dominated power systems represent typically less than 10% of the total system costs [32], [33]. However, capacity expansion models (CEMs) that cover GEP and TEP simultaneously (co-optimization) can identify solutions that are economically more efficient compared to solutions identified by a decoupled approach. This is especially the case for capacity expansion planning with RES-E as models can identify if it is more cost efficient to invest largely in grid expansion to tap the best available RE resources or to use less excellent resources that are however closer to demand centers and hence require less investments in the transmission grid. However, the drawback of co-optimizing GEP and TEP within one integrated CEM is the higher complexity that causes higher computational efforts.

CEMs have typically a significant lower temporal resolution than PCMs due to the multi-annual planning time frame and the resulting large problem size. In order to keep CEMs manageable only a limited number of annual dispatch periods is used to model the operation of the system within a year. Historically, CEMs used LDCs to describe electricity demand over the year and applied screening-curve algorithms to determine the least-cost expansion plan to balance demand and supply over the planning time frame, following a merit order dispatch rule. Haydt et al. call this approach integral balance method [97]. The integral balance method estimates the utilization of each investment option, based on its variable generation costs and its average (annual or seasonal) capacity factor for resource availability, and select the appropriate units for investments by optimizing capital and operating expenditures compared to expected operating hours (see Figure 7). The advantages of the integral balance method are its computational simplicity and low data requirements to describe the demand and the supply side.

Within the integral balance method, UCCs of conventional thermal generators, such as start-up costs, minimum generation levels, or minimum on- and offline times are neglected. Hence, generators are dispatched solely according to their position in the merit order without considering any flexibility constraints. Furthermore, the value of energy at its time of the delivery for the various supply options cannot be taken into account because using LDCs comes along with the loss of load chronology and information about the correlation of technology specific resource availability and electricity demand. These simplifications weren’t an issue

during times when most CEMs were initially developed because existing power systems and investment options were dominated by dispatchable conventional thermal and hydro power plants, daily load patterns were highly predictable, and (residual) load ramps were only moderate. However, this has changed fundamentally today because VRE (PV, wind power) have become a very competitive investment option and have been integrated into power systems on a large-scale in many power systems. Recently it becomes more and more clear that the described simplifications of the integral balance method are inadequate for capacity expansion planning with VRE because the impacts of a large-scale integration of VRE into the power system cannot be captured sufficiently [96].

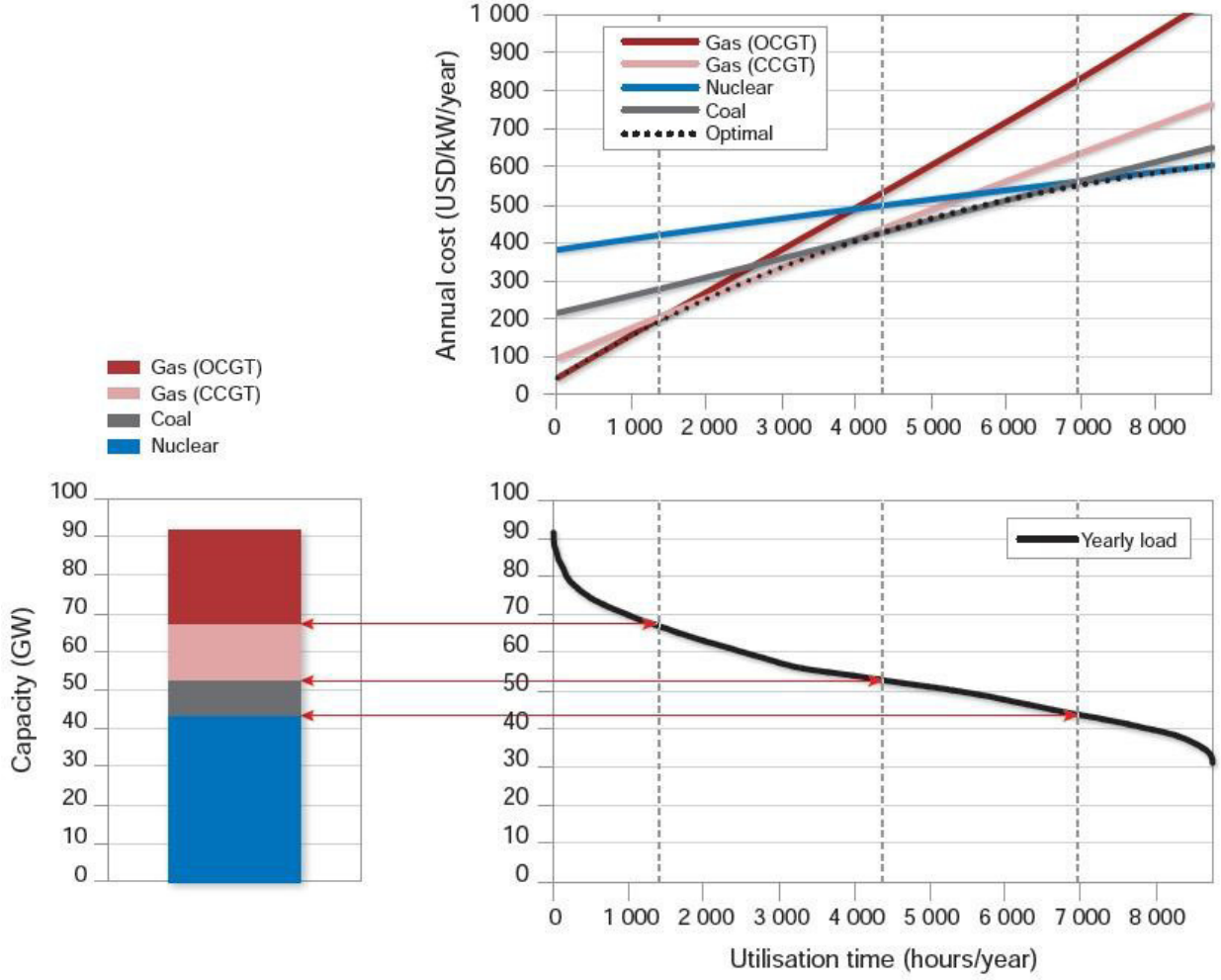

Figure 7: Integral balance method based on LDCs and screening curve algorithms to describe annual electricity demand and to determine the least-cost expansion plan to balance demand and supply [34]

3.2 Impacts of a large-scale integration of VRE into the power system

Today, onshore wind power and PV are well established and mature power generation technologies. Global wind power and PV capacity reached about 430 GW and 230 GW respectively in the end of 2015 [35]. This large-scale deployment has resulted in a significant cost reduction making these VRE technologies an attractive investment option from a single investor but also from an entire system perspective. Today, LCOEs of onshore wind power are in the range of 0.06-0.12 USD/kWh and generation cost of utility-scale PV has fallen around 50% between 2010 and 2014 resulting in LCOEs of 0.06 - 0.08 USD/kWh or lower at sites with excellent resources [36]. Therefore, LCOEs of onshore wind power and utility-scale PV are in the range of variable generation costs of conventional thermal generators fired by oil, natural gas, and sometimes even coal. This makes them a very attractive fossil “fuel saver”. There is no doubt that PV and wind power will play a major role within the transition towards RES-E dominated power systems and that a large share of electricity demand will be supplied by these VRE technologies in the future.

However, due to the inherent characteristics of VRE, i.e. the site-specific, highly variable, and unreliable power generation, as well as their low variable generation costs, the large-scale deployment of PV and wind power has significant impacts on the power system and creates challenges on different timescales that need to be considered by power system planners and operators [37], [39]. An overview of studies covering the impacts of integrating VRE into the power system is given e.g. by [38] where impacts and related integration costs (often also called external costs of VRE) from a long-term planning and short-term system operation perspective are distinguished into i) adequacy ii) balancing, and iii) grid-related impacts (see Figure 8).

Adequacy impacts and related costs refer to the fact that on the one hand deployment of VRE contributes only marginally to adequacy of the system due to their comparably low capacity credits, but on the other hand reduce significantly the utilization of conventional thermal generators due to their low variable generation costs. This effect is referred to as utilization effect [40]. The utilization effect can be further distinguished into the transitional utilization effect and the persistent utilization effect [39].

The transitional utilization effect describes the effect of decreasing utilization of existing conventional thermal generators with increasing VRE deployment. In a first step, utilization of peaking generators with high variable generation costs, e.g. oil-fired open-cycle gas turbines, will be reduced. With increasing VRE deployment, also mid-merit and base-load generators will be affected. The persistent utilization effect describes the structural shift of the residual generation fleet dominated originally by base-load generators towards a higher share of flexible mid-merit and peaking generators. In the framework of a large-scale VRE deployment, future investments in new dispatchable generators will be dominated by investments in flexible generation technologies with rather low investment costs (mid-merit and peaking units) due to expected low capacity factors and the need for flexible generation capacity that is capable to serve the highly variable residual load and the increased need for operating reserve.

Both, the transitional utilization effect and the persistent utilization effect imply an increase in average generation costs of the residual system. Decreasing capacity factors of the existing conventional thermal generation fleet will increase the generation costs of the residual system due to lower utilization but constant investment related capital costs (transitional utilization effect). With proceeding transformation towards a VRE dominated power system the transitional utilization effect will be more and more absorbed due to the shift of the residual system towards flexible mid-merit and peaking generators (persistent utilization effect). However, even with a shift towards a more flexible residual generation fleet, the average generation costs of the residual system will increase due to the higher share of mid-merit and peaking generators with higher generation costs than base load generators.

Balancing impacts and related costs refer to an increasing demand for operating reserves due to forecast errors of VRE generation and the need for more extensive cycling of dispatchable generators caused by an increasing variability of the residual load. Following [40], the latter circumstance is referred to as flexibility effect. Balancing impacts and associated costs have been investigated in several studies, with the emphasis on wind power in e.g. [41–43], [47] and for PV in e.g. [44–46], [75]. An increase in operating reserve requirements implies that an increasing number of dispatchable units, mainly conventional thermal generators, need to be operated in part-load mode meaning less fuel efficiency and consequently higher generation

costs and emissions. The higher variability of the residual load leads to more extensive cycling of dispatchable generators, which causes higher specific generation costs and emissions of the residual asset fleet (flexibility effect). To avoid an extensive cycling of dispatchable generators the flexibility of the residual load must be increased, e.g. by an increased deployment of electricity storage facilities and demand-side measures or spatial smoothing of VRE generation by long-distance electricity exchange via transmission lines. However, this causes additional integration costs of VRE and therefore increases overall system costs.

Grid-related impacts and associated costs occur due to the location-specific and modular characteristics of VRE. In most cases, relevant VRE resources are located far away from demand centers making considerable investments in new transmission capacity necessary to tap these resources for power generation[5]. Furthermore, the large-scale deployment of VRE leads to large amounts of variable output that requires a reinforcement of the existing transmission grid due to increased load flows with associated network losses and constraints [47].

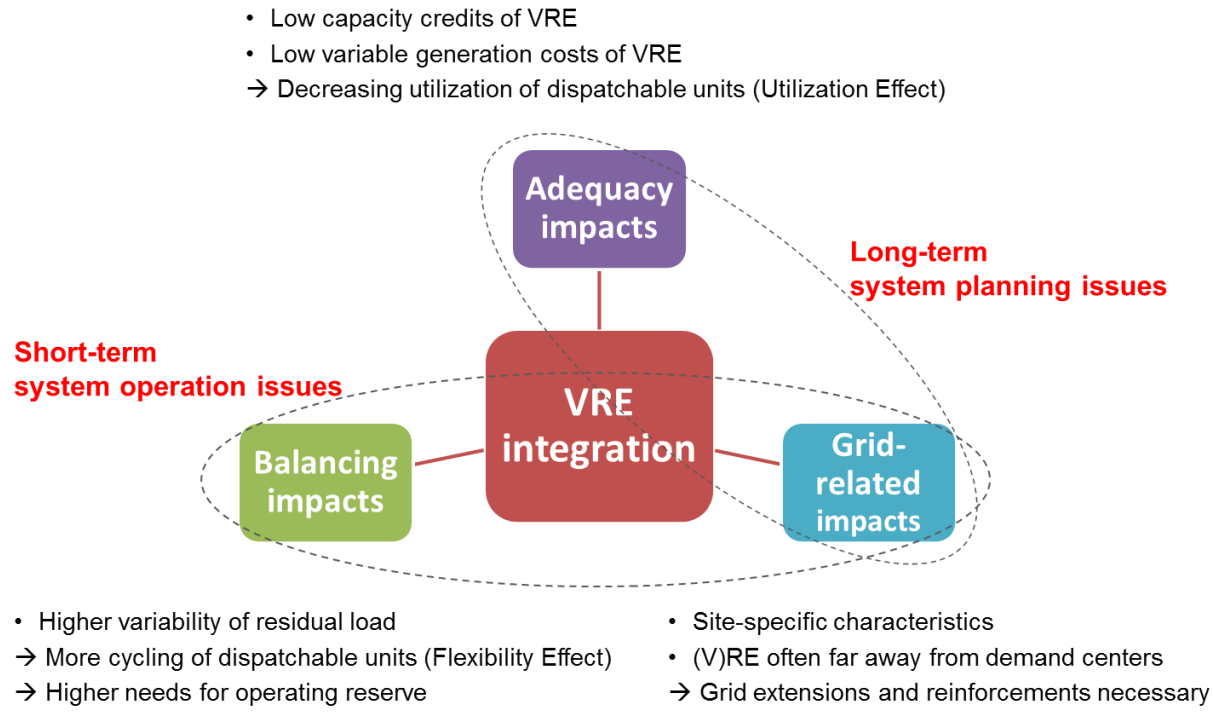

Figure 8: Impacts of integrating VRE into the power system

[5] This is also true for DRE technologies like reservoir hydro power or CSP

3.3 Recent developments in capacity expansion planning with VRE

Recently it becomes clear that the historically applied integral balance method is insufficient for capacity expansion planning with VRE because flexibility challenges and the value of energy at its time of the delivery cannot be represented correctly. The low temporal resolution and the consideration of LDCs by the integral balance method cannot capture the fluctuating nature of VRE electricity production and its impact on the residual system (balancing impacts). Furthermore, a simultaneous capacity expansion planning with dispatchable and non-dispatchable technologies requires that the competiveness of an investment option is evaluated not only on the basis of its generation costs but also on its value for the system, mainly described by the capability to deliver energy reliably at high (residual) demand. As using LDCs within capacity expansion planning comes along with the loss of load chronology and information about the correlation of VRE availability with system load, the value of energy at its time of the delivery of VRE technologies cannot be considered for the investment decision. Hence, in many cases system planners set VRE deployment model exogenously and use the integral balance method to optimize capacity expansion for the conventional residual system to balance residual demand and supply [48], [49]. This approach allows considering the utilization effect caused by a large-scale integration of VRE into the power system but does not allow a simultaneous and concerted capacity expansion optimization for VRE, dispatchable generators, and additional flexibility options, such as e.g. energy storage. Furthermore, the flexibility effect cannot be considered within capacity expansion optimization because UCCs of conventional thermal generators cannot be modeled by the integral balance method.

In order to improve long-term capacity expansion planning with VRE, several researchers attempt to bridge the gap between traditional long-term CEMs and short-term system operation planning models (PCMs or UCMs), which have a significant higher system-operational detail (see Figure 9). Thereby, it can be distinguished between two fundamentally different approaches. A first group of approaches examines results of the CEM with a detailed system operation model with the aim to better interpret results of the, in terms of system operation, less detailed long-term planning model (unidirectional soft-link, e.g. [50]) or to adjust input parameters of the planning model (bidirectional soft-link, e.g. [51], [52]).

In a second group of approaches researchers put efforts in increasing the level of system-operational detail directly in the long-term CEM. Some researchers improved the temporal representation [53], [54], [97], [102] whereas others focus on a higher modelling detail for conventional thermal generator and operating reserve requirements [56], [77]. The increased system-operational detail increases computational complexity significantly. However, it can be concluded that the higher computational effort is justified by a significant higher accuracy for capacity expansion planning with VRE. It was shown that long-term CEMs which apply a low temporal resolution tend to overestimate competiveness of less flexible baseload technologies (nuclear, lignite) and non-dispatchable VRE (PV, wind power), while competiveness of flexible dispatchable mid-merit and peaking generators is underestimated [53], [54]. Nweke et al. [55], Palmintier and Webster [77], and Welsch et al. [56] demonstrated that neglecting UCCs of thermal generators and other flexibility requirements, such as operating reserve requirements, during capacity expansion planning with VRE can lead to non-optimal investment decisions resulting in significant higher generation costs and CO_2 emissions of the system.

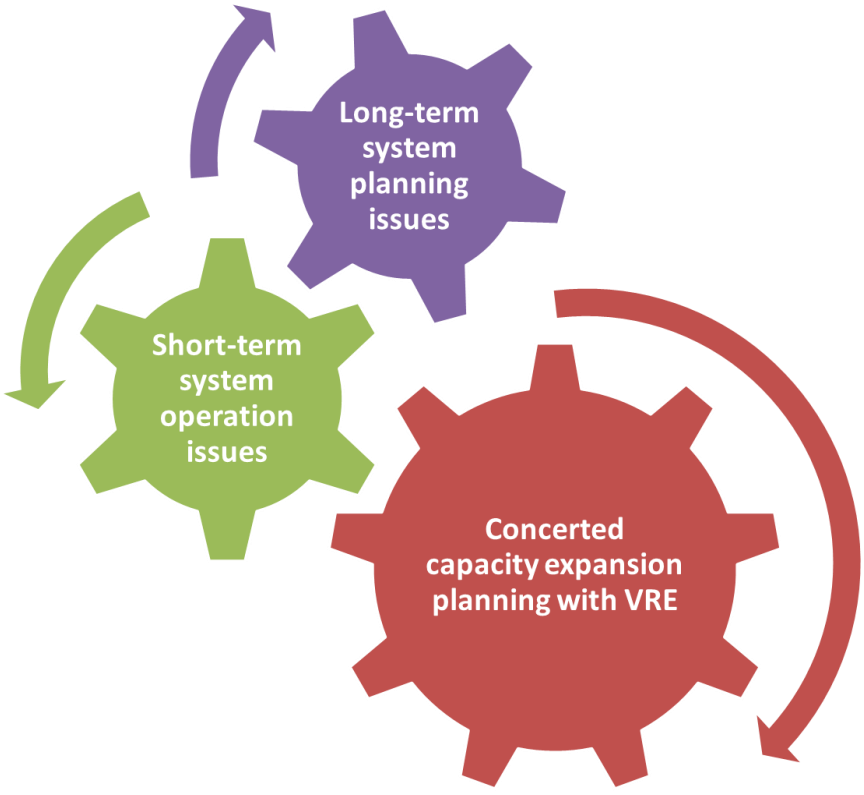

Figure 9: Combining long-term system planning with short-term system operation issues for a concerted capacity expansion planning with VRE

In countries with high solar resource potentials, one option to meet increased system flexibility requirements due to a large-scale integration of VRE is the utilization of CSP with thermal energy storage and fossil/bio fuel fired back-up burner system. However, as CSP is a relatively new commercially available technology, many long-term capacity expansion models do not have the capability to include CSP at all in the analysis or do apply an insufficient modelling approach, which underestimates the value of the technology from a system perspective and its capability to support VRE integration. In the case CSP is included in the analysis, in many cases CSP is modeled as a non-dispatchable VRE technology instead of a DRE technology. In such models, the only difference between CSP and PV is that non-dispatchable power generation of CSP is extended for several hours after sunset in the case CSP units are equipped with a thermal energy storage system [57]. An example of this CSP modelling approach is given in [58]. Some researchers have improved the modelling approach for CSP within long-term capacity expansion planning by enabling CSP generators to be dispatched according to the needs of the system. This modelling approach represents already a significant improvement because the value of energy at its time of the delivery is captured for dispatchable CSP generators [59], [131]. However, the value of entirely firm power generation from CSP by the back-up burner system is not considered in these models, even though this represents a major advantage especially for power systems with increasing peak load and total annual electricity demand like it is the case in MENA, Southern Africa, Latin America, China, and India.

4 Capacity expansion optimization model REMix-CEM

This chapter introduces the optimization model REMix-CEM that was developed in this work. REMix-CEM aims to bridge the gap between traditional long-term CEMs and detailed short-term PCMs to consider the different impacts of a large-scale deployment of VRE (adequacy, balancing, and grid-related impacts) and the value of energy at its time of the delivery for the various supply options during capacity expansion optimization. A qualitative description of the model is provided in Section 4.1. The mathematical formulation of the major enhancements compared to the initial REMix-OptiMo version is presented in Section 4.2.

4.1 Qualitative model description

REMix-CEM was developed to support national system planning authorities of developing and emerging economies in the process of defining concerted and reliable transition pathways towards a sustainable electricity supply. Figure 10 shows how REMix-CEM is typically embedded in the overall advisory process for national system planning authorities.

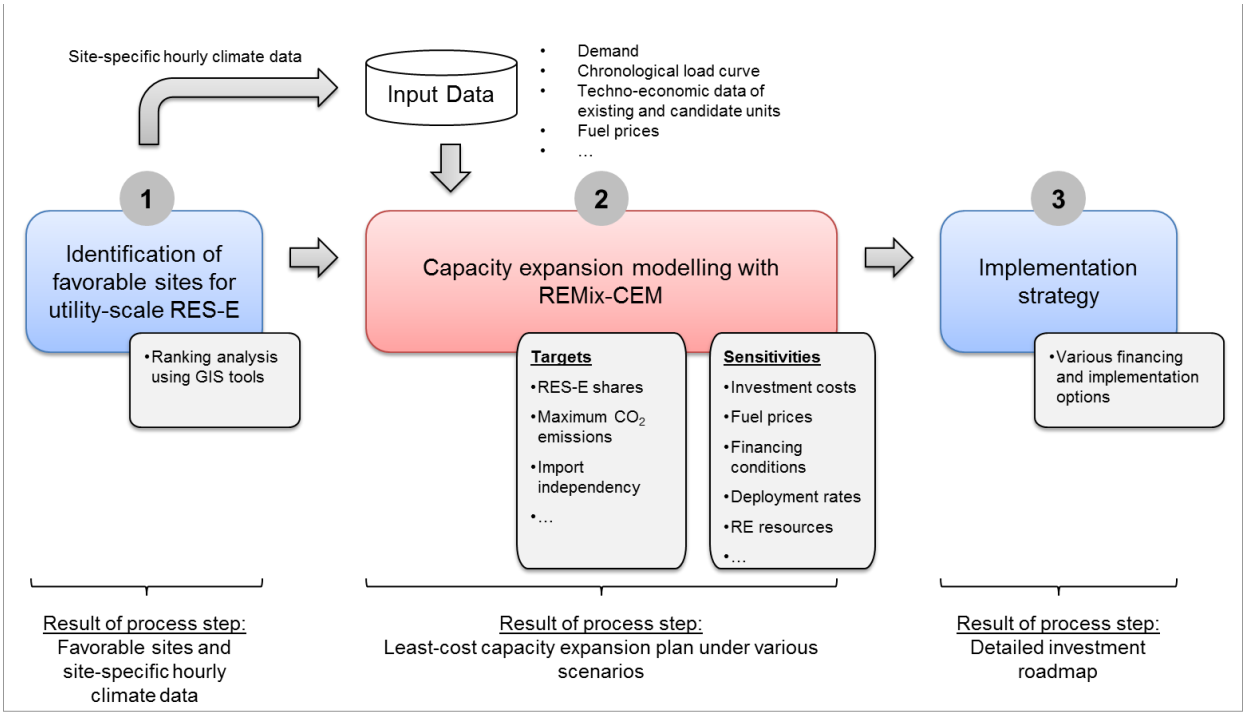

Figure 10: Methodology for national power system planning consultancy

In the first step of the advisory process, a geographical information system (GIS) is applied to quantify overall potentials and to identify favorable sites for utility-scale RES-E using geospatial data for resource availability and land coverage (see Figure 11). Hourly meteorological data at the identified RES-E sites serve as input for the optimization model REMix-CEM. Additionally, parameters describing demand over the planning time frame (chronological load curve, annual peak load, and electricity demand), the techno-economic characteristics of existing units and available investment options (investment and fuel costs, generator efficiencies, etc.) and the storyline of the analysis (e.g. political targets) serve as input for the optimization model.

In the second step of the advisory process, REMix-CEM is used to compute the least-cost capacity expansion plan to meet future electricity demand over the planning time frame, while ensuring adequacy of the system from a long-term planning perspective and a reliable system operation from a short-term system operation perspective. The least-cost system expansion plan can be computed for various targets over the planning time frame, such as maximum threshold for CO_2 emission or minimum RES-E quotas. To investigate the consequences of certain policy targets and robustness of results, capacity expansion modelling for the power system typically contains several what-if analyses and sensitivity studies.

In the third and last step of the advisory process, investment and implementation strategies are developed based on the results and lessons learned from capacity expansion modelling. Thereby, various implementation and financing options are considered and evaluated to define a detailed investment roadmap for the power sector (e.g. different types of project financing, concessional financing, tax incentives, de-risking measures, feed-in tariffs, etc.).

REMix-CEM is a power sector specific deterministic mixed integer linear programming (MILP) optimization model, formulated in the modelling language GAMS. From a central system planning perspective the bottom-up optimization model optimizes capacity expansion for a given power system to meet future electricity demand within defined reliability standards by minimizing the net present value of total systems costs over the planning time frame. The geographical coverage of the model is typically at national level. However, multi-national or sub-national power systems can also be modelled.

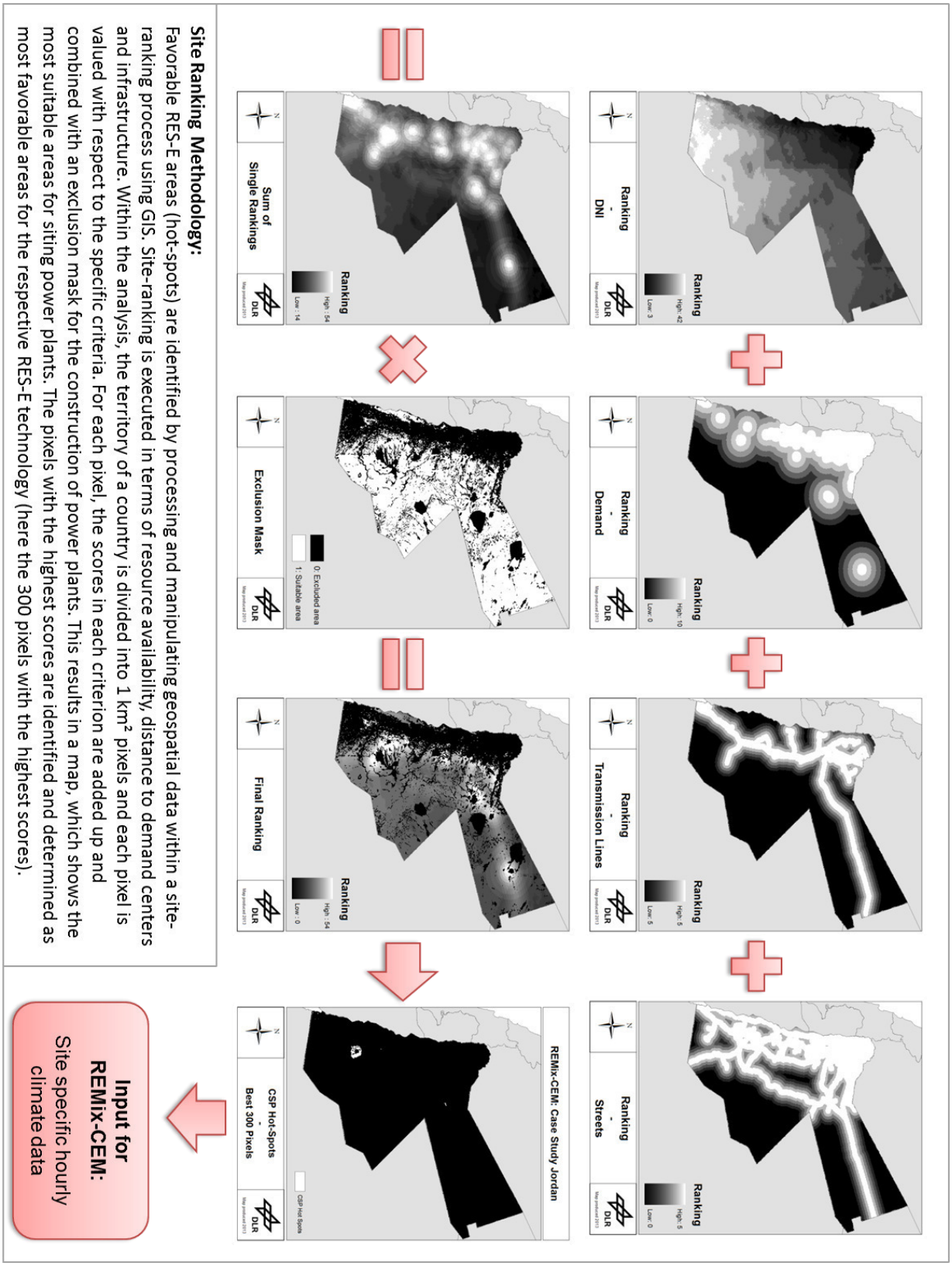

Figure 11: Site-ranking analysis for identifying favorable RES-E sites using geo-spatial data and GIS. The example shows a site-ranking analysis to identify favorable CSP areas in the Hashemite Kingdom of Jordan. For a more detailed description please refer to Fichter et al. [60]**.**

Planning time frames can be defined flexibly and are typically between 10 - 40 years. Formulated as multi-node model, REMix-CEM provides not only optimal investment strategies for new generation and storage assets and their spatial distribution and operation but also delivers first indications for required transmission grid reinforcements and extensions associated with the respective supply side expansion plan[6]. The least-cost expansion plan for the system is complemented by detailed information about generation costs (separated by capital and operational related costs), utilization, emissions (CO_2, NOx, SO_2, and $PM_{2.5}$), and water usage over the planning time frame for single assets and the entire system.

REMix-CEM is formulated in a modular way. The model structure and the available modules are presented in Figure 12. The module System Planner & Operator contains the objective function of the optimization model (minimizing total system costs) and all restrictions on system level, which are required to ensure a reliable system design over the planning time frame. Furthermore, the module contains so-called user constraints which can be applied flexibly. User-constraints can be applied to perform the least-cost capacity expansion optimization for the power system under defined targets or boundary conditions (e.g. annual CO_2 emissions of the power system or maximum deployment rates for a certain technology). Hence, the user-constraints have the function of guide rails that restrict the solution space for the optimization problem. The System Planner & Operator can make use of several supply side options to meet electricity demand, reliability standards, and targets for the power system with highest economic efficiency (least-cost). The different supply side options are modeled in technology specific modules whereby several sub-technologies are represented by each module. The modelling approach applied for the various sub-technologies of a module is always the same but techno-economic input parameters describing the respective sub-technology differ. For example, in the module Conventional Thermal Generators, nuclear power plants and open-cycle gas turbines are modeled with the same set of equations, but different techno-economic input parameters are utilized.

[6] This however does not replace a subsequent detailed transmission grid expansion study.

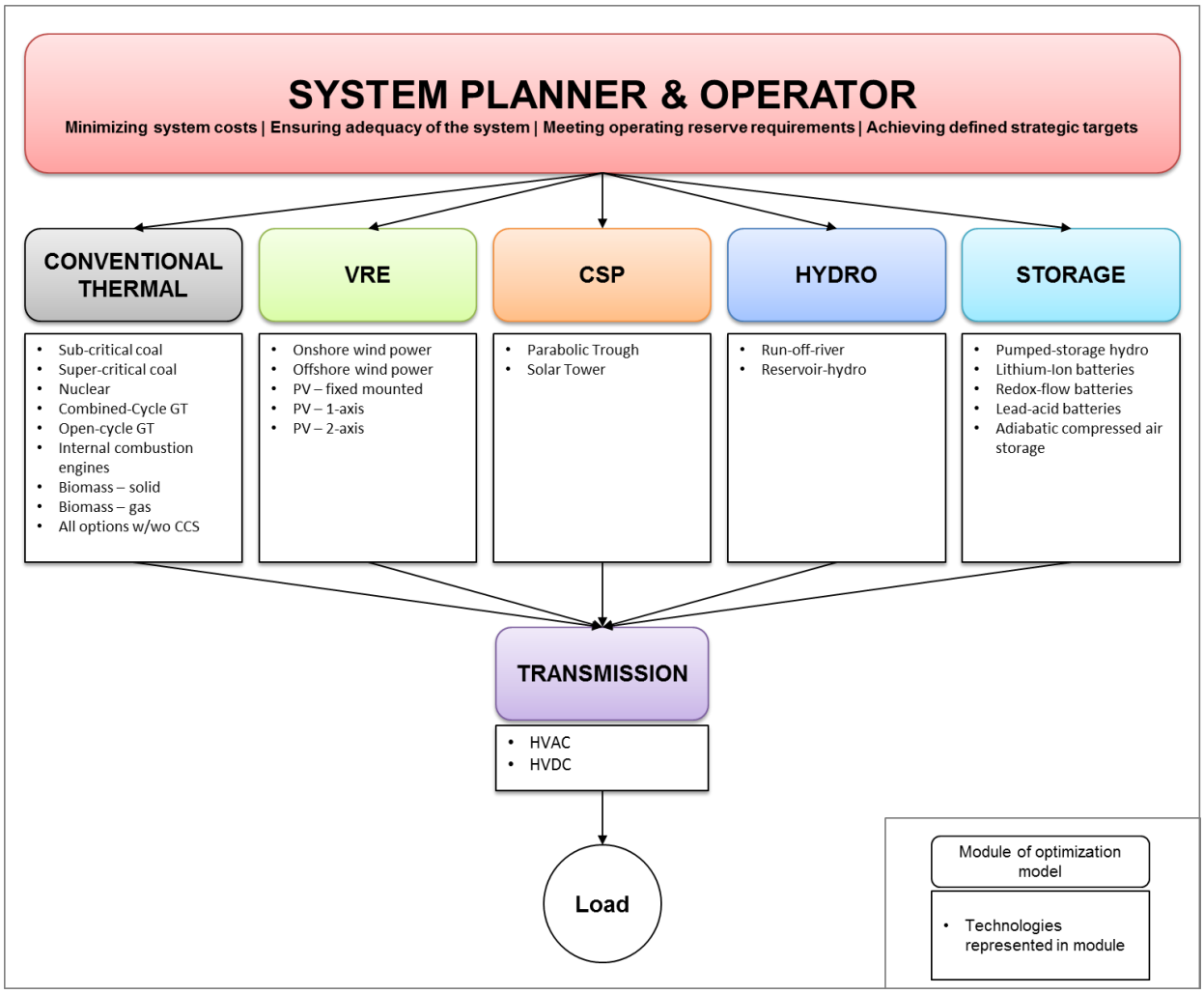

Figure 12: Overview of modules and available technologies in REMix-CEM

REMix-CEM can be used to test innovative, explorative, or normative scenarios, in order to investigate the impact of innovative technologies in future power systems (e.g. the role of CSP or energy storage), to identify optimal strategies to achieve specific targets (e.g. GHG mitigation), or to analyze the consequence of policy decisions (e.g. quotas for RES-E or implementation of CO_2 certificate prices) respectively. The least-cost system expansion plan for the planning time frame can be identified under different foresight approaches. The user can chose between a perfect, a rolling horizon, and a myopic foresight approach (see Figure 13). Examples for the model application with myopic foresight are given in [60], [61] where capacity expansion optimization is executed for the power system of Jordan. An example for applying the perfect foresight approach is provided in [62], where capacity expansion is optimized for the Northeast power system of Brazil.

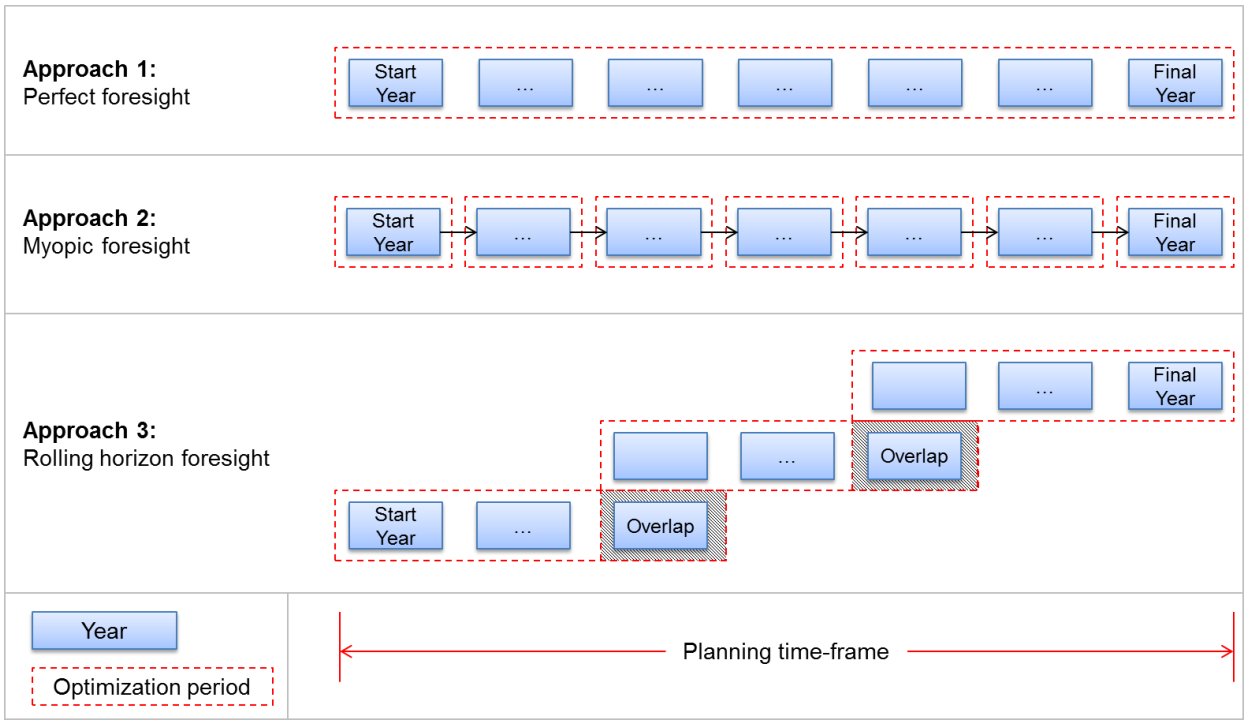

Figure 13: Different foresight approaches available in REMix-CEM

Under the perfect foresight approach, REMix-CEM calculates the optimal (least-cost) capacity expansion pathway for the power system to meet electricity demand over the planning time frame in one single model run. This approach enables decision makers to identify optimal short- and long-term investment strategies under defined boundary conditions (scenario story lines) because the results represent the global optimum to meet electricity demand over the planning time frame. However, a disadvantage of the perfect foresight approach is its high computational effort (due to the large optimization problem) and the implicit assumptions that all information characterizing the investigated planning time frame is known apriori, which not fully captures the decision framework of system planning authorities.

Another available approach in REMix-CEM is the single-year myopic foresight approach. In this approach, the capacity expansion problem is solved for each year of the planning time frame sequentially, taking into account results of the previous optimization period. The large optimization problem created under the perfect foresight approach is separated into several smaller sub-problems, which can be solved with significant less computational effort. However, the disadvantage of this approach is that the optimization model is provided with no information that goes beyond the current optimization period (one year). Hence, investment

decisions are made exclusively on the basis of the current situation (e.g. electricity demand, fuel and technology costs, political targets) without anticipating any changes in future years of the planning time frame. The assumption that system planning authorities have no information about future occurrences of the planning time frame at all is just as unrealistic as the assumption of having perfect foresight about all future developments as it is the case in the perfect foresight approach. Naturally, computed solutions for capacity expansion optimization under the myopic foresight approach are more costly than under the perfect foresight approach because results of the former approach do not represent the global optimum for the planning time frame anymore.

The third available foresight approach in REMix-CEM is the multi-annual rolling horizon approach. This approach is a compromise between the perfect foresight and the single-year myopic foresight approach. Several years of the planning time frame are grouped together and are optimized simultaneously under perfect foresight. After solving the sub-problem of the first optimization period, the foresight horizon rolls forward to the next group of years while taking into account investment decisions made in the previous optimization periods. If desired, an overlap between the defined optimization periods can be applied.

In order to avoid so-called end effects during capacity expansion optimization, annualized investment costs are considered in REMix-CEM and perpetuity is applied for all system costs of the final year of the finite planning horizon. Neglecting end effects during long-term capacity expansion optimization lead to anomalies in investment decisions towards the end of the finite planning horizon. A typical anomaly is that in the final years of the planning time frame candidate units with low investment costs but high operational costs are installed. Due to the truncation of the (in reality) infinite planning horizon, the advantage of candidate units with low operational costs over their lifetime but rather high investment costs cannot be considered. By using annualized investment costs this end effect can be mitigated. Another effect of a finite planning horizon is that potentially decreasing utilization of assets (e.g. conventional thermal generators) towards the end of the planning time frame and beyond is not fully captured due to the truncation of the planning horizon itself and the highly discounted costs towards the end of the planning time frame. Considering decreasing utilization of conventional thermal generators

is however of high importance for capacity expansion planning with VRE (utilization effect). By applying perpetuity for the system costs of the final year of the planning time frame, the importance of the finite year of the planning time frame increases considerably. This accommodates the utilization effect within capacity expansion planning with VRE. For further reading about end effects and different strategies for mitigation please refer e.g. to [63].

To overcome the limitations of the integral balance method described in Chapter 3, capacity expansion modelling in REMix-CEM is based on high temporal resolution (typically hourly) using chronological time-series for system loads and RE resource availability for representative periods of the year (e.g. one representative week per season or one representative day per month). The utilized periods have the aim to represent seasonal and diurnal load and RE resource variability over the year as accurately as possible. According to Haydt et al. this approach is referred to as semi-dynamic balance method [97]. Taking into account all days of a year (dynamic balance method) would result in the highest accuracy in terms of considering temporal load and RE resource variability over the year. However, this would increase computational effort for long-term capacity expansion optimization extremely. Hence, the semi-dynamic balance method represents a compromise between capturing in some extent the short-term dynamics of demand and supply of the power system and being in the same time less data intensive and computationally demanding. Applying the semi-dynamic balance method enables REMix-CEM to consider the value of energy at its time of the delivery during least-cost capacity expansion optimization from a central planning perspective. This is crucial for capacity expansion planning with VRE because the competiveness of a technology from a system perspective is not only determined by its generation costs over the planning time frame but also by its value for the system (e.g. capability to produce electricity during high demand and contributing to system adequacy and a reliable system operation).

REMix-CEM has a flexible inter- and intra-annual temporal resolution (see Figure 14). The applied temporal resolution determines the number of dispatch periods that are considered over the planning time frame.[7] As the number of dispatch periods influences computational

[7] Time slices is another expression for dispatch periods often used in the literature

efforts directly, a trade off exists in terms of accuracy and manageability of the model. The multi-annual planning time frame can be separated into several periods with user-defined durations (inter-annual dimension). For each period only one so-called milestone year is modelled, assuming system costs and operational behavior are constant over the period represented by the milestone year. In addition, a year can be represented by several dispatch periods for which values for system load and RE resource availability are assigned. Three intra-annual dimensions are available to represent seasonal and diurnal load and RE resource variability over the year. For example, a year can be split into several seasons (intra-annual dimension 1), each represented by a representative day or week (intra-annual dimension 2), which in turn can be described by a defined number of chronological dispatch periods (intra-annual dimension 3). In the optimization model, only the representative dispatch periods are used to model the operation of the system. However, each dispatch period is multiplied with a weighting factor to ensure that the time period of the year which is represented by the representative dispatch period is considered correctly. To reduce computational effort, the intra-annual dimensions 1 and 2 are typically not linked chronologically. However, this approach limits the possibility to model seasonal storage technologies.

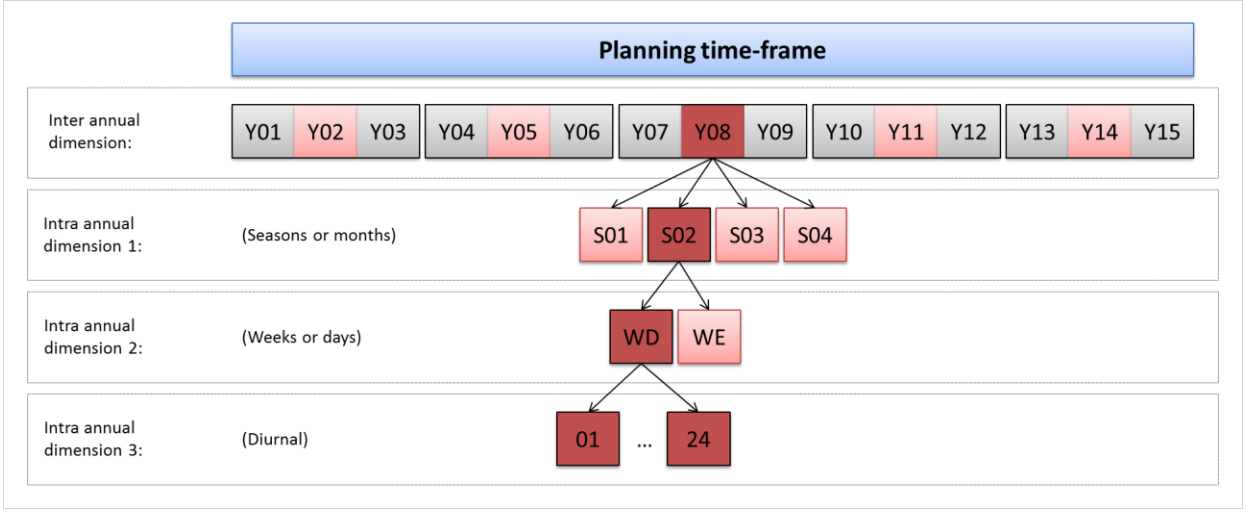

Figure 14: Exemplary dispatch period tree of REMix-CEM. Inter- and intra-annual temporal resolution can be determined flexibly. The example shows a 15 year planning time frame represented by five milestone years (Y), four seasons (S), one working and one weekend day (WD, WE), each described by 24 diurnal dispatch periods.

In addition to the value of energy at its time of the delivery, the semi-dynamic balance method enables REMix-CEM to consider the flexibility effect caused by a large-scale deployment of VRE

within capacity expansion optimization. The utilization of chronological dispatch periods allows for considering inter-temporal operational constraints of thermal generators (UCCs) which describe the flexibility characteristics of a generator. Only when considering these UCCs the flexibility effect can be captured within capacity expansion optimization. However, considering UCCs of thermal generators within capacity expansion optimization comes at high computational costs because a large number of integer variables are required to describe the commitment status of each unit in each considered dispatch period of the planning time frame. Therefore, REMix-CEM has a flexible formulation that allows a flexible application of UCCs where single constraints, such as start-up costs, minimum generation level, or minimum offline times, can be included individually. Furthermore, a linear relaxation for integer variables that describe the unit commitment status of a generator can be applied. With this flexibility, the user can identify the optimal trade-off between computational effort and accuracy of the model in capturing the flexibility effect.

Due to its flexible formulation, the developed optimization model can be applied not only as CEM but also as detailed PCM. The possible forms of application are highlighted in Figure 15. One option is to execute long-term capacity expansion optimization in a first step (REMix-CEM) and a detailed annual production cost modelling (REMix-PCM) for the proposed asset fleet of the CEM in a subsequent second step (soft-link). Typically, the CEM uses the semi-dynamic balance method to keep computational effort of the CEM manageable. Furthermore, also to reduce computing time, operational details of thermal generators are often simplified (e.g. considering not the full set of UCCs of thermal generators). Results of the CEM are the least-cost capacity expansion plan (asset fleet) and a first indication for the operation of the proposed system over the planning time frame. Applying the optimization model subsequently as a detailed PCM provides further insights into the operation of the proposed asset fleet and validates how reduced temporal resolution and simplified operational details bias results for the operation of the system assumed in the CEM. The subsequent PCM optimizes the annual operation of the proposed asset fleet with at least hourly resolution (dynamic balance method) for a certain year of the planning time frame (e.g. the final year) taking into account the full set of UCCs of thermal generators.

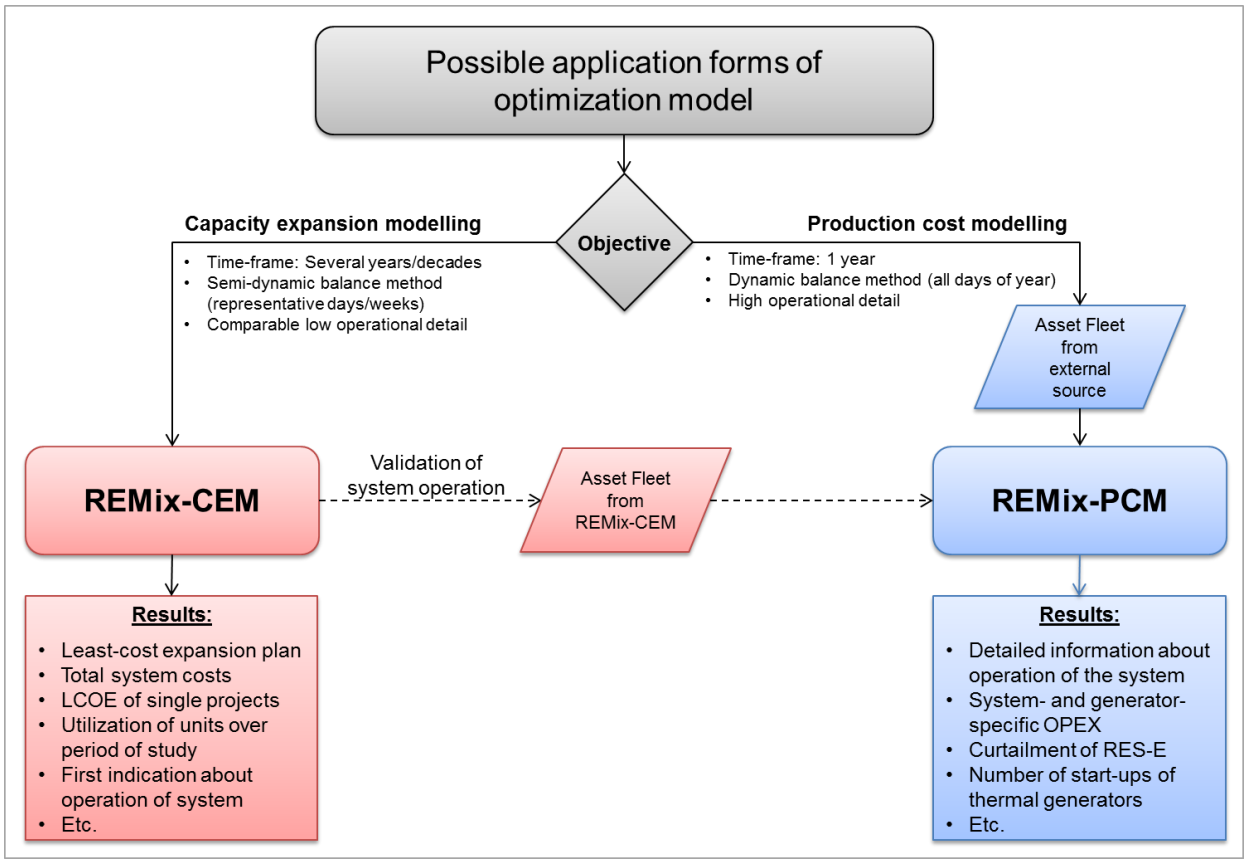

Figure 15: Possible forms of application of the developed optimization model

Another form of application is using the optimization model solely as PCM to perform production cost modelling for an asset fleet derived from an external source to provide further insights about the operation of the power system or to analyze the role of a certain technology for the operation of the system in detail. Examples for this form of model application are given e.g. in Soria et al. [64], where the model is used to validate results of capacity expansion optimization for the Brazilian power sector derived from the energy system models TIMES and MESSAGE, or in Cebulla and Fichter [65], where the model is applied to highlight the need of a detailed modelling approach for conventional thermal generators to assess electricity storage requirements for power systems with high shares of VRE. In Moser et al. the model is used to optimize the dispatch of dry-cooled CSP generators for different operation strategies [66].

Table 9 summarizes the characteristics of the developed power system optimization model, which aims to bridge the gap between traditional long-term CEMs and short-term PCMs for a concerted capacity expansion planning with VRE.

Table 9: Characteristics and features of the optimization model REMix-CEM

	REMix-CEM
Model type	Bottom-up optimization model
Methodology	Deterministic mixed integer linear programming (MILP)
Scope	Co-optimization for capacity expansion of generation, storage and transmission assets
Objective	Minimization of net present value of total system costs
Perspective	Central system planning authority
Sectoral scope	Power sector
Planning time frame	Flexible, typically 10 - 40 years
Spatial resolution	Flexible, typically national with multiple sub-regions
Temporal resolution	Flexible, typically hourly for representative days (semi-dynamic balance method)
Model foresight	Flexible, perfect foresight, rolling horizon foresight, or myopic foresight
Operational details for thermal units	Flexible application. Single constraints can be included individually. Constraints comprises: Start-up and shut down costs, minimum generation level, minimum online and offline times, online ramping costs, part-load efficiency
Reliability constraints	Long-term planning (adequacy reserve) and short-term operating reserve capacity (spinning and standing reserve) can be considered
Environmental aspects	Consideration of CO_2, SO_2, NOx, and PM2.5 emissions and water consumption of thermal generators
Additional feature	Can be applied solely as detailed production cost model (REMix-PCM)

4.2 Mathematical formulation of the major enhancements of the REMix energy system modelling framework

The following section provides the mathematical formulation of the major enhancements of the REMix energy system modelling framework within this work (see section 2.2), i.e. the conversion from a scenario validation tool to a dynamic, long-term capacity expansion optimization model that allows path-optimization over the planning time frame, an increased modelling detail for conventional thermal power plants in order to consider flexibility constraints of generators, a detailed consideration of system reliability constraints in order to ensure a reliable system design, and an enhanced modelling approach for CSP in order to assess the potential role of this DRE technology in countries with high solar resource potentials.

These enhancements led to the development of the capacity expansion optimization model REMix-CEM. In the following, only the mathematical formulation of the modules System Planner & Operator, Conventional Thermal Generators, and Concentrating Solar Power of REMix-CEM are described as these modules compromise the major enhancements within this work.

However, all other modules of the original REMix-OptiMo version developed by Scholz [70] have been enhanced to be used for long-term capacity expansion optimization. This comprises additional equations necessary to perform capacity expansion optimization over a multi-annual planning time frame under different foresight approaches and equations to consider system adequacy and operating reserve allocations. For a detailed description of the principle and the basic mathematical formulation of modules that are not described in this work, please refer to [67–70].

4.2.1 Module System Planner & Operator

The module System Planner & Operator contains the objective function of the optimization problem and all restrictions on system level that are required to ensure a reliable system design over the planning time frame. Furthermore, the module contains so-called user-constraints, which can be applied to perform least-cost capacity expansion optimization under defined targets and boundary conditions for the investigated power system (e.g. RES-E quotas or CO_2 emission limits). The user-constraints act as guide rails for the optimization model and restrict the solution space for the least-cost capacity expansion plan to meet the electricity demand over the planning time frame.

A power system represented in REMix-CEM can be composed of multiple balancing regions (R). Each balancing region comprises at least one model node (N) with a time-dependent load that might vary over the planning time frame. Power demand at each model node can be covered by existing and candidate supply side assets sited at the model node or by power transmission from other nodes of the system via existing and candidate transmission lines. At each balancing region enough firm generation and operating reserve capacity must be hold available to ensure generation adequacy from a long-term planning perspective and a reliable system operation from a short-term operation perspective. An illustrative example of a power system composed of multiple balancing regions, nodes, as well as existing and candidate generation and transmission assets is shown in Figure 16.

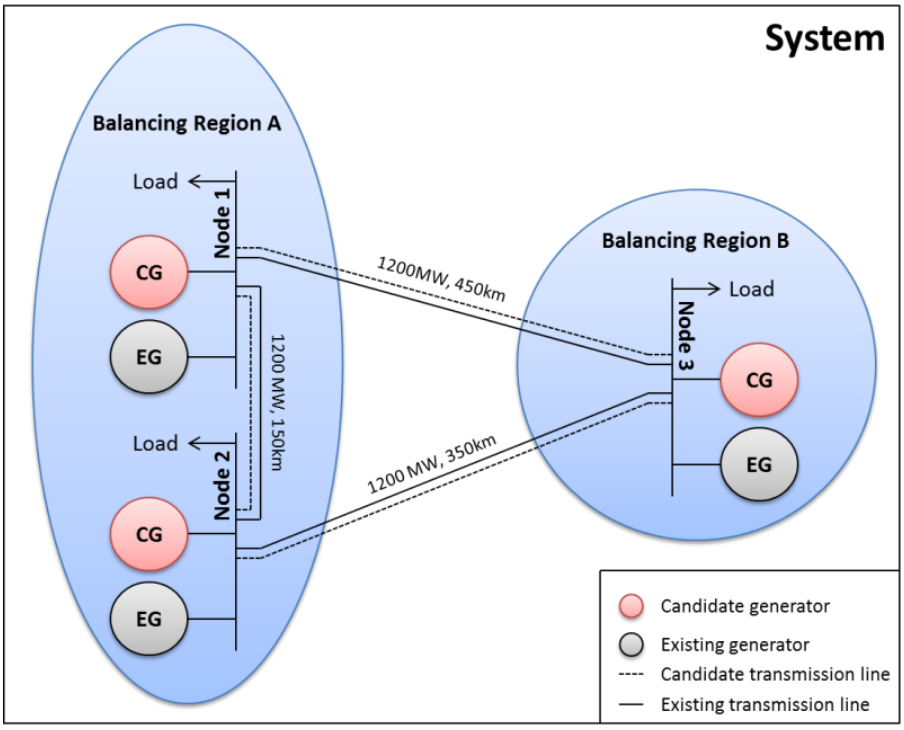

Figure 16: Illustrative example of a power system represented in REMix-CEM

Objective function

The objective function of the optimization problem is presented in equation (1). The model seeks to minimize the net present value of total system costs [NPV^{System}] by discounting annual capital and operational expenditures of all existing and candidate generation, storage, and transmission projects [p] over the planning time frame [$CAPEX_{p,y}$, $OPEX_{p,y}$]. The planning time frame is represented by a set of milestone years [y]. Annual CAPEX and OPEX are multiplied by the duration of each period represented by the respective milestone year [d_y^{MY}], and discounted to the base year of the analysis by a discount factor [df_y]. Additionally, the objective function contains a cost component that deals with end effects. End effects are treated within REMix-CEM by assuming that results of the final year of the planning time frame [LPY] are repeated an infinite number of times. The perpetuity calculated in equation (2) is applied for all CAPEX and OPEX of the final year of the planning time frame.

$$NPV^{System} = \sum_{y} \sum_{p} df_y \cdot d_y^{MY} \cdot \left(CAPEX_{p,y} + OPEX_{p,y}\right) + END\ EFFECT \implies Minimize! \quad (1)$$

$$END\ EFFECT = \frac{df_{LPY} \cdot \left(CAPEX_{p,LPY} + OPEX_{p,LPY}\right)}{discount\_rate} \quad (2)$$

Annual capital expenditures

Annual CAPEX of each candidate project are computed in equation (3). Total overnight investment costs are multiplied with a factor for interests during construction and transformed into equal annual annuities using an annuity factor. The factor for interests during construction is calculated according to equation (4). Equation (5) determines the annuity factor based on the project specific weighted average cost of capital (WACC) and the economic lifetime of the project.

$$CAPEX_{p,y} = C_{p,y}^{Invest} \cdot \left(1 + idc_p\right) \cdot af_p \qquad \forall p \in CP \qquad (3)$$

$$idc_p = \frac{wacc_p \cdot ct_p}{2} \qquad \forall g \in CP \qquad (4)$$

$$af_p = \frac{(1 + wacc_p)^{Ec.life_p} \cdot wacc_p}{(1 + wacc_p)^{Ec.life_p} - 1} \qquad \forall p \in CP \qquad (5)$$

Supply and demand balance

The supply and demand balance for each model node of the power system is given in equation (6). In each dispatch period of the planning time frame, power generation of the node's generation fleet plus imports from other nodes must be equal to the load, electricity consumption from storage facilities and CSP generators, and exports to other nodes of the system. CSP generators can use electricity from the grid to cover auxiliaries required to operate the solar field and the thermal energy storage. Power generation and grid consumption of assets is reduced by an availability factor [a_g] that depends on the unit specific forced and maintenance outage rate [for_g, mor_g]. The power transmission network is modeled as generic transportation model with maximum transfer capacities and defined network losses between model nodes [70].

$$\sum_{g \in N} P_{g,y,s,d,t}^{Net} \cdot a_g + IMPORT_{n,y,s,d,t} = load_{n,y,s,d,t} + EXPORT_{n,y,s,d,t} + \left[\sum_{\substack{g \in STO \\ g \in N}} P_{g,y,sd,,t}^{Charge} + \sum_{\substack{g \in CSP \\ g \in N}} P_{g,y,s,d,t}^{Grid,Aux} \right] \cdot a_g \qquad \begin{matrix} \forall n, \forall y, \\ \forall s, \forall d, \forall t \end{matrix} \qquad (6)$$

$$\text{with } a_g = 100\% - for_g - mor_g$$

Generation adequacy reserve (long-term planning reserve)

Generation adequacy can be defined as a measure for the ability of the available domestic generation capacity to satisfy the load of a system in all steady states that may exist. Reasonable amounts of unavailable capacities due to operating reserve requirements, overhauls, forced and planned outages, and non-usable capacities due to a lack of primary energy resources of RES-E technologies must be considered when assessing the adequacy of the system [71]. To maintain a reliable system design over the planning time frame a dynamic approach to ensure generation adequacy for each balancing region of the system is applied. For each considered dispatch period of the planning time frame equation (7) ensures that in each balancing region of the system the sum of the domestic firm net capacity is equal or greater than the domestic load including a defined reserve margin (rm). The asset-specific firm net capacity is calculated by multiplying the gross capacity with a factor for auxiliary requirements [aux_g], a time-dependent correction factor for the influence of ambient temperature on available capacity [$cf^{p}_{g,s,d,t}$], and a time-dependent capacity credit [$cc_{g,s,d,t}$].[8]

$$load_{r,y,s,d,t} \cdot (1 + rm) \leq \sum_{g \in R} CAP_{g,y} \cdot \left(1 - aux_g\right) \cdot cf^{p}_{g,s,d,t} \cdot cc_{g,s,d,t} \qquad \forall r, \forall y, \forall s, \forall d, \forall t \qquad (7)$$

For conventional thermal, CSP, and reservoir hydro generators as well as for energy storage systems, the time-dependent capacity credit is assumed to be constant for each dispatch period. The capacity credit of conventional thermal generators depends entirely on the technically forced outage rate because it is assumed that there is a very low risk for a lack of primary energy resources (fuel shortages). For CSP generators the capacity credit depends on the capacity of the back-up burner, which is subject for optimization, and the assumed technically forced outage rate for the entire CSP generator. For energy storage systems and reservoir hydro generators the capacity credit depends on the size of the storage reservoir and the technically forced outage rate. The capacity credit of VRE generators varies for each considered intra-annual dispatch period because the capacity credit of VRE generators depends not only on the technically forced outage rate (probability of generator tripping) but also on the

[8] The correction factor $cf^{p}_{g,s,d,t}$ for thermal generators is calculated according to equation (36) (see following section). For all other technologies the correction factor is set to one.

seasonal and diurnal availability of the primary energy resource. The methodology to determine time-dependent capacity credits of VRE generators using the simulation software INSEL[9] is presented and explained in Figure 17.

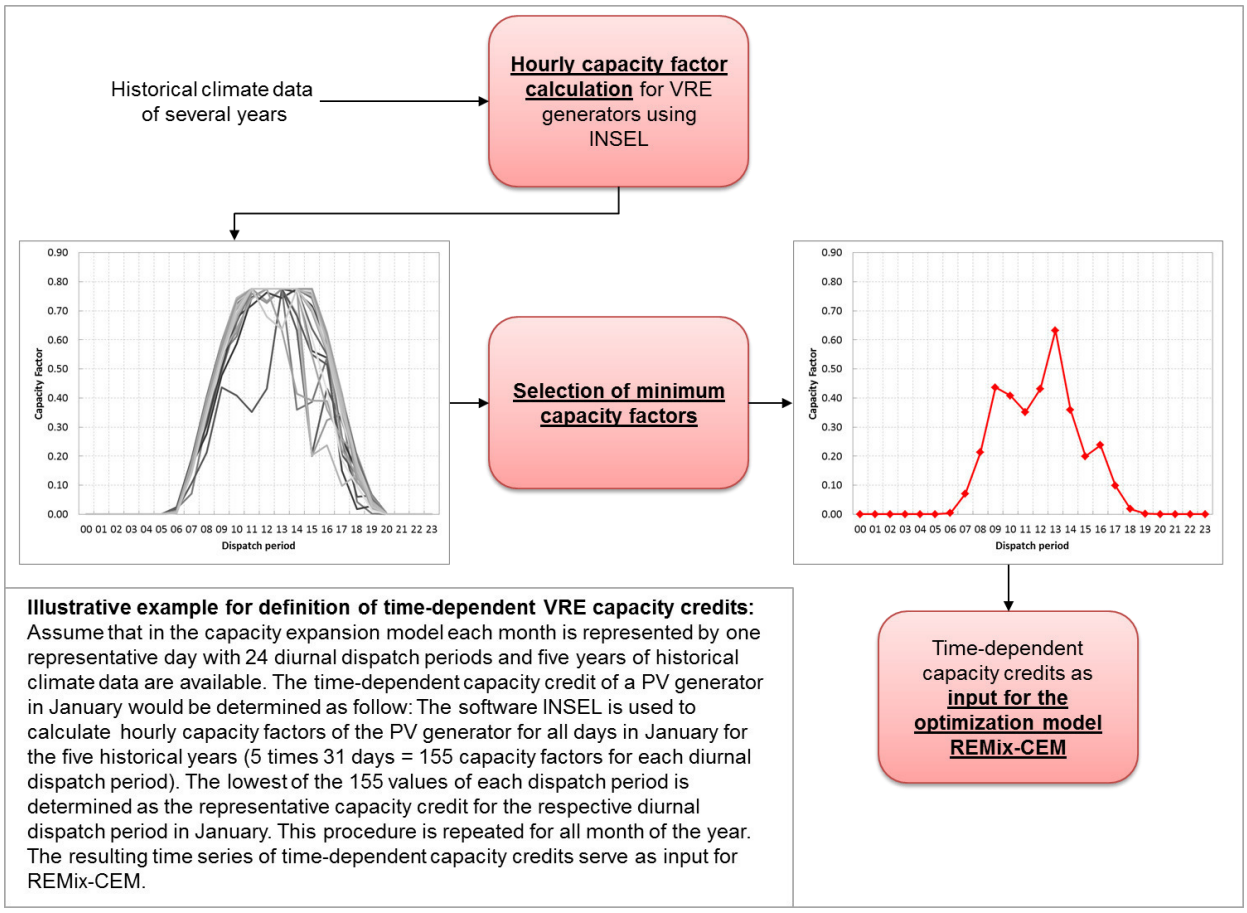

Figure 17: Methodology for determining temporal capacity credits of VRE generators

The dynamic approach for ensuring generation adequacy for each balancing area in combination with the concept of time-dependent capacity credits of VRE generators allows for considering the effect of decreasing contribution of VRE generators that rely on the same primary energy resource to meet critical load periods (diurnal peak loads) with increasing penetration rates. This effect is highlighted in Figure 18. With increasing penetration rates of a VRE technology the critical diurnal load periods shift towards periods of low availability of the VRE technology (diurnal residual peak load periods). Due to the correlated generation patterns

[9] Integrated Simulation Environment Language, www.insel.eu

of VRE generators that rely on the same primary energy resource, there is a high probability that an additionally installed VRE generator will produce electricity just in the same moment as an already existing VRE generator of this technology type. This results in a low contribution of the additionally installed VRE generator to serve the critical residual load periods. This effect can be reduced by a spatial distribution of VRE generators [72–76].

However, also a more conservative and straight forward approach can be applied for the generation adequacy reserve restriction in REMix-CEM by setting the capacity credit of VRE to zero for all intra-annual dispatch periods. In this case, generation adequacy depends entirely on the assumptions for capacity credits of dispatchable generators. A variation of VRE resource availability from year to year would than only influence the utilization of the different assets of the system but not generation adequacy of the system.

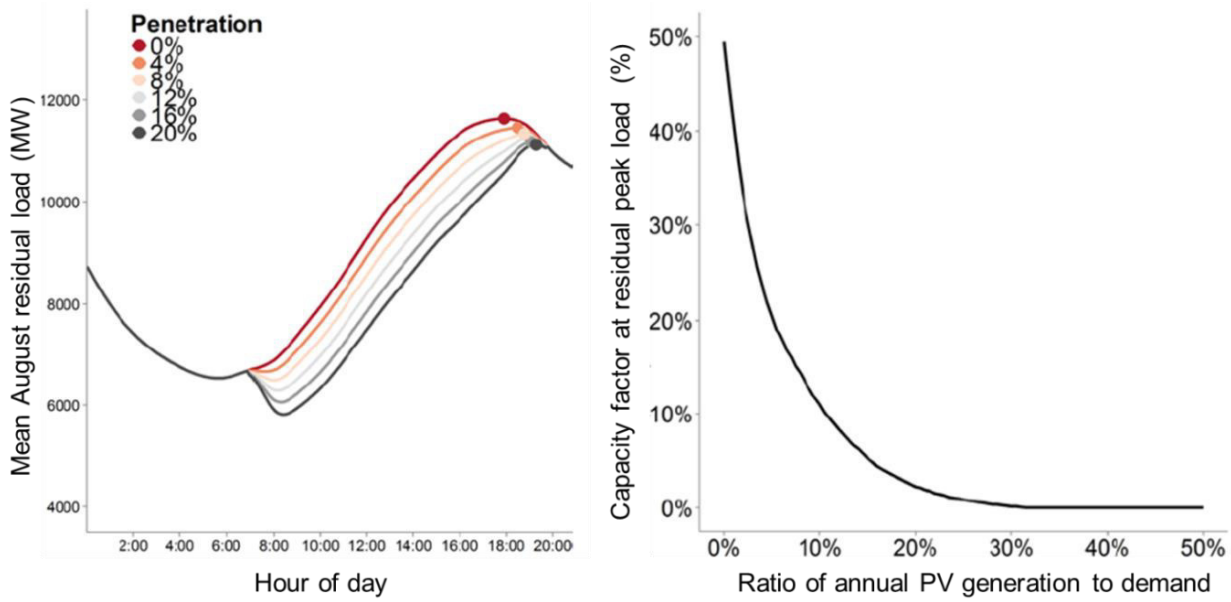

Figure 18: Decreasing contribution of VRE (example PV) to meet residual peak load demand. Left: Mean diurnal residual load curve of a balancing region in Arizona for increasing PV shares. The dot marking the diurnal residual peak load that continuously shifts later into the evening as the PV share increases. Right: Average capacity factor of all PV generators at diurnal residual peak load as a function of PV penetration for a balancing region in Arizona in August [76]**. (Note: Original axis label of figures have been adjusted to the terminology of this work).**

Spinning and standing reserve (short-term operating reserve)

Operating reserve capacity has the aim to ensure a reliable system operation by performing frequency stabilization actions in the case of an imbalance between demand and supply. Imbalances can occur due to unforeseen events (e.g. generator tripping) or forecast errors for expected load and VRE generation. The optimization model contains three types of operating reserve capacities that must be kept available in each considered dispatch period of the planning time frame:

- Positive spinning reserve:
  - Fully activated within 10 min and maintained for 1h
- Negative spinning reserve:
  - Fully activated within 10 min and maintained for 1h
- Positive standing reserve:
  - Fully activated within 60 min and maintained for 24h

Positive and negative spinning reserve capacity is restricted by equation (8) and (9) respectively and can be provided by dispatchable units (generation and storage assets) that operate below (above) their maximum (minimum) generation level. Negative spinning reserve can also be provided by VRE generators through curtailment. The minimum available positive standing reserve capacity is restricted in equation (10). Standing operating reserve can be offered by offline dispatchable generators with fast start-up capabilities. Operating reserve requirements to cover load and VRE generation forecast errors are modeled dynamically to avoid an overestimation of reserve requirements (e.g. during night no reserve capacity is necessary to balance out forecast errors for PV generation).

$$\sum_{\substack{g\in DG\\ g\in R}} OR^{Spin+}_{g,y,s,d,t} \geq orc^{10min+}_{r,y,s,d,t} \qquad \forall r, \forall y, \forall s, \forall d, \forall t \qquad (8)$$

$$\sum_{\substack{g\in DG\\ g\in R}} OR^{Spin-}_{g,y,s,d,t} + \sum_{\substack{g\in VRE\\ g\in R}} P^{Net}_{g,y,s,d,t} \geq orc^{10min-}_{r,y,s,d,t} \qquad \forall r, \forall y, \forall s, \forall d, \forall t \qquad (9)$$

$$\sum_{\substack{g\in FSG\\ g\in R}} OFF_{g,y,s,d,t} \cdot \overline{p}_g \cdot \left(1 - aux_g\right) \geq orc^{60min+}_{r,y,s,d,t} \qquad \forall r, \forall y, \forall s, \forall d, \forall t \qquad (10)$$

User constraints (guide rails)

Several user constraints are available that can be applied flexibly. User-constraints are applied to execute least-cost capacity expansion optimization under defined targets or to narrow down the solution space by introducing guide rails for the optimization model. The introduction of guide rails is especially important when least-cost and a reliable system design is not the only criterion for defining the system expansion plan but other issues such as security of supply, environmental aspects, job creation or steady growth rates for certain industries (e.g. PV industry) are aimed to be considered during capacity expansion optimization. Hence, user-constraints/guide rails are often applied when policy driven least-cost expansion pathways for power systems are aimed to be computed by REMix-CEM. Available user-constraints comprise:

- Maximum annual CO_2 emission of the system by year
- Maximum total CO2 emissions over the planning time-frame
- Minimum share of RES-E generation by year
- Minimum/maximum annual offtake of a specific fuel
- Minimum/maximum annual capacity addition by technology
- Minimum/maximum total capacity expansion over planning time frame by technology
- Minimum annual utilization for certain types of generators

4.2.2 Module Conventional Thermal Generators

The module Conventional Thermal Generators comprises all generators fired by fossil- and bio-fuels. The accuracy of the modelling approach for conventional thermal generators applied in the module was validated with the thermal cycle simulation software KPRO[10] during the THERMVOLT project. Maximum deviations for variables describing the performance of conventional thermal generators at defined load levels were below 0.3% [132]. The module for conventional thermal generators is formulated in that way that the level of modelling detail can be defined flexibly. More precisely, this means that single UCCs, which describe the flexibility characteristics of conventional thermal generators, such as start-up and shut-down costs, minimum online and offline times, part-load efficiencies, minimum generation levels, maximum

[10] KPRO software, www.kpro-fichtner.de

ramping and load following costs, can be applied individually. Furthermore, a linear relaxation for the unit commitment decision variables can be applied. In the case UCCs are not applied at all, units are dispatched according to their position in the merit-order. The merit-order dispatch is determined by the short run marginal costs (SRMC) of the various existing and candidate generators.

One approach to model UCCs is to use binary variables to describe the commitment status (on/off) for each unit in each dispatch period of the planning time frame. However, due to the large number of required binary variables this approach comes at very high computational cost. One strategy to reduce the number of binary variables is the application of a so-called unit clustering approach, as proposed e.g. by Palmintier and Webster [77]. Figure 19 shows the principle concept of the clustering approach. Units with similar techno-economic characteristics are grouped together and modeled as one generator with multiple units (generator = cluster). In the unit clustering approach, investment and unit commitment decisions at each generator are represented by integer variables instead of using binary variables for each single unit. This leads to a large space reduction for the optimization problem, which in turn reduces computational efforts significantly.

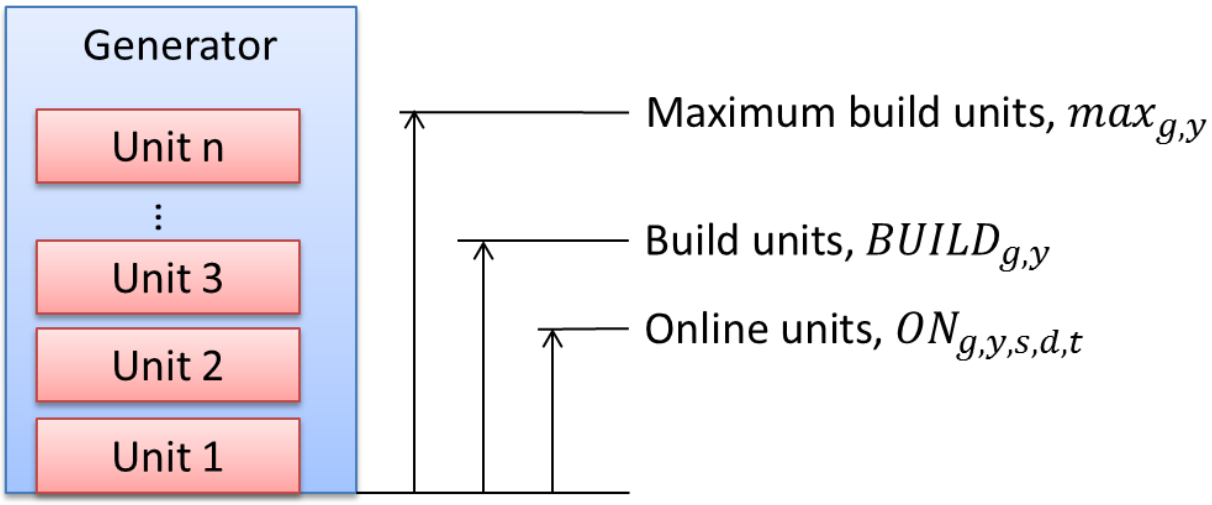

Figure 19: Clustering approach for capacity expansion optimization with unit commitment constraints of thermal generators

Maximum number of units and cumulative installed capacity at generator

The maximum number of units that can be built at each candidate generator over the planning time frame is restricted by equation (11). The cumulative number of built units at each generator over the period of study is calculated in equation (12). Resulting gross capacity is determined in equation (13). For already existing generators equation (11) is reformulated to a strict equality and $[\max_{g,y}]$ represents the number of existing units at the generator.

$$\sum_{y} BUILD_{g,y} \leq \bar{u}_{g,y} \qquad \forall g \in CTG, with\ BUILD_{g,y} = 0\ if\ fy_g > y \qquad (11)$$

$$BUILD_{g,y}^{Cum} = BUILD_{g,y-1}^{Cum} + BUILD_{g,y} \qquad \forall g \in CTG, \forall y, with\ BUILD_{g,y}^{Cum} = 0\ if\ ly_g < y \qquad (12)$$

$$CAP_{g,y} = BUILD_{g,y}^{Cum} \cdot \overline{p}_g \qquad \forall g \in CTG, \forall y \qquad (13)$$

Maximum online units at generator

The maximum number of units that can be online at each generator is restricted by equation (14). The number of online units in each dispatch period of the planning time frame must be smaller than the cumulative number of installed units at the generator in the respective year. Equation (15) determines the number of units that are offline and thus can offer standing reserve capacity in the case they have fast start-up capabilities.

$$ON_{g,y,s,d,t} \leq BUILD_{g,y}^{Cum} \qquad \forall g \in CTG, \forall y, \forall s, \forall d, \forall t \qquad (14)$$

$$OFF_{g,y,s,d,t} = BUILD_{g,y}^{Cum} - ON_{g,y,s,d,t} \qquad \forall g \in CTG, \forall y, \forall s, \forall d, \forall t \qquad (15)$$

Minimum online and offline times

Restrictions for minimum on- and offline times are formulated aligned to [78] but adjusted to the unit clustering approach as given in equation (16) and (17) respectively. In addition, equation (18) ensures the logical condition for the online, start-up, and shut-down status of each unit of the generator. Equation (19) ensures that the commitment status of each generator in the first and the last dispatch period [*FT*, *LT*] of the second intra-annual dimension (representative week or day) are equal to avoid biased results for generator start-ups.

$$\sum_{k=t-mut_g+1}^{t} SU_{g,y,s,d,k} \leq ON_{g,y,s,d,t} \qquad \forall g \in CTG, \forall y, \forall s, \forall d, t \in [mut_g, T] \tag{16}$$

$$\sum_{k=t-mdt_g+1}^{t} SD_{g,y,s,d,k} \leq BUILD_{g,y}^{Cum} - ON_{g,y,s,d,t} \qquad \forall g \in CTG, \forall y, \forall s, \forall d, t \in [mdt_g, T] \tag{17}$$

$$ON_{g,y,s,d,t} - ON_{g,y,s,d,t-1} = SU_{g,y,s,d,t} - SD_{g,y,s,d,t} \qquad \forall g \in CTG, \forall y, \forall s, \forall d, \forall t \tag{18}$$

$$ON_{g,y,s,d,FT} = ON_{g,y,s,d,LT} \qquad \forall g \in CTG, \forall y, \forall s \tag{19}$$

Generation limits

Equations (20) – (23) restrict the generation limits and the available spare capacity of each generator. The formulation of these constraints is aligned to [79] and [82] but also adjusted for the unit clustering approach. The total generation of a single unit of a generator is modelled in two blocks: the minimum electricity generation [$\underline{p}_g$] that is generated by the unit just by being committed, and the electricity generation above this minimum [$P_{g,y,s,d,t}$]. The minimum generation and the available negative spare capacity are restricted by equation (20). For units with a minimum up and down time of one dispatch period (e.g. 1h), the upper generation limits over the power output and the positive spare capacity are restricted by equation (21) and (22). Note that power generation above the minimum level and the available positive spare capacity are restricted also by unit start-up and shut-down capabilities. A tighter and more compact formulation for units with a minimum online time of at least two dispatch periods is given in equation (23), which replaces both constraints formulated in equation (21) and (22).

$$0 \leq P_{g,y,s,d,t} - OR_{g,y,s,d,t}^{Spare-} \qquad \forall g \in CTG, \forall y, \forall s, \forall d, \forall t \tag{20}$$

$$P_{g,y,s,d,t} + OR_{g,y,s,d,t}^{Spare+} \leq \left(\overline{p}_g - \underline{p}_g\right) \cdot ON_{g,y,s,d,t} - \left(\overline{p}_g - p_g^{SU}\right) \cdot SU_{g,y,s,d,t} \qquad \forall g \in CTG, \forall CTG \in mut_g = 1, \forall y, \forall s, \forall d, \forall t \tag{21}$$

$$P_{g,y,s,d,t} + OR_{g,y,s,d,t}^{Spare+} \leq \left(\overline{p}_g - \underline{p}_g\right) \cdot ON_{g,y,s,d,t} - \left(\overline{p}_g - p_g^{SD}\right) \cdot SD_{g,y,s,d,t+1} \qquad \forall g \in CTG, \forall CTG \in mdt_g = 1, \forall y, \forall s, \forall d, \forall t \tag{22}$$

$$P_{g,y,s,d,t} + OR^{Spare+}_{g,y,s,d,t} \leq \left(\overline{p}_g - \underline{p}_g\right) \cdot ON_{g,y,s,d,t} - \left(\overline{p}_g - p^{SU}_g\right) \cdot SU_{g,y,s,d,t} - \left(\overline{p}_g - p^{SD}_g\right) \cdot SD_{g,y,s,d,t+1} \quad \forall g \in CTG, \forall CTG \in mut_g \neq 1, \forall y, \forall s, \forall d, \forall t \quad (23)$$

Ramping limits

Equation (24) - (26) restrict the maximum upwards- and downwards-ramping of each unit at the generator per dispatch period as proposed by [80]. The maximum upwards ramping for units with a minimum online time of maximum one dispatch period is constraints by equation (24). Equation (25) does the same for downwards ramping. A tighter formulation of the upwards ramping restriction for units with a minimum online time of two or more dispatch periods is given in equation (26), which is aligned to the formulation given in [81].

$$P_{g,y,s,d,t} + OR^{Spare+}_{g,y,s,d,t} - P_{g,y,s,d,t-1} \leq \bar{r}_g \cdot ON_{g,y,s,d,t-1} + \left(p^{SU}_g - \underline{p}_g\right) \cdot SU_{g,y,s,d,t} \quad \forall g \in CTG, \forall y, \forall s, \forall d, \forall t \quad (24)$$

$$P_{g,y,s,d,t-1} - OR^{Spare-}_{g,y,s,d,t} - P_{g,y,s,t} \leq \bar{r}_g \cdot ON_{g,y,s,d,t} + \left(p^{SD}_g - \underline{p}_g\right) \cdot SD_{g,y,s,d,t} \quad \forall g \in CTG, \forall y, \forall s, \forall d, \forall t \quad (25)$$

$$P_{g,y,s,d,t} + OR^{Spare+}_{g,y,s,d,t} - P_{g,y,s,d,t-1} \leq \bar{r}_g \cdot ON_{g,y,s,d,t} - \left(\bar{r}_g - p^{SD}_g + \underline{p}_g\right) \cdot SD_{g,y,s,d,t+1} + \left(p^{SU}_g - \underline{p}_g - \bar{r}_g\right) \cdot SU_{g,y,s,d,t} \quad \forall g \in \forall CTG, \forall CTG \in mdt_g \geq 2 \;\&\; \bar{r}_g > p^{SD}_g - \underline{p}_g, \forall y, \forall s, \forall d, \forall t \quad (26)$$

Positive and negative spinning reserve capacity

Positive and negative spinning reserve capacity that can be offered by a conventional thermal generator within 10 minutes is restricted in equation (27) - (30) respectively. Equation (27) constraints the maximum spinning reserve that can be theoretically provided by each unit of the generator. When units operate very close to their upper generation level, the actual spare capacity might be smaller than the maximum possible spinning reserve capacity that can be provided within ten minutes. Equation (28) ensures that the maximum spinning reserve capacity offered by the generator is smaller or equal than its actual spare capacity. Equation (29) and (30) do the same for negative spinning reserve capacity.

$$OR^{Spin+}_{g,y,s,d,t} \leq ON_{g,y,s,d,t} \cdot \overline{p}_g \cdot r^{Max}_g \cdot 10 \quad \forall g \in CTG, \forall y, \forall s, \forall d, \forall t \quad (27)$$

$$OR^{Spin+}_{g,y,s,d,t} \leq OR^{Spare+}_{g,y,s,d,t} \qquad \forall g \in CTG, \forall y, \forall s, \forall d, \forall t \qquad (28)$$

$$OR^{Spin-}_{g,y,s,d,t} \leq ON_{g,y,s,d,t} \cdot \overline{p}_g \cdot r_g^{Max} \cdot 10 \qquad \forall g \in CTG, \forall y, \forall s, \forall d, \forall t \qquad (29)$$

$$OR^{Spin-}_{g,y,s,d,t} \leq OR^{Spare-}_{g,y,s,d,t} \qquad \forall g \in CTG, \forall y, \forall s, \forall d, \forall t \qquad (30)$$

Part-load efficiency and influence of ambient temperature

REMix-CEM is a MILP optimization model. Hence, nonlinear functions cannot be represented directly. For considering non-linear part-load efficiency of thermal generators, a piecewise linear fuel consumption approach can be applied as proposed e.g. in [82]. The approach is adapted to the unit clustering approach. Figure 20 presents the principle of the piecewise linear fuel consumption approach.

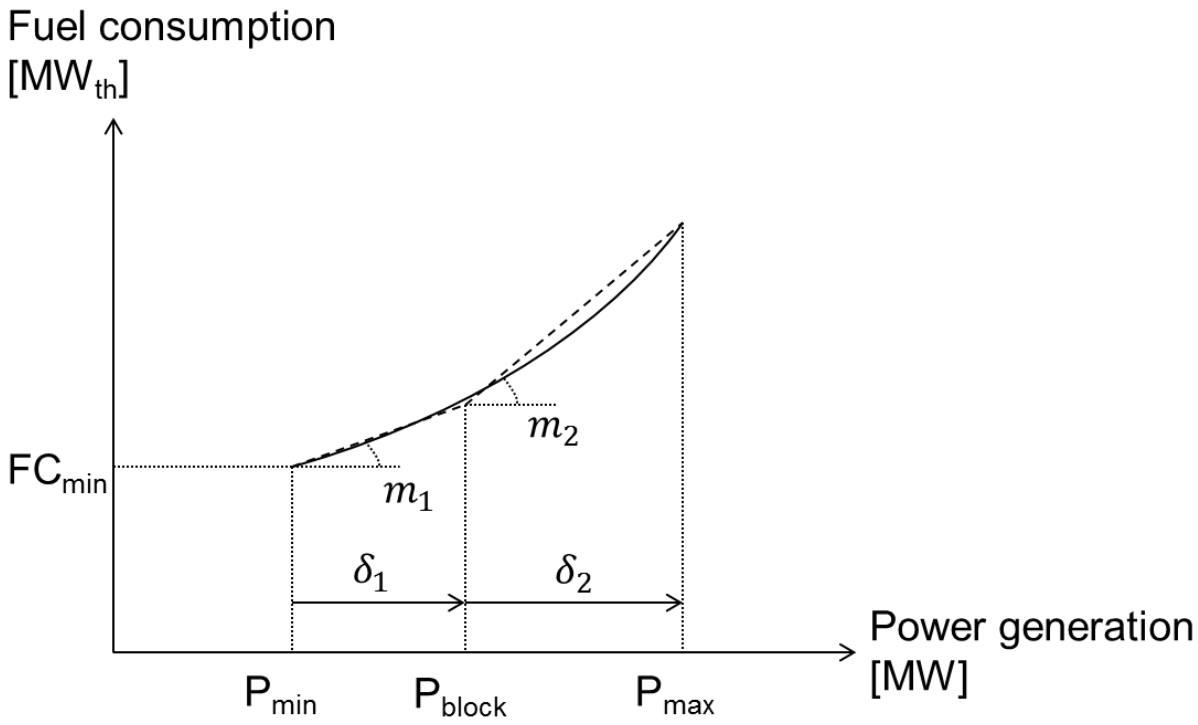

Figure 20: Piecewise linear fuel consumption approach:
Piecewise linear approximation of a convex fuel consumption curve with two blocks

The possible generation range of a single unit is subdivided into a user-defined number of generation blocks (here two). Equation (31) limits the maximum power generation within each defined generation block. Total power generation above the minimum generation level is calculated in equation (32) by adding up generation within the individual blocks. Total fuel

consumption of the generator is calculated in equation (33) by summing up fuel consumption at minimum load and fuel consumption within the individual generation blocks. Fuel consumption in each generation block is calculated by multiplying the block-specific slope $[m_{g,b}]$ of the piecewise linear fuel consumption curve with the power generation within the respective generation block $[\delta_{g,b,y,s,d,t}]$.[11]

$$\delta_{g,b,y,s,d,t} \leq ON_{g,y,s,d,t} \cdot \Delta_{g,b} \qquad \forall g \in CTG, \forall b, \forall y, \forall s, \forall d, \forall t \qquad (31)$$

$$P_{g,y,s,d,t} = \sum_{b} \delta_{g,b,y,s,d,t} \qquad \forall g \in CTG, \forall y, \forall s, \forall d, \forall t \qquad (32)$$

$$FC_{g,y,s,d,t} = \left[\frac{ON_{g,y,s,d,t} \cdot \underline{p}_g}{\underline{\eta}_g} + \sum_{b} m_{g,b} \cdot \delta_{g,b,y,s,d,t} \right] \cdot \frac{1}{cf^{\eta}_{g,s,d,t}} \qquad \forall g \in CTG, \forall y, \forall s, \forall d, \forall t \qquad (33)$$

$$cf^{\eta}_{g,s,t} = \begin{cases} \left(tc_g^{\eta,01} \cdot at_{g,s,d,t} + tc_g^{\eta,02}\right), & at_{g,s,d,t} \leq 5°C \\ \left(tc_g^{\eta,03} \cdot at_{g,s,d,t} + tc_g^{\eta,04}\right), & 5°C < at_{g,s,d,t} \leq 15°C \\ \left(tc_g^{\eta,05} \cdot at_{g,s,d,t} + tc_g^{\eta,06}\right), & 15°C < at_{g,s,d,t} \leq 25°C \\ \left(tc_g^{\eta,07} \cdot at_{g,s,d,t} + tc_g^{\eta,08}\right), & 25°C < at_{g,s,d,t} \leq 35°C \\ \left(tc_g^{\eta,09} \cdot at_{g,s,d,t} + tc_g^{\eta,10}\right), & at_{g,s,d,t} > 35°C \end{cases} \qquad \forall g \in CTG, \forall y, \forall s, \forall d, \forall t \qquad (34)$$

The ambient temperature can have a significant, nonlinear impact on the efficiency of thermal generators. This is especially the case for open-cycle and combined-cycle gas turbines but also for air-cooled steam power plants [83–85]. Therefore, fuel consumption calculated in equation (33) is adjusted by a time-dependent correction factor for the influence of the ambient temperature on generator efficiency. This correction factor is calculated in equation (34). Similar to the approach to approximate non-linear part-load performance, a piecewise linear approach is applied to approximate the non-linear influence of the ambient temperature on generator efficiency. Figure 21 (left-hand side) shows exemplarily the nonlinear development of the efficiency of an combined-cycle gas turbine power plant as function of ambient temperature calculated by the thermal cycle simulation software KPRO [132]. The piecewise linear approximation used in REMix-CEM is presented in Figure 21 (right-hand side). The ambient

[11] For convex fuel consumption curves, the linearization as described in equations (31) - (33) ensures a correct order of use of the different blocks of the piecewise linear fuel consumption curve. For concave fuel consumption curves an additional binary/integer variable has to be used to enforce a correct order of use.

temperature range is subdivided into five blocks. The correction factor for each temperature range is calculated by a linear function.

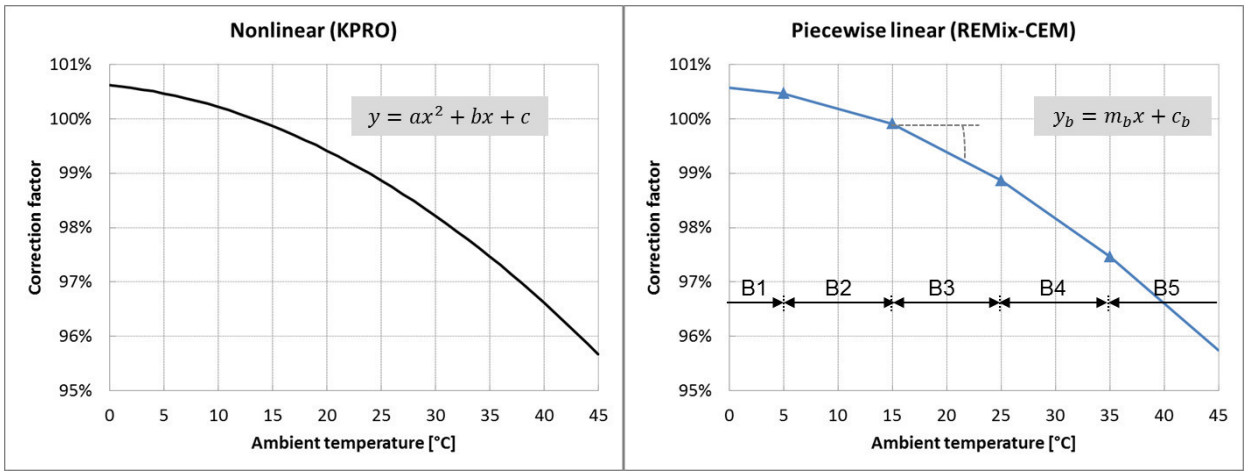

Figure 21: Correction factor for the efficiency of a combined-cycle gas turbine as function of ambient temperature. Left-hand side: Nonlinear function as modeled by KPRO. Right-hand side: Piecewise linear approximation by REMix-CEM

Net power generation and influence of ambient temperature

The ambient temperature has not only a non-linear impact on generator efficiency but also on the available net capacity [83–85]. Hence, when calculating net power generation of conventional thermal generators in equation (35), gross power generation is not only reduced by the share for auxiliary power but also adjusted by a time-dependent correction factor for the impact of the ambient temperature. To approximate the non-linear impact of the ambient temperature, again a piecewise linear approach is applied (see Figure 22). The ambient correction factor is calculated in equation (36).

$$P^{Net}_{g,y,s,d,t} = \left(ON_{g,y,s,d,t} \cdot \underline{p}_g + P_{g,y,s,d,t}\right) \cdot \left(1 - aux_g\right) \cdot cf^{p}_{g,s,d,t} \qquad \forall g \in CTG, \forall y, \forall s, \forall d, \forall t \quad (35)$$

$$cf^{p}_{g,s,d,t} = \begin{cases} \left(tc^{p,01}_g \cdot at_{g,s,d,t} + tc^{p,02}_g\right), & at_{g,s,d,t} \leq 5°C \\ \left(tc^{p,03}_g \cdot at_{g,s,d,t} + tc^{p,04}_g\right), & 5°C < at_{g,s,d,t} \leq 15°C \\ \left(tc^{p,05}_g \cdot at_{g,s,d,t} + tc^{p,06}_g\right), & 15°C < at_{g,s,d,t} \leq 25°C \\ \left(tc^{p,07}_g \cdot at_{g,s,d,t} + tc^{p,08}_g\right), & 25°C < at_{g,s,d,t} \leq 35°C \\ \left(tc^{p,09}_g \cdot at_{g,s,d,t} + tc^{p,10}_g\right), & at_{g,s,d,t} > 35°C \end{cases} \qquad \forall g \in CTG, \forall y, \forall s, \forall d, \forall t \quad (36)$$

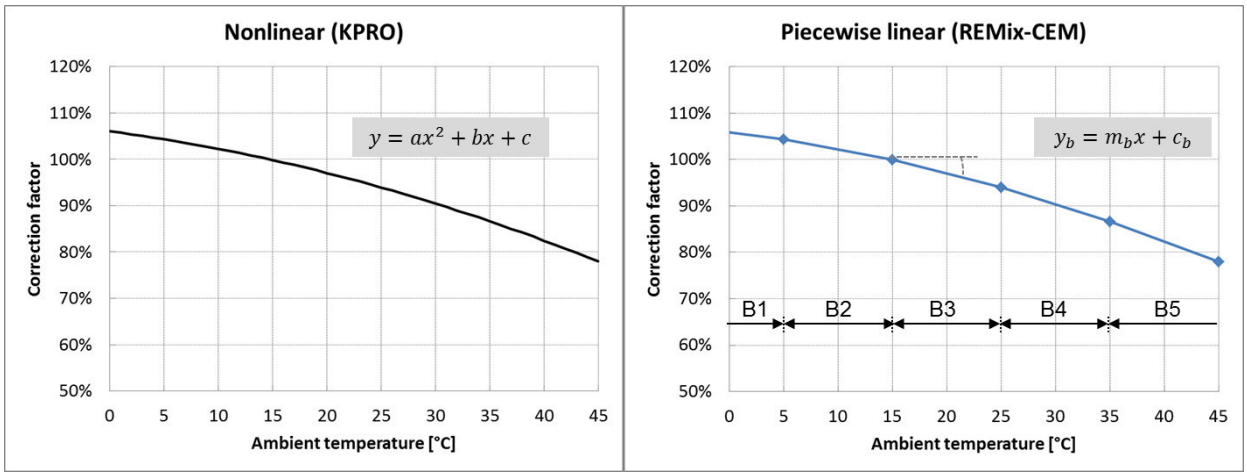

Figure 22: Correction factor for the available capacity of an open-cycle gas turbine as function of ambient temperature. Left-hand side: Nonlinear function as modeled by KPRO. Right-hand side: Piecewise linear approximation utilized in REMix-CEM

Short run marginal costs (SRMC)

SRMC of each conventional thermal generator are calculated in equation (37). Cost components are fuel costs, emission costs and variable operation and maintenance costs.

$$C^{SRMC}_{g,y,s,d,t} = FC_{g,y,s,d,t} \cdot \left(c^{Fuel}_{g,y} + c^{E}_{y} \cdot e_g\right) + \left(ON_{g,y,s,d,t} \cdot \underline{p}_g + P_{g,y,s,d,t}\right) \cdot c^{VOM}_{g} \qquad \forall g \in CTG, \forall y, \forall s, \forall d, \forall t \quad (37)$$

Start-up and shut-down costs

Equation (38) and (39) determine the start-up and shut-down costs for conventional thermal generators respectively. Start-up costs are composed of fuel and emission costs during the start-up procedure and other costs related to a unit start-up, such as additional capital and maintenance expenditures, and costs for chemicals, water, etc. For unit shut-downs, no additional fuel consumption is considered.

$$C^{SU}_{g,y,s,d,t} = SU_{g,y,s,d,t} \cdot \left[fuel^{SU}_{g} \cdot \left(c^{Fuel}_{y} + c^{E}_{y} \cdot e_g\right) + c^{SU}_{g}\right] \qquad \forall g \in CTG, \forall y, \forall s, \forall d, \forall t \quad (38)$$

$$C^{SD}_{g,y,s,d,t} = SD_{g,y,s,d,t} \cdot c^{SD}_{g} \qquad \forall g \in CTG, \forall y, \forall s, \forall d, \forall t \quad (39)$$

Load following costs (ramping costs)

Extensive ramping of thermal generators causes additional wear and tear costs. Load-following costs due to ramping-up and -down the single units of a generator between their minimum and maximum generation level are taken into account by equation (40) and (41) respectively.

$$C^R_{g,y,s,d,t} \geq c^R_g \cdot \left(P_{g,y,s,d,t} - P_{g,y,s,d,t-1} - SU_{g,y,s,d,t} \cdot \overline{p}_g\right) \qquad \forall g \in CTG, \forall y, \forall s, \forall d, \forall t \quad (40)$$

$$C^R_{g,y,s,d,t} \geq c^R_g \cdot \left(P_{g,y,s,d,t-1} - P_{g,y,s,d,t} - SD_{g,y,s,d,t} \cdot \overline{p}_g\right) \qquad \forall g \in CTG, \forall y, \forall s, \forall d, \forall t \quad (41)$$

Overnight investment costs and annual operational expenditures

Overnight investment costs are calculated in equation (42), where cumulative installed gross capacity at the generator is multiplied with the specific investment costs. Total OPEX are calculated by equation (43) and are composed of a variable and fix component. Variable OPEX include SRMC, start-up, shut-down, and ramping costs. Variable OPEX are multiplied with the availability factor of the generator [a_g] and the weighting factor for the respective dispatch period [$d^{DP}_{s,d,t}$] to ensure that variable OPEX are scaled correctly to an annual level.

$$C^{Invest}_{g,y} = CAP_{g,y} \cdot c^{Invest}_g \qquad \forall g \in CTG, \forall y \quad (42)$$

$$OPEX_{g,y} = \sum_s \sum_d \sum_t \left(C^{SRMC}_{g,y,s,d,t} + C^{SU}_{g,y,s,d,t} + C^{SD}_{g,y,s,d,t} + C^R_{g,y,s,d,t}\right) \cdot a_g \cdot d^{DP}_{s,d,t} + C^{Invest}_{g,y} \cdot c^{FOM}_g \qquad \forall g \in CTG, \forall y \quad (43)$$

4.2.3 Module Concentrating Solar Power

Figure 23 presents the principle design of a CSP generator. A CSP plant is typically composed of four major subsystems: The solar field, the back-up burner, the thermal energy storage, and the power block. The power block is equipped with a steam turbine and a wet or dry cooling system to transform thermal energy into electricity. Through the application of the energy storage system and the back-up burner, CSP generators can provide firm and dispatchable capacity similar to conventional thermal power plants. With comparably low techno-economic effort, thermal energy generated by the solar field during the day can be stored in the thermal energy storage system for later use after sunset. The size of the solar field and storage system determine the annual electricity generation from solar energy. The back-up burner, which can be fired with fossil- or bio-fuels, is used to compensate longer periods without sunshine whereby power generation from CSP can be entirely guaranteed. Hence, the capacity of the back-up burner ultimately defines the firm capacity of the CSP generator. Utilized steam turbines are designed for fast unit start-ups, high ramping rates, and efficient part-load operation. Hence, CSP generators can provide several system services, such as firm and flexible

capacity, different kind of operating reserves, or reactive power. All of these system services become particularly important with increasing shares of VRE in the power system. Therefore, CSP generators can support grid-integration of VRE considerably while at the same time increasing the overall share of power generation from RES-E.

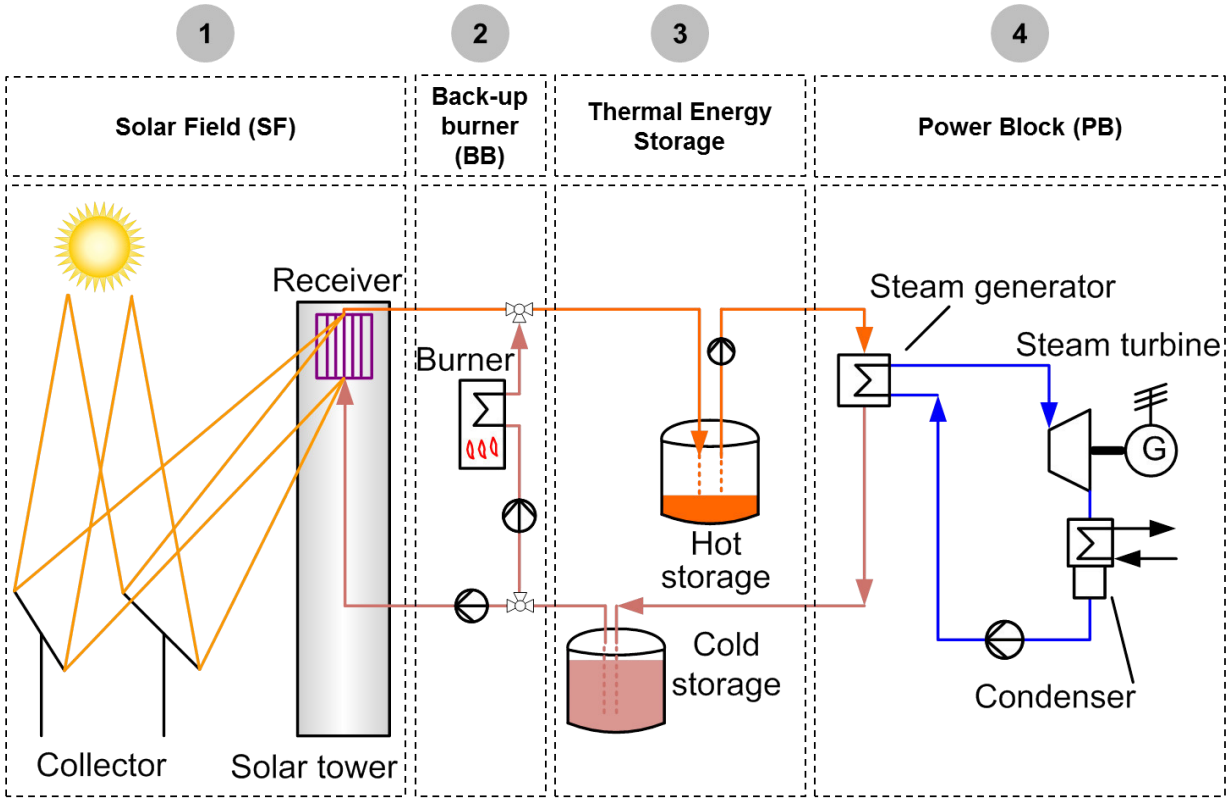

Figure 23: Principle design of a CSP generator (Solar Tower) with its major components. Own illustration based on [132]**.**

CSP generators can be designed to operate in a defined load segment (peak-, mid-merit or base-load), which can facilitate system integration. First CSP generators could be equipped with a relatively small solar field and storage system and operate in the peak- and upper mid-merit segment with a relatively low number of full load hours. In this load segment CSP generators compete with combined-cycle and open-cycle gas turbines, which typically have significantly higher generation costs than base load generators like e.g. coal power plants. With decreasing investment costs due to technological learning, the solar field and storage size, and therefore the number of full load hours, of subsequent CSP generators can be increased to operate in the lower mid-merit and even base load segment where competiveness is harder to achieve [86], [87].

The modelling approach for CSP generators in REMix-CEM is presented in Figure 24. In a first step, the hourly performance of the solar field of a Parabolic Trough or Solar Tower power plant is simulated using a detailed CSP solar field model. The solar field model is implemented in the modular simulation software INSEL and was developed during the PhD thesis of Moser [88]. Site-specific annual climate data with hourly resolution, such as direct normal irradiation (DNI), ambient temperature, and wind velocity, serve as input for the solar field model. In a second step, the hourly thermal generation profile of the solar field is normalized and feed into the optimization model REMix-CEM.

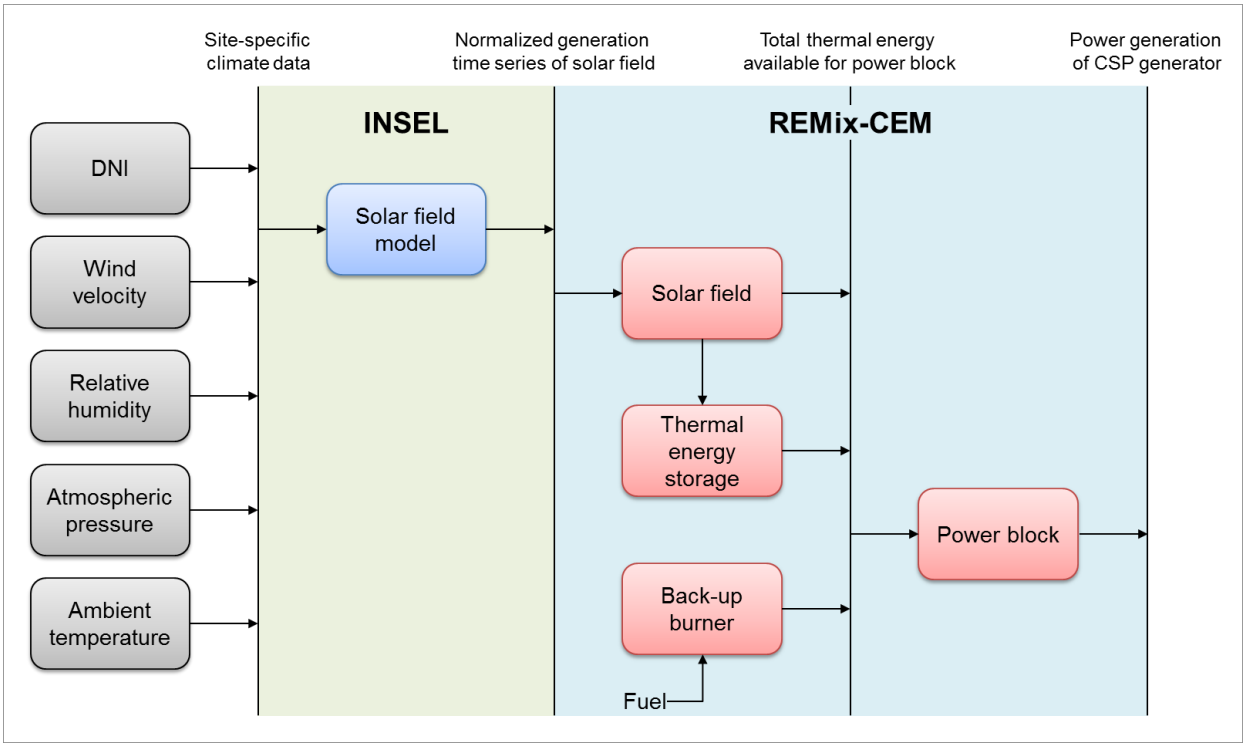

Figure 24: INSEL - REMix-CEM soft-link

In the optimization model the four major subsystems of a CSP generator, i.e. solar field, thermal energy storage system, back-up burner, and power block, are modeled individually (investment decision and operation), applying a unit clustering approach similar to the approach for conventional thermal power plants. Hence, a CSP generator can be composed of several units. The size of the solar field, storage and back-up burner of each CSP generator is optimized model-endogenously from a system perspective. Optimizing the configuration of a CSP generator from a system perspective means that the determined configuration for the CSP generator by the optimization model is not necessarily the configuration which leads to the

lowest LCOE for the CSP generator itself, but the configuration which provides the highest value for the system. The accuracy of the modelling approach of the CSP module was validated with specialized CSP modelling tools of the Solar Research Institute of DLR during the THERMVOLT project. Maximum deviations in variables describing the operational performance of a CSP generator were below 2% [132].

In the following the mathematical formulation of the module Concentrating Solar Power is presented. The performance of the CSP power block is modeled in the same way as conventional thermal power plants (see section 4.2.2). This comprises also the consideration of UCCs if desired. The relevant equations to model the power block are not repeated in this section.

Maximum number of power blocks and cumulative installed capacity at generator

Equation (44) restricts the maximum number of power blocks (PBs) that can be built at each candidate CSP generator over the planning time frame. Equation (45) and (46) determine the cumulative number of built PBs and the resulting installed gross capacity at the CSP generator respectively. For already existing generators equation (44) is reformulated to a strict equality and $[\overline{pb}_{g,y}]$ represents the number of existing PBs at the CSP generator in the respective year.

$$\sum_{y} BUILD_{g,y}^{PB} \leq \overline{pb}_{g,y} \qquad \forall g \in CSP, with\ BUILD_{g,y} = 0\ if\ fy_g > y \qquad (44)$$

$$BUILD_{g.y}^{Cum,PB} = BUILD_{g.y-1}^{Cum,PB} + BUILD_{g,y}^{PB} \qquad \forall g \in CSP, \forall y, with\ BUILD_{g.y}^{Cum,PB} = 0\ if\ ly_g < y \qquad (45)$$

$$CAP_{g,y} = BUILD_{g.y}^{PB} \cdot \overline{p}_g \qquad \forall g \in CSP, \forall y \qquad (46)$$

CSP configuration

Equations (47) – (52) are used to optimize the configuration of the CSP generator. Equation (47) restricts the maximum and minimum size of the SF of the CSP generator (expressed as solar multiple (SM)[12]) as a function of the number of installed PBs. Similar to that, the total capacity of

[12] In the optimization model, the term solar multiple (SM) is defined as follow: A SM of 1 means that the size of the solar field and the related capacity at design condition equals the thermal capacity of the steam turbine at maximum load. A SM 2 means that the thermal capacity of the solar field at the design point is twice as much as the thermal capacity of the steam turbine.

the thermal energy storage (TES) and the back-up burner (BB) of the CSP generator is restricted by equation (48) and (49) respectively. The capacity of the TES is expressed as number of full load hours for which the PB can be solely operated by the TES with full capacity. The size of the BB is expressed as percentage of gross turbine capacity. For example, a BB with 100% capacity would allow the operation of one power block at the CSP generator with full capacity solely by the BB. Equations (50) - (52) determine the cumulative size of the SF and the capacity of the TES and BB of each CSP generator over the planning time frame.

$$\underline{sm}_g \cdot BUILD_{g,y}^{PB} \leq BUILD_{g,y}^{SF} \leq \overline{sm}_g \cdot BUILD_{g,y}^{PB} \qquad \forall g \in CSP \quad (47)$$

$$\underline{tes}_g \cdot BUILD_{g,y}^{PB} \leq BUILD_{g,y}^{TES} \leq \overline{tes}_g \cdot BUILD_{g,y}^{PB} \qquad \forall g \in CSP \quad (48)$$

$$\underline{bb}_g \cdot BUILD_{g,y}^{PB} \leq BUILD_{g,y}^{BB} \leq \overline{bb}_g \cdot BUILD_{g,y}^{PB} \qquad \forall g \in CSP \quad (49)$$

$$SM_{g,y}^{SF} = SM_{g,y-1}^{SF} + BUILD_{g,y}^{SF} \qquad \forall g \in CSP, \forall y \quad (50)$$

$$CAP_{g,y}^{TES} = CAP_{g,y-1}^{TES} + BUILD_{g,y}^{TES} \qquad \forall g \in CSP, \forall y \quad (51)$$

$$CAP_{g,y}^{BB} = CAP_{g,y-1}^{BB} + BUILD_{g,y}^{BB} \qquad \forall g \in CSP, \forall y \quad (52)$$

Performance of solar field and back-up burner

Thermal energy can be produced by the SF and the BB. Equation (53) determines the thermal energy produced by the SF for each dispatch period of the planning time frame. The site-specific normalized generation profile of a SM 1 SF (calculated by INSEL) is multiplied by the SM of the CSP generator and the thermal capacity of a single PB. The maximum generation of the BB is restricted by equation (54). The share of thermal energy produced by the BB over the year is constrained by equation (55) as a function of the annual SF generation.

$$Q_{g,y,s,d,t}^{SF} = q_{g,s,d,t}^{norm,SF} \cdot SM_{g,y}^{SF} \cdot \bar{q}_g^{PB} \qquad \forall g \in CSP, \forall y, \forall s, \forall d, \forall t \quad (53)$$

$$Q_{g,y,s,d,t}^{BB} \leq CAP_{g,y}^{BB} \cdot \bar{q}_g^{PB} \qquad \forall g \in CSP, \forall y, \forall s, \forall d, \forall t \quad (54)$$

$$\sum_s \sum_d \sum_t Q_{g,y,s,d,t}^{BB} \leq max^{BB} \cdot \sum_s \sum_d \sum_t Q_{g,y,s,d,t}^{SF} \qquad \forall g \in CSP, \forall y \quad (55)$$

Performance of thermal energy storage

The maximum fill level of the TES is restricted by equation (56). Equation (57) ensures that the fil level in the first and the last dispatch period (FT, LT) of the second intra-annual dimension (e.g. representative week or day) are equal. The energy balance of the TES for each dispatch period is calculated in equation (58).

$$L^{TES}_{g,y,s,d,t} \leq CAP^{TES}_{g,y} \cdot \bar{q}^{PB}_{g} \qquad \forall g \in CSP, \forall y, \forall s, \forall d, \forall t \quad (56)$$

$$L^{TES}_{g,y,s,d,FT} = L^{TES}_{g,y,s,d,LT} \qquad \forall g \in CSP, \forall y, \forall s, \forall d \quad (57)$$

$$\left(Q^{C,TES}_{g,y,s,d,t} \cdot \eta^{c,TES}_{g} - \frac{Q^{D,TES}_{g,y,s,d,t}}{\eta^{d,TES}_{g}}\right) \cdot \Delta t = L^{TES}_{g,y,s,d,t} - L^{TES}_{g,y,s,d,t-1} \cdot \left(1 - \eta^{Self,TES}_{g}\right) \qquad \forall g \in CSP, \forall y, \forall s, \forall d, \forall t \quad (58)$$

Performance of power block

The modelling approach for the PB of a CSP generator is identical to the approach for modelling the operational performance of conventional thermal generators. Please refer to Section 4.2.2.

Energy balance of CSP generator

The thermal energy balance for the entire CSP generator is determined by equation (59). The sum of thermal energy generated by the SF and the BB, plus the thermal energy discharged from the TES must be equal to thermal energy consumption due to power generation and unit start-ups, plus thermal energy stored in the TES and thermal energy that is curtailed. Thermal energy consumption due to power generation is calculated like for conventional thermal generators according to the piecewise linear fuel consumption approach (see equation (33)).

$$\begin{aligned} Q^{SF}_{g,y,s,d,t} + Q^{BB}_{g,y,s,d,t} + Q^{D,TES}_{g,y,s,d,t} & \qquad \forall g \in CSP, \\ = FC_{g,y,s,d,t} + SU_{g,y,s,d,t} \cdot fuel^{SU}_{g} + Q^{C,TES}_{g,y,s,d,t} + Q^{Curtail}_{g,y,s,d,t} & \qquad \forall y, \forall s, \forall d, \forall t \end{aligned} \quad (59)$$

Auxiliary power and net power generation

Auxiliary power for the SF and TES operation can be significant, especially for Parabolic Trough power plants. Equation (60) calculates the auxiliaries for the SF and TES simplified as linear function of SF generation and TES charging. As CSP generators can consume electricity from the grid to cover auxiliaries for SF and TES operation, in equation (60) auxiliary power is reduced by the grid consumption of the CSP generator.

$$AUX_{g,y,s,d,t}^{SF,TES} = q_{g,s,d,t}^{norm,SF} \cdot SM_{g,y}^{SF} \cdot aux_g^{SF} + Q_{g,y,s,d,t}^{C,TES} \cdot aux_g^{TES} - P_{g,y,s,d,t}^{Grid,AUX} \qquad \forall g \in CSP, \forall y, \forall s, \forall d, \forall t \quad (60)$$

Net power generation of the CSP generator is calculated in equation (61). Gross power generation is reduced by the auxiliaries of the PBs and adjusted by a correction factor for ambient temperature. The correction factor is calculated in the same way as for conventional thermal generators (see equation (36) in Section 4.2.2). In addition, auxiliary power for SF and TES operation is subtracted.

$$P_{g,y,s,d,t}^{Net} = \left(ON_{g,y,s,d,t} \cdot \underline{p}_g + P_{g,y,s,d,t}\right) \cdot \left(1 - aux_g\right) \cdot cf_{g,s,d,t}^{p} - AUX_{g,y,s,d,t}^{SF,TES} \qquad \forall g \in CSP, \forall y, \forall s, \forall d, \forall t \quad (61)$$

Overnight investment costs and annual operational expenditures

Overnight investment costs are calculated by equation (62) as a function of the CSP generator configuration. Total annual OPEX are calculated by equation (63). OPEX are composed of variable and fix OPEX. The variable OPEX include costs for the back-up fuel itself and eventually related emissions as well as start-up, variable O&M, shut-down, and ramping costs. Variable OPEX are reduced by the availability factor of the generator [a_g] and multiplied with the weighting factor for the respective dispatch period [$d_{s,d,t}^{DP}$]. Fix OPEX are calculated as function of the overnight investment costs.

$$C_{g,y}^{Invest} = CAP_{g,y} \cdot c_g^{PB} + SM_{g,y}^{SF} \cdot c_g^{SM1} + \left(CAP_{g,y}^{TES} \cdot c_g^{TES} + CAP_{g,y}^{BB} \cdot c_g^{BB}\right) \cdot \bar{q}_g^{PB} \qquad \forall g \in CSP, \forall y \quad (62)$$

$$OPEX_{g,y} = \sum_s \sum_d \sum_t \Big[Q_{g,y,s,d,t}^{BB} \cdot \left(c_{g,y}^{Fuel} + c_{g,y}^{E} \cdot e_g\right) + \left(ON_{g,y,s,d,t} \cdot \underline{p}_g + P_{g,y,s,d,t}\right) \cdot c_g^{VOM} + C_{g,y,s,d,t}^{SU} + C_{g,y,s,d,t}^{SD} + C_{g,y,s,d,t}^{R}\Big] \cdot a_g \cdot d_{s,d,t}^{DP} + C_{g,y}^{Invest} \cdot c_g^{FOM} \qquad \forall g \in CSP, \forall y \quad (63)$$

5 Impact of applied modelling approach on results of capacity expansion optimization

The flexible formulation of REMix-CEM allows the application of different approaches for capacity expansion optimization. On the one hand, the user can select between different foresight approaches (myopic foresight, rolling horizon, and perfect foresight) to solve the least-cost optimization problem. On the other hand, the user has the possibility to define the system-operational detail during capacity expansion optimization in a flexible way. The selected approach has an impact on the accuracy of the computed results but also on required computing time to solve the capacity expansion optimization problem. The following chapter has the aim to investigate the impact of the available modelling approaches of REMix-CEM on results and computational effort. This is achieved by executing long-term capacity expansion optimization for a fictitious power system for the planning time frame 2016 - 2040 under the different available modelling approaches. The fictitious power system has typical characteristics of power systems of developing and emerging countries of the Sunbelt, i.e. excellent solar and wind resources but also a strong increase of annual electricity demand and peak load. Section 5.1 describes the utilized power system and the basic model setup of the optimization model. Section 5.2 investigates the impact of the foresight approach on results for capacity expansion optimization. The impact of the applied system-operational detail on results for capacity expansion optimization is investigated in Section 5.3.

5.1 Description of reference power system and model setup

The fictitious reference power system is composed of four model nodes. Figure 25 shows the transmission grid topology of the power system and the principle characteristics of each model node. 90% of total electricity demand occurs at model node N1 (25%) and model node N2 (65%). N1 and N2 represent the industrialized region of the power system. Coal, natural gas, oil, and biomass are available for power generation at these model nodes. Both model nodes are characterized by good PV resources with an annual global horizontal irradiation (GHI) of 1950 kWh/m². In addition, N1 has good wind resources (average 7.5 m/s at 60m hub height) and some moderate hydro resources (annual capacity factor of 29%). However, two thirds of the hydro potential is already deployed. Model node N3 and N4 together represent only 10% of

the annual electricity demand of the system. Both model nodes are characterized by a low population density. N3 has excellent wind resources (average 9 m/s at 60m hub height) and very good PV resources (annual GHI 2050 kWh/m²). Potentials for CSP installations exist only at model node N4. The annual GHI and direct normal irradiation (DNI) is 2250 kWh/m² and 2700 kWh/m² respectively at N4. Coal, natural gas, and biomass are not available for power generation at N3 and N4. Hence, CSP generators can use only oil for hybrid operation. At the beginning of the planning time frame in 2016, the net transfer capacity (NTC) between model N1 and N2 is 1.8 GW. The NTC between model nodes N2/N3 and N2/N4 is 0.6 GW. No transmission lines exist between N1/N4 and N3/N4 at the beginning of the planning time frame.

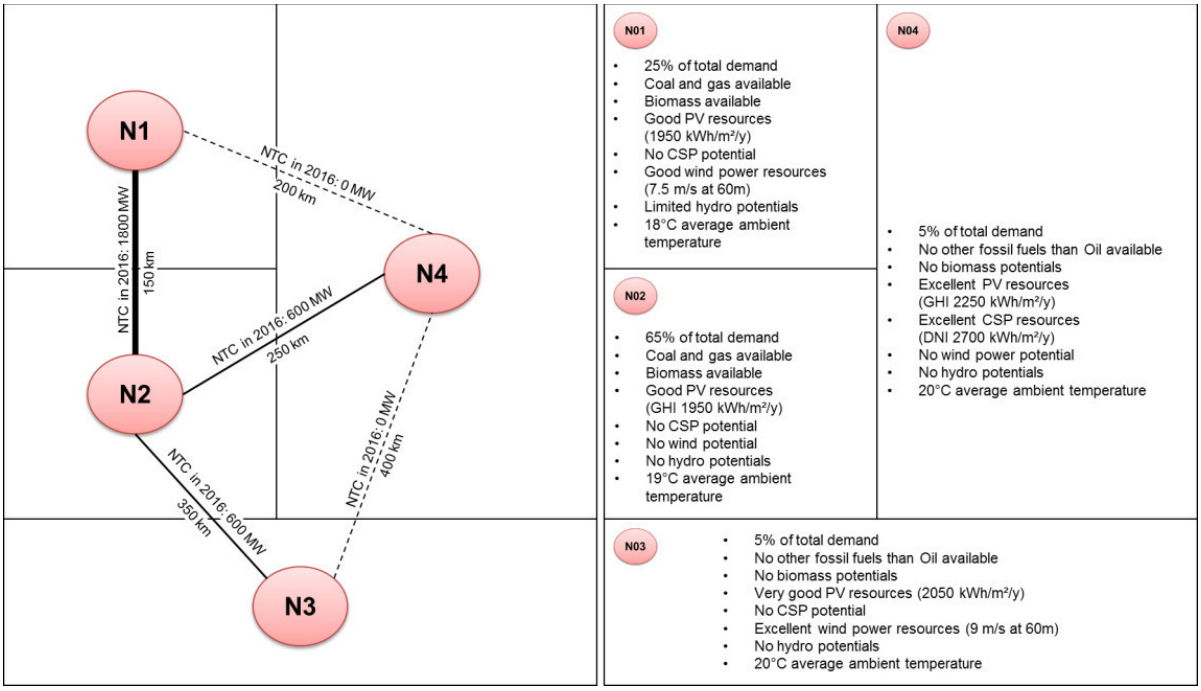

Figure 25: Overview of fictitious reference power system.
Left-hand side: Transmission grid topology; Right-hand side: Principle characteristics of model nodes

The planning time frame for the reference system is set from 2016 - 2040 (24 years). In the beginning of the planning time frame in 2016, the peak load of the system is 10 GW. Due to strong demand growth rates, the system peak load increases to about 27.5 GW until 2040. In the same time frame, annual electricity demand grows from 63 TWh to 170 TWh (see Table 10).

Figure 26 shows the annual chronological load curve and the annual load duration curve of the system in 2016. The absolute annual peak load of the system occurs at 10pm during a summer day in August.

Table 10: Demand development for the reference system

Year		2016	2019	2022	2025	2028	2031	2034	2037	2040
Growth rate	[%/a]	6.5%	6.0%	5.5%	5.0%	4.0%	3.5%	3.0%	2.5%	2.0%
Peak load	[GW]	10.00	12.02	14.25	16.66	19.1	21.38	23.59	25.65	27.49
Demand	[TWh]	62.7	74.1	87.9	102.7	117.8	131.9	145.5	158.2	169.5

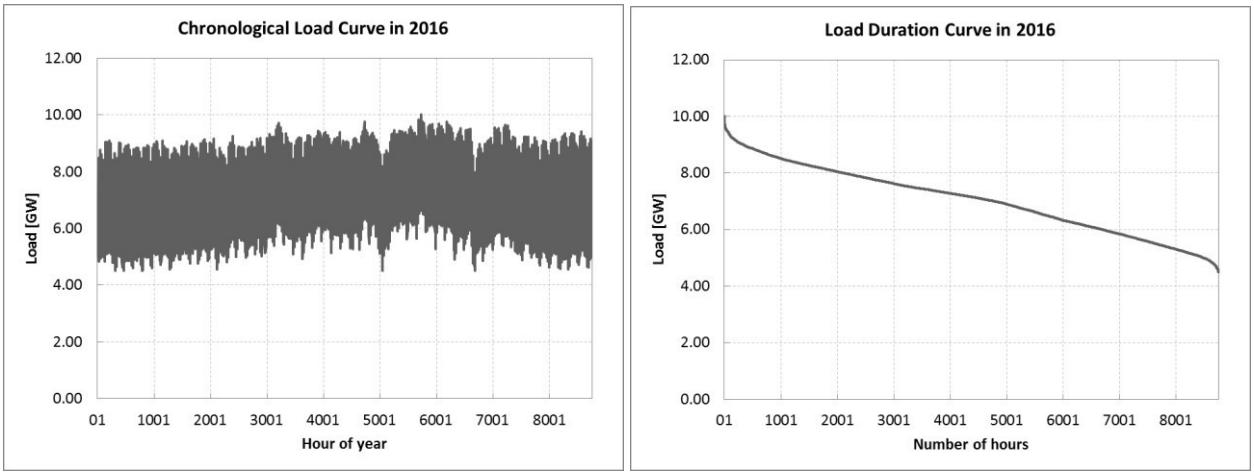

Figure 26: Hourly chronological load and load duration curve of the reference system in 2016

Figure 27 presents the average daily load curve of a winter and summer day respectively. Daily load curves in summer and winter are characterized by a pronounced evening peak. However, in summer a second peak occurs during noon mainly driven by air conditioning. For simplicity, the shape of the load curve in each model node is assumed to be identical but absolute values depend on the share on overall electricity demand at the model node.

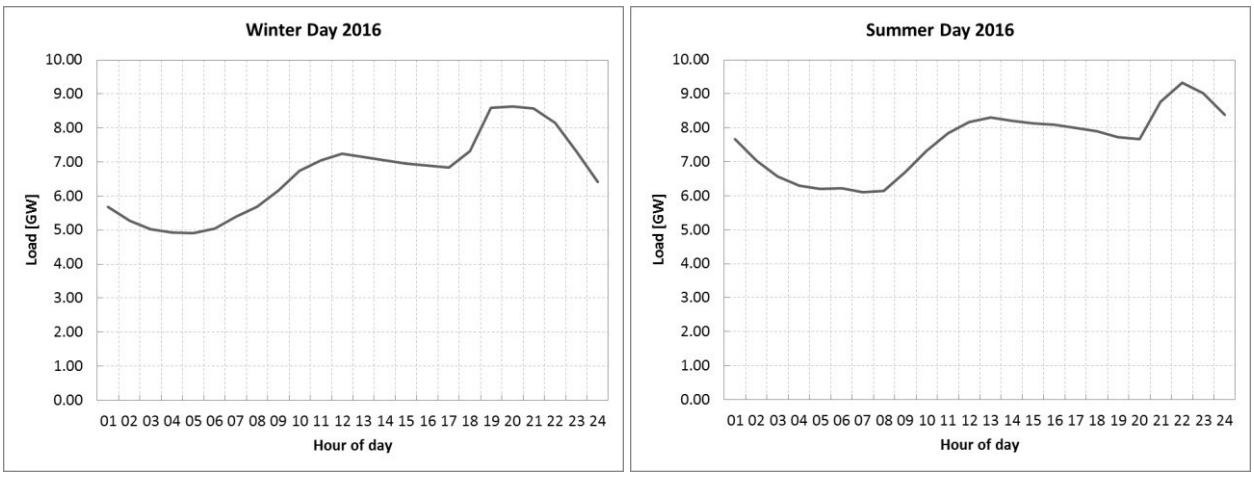

Figure 27: Average daily load of a winter and summer day of the reference system

The installed gross capacity at the beginning of the planning time frame and its spatial distribution is given in Figure 28. A total gross generation capacity of 13.3 GW is installed in 2016. Coal power plants represent about 50% of the total installed system capacity. Other conventional thermal capacities account for roughly 22% of installed system capacity. RES-E installations represent 28% of the total installed capacity of the system. Most RES-E capacity is provided by hydro power (15%) and onshore wind power (7.5%). Biomass, PV, and CSP together represent about 5% of total installed capacity. Almost the entire existing generation capacity is located at model node N1 and N2 (94%). Table 11 presents the spatial distribution of the existing generator fleet by model node.

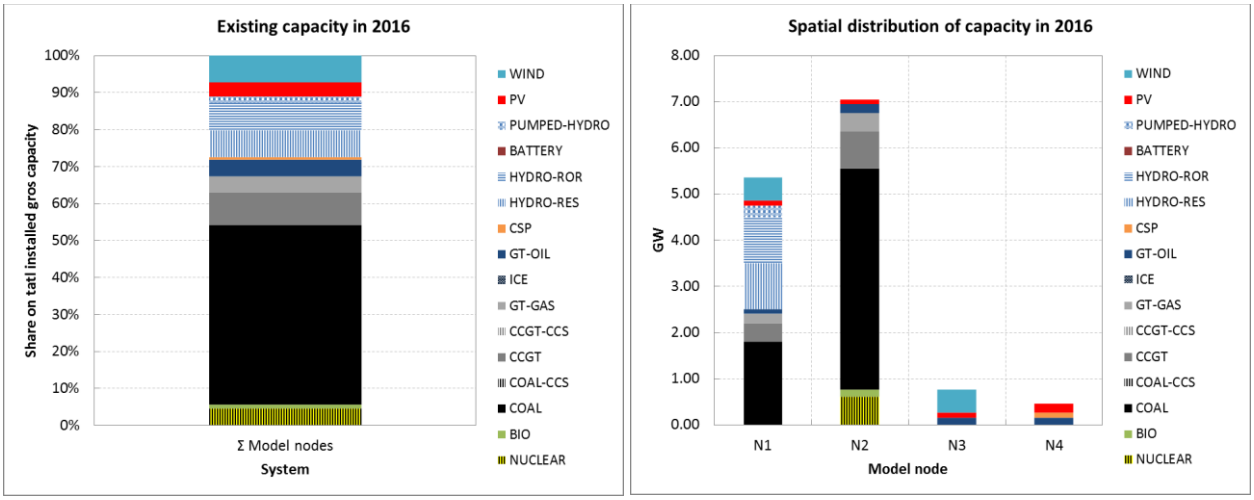

Figure 28: Shares on total installed gross capacity and its spatial distribution in 2016

Table 11: Total installed gross capacity and spatial distribution of existing units

Generator/storage type	Gross capacity per unit [MW]	Total number of installed units [-]	Total installed capacity [MW]	Installed units at model node			
				N1	N2	N3	N4
NUCLEAR	600	1	600	1			
COAL	600	11	6600	3	8		
CCGT	400	2	800	1	2		
GT-GAS	50	12	600	4	8		
GT-OIL	50	12	600	2	4	3	3
BIO	150	1	150		1		
HYDRO-ROR	250	4	1000	4			
HYDRO-RES	250	4	1000	4			
PUMPED-HYDRO	250	1	250	1			
CSP	100	1	100				1
PV	100	1	500	1	1	1	2
WIND	100	1	1000	5		5	

Figure 29 shows the scheduled decommissioning of existing generation capacity until the end of the study period. Until 2040, 6.4 GW of generation capacity is decommissioned. This represents almost 50% of the entire existing capacity in 2016. The simultaneous increase of electricity demand leads to a large capacity gap until 2040.

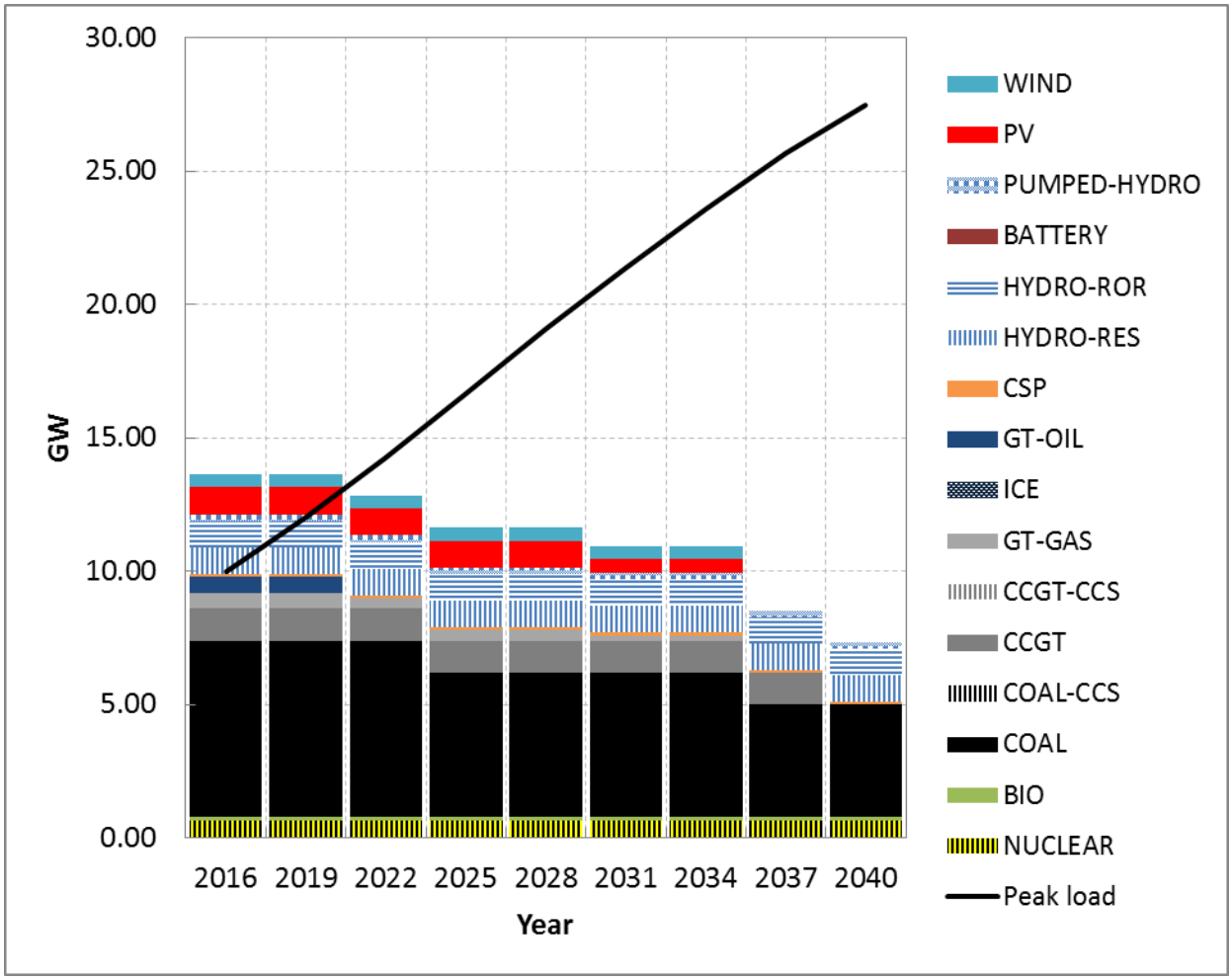

Figure 29: Peak load development over the planning time frame and remaining existing gross capacity after decommissioning of facilities that have reached the end of the technical lifetime

To meet growing electricity demand until 2040 several investment options are available (see Table 12). Candidate conventional thermal power plants are nuclear power plants (NUCLEAR), supercritical coal power plants (COAL) with and without carbon capture and storage (CCS), combined-cycle gas turbines (CCGT) with and without CCS, open-cycle gas turbines (GT), and internal combustion engines (ICE). Candidate RES-E technologies are onshore wind power (WIND), fixed-mounted PV, CSP (Solar Tower), hydro-reservoir (HYDRO-RES), and biomass steam power plants (BIO). Hydro pumped-storage (PUMPED-HYDRO) and Lithium-ion batteries

(BATTERY) are candidate storage technologies. The candidate units have a fix size and discrete investment decisions are represented by integer variables. Hence, capacity can be added only in increments of units. Exceptions of this are PV, wind power, and Lithium-ion batteries, which are considered as easily scalable technologies. The configuration of CSP generators (size of solar field, storage, and back-up burner) is optimized model endogenously. Hydro pumped-storage and Lithium-ion batteries have a fixed storage size of 8 Flh and 4 Flh respectively. High voltage alternating current (HVAC) transmission lines (TL) are available to increase the NTC between model nodes.

Table 12: Overview investment options

Conventional Thermal Technologies	RES-E Technologies	Storage and Transmission Technologies
NUCLEAR (600 MW)	WIND (scalable, min. 100 MW)	PUMPED-HYDRO (250 MW)
COAL with and w/o CCS (600 MW)	PV (scalable, min. 100 MW)	BATTERY (scalable, min. 50 MW)
CCGT with and w/o CCS (400 MW)	CSP (Solar Tower, 100 MW)	HVAC 400kV TL (NTC 600 MW)
GT (50 MW)	HYDRO-RES (250 MW)	
ICE (50 MW)	BIO (100 MW)	

Figure 30 presents the assumptions for the development of overnight investment costs for the different investment options over the planning time frame. Investment costs for conventional thermal, hydro reservoir, and pumped-hydro units are constant over the planning time frame. Investment costs for PV, wind power, CSP, Lithium-ion batteries, and CCS technologies decrease considerably until the end of the planning time frame. Investment costs for conventional thermal generators are taken from the New Policy Scenario of the International Energy Agency (IEA) [116]. Investment costs for RES-E and storage technologies are aligned to cost data provided in [121–123], [125], [128–130], [132]. For all investment options a WACC of 5.8% is applied. Additional techno-economic input data for the candidate units as well as other relevant input data for the case studies conducted in this work is presented in the Appendix.

Figure 31 presents the development of fuel prices over the planning time frame. Assumptions for fossil fuel price development are aligned to the New Policy Scenario of the IEA [116]. Fuel prices for biomass and nuclear power are also taken from the IEA and are assumed to be constant over the study period [114], [115].

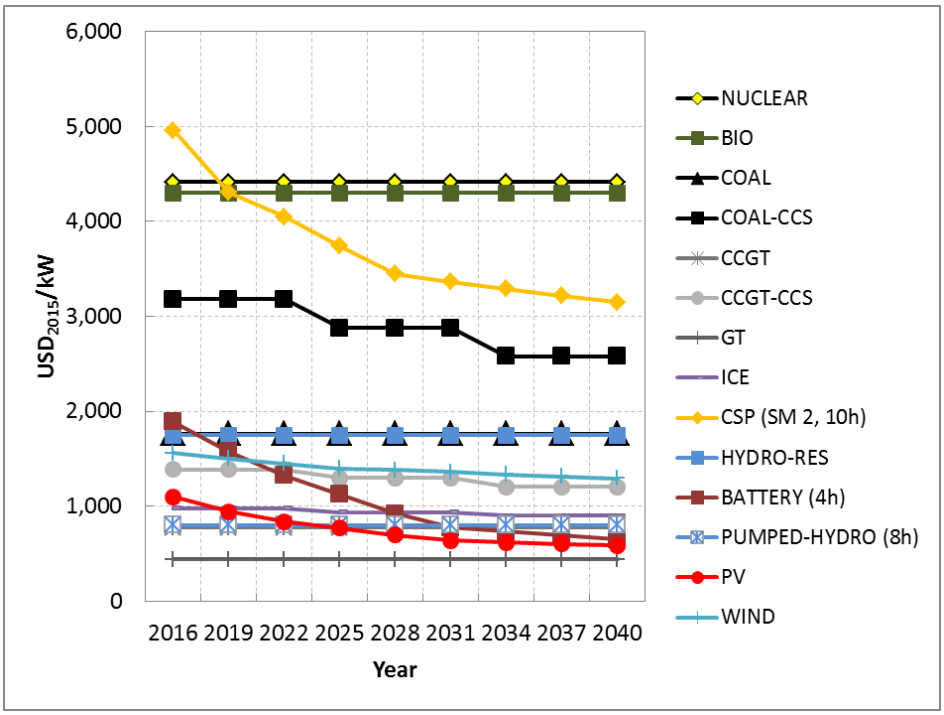

Figure 30: Assumptions for overnight investment costs for candidate technologies [116]**,** [123], [128], [132] **(more techno-economic data for the candidate units is presented in the Appendix)**

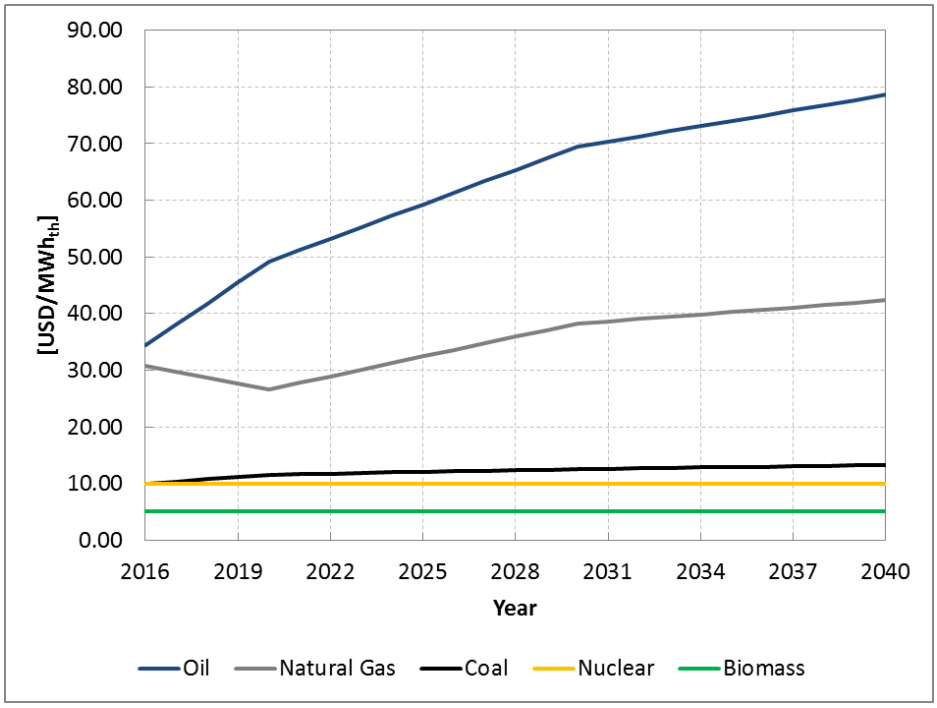

Figure 31: Fossil fuel price assumption (New Policy Scenario of IEA) [116]

Table 13 summarizes the resource availability at each model node. Coal, gas, and biomass are only available at model node N1 and N2. Wind resources are only available at N1 and N3, hydro resources at N1, and CSP resources at N4. PV resources are available at all model nodes.

Table 13: Overview resource availability at model nodes

	N1	N2	N3	N4
PV	GHI: 1950 kWh/m² Unlimited	GHI: 1950 kWh/m² Unlimited	GHI: 2050 kWh/m² Unlimited	GHI: 2250 kWh/m² Unlimited
Wind*	Wind speed: 7.5 m/s Unlimited	Not available	Not available	Wind speedy: 9 m/s Unlimited
Hydro	Capacity factor: 29% Maximum potential: 1.0 GW Run-of-river 2.5 GW Reservoir 1.25 GW Pumped-storage	Not available	Not available	Not available
CSP	Not available	Not available	Not available	DNI: 2700 kWh/m² Unlimited
Biomass	Potential: 1 TWh/y	Potential: 1 TWh/y	Not available	Not available
Fossil fuels	Coal: Unlimited Gas: Unlimited Oil: Unlimited	Coal: Unlimited Gas: Unlimited Oil: Unlimited	Coal: Not available Gas: Not available Oil: Unlimited	Coal: Not available Gas: Not available Oil: Unlimited

*) Wind speed at 60m hub height

The seasonality of PV, CSP, wind power, and hydro power resource availability is shown in Figure 32. Highest resource availability for PV is during summer whereas the highest CSP resource availability appears during spring and autumn. Wind power resources are highest during spring and summer. The largest hydro resources are available during the winter and spring months.

Table 14 presents the basic model setup of REMix-CEM, which is used for all executed model runs of the following case studies. The 24 year planning time frame from 2016 - 2040 is represented by nine milestone years. All investment options are available from 2019. The power system is represented by four model nodes, which are located all in the same balancing region. A 15% adequacy reserve margin is applied to ensure adequacy of the system over the planning time frame. The spinning and standing operating reserve capacity must be able to cover the failure of the largest unit of the system and to cover forecast errors for expected load and VRE generation. The system discount rate is set to 5%. Finally, it is assumed that for the fictitious power system the annual capacity additions per technology are not unlimited but restricted to some extent due to limited administrative and construction resources. This is a common situation in many developing and emerging countries. Therefore, a user-constraint is applied that limits the maximum deployment per technology to 4.8 GW per milestone year.

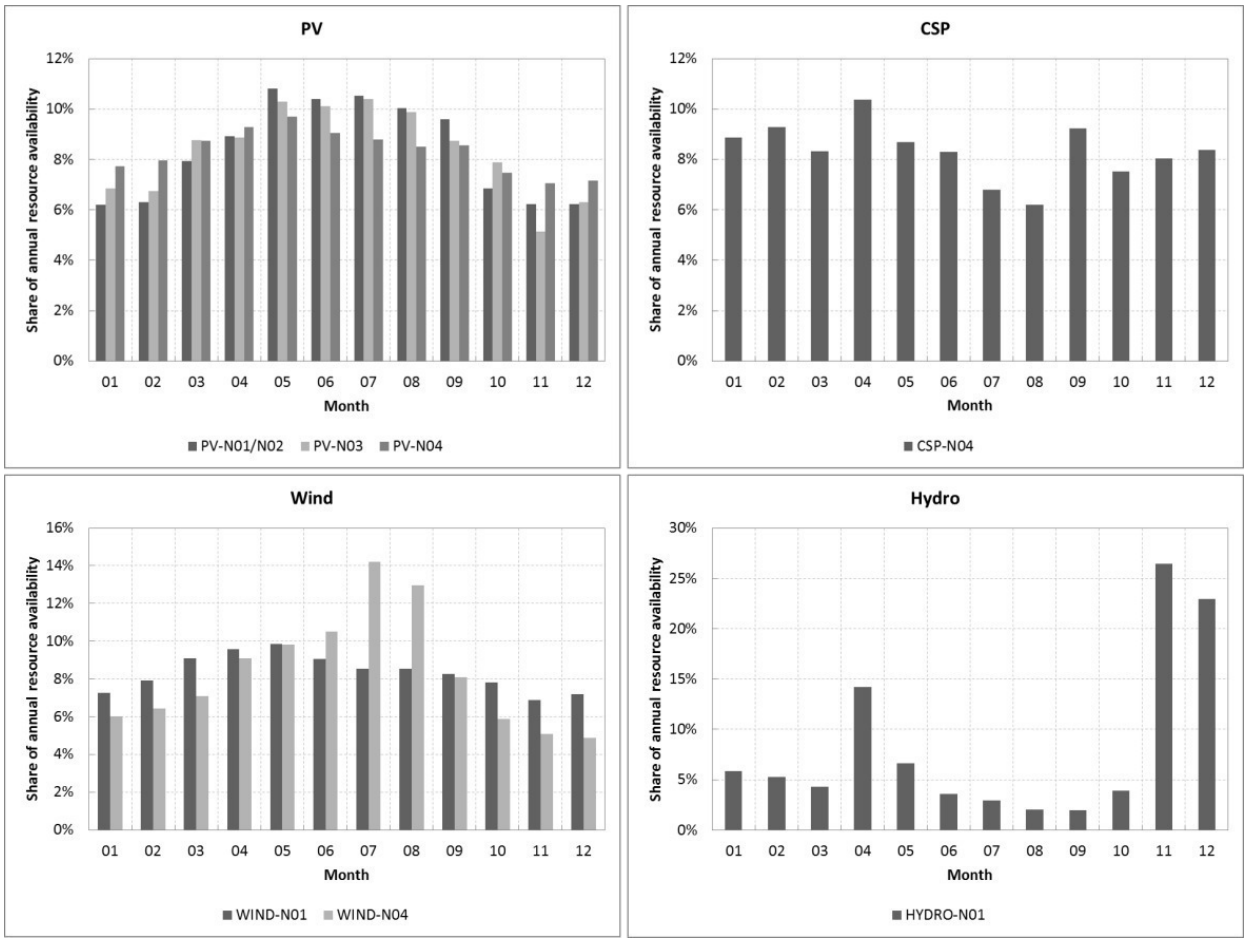

Figure 32: Seasonality of resource availability for PV, CSP, wind and hydro power

Table 14: General model setup for case study 1 and 2

	REMix-CEM setup
Planning time frame	2016 - 2040
Milestone years	2016, 2019, 2022, 2025, 2028, 2031, 2034, 2037, 2040
First investment year	2019
Spatial resolution	Country level, one balancing area with four model nodes
Temporal resolution	Case study specific (see Table 15 and Table 19)
Model foresight	Case study specific (see Table 15 and Table 19)
Operational details for thermal units	Case study specific (see Table 15 and Table 19)
Adequacy reserve restriction	15% generation adequacy reserve margin
Spinning reserve restriction	Failure of largest single unit + 2% of load + 10% of VRE capacity, no reserve capacity required for PV from dusk till dawn
Standing reserve restriction	Failure of largest single unit + 2% of load + 20% of VRE capacity, no reserve capacity required to back-up PV from dusk till dawn
System discount rate	5%
User constraints	Maximum deployment per technology: 4.8 GW per milestone year

5.2 Impact of model foresight

5.2.1 Hypothesis

Considering the uncertainty for certain input parameters is important for long-term capacity expansion and short-term system operation planning. This is all the more important when RES-E technologies are included in the analysis due to uncertainty about the development of their investment costs (long-term planning perspective) and the temporal and spatial availability of their intermittent primary energy resources (short-term operation perspective). Besides sensitivity analyses and stochastic programing, the application of different foresight assumptions can be used to address the highly uncertain nature of certain input parameters, such as e.g. the development of electricity demand, investment costs, fossil fuel prices, or resource availability of RES-E technologies [89–91], [94], [95]. In this section the impact of the applied model foresight on results and computational effort for capacity expansion optimization is investigated. As described in Chapter 4, REMix-CEM can be applied with three different foresight approaches:

I) Perfect foresight over the entire planning time frame
II) Multi-annual rolling horizon foresight
III) Single-year myopic foresight

Each foresight approach has its advantages and disadvantages. Providing the optimization model with perfect foresight enables the model to identify the intertemporal global optimum to meet demand over the planning time frame, while ensuring reliability standards and meeting defined strategic targets. Future developments, such as electricity demand, RES-E technology learning rates, or fuel and CO_2 price development, can be anticipated by the model and investment decisions can be adapted accordingly. This makes the perfect foresight approach especially suitable for e.g. policy makers to identify economically efficient transition pathways towards a sustainable electricity supply under a set of input parameters. However, the drawback of the approach is the high computational effort caused by the large optimization problem which must be solved in one single model run. Another issue of the perfect foresight approach is the unrealistic assumption that decision makers have perfect information about future occurrences of the entire planning time frame that often covers several decades.

Whereas the perfect foresight approach provides the CEM with information about all future developments until the end of the planning time frame, the single- year myopic foresight approach provides the CEM with no information at all about future occurrences. Hence, investment decisions are made only on the basis of current demand and cost figures (e.g. fuel or investment costs) in the respective optimization period (milestone year) without anticipating any changes in future years. The advantage of the myopic approach is a significant reduction of the problem size. The large optimization problem of the perfect foresight approach is separated into several smaller sub-problems, which can be solved sequentially. Consequently, this leads to a reduced computational effort. The drawback of the myopic approach is the unrealistic assumption that decision makers have no information about the future at all and that computed solutions are more costly compared to solutions determined under perfect foresight. The very limited foresight of the single-year myopic approach is especially problematic for capacity expansion planning with RES-E, as future savings due to early investments into RES-E with almost constant generation costs over their economic life-time cannot be anticipated. Also the utilization effect for conventional thermal generators cannot be taken into account, which can lead to stranded investments for conventional thermal generators, as decreasing future utilization is not considered during the investment decision.

The multi-annual rolling horizon approach is a compromise between the perfect foresight and single-year myopic foresight approach. Several milestone years of the planning time frame are grouped together and are optimized simultaneously. After solving the sub-problem of the first group of milestone years, the foresight horizon rolls forward to the next group of milestone years, while taking into account investment decisions made in the previous optimization periods. Hence, investment decisions are not only based on the current situation but also on information of some future periods.

It can be expected that differences in investment decisions under the different foresight approaches are relatively small for a continuous development of input parameters (e.g. fossil fuel or CO_2 prices). In the case input parameters change suddenly at one or more stages during the planning time frame, the difference between results is expected to be more pronounced because these occurrences can only be foreseen by the perfect foresight and partially by the

multi-annual rolling horizon approach. As providing the CEM with perfect foresight leads to the largest optimization problem, it can also be expected that computing time to solve the capacity expansion optimization problem for the 24 year planning time frame is highest for the perfect foresight approach.

5.2.2 Methodology

The fictitious power system described in the previous section is used to investigate the impact of the foresight approach on results for capacity expansion optimization. REMix-CEM is applied to calculate the least-cost expansion plan to meet electricity demand from 2016 to 2040, while ensuring applied reliability standards of the system. Two groups of model runs are executed, each composed of three CEM runs. Within one group, all three CEM runs are based on the same input data and differ only in the applied foresight approach. The only difference between input parameters of the two groups of model runs is the assumed development of CO_2 prices over the planning time frame (see Figure 33). For the CEM runs of Group 1, a monotone development of CO_2 prices is assumed, starting with 6 USD/t in 2016 and ending up with 37 USD/t in 2040. In Group 2, the introduction of CO_2 prices occurs more suddenly. Until 2025, no CO_2 prices exist. Afterwards, CO2 prices are introduced and the price development follows a s-curve function to reach 37 USD/t in 2040.

For the first CEM run of each group, the single-year myopic foresight approach is applied, meaning that each single milestone year is optimized consecutively (nine optimization periods). In the second CEM run of Group 1 and Group 2, the multi-annual rolling horizon approach is applied to calculate the least-cost expansion plan over the planning time frame. The nine milestone years are grouped together into three optimization periods (period 1: 2016 - 2022; period 2: 2025 - 2031; period 3: 2034 - 2040). In the third CEM run of each group, the perfect foresight approach is applied and hence, the entire planning time frame is optimized as one large optimization period. Results of the three foresight approaches applied within each group are compared in terms of investment decisions, composition of power supply, overall system costs, and computing time (see Figure 34).

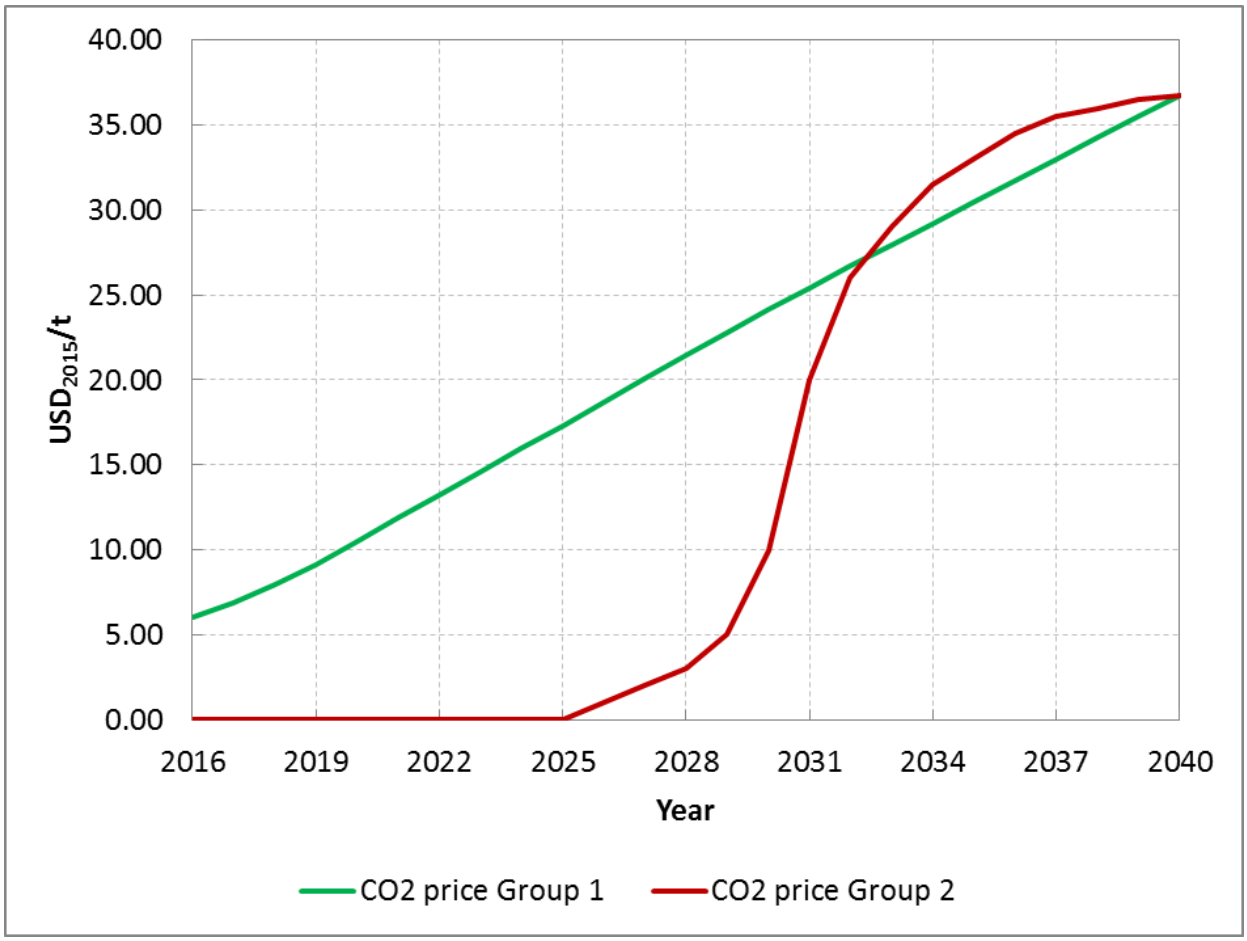

Figure 33: CO_2 price assumption for CEM runs of Group 1 and Group 2. CO_2 prices in 2040 are aligned to assumed CO_2 prices in China according to the New Policy scenario of the IEA [116].

Table 15 presents the model setup for the CEM runs. The only difference between the CEM runs is the applied foresight approach and the resulting number of optimization periods into which the entire planning time frame is divided. Each milestone year in the CEMs is represented by 24 representative days (one working and one weekend day per month). Each day is composed of 24 chronological dispatch periods (hours). UCCs of thermal generators are neglected in this analysis, meaning that generators are dispatched according to their position in the merit order. Hence, the flexibility effect is not considered here. The optimization problem is solved on a 2 x Intel Xeon E5-2640v3 @ 2.60 GHz with 12 x 16 GB RAM.

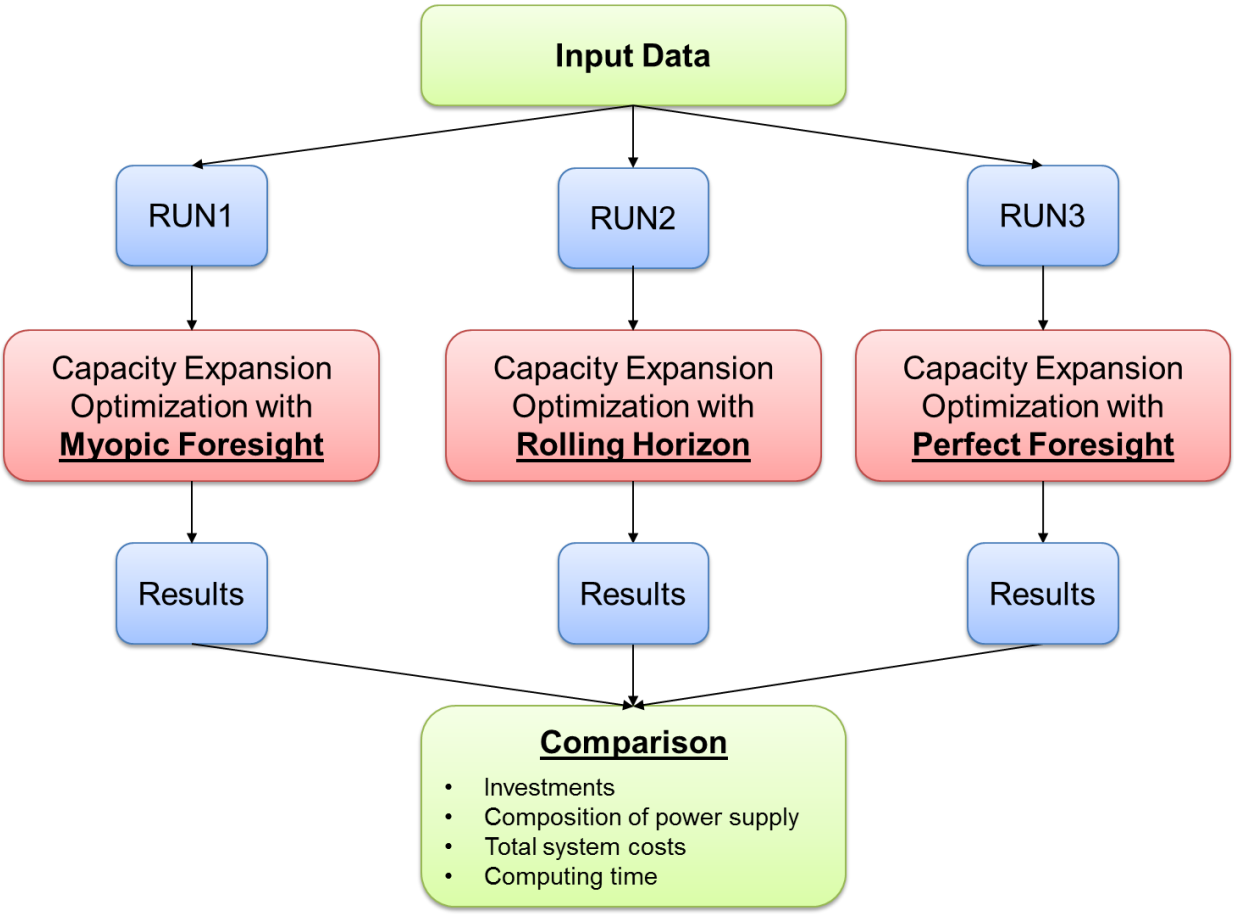

Figure 34: Approach for analyzing the impact of the applied foresight approach on results for capacity expansion optimization

Table 15: Model setup for the different CEMs of case study 1

	Myopic Foresight	Rolling Horizon	Perfect Foresight
Planning horizon	2016 - 2040		
Milestone years	2016, 2019, 2022, …, 2040		
# Milestone years	9		
# Seasons	12 (each month of the year)		
# Representative days per season	2 (1 working and 1 weekend day)		
# Dispatch periods per day	24		
# Total annual dispatch periods	576		
System-operational detail	No unit commitment constraints of thermal generators		
# Optimization periods	**9**	**3**	**1**

5.2.3 Results for monotone CO_2 price development

Figure 35 presents the total added generation capacity over the planning time frame for the three CEM runs of Group 1. Several differences can be observed between the model runs:

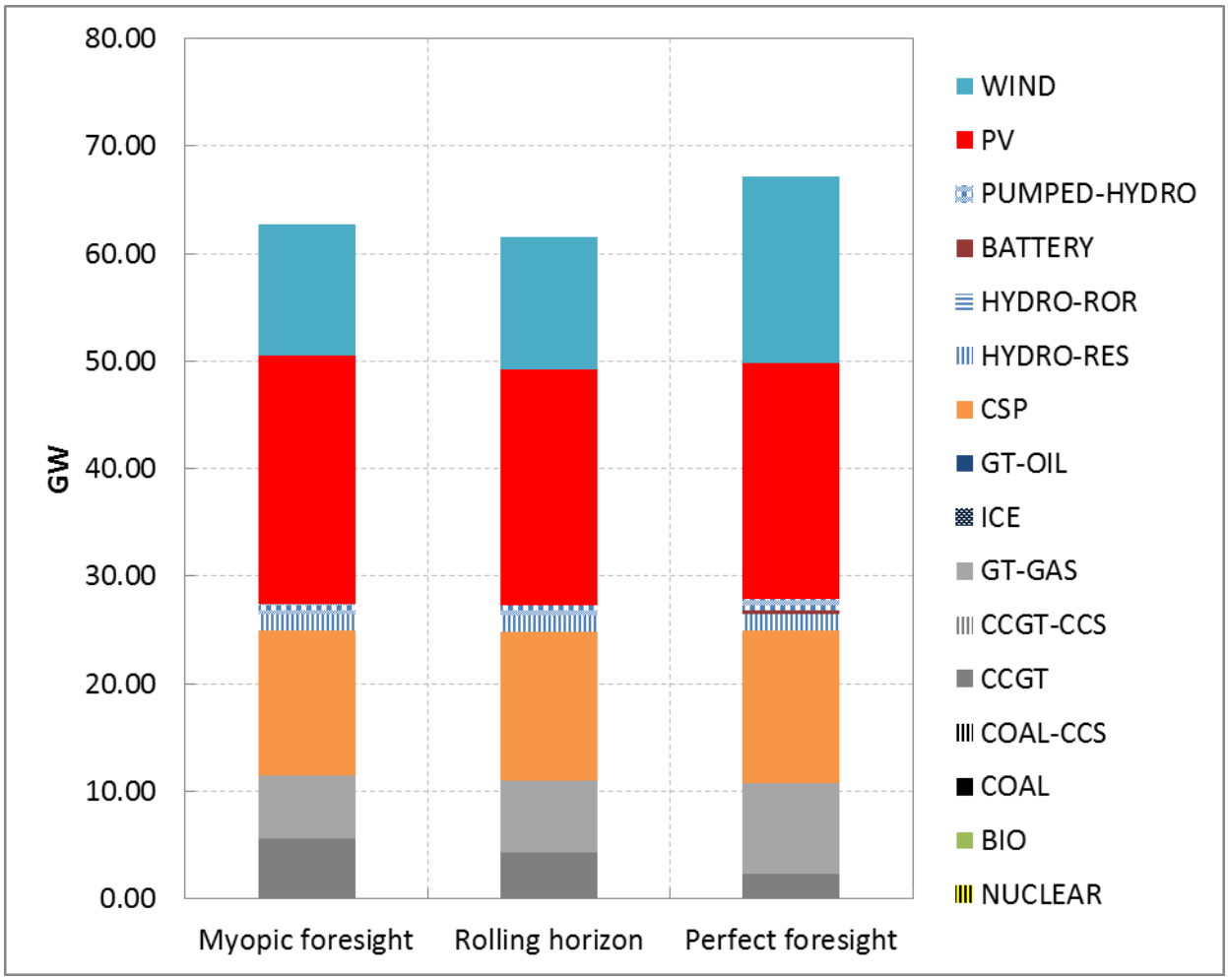

Figure 35: Total added gross capacity by foresight approach (Group 1)

Providing the CEM with perfect foresight leads to the largest overall capacity expansion. Almost 67 GW of new capacity is added until 2040 by the perfect foresight model. The myopic foresight and rolling horizon model invest only in 63 GW and 62 GW of new capacity respectively. The higher capacity expansion by the perfect foresight model is driven by larger investments in VRE compared to the myopic foresight and rolling horizon model. VRE generators with a capacity of more than 39 GW are added by the perfect foresight model. This represents 59% of the total capacity expansion over the planning time frame. In contrast, the myopic foresight and rolling horizon model install VRE generators with a capacity of 35 GW and 34 GW respectively (about

56% of total installations). With more than 17 GW, most wind power capacity is installed by the perfect foresight model. The myopic foresight and rolling horizon model invest only in about 12 GW of wind power. In all three CEM runs significantly more PV than wind power capacity is added. PV generators with a total capacity of 23 GW are installed by the myopic foresight model. The rolling horizon and perfect foresight model invest in about 22 GW of new PV capacity.

Also for the residual asset fleet differences in investment decisions can be observed. Most CCGT capacity is installed by the myopic foresight model. 14 units, each with a capacity of 0.4 GW, are added to the system (in total 5.6 GW). The rolling horizon model installs three CCGT units less than the myopic foresight model (4.4 GW) because it can partially foresee increasing fossil fuel and CO_2 prices as well as a reduced utilization of conventional thermal generators in the future (utilization effect). The perfect foresight model has information about all occurrences over the planning time frame. Based on this perfect information, the perfect foresight model evaluates investments in CCGT as considerably less attractive than the other two CEMs. Only 2.4 GW of CCGT (6 units) are installed over the planning time frame. Instead, the perfect foresight model installs more CSP and GT units. CSP generators have nearly constant generation costs over their economic life-time, which compensates slightly higher generation costs compared to CCGT in the short-term. Very flexible GT with low investment costs ideally complement the larger deployment of VRE in the perfect foresight model. Compared to the myopic foresight model, 2.45 GW more GT and 0.8 GW more CSP capacity is installed. The differences between the rolling horizon model and the perfect foresight model are less pronounced but still considerably. 1.7 GW more GT and 0.5 GW more CSP capacity is added. In total, the perfect foresight model invests in 14.3 GW of CSP and 8.35 GW of GT generators over the planning time frame. In all CEM runs, CSP units are equipped with a 10h TES and a BB with 100% of thermal turbine capacity.

All CEMs deploy the entire additional available reservoir hydro (1.5 GW) and pumped-storage (1 GW) potential. Investments in Lithium-ion batteries do not belong to the least-cost expansion plan in the myopic foresight and rolling horizon model. Only in the perfect foresight model Lithium-ion batteries with a total capacity of 0.35 GW are installed. In all CEM runs, no

investments in nuclear, coal, and biomass power plants are executed. Also fossil fuel fired generators equipped with CCS are not part of the least-cost solution in all CEM runs of Group 1.

The newly added net transfer capacity (NTC) between the model nodes of the system is presented in Figure 36. The perfect foresight model installs the most additional NTC over the planning time frame (17.4 GW). The myopic foresight and rolling horizon models invest in 15.0 GW and 16.2 GW of NTC respectively. In all CEM runs most NTC is added between N2/N3 and N2/N4. At model node N3 the highest wind power resources of the power system are located. The excellent CSP resources of the power system are located at model node N4.

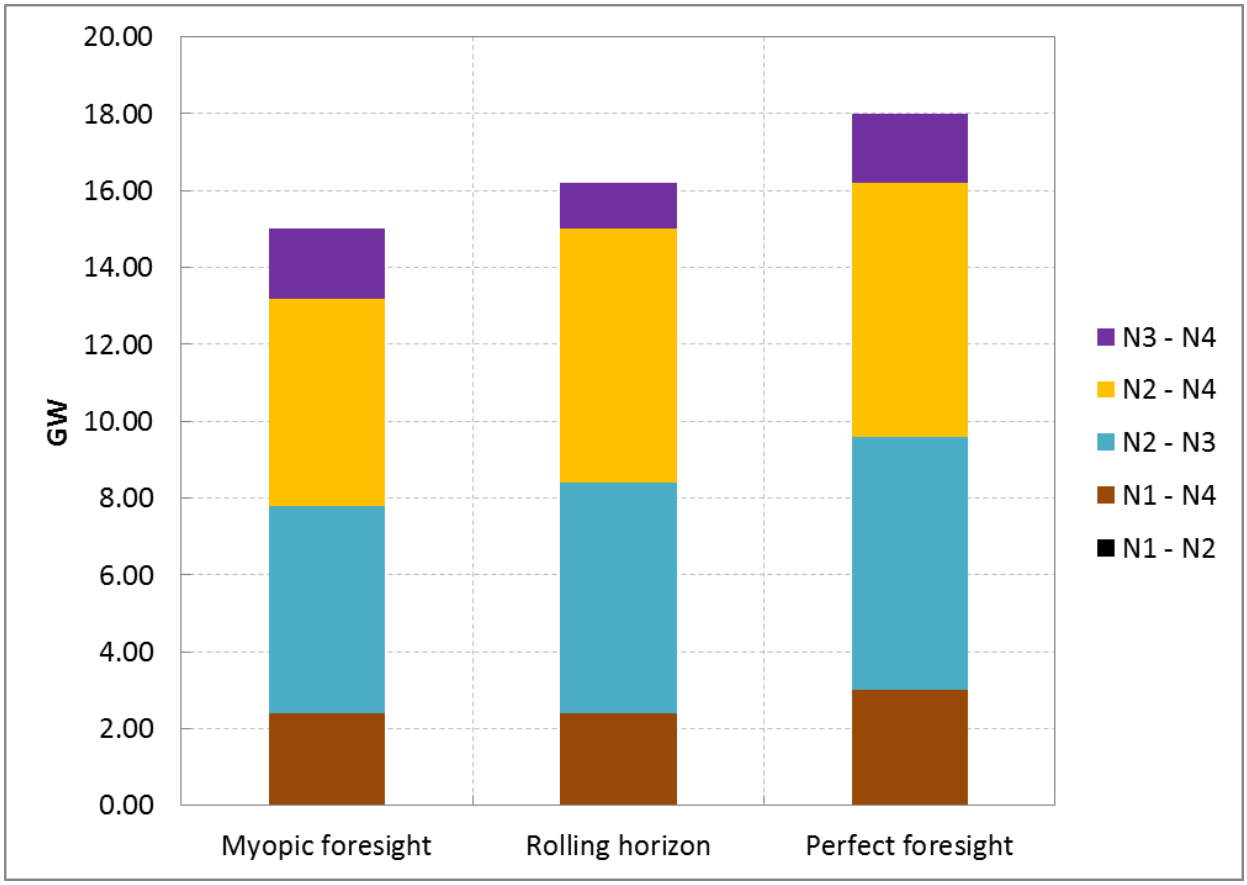

Figure 36: Total added NTC between model nodes by foresight approach (Group 1)

The results of the three CEM runs confirm the theory of the persistent utilization effect (see Section 3.2). A large-scale deployment of VRE is accompanied by investments in flexible mid-merit and peaking generators with rather low investment costs. The structural shift of the residual system from a base-load generator dominated system to a system dominated by mid-merit and peaking generators can be observed in Figure 37, where the cumulative installed

generation capacity over the planning time frame for the three different foresight approaches is presented. Figure 38 highlights the corresponding cumulative NTC between each pair of model node. The existing system in 2016 is dominated by coal and nuclear base-load generators. Over the planning time frame this changes fundamentally for all CEM runs due to large investments in mid-merit and peaking generators that accompany the large-scale deployment of VRE.

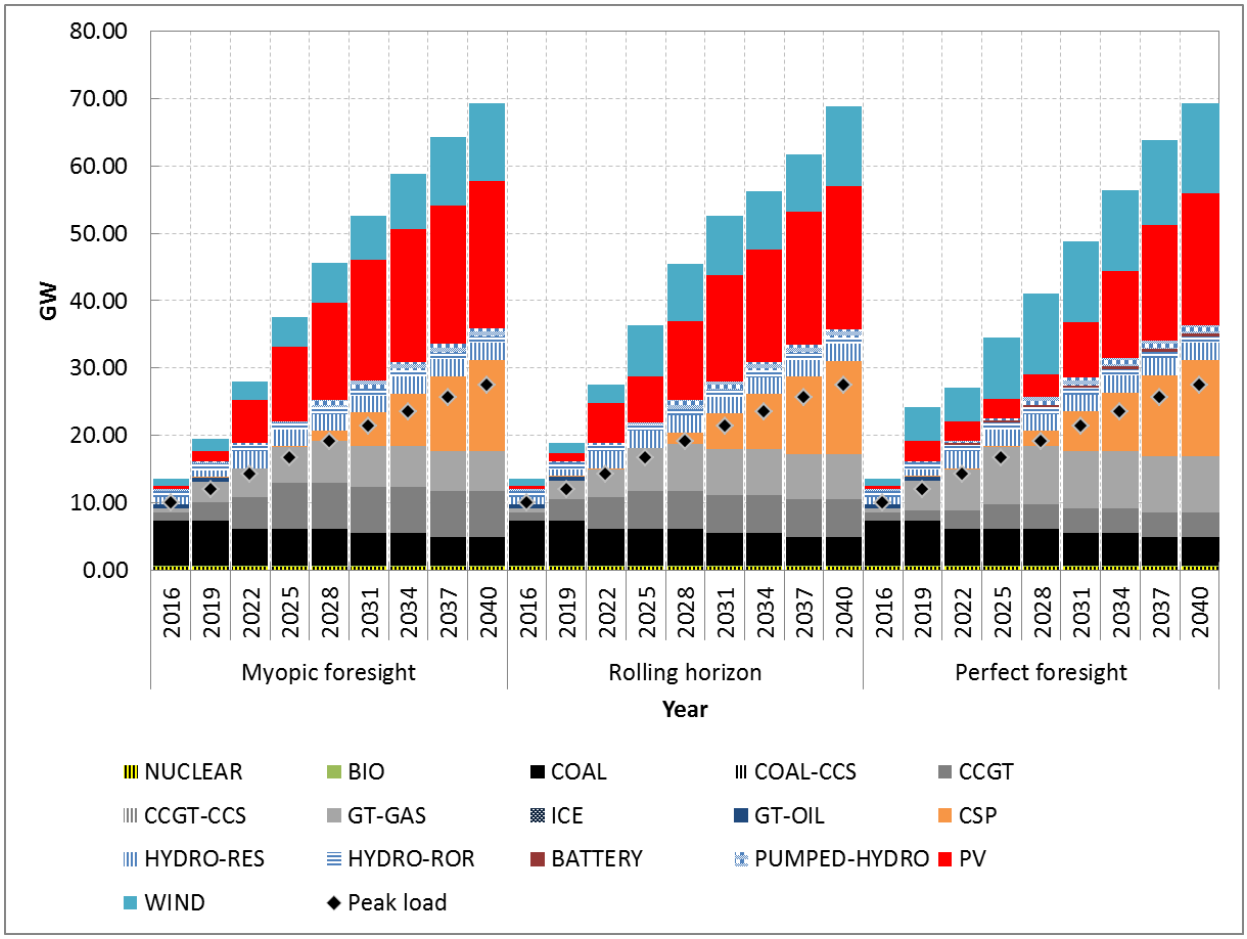

Figure 37: Cumulative installed gross capacity by foresight approach (Group 1)

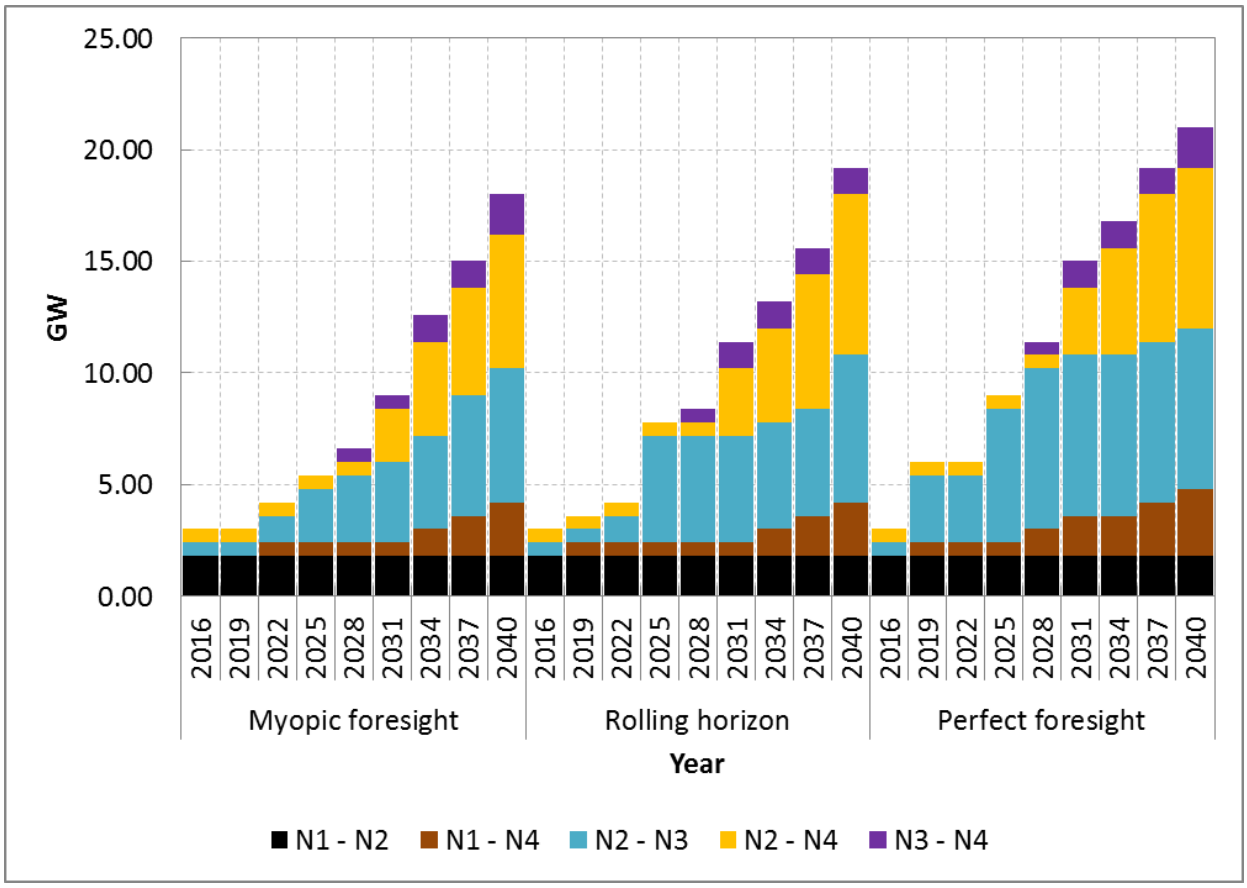

Figure 38: Cumulative installed NTC between model nodes by foresight approach (Group 1)

In 2016, base-load generators represented 54% of total installed generation capacity and 61% of the capacity of the residual system. Until 2040, the share of base-load generators is reduced to 43% of the total installed generation capacity. Related to the residual system, the share of base-load generators even decrease to 14%. The share of VRE on total installed system capacity is increased from 18% in 2016 to about 48% in 2040 in all three CEM runs. As a consequence of the persistent utilization effect, the share of flexible mid-merit and peaking units on the residual asset fleet increases from 26% to 83% and from 23% to 43% related to the total installed generation capacity.

Major differences between the three CEM runs can also be observed for the timing of investments. Figure 39 and Figure 40 present the newly installed generation capacity and NTC respectively in each milestone year by CEM run. The general trend is that the perfect foresight model installs more generation capacity in the second half of the planning time frame (after 2028) in contrast to the other two CEMs. Roughly 57% of the entire generation capacity is

installed after 2028 by the perfect foresight model. In contrast, the myopic foresight and rolling horizon model add about 55% of the entire new generation capacity before 2028. Investments in the transmission grid are larger in the second half of the planning time frame in all CEM runs, even though for the perfect foresight model investments are almost equally distributed between the first and the second half of the planning time frame.

All CEMs have in common that the entire newly added fossil fuel fired generation capacity is installed between 2019 and 2028 and that CSP generators are not installed before 2028. Investments in VRE are economically efficient already in 2019 in all CEM runs, as they reduce power generation from the most expensive elements of the asset fleet such as GT or old and inefficient coal power plants ("fuel saver"). However, a significant difference in the timing of VRE investments exists between the CEM runs. The myopic foresight and rolling horizon model install 14 GW of PV until 2028. Compared to that, the perfect foresight model installs only 3 GW of PV in the same time frame. Instead of installing large PV capacities, the perfect foresight model invests in large wind power capacities until 2028 (about 11 GW). In the same time frame, the myopic foresight and rolling horizon model invest only in 5 GW and 7.5 GW of wind power respectively. The large investments in wind power in the perfect foresight model are accompanied by large-scale investments for transmission grid expansion between model node N2 and N3 (see Figure 40).

The difference in timing of VRE capacity is a direct consequence of the different foresight approaches applied in the CEMs. The perfect foresight model has the capability to anticipate strongly decreasing PV investment costs until the end of the planning time frame. To not blocking cheap future PV investments with early investments in comparably expensive PV generators, the perfect foresight model postpones major PV investments until 2028. Instead, large investments in wind power are executed until 2028 by the perfect foresight model for which cost reduction is less pronounced over the planning time frame (less steep learning rate).

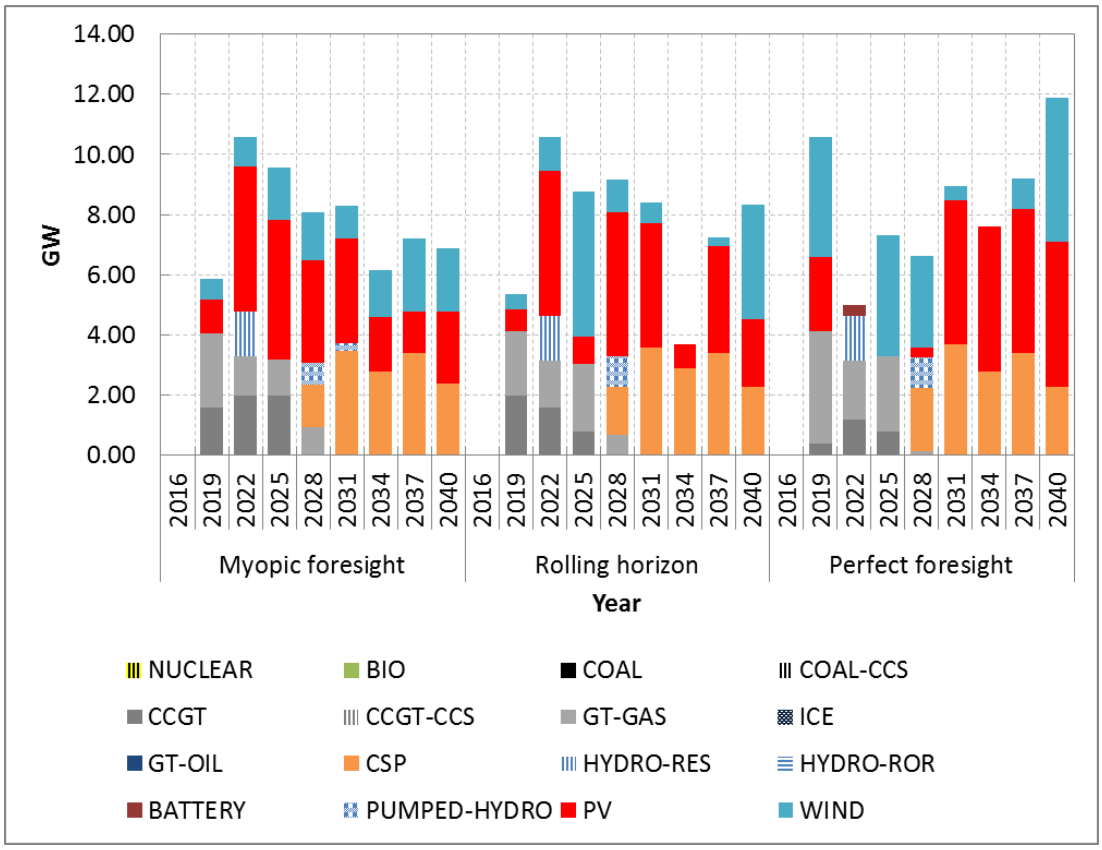

Figure 39: Newly added gross capacity by milestone year and foresight approach (Group 1)

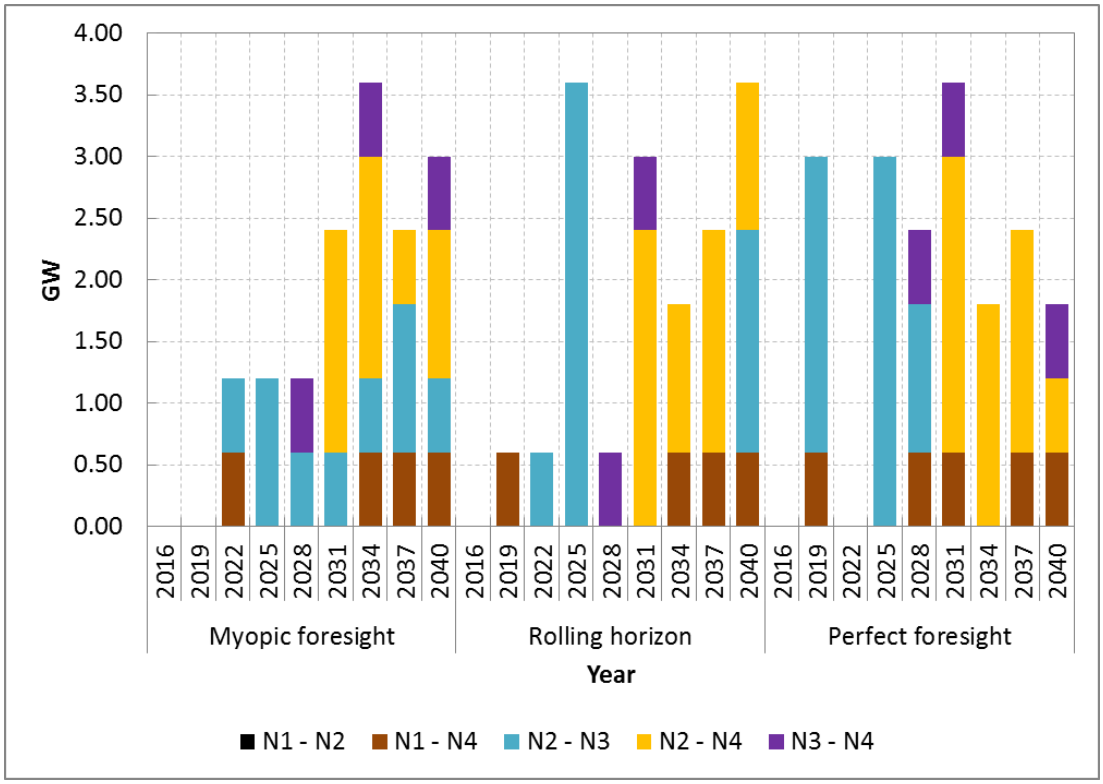

Figure 40: Newly added NTC between model nodes by foresight approach (Group 1)

Figure 41 presents the spatial distribution of the cumulative installed generation capacity computed by the three CEM runs. The major difference is the siting of PV generators. Despite the lower solar resource availability compared to model node N4, the myopic foresight model installs most PV capacity at model node N2. At the end of the planning time frame in 2040, 9.7 GW of PV is installed at model node N2. At N1 and N4, only 3.7 GW and 8.5 GW are installed respectively. In contrast, the rolling horizon and perfect foresight model installed most PV capacity at model node N4, where the highest solar resources are located. At the final year of the planning time frame, PV generators with an installed capacity of 3.6 GW, 6.7 GW, and 11 GW are sited at model node N1, N2, and N4 respectively by the rolling horizon model. In the perfect foresight model 2.5 GW, 4.2 GW, and 12.8 GW of PV are installed at model node N1, N2, and N4 respectively. The difference between the model runs is a consequence of the different capability of the CEMs to adapt investment decisions over the planning time frame according to future occurrences. The myopic foresight model does not foresee the large-scale CSP deployment at model node N4, starting in 2028, and the associated large investments in the transmission grid that allows also the transportation of electricity generated by PV from N4 to the demand centers of the power system (N1 and N4). Without this knowledge, the myopic foresight model executes large-scale PV investments at model node N2 in the milestone years 2022 and 2025 because higher solar resources at N4 do not compensate additional costs required to increase the NTC between N4 and the rest of the power system to transport electricity generated by PV at N4 (grid-related impacts of VRE).

Figure 42 presents the composition of the power supply for the entire planning time frame aggregated by technology. As longer the foresight of the CEM as higher is the share of RES-E on power supply. Hence, the highest RES-E share is computed by the perfect foresight model. About 60% of the entire electricity demand for the 24 year planning time frame is served by RES-E. The myopic foresight and rolling horizon model cover 56% and 57% of the electricity demand by RES-E. Due to the earlier large-scale wind power investments, the share of wind power on total produced electricity over the planning time frame is highest in the perfect foresight model.

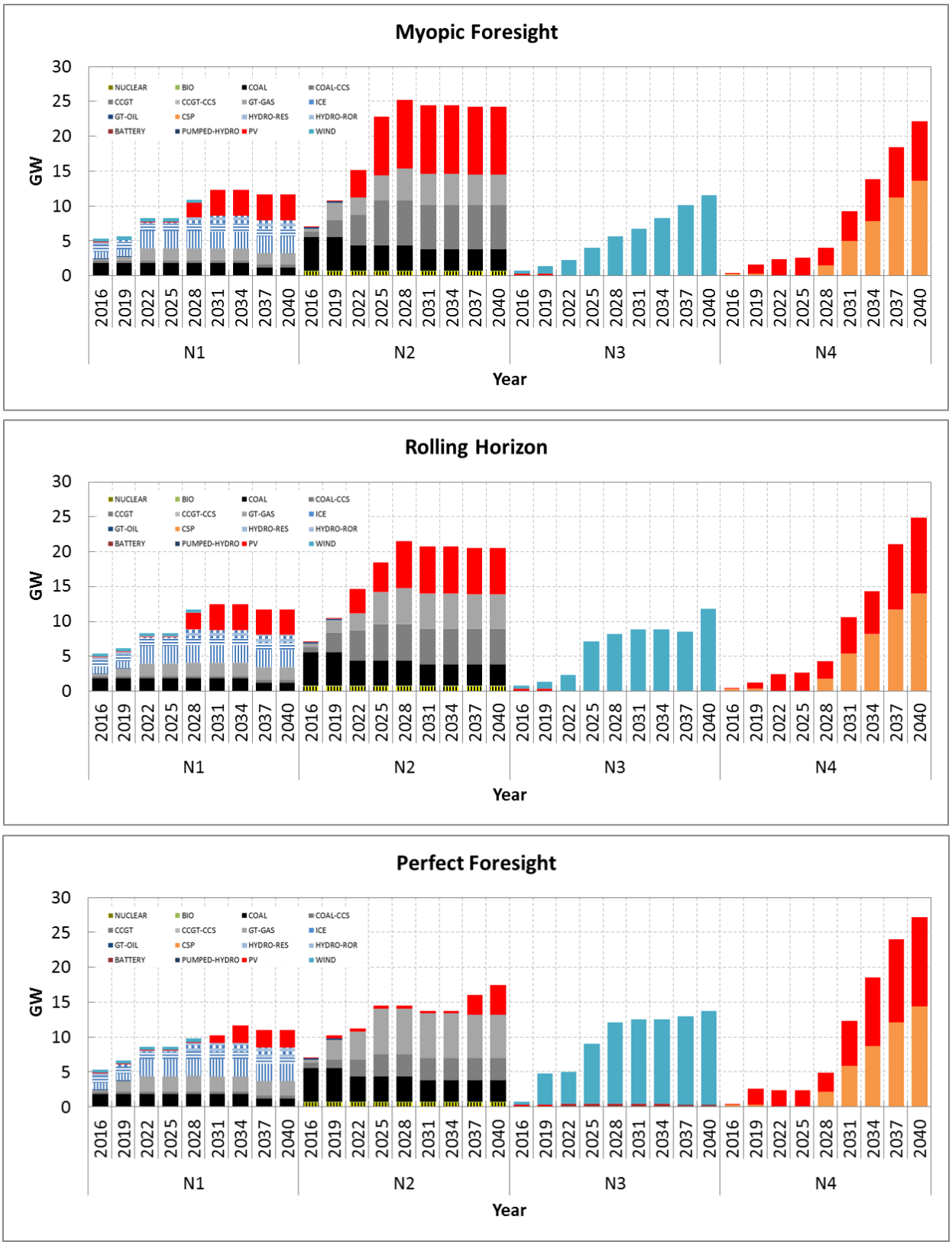

Figure 41: Spatial distribution of cumulative installed gross capacity foresight approaches (Group 1)

Also power generation from CSP is highest for the perfect foresight model. The share of power generation from PV and CCGT is largest in the myopic foresight model, which is a result of investment decisions in the first half of the planning time frame. Power generation shares from coal, nuclear, hydro power, and biomass are similar in all three models.

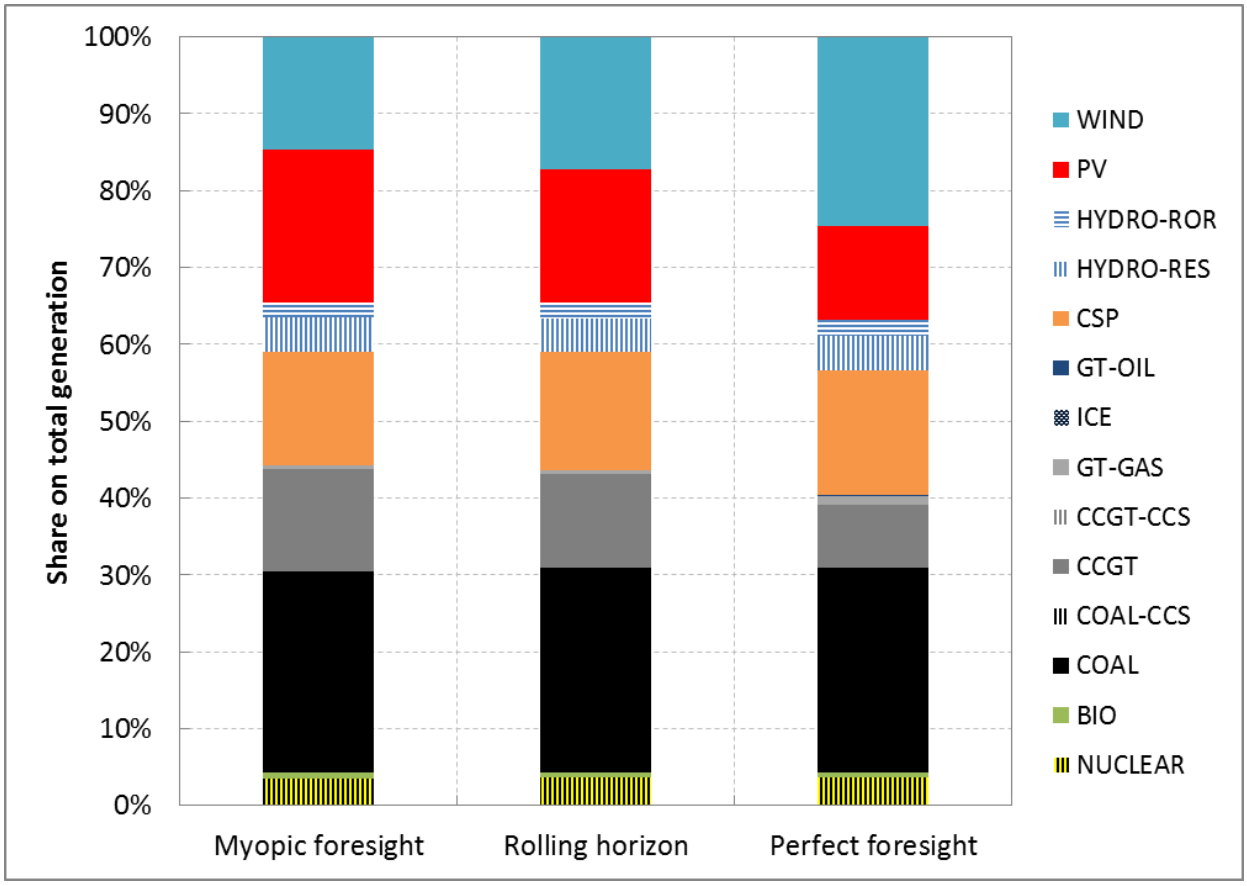

Figure 42: Composition of total power supply for the planning time frame (Group 1)

The asset fleet determined by the perfect foresight model reaches with 82% the highest RES-E share at the end of the planning time frame in 2040 (see Figure 43). Compared to that, the least-cost asset fleets computed by the myopic foresight and rolling horizon model reach only a RES-E share of 78% and 79% respectively in 2040. The results of the three CEM runs are in line with the theory of the transitional utilization effect. For example, capacity factors of existing coal generators are reduced by about 50% over the planning time frame in all three CEM runs.

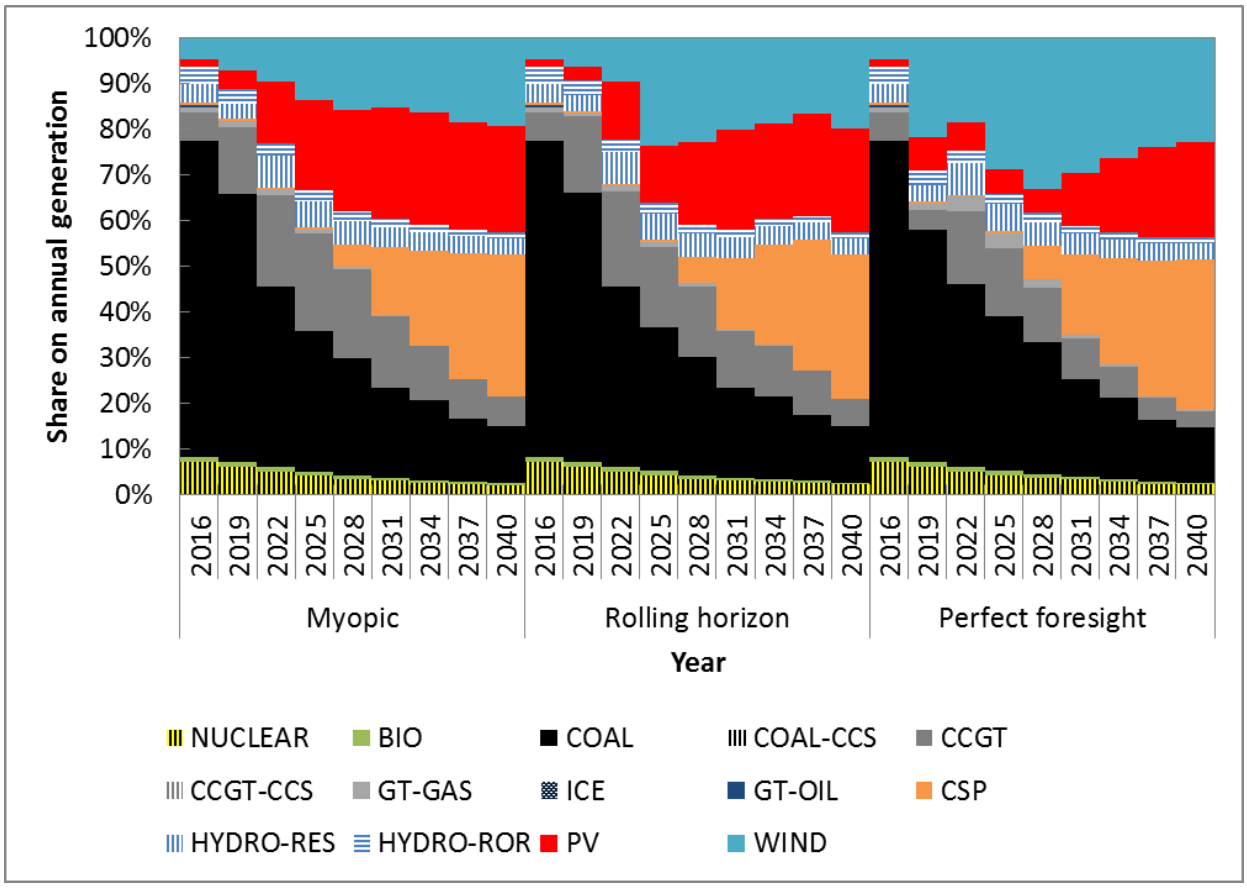

Figure 43: Composition of power supply by milestone year (Group 1).

Figure 44 presents the average supply costs of the power system over the planning time frame for the three foresight approaches. Average supply costs are defined according to equation (64). The sum of annual system CAPEX and OPEX is divided by the annual electricity demand of the system.

$$Averrage\ Supply\ Costs_y = \frac{CAPEX_y^{System} + OPEX_y^{System}}{Demand_y^{System}} \quad (64)$$

As the existing asset fleet in 2016 is the same for all CEM runs, average supply costs of the system in 2016 are identical for all three CEM runs (71.8 USD/MWh). Average supply costs increase almost identical until the end of the planning time frame in the myopic foresight and rolling horizon model and reach 81.0 USD/MWh and 80.6 USD/MWh respectively in 2040. Average supply costs of the perfect foresight model increase more sharply in the first part of the planning time frame but this level off after 2028. In 2031, average supply costs are almost similar to those of the myopic foresight and rolling horizon model. Afterwards, average supply

costs are considerably lower and reach 79.2 USD/MWh in 2040. The development of the average supply costs of the power system highlights again the advantage of the perfect foresight model to adapt investment decisions according to future occurrences. Higher costs in the short-term are accepted to a certain degree if its pay out in the long-term. In a less extent this behavior can also be observed for the rolling horizon model.

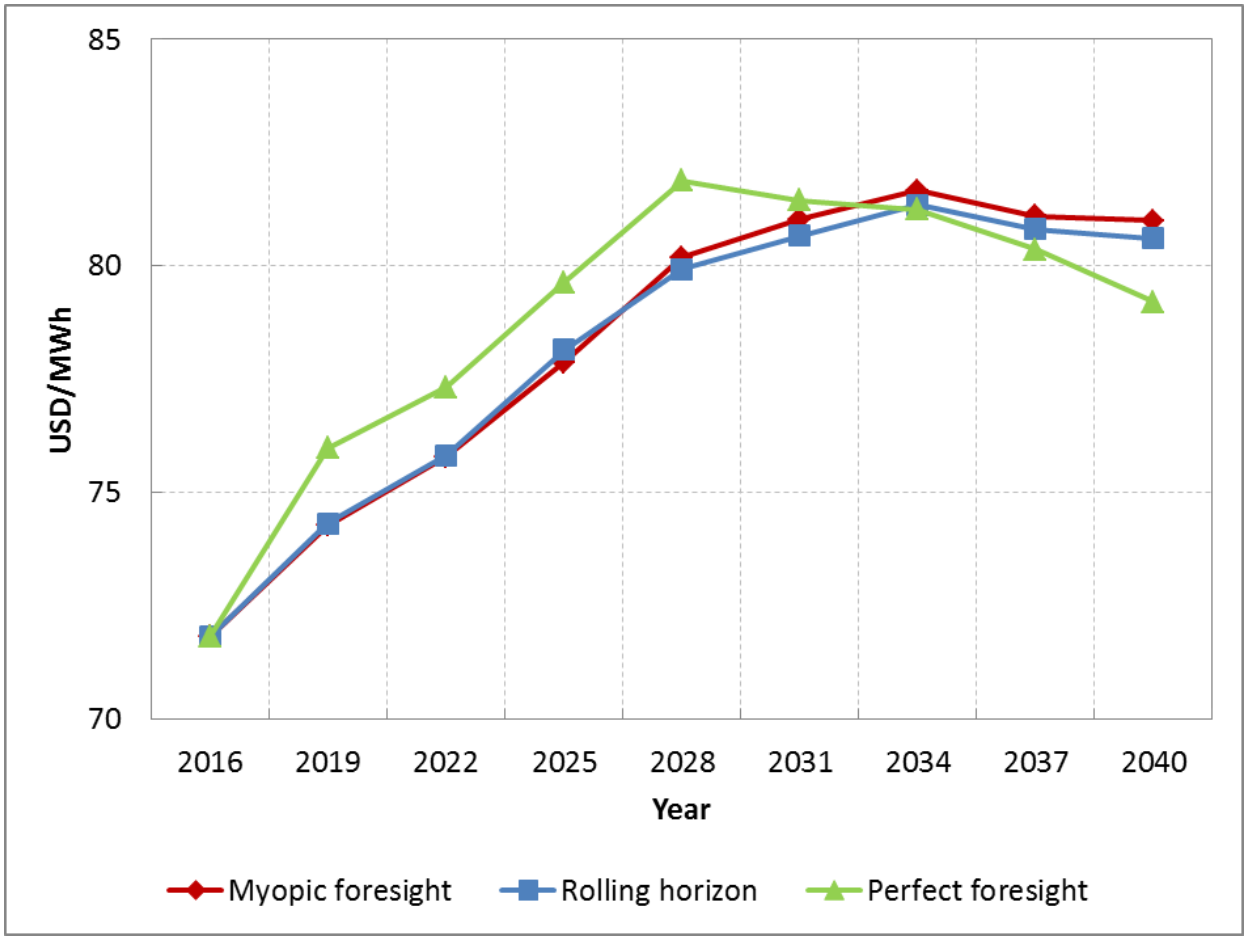

Figure 44: Development of average supply costs over the planning time frame by foresight approach (Group 1)

Table 16 presents the net present value (NPV) of the total system costs over the planning time frame as well as computing time to solve the optimization problem (expressed in percentage of the myopic foresight model). While significant differences in investment decisions could be observed for the three different foresight approaches, total system costs over the planning time frame are very similar. Compared to the myopic foresight model, total system costs of the rolling horizon and perfect foresight model are only 0.39% and 1.23% lower respectively. This

indicates that the capacity expansion optimization problem has a very flat optimum, meaning that several solutions exist with very similar total system costs over the planning time frame.

The myopic foresight model required the less computing time to solve the capacity expansion optimization problem. However, the computing time of the rolling horizon model was only 8% higher. The perfect foresight model required significantly more computational effort than the other two CEMs. Solving the optimization problem in one large optimization period with perfect foresight requires almost four times more computational effort than solving the optimization problem with a single-year myopic foresight. The relatively low difference in computing time between the myopic foresight and the rolling horizon model can be explained by the fact that for each optimization period (nine in the myopic foresight, three in the rolling horizon model), the CEM must be compiled again before the actual optimization period can be solved. This process can take a considerable amount of time and partially levels off reduced computing time to solve the optimization problem of the respective optimization period.

Table 16: Total system costs and computing time by foresight approaches (Group 1)

	Myopic foresight	Rolling horizon	Perfect foresight
Total system costs (NPV)	100%	99.61%	98.77%
Computing time	100% 343 sec.	108% 370 sec.	396% 1360 sec.

5.2.4 Results for sudden introduction of CO_2 prices

Figure 45 presents the total newly installed generation capacity over the planning time frame for the three CEM runs of Group 2. Similar to the CEM runs of Group 1, more than 60 GW of new capacity is added until 2040 in each CEM run. Again, the perfect foresight model installs most capacity (66 GW). Investments in VRE by the three CEM runs are also very similar compared to the CEM runs of Group 1. Firstly, most VRE capacity is installed by the perfect foresight model due to larger wind power investments, and secondly significantly more PV than wind power is installed by all CEMs. The share of VRE on total generation capacity expansion is about 56% in the myopic foresight and rolling horizon model and almost 59% in the perfect foresight model.

Whereas investments in VRE are very similar in the respective CEM runs of Group 1 and Group 2, significant differences can be observed for the residual system. In Group 1, no investments in coal generators are executed in any of the three CEM runs. In contrast, the myopic foresight and rolling horizon model of Group 2 make considerable investments in coal power plants due their limited information about future CO_2 price developments. The myopic foresight model invests in 4.8 GW of new coal capacity (eight units). The rolling horizon model installs new coal power plants with a capacity of 3.6 GW (six units). The perfect foresight model has information about all future occurrences over the planning time frame and adapts its investment decisions accordingly. Due to the high CO_2 prices in the second half of the planning time frame and the large-scale deployment of VRE, the perfect foresight model avoids investments in coal generators.

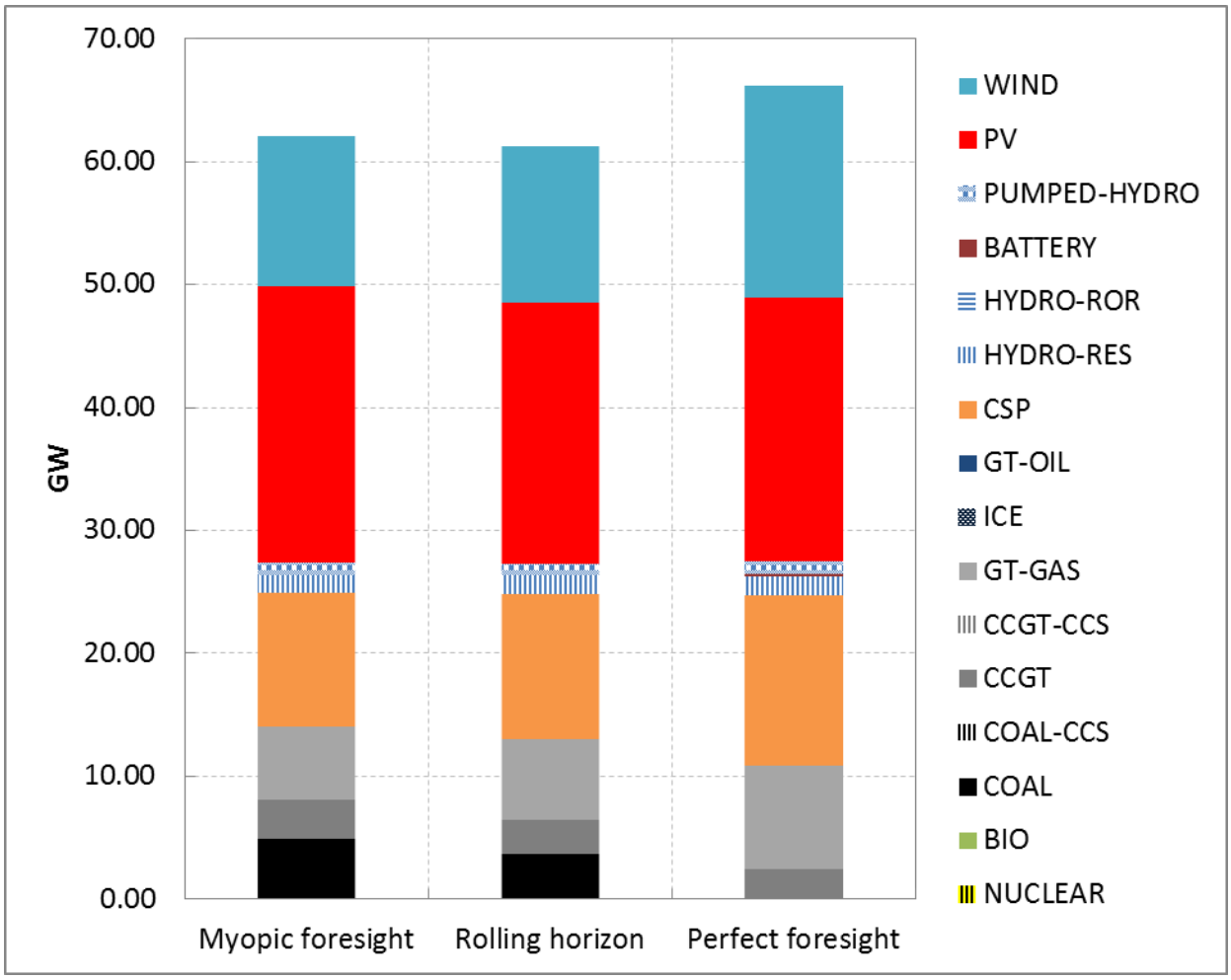

Figure 45: Total added gross capacity by foresight approach (Group 2)

Also regarding investments in CCGT generators some differences can be observed between the three CEM runs of Group 2. The perfect foresight model installs the less CCGT capacity (2.4 GW) over the planning time frame. The myopic foresight and rolling horizon model install 3.2 GW (two more units) and 2.8 GW (one more unit) of CCGT capacity respectively. Instead investing in fossil fuel fired CCGT generators, which would lead to significant CO_2 emissions, the perfect foresight model installs significantly more dispatchable CSP generators. CSP units with a total capacity of 13.9 GW are installed until 2040 by the perfect foresight model. This is 3.1 GW and 2.1 GW more CSP capacity than installed by the myopic foresight and rolling horizon model respectively. Similar to the CEM runs of Group 1, CSP units are equipped with a 10h TES and a BB with 100% of thermal turbine capacity in all CEM runs. Also more GT capacity is installed by the perfect foresight model compared to the other two CEMs. 8.35 GW of GT power plants are added by the perfect foresight model. The myopic foresight and rolling horizon models invest only in 6.0 GW and 6.55 GW of new GT capacity respectively. Similar to the CEM runs of Group 1, all CEMs runs of Group 2 deploy the entire additional available reservoir hydro (1.5 GW) and pumped-storage (1 GW) potential. Also in Group 2, investments in Lithium-ion batteries do not belong to the least-cost expansion plan in the myopic foresight and rolling horizon model but do in the perfect foresight model. The perfect foresight model invests in 0.25 GW of Lithium-ion batteries. Also in the CEM runs of Group 2, nuclear and biomass generators as well as CCS technologies are not part of the least-cost expansion plan.

The newly added NTC between model nodes of the system is presented in Figure 46. With 18 GW, the perfect foresight model installs the most additional NTC (similar as in Group 1). The myopic foresight and rolling horizon models invest in 13.8 GW and 15.6 GW of NTC respectively. Hence, the differences between investments in the transmission grid between CEM runs of Group 2 are significantly higher than between the CEM runs of Group 1 (maximum difference between CEM runs of Group 1 was 2.4 GW). The higher difference between the perfect foresight and the other two CEMs is mainly driven by the significant larger investments in CSP in the perfect foresight model, which requires larger grid investments to transport electricity from model node N4 to the demand centers of the power system that are located at N1 and N2.

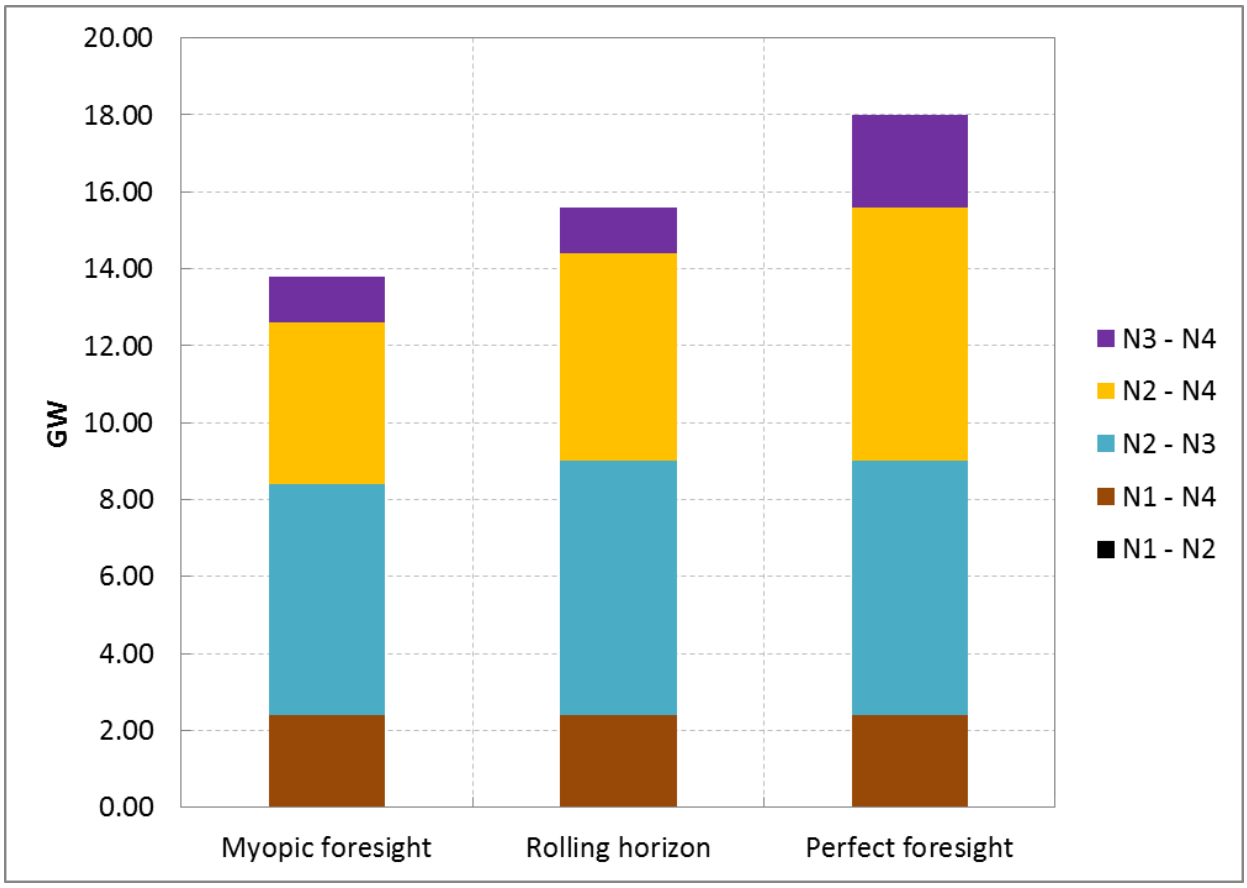

Figure 46: Total added NTC between model nodes by foresight approach (Group 2)

The timing of investments in new generation capacity for the CEM runs of Group 2 is shown in Figure 47. The limited foresight and its consequences on investment decisions made by the myopic foresight and rolling horizon models can be clearly recognized. The myopic foresight model invests in 4.8 GW of coal power plants until 2028 as the strong increase of CO_2 prices after 2028 cannot be foreseen by the CEM. The rolling horizon model has partial information about the strongly increasing CO_2 prices between 2028 and 2040 and therefore adapts its investment decisions. In the first of the three sub-periods of the rolling horizon model (2016 - 2022) 3.0 GW of coal power plants are installed, which is the same quantity that is installed by the myopic foresight model until 2022. However, in the second optimization period of the rolling horizon model (2025 - 2031) only one more coal power plant (0.6 GW) is added because increasing CO_2 prices in the future can be partially foreseen by the CEM. Compared to that, the myopic foresight model invests in another three coal units (1.8 GW) until 2028. Instead of installing additional coal power plants, the rolling horizon model invests in more wind power and CSP generators. As the perfect foresight model has information about all future

occurrences, investments in coal power plants are completely avoided because high generation costs of coal power plants due to increasing CO_2 prices and a large-scale deployment of VRE over the planning time frame are anticipated by the CEM.

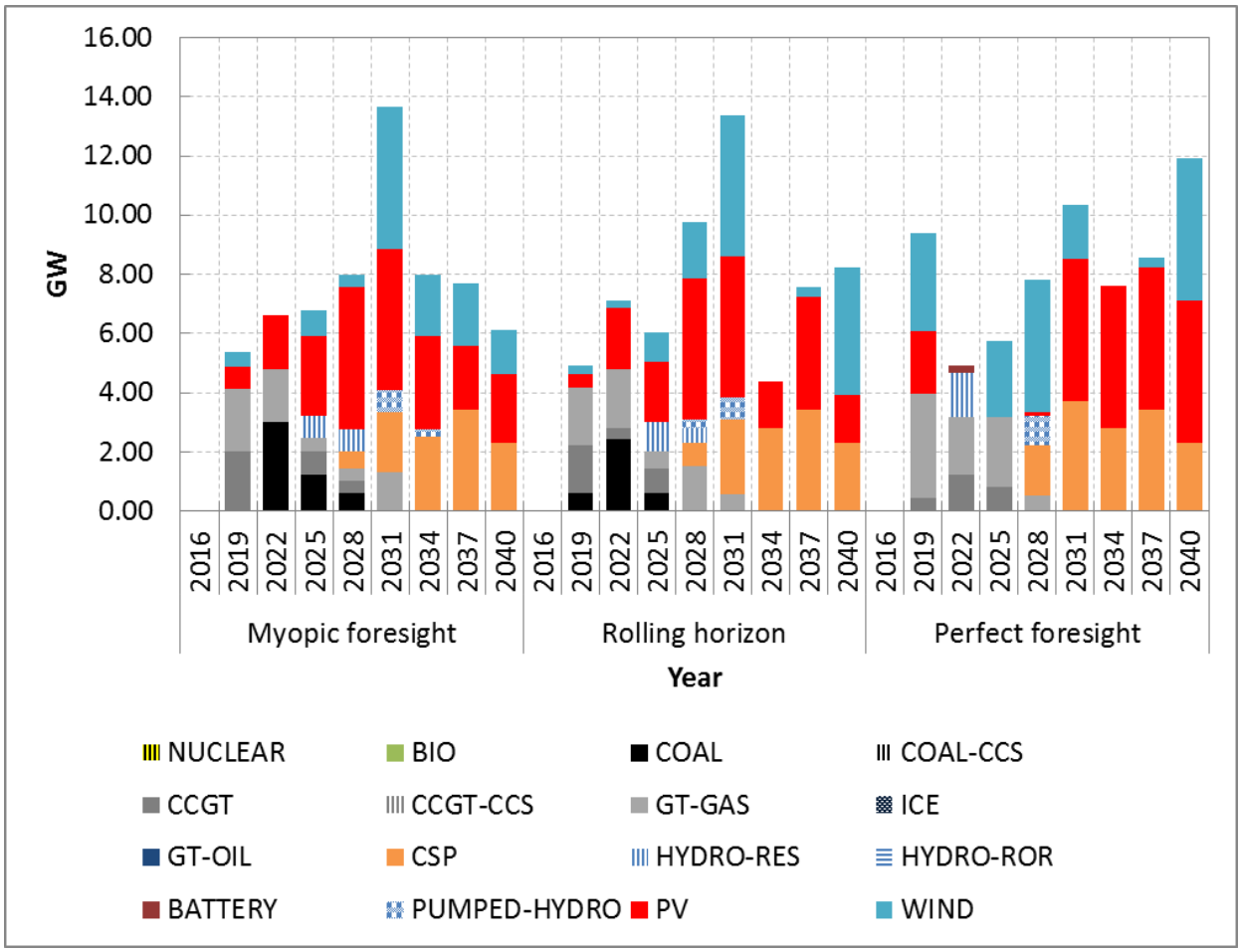

Figure 47: Newly added gross capacity per milestone year by foresight approach (Group 2).

Table 17 compares the development of the capacity factor, SRMC, and long run marginal costs (LRMC) of the coal and the CSP units installed in 2028 by the myopic foresight model. The capacity factor of the coal unit decreases from 75% in 2028 to 50% in 2040, due to a large-scale deployment of VRE. According to the assumptions for fossil fuel and CO_2 price development, the SRMC of the coal unit increase from 37 USD/MWh in the first year of operation to 71 USD/MWh at the final year of the planning time frame. Combined with the decreasing capacity factor, this leads to an increase of the LRMC from 67 USD/MWh in 2028 to 117 USD/MWh in 2040. In contrast, the installed CSP units have a constant capacity factor of 45% until the end of the planning time frame. The capacity factor is not affected by the large-scale deployment of VRE

due to the low SRMC of the CSP units. As a consequence of a constant capacity factor and stable SRMC, also the LRMC of the CSP units are constant until the end of the planning time frame (86 USD/MWh). The rolling horizon (partially) and the perfect foresight model do have information about these future occurrences and therefore install significantly more CSP units in 2028 than the myopic foresight model.

Table 17: Performance of coal and CSP units installed by the myopic foresight model in 2028 (Group 2)

	COAL (1 unit, 0.6 GW)			CSP (6 units, each 0.1 GW)		
	Capacity factor [%]	SRMC [USD/MWh]	LRMC [USD/MWh]	Capacity factor [%]	SRMC [USD/MWh]	LRMC [USD/MWh]
2028	75	37	67	45	18	86
2031	62	54	90	45	18	86
2034	54	65	107	45	18	86
2037	51	69	113	45	18	86
2040	50	71	117	45	18	86

The cumulative installed generation capacity over the planning time frame and its spatial distribution is shown in Figure 48 and Figure 49 respectively. In all CEM runs, the installed VRE capacity in 2040 represents about 50% of total installed capacity. The persistent utilization effect for the residual system is significantly more pronounced in the perfect foresight model due to the abdication of investments in coal power plants. In 2040, base-load generators represent only 14% of the residual asset fleet due to large investments in dispatchable peak- and mid-merit generators, such as GT, CCGT, and CSP, which accompanies the large-scale integration of VRE. The share of base-load generators is considerably higher in the myopic foresight (30%) and rolling horizon models (25%), which do not at all (myopic foresight) or only partially (rolling horizon) foresee the strongly increasing CO_2 prices and high shares of VRE towards the end of the planning time frame. Similar to the CEM runs of Group 1, significant PV capacities are installed at model node N2 in the myopic and rolling horizon models, whereas the perfect foresight model installs most PV capacity at N1 and N4. The additional coal power plants that are built in the myopic and rolling horizon model are installed at model node N2 where the largest electricity demand exists. The perfect foresight model instead avoids these coal installations at N2 and starts to invest earlier in wind power at model node N3. The wind power

installations are accompanied by large investments in GT at model node N2 in order to ensure adequacy of the system from a long-term planning and a reliable system operation from short-term operation perspective.

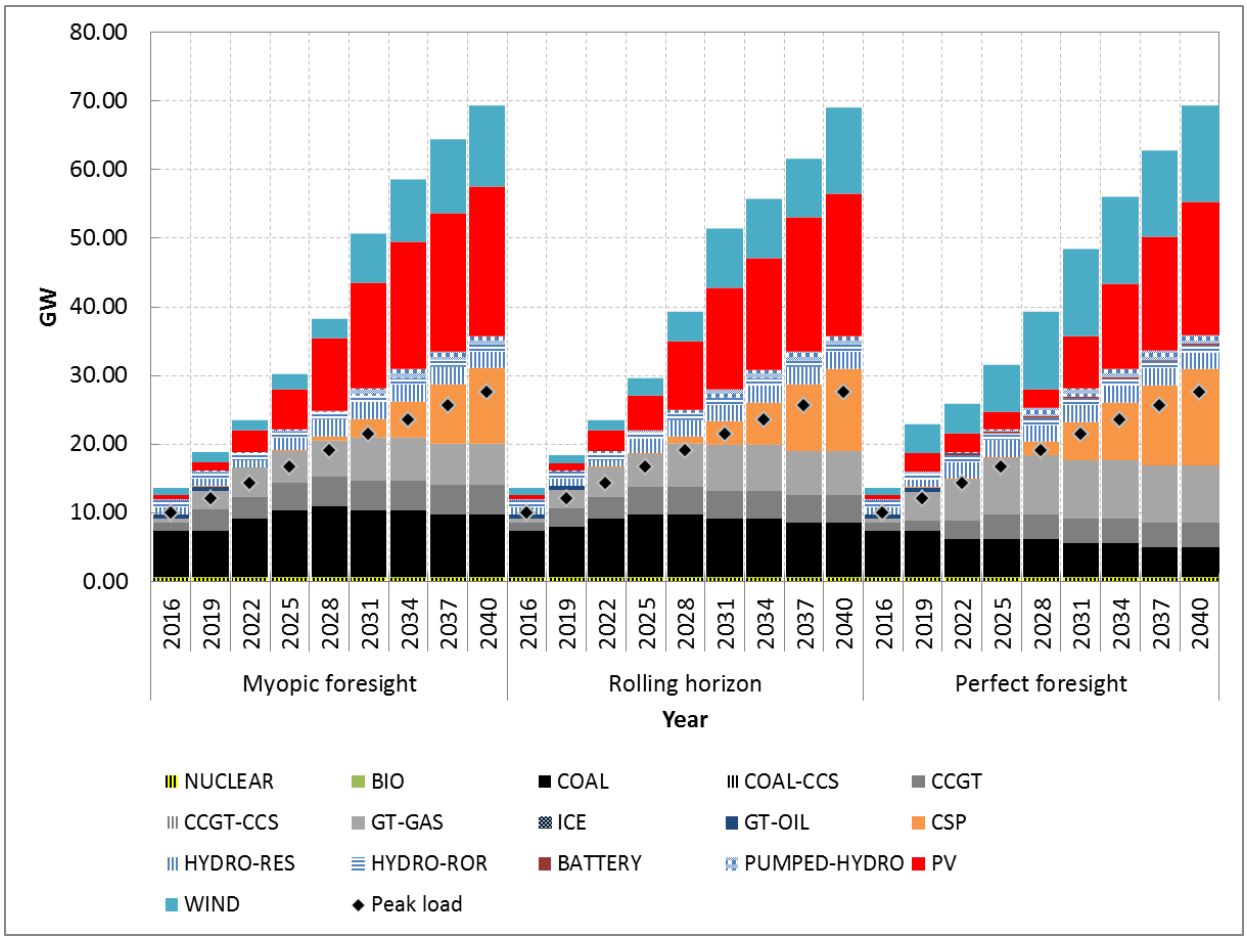

Figure 48: Cumulative installed gross capacity by foresight approach (Group 2)

Figure 50 and Figure 51 present the composition of total power supply over the total planning time frame and its development by milestone year respectively aggregated by technology. As the myopic foresight and the rolling horizon model invests significantly in coal generators while the perfect foresight model does not, the share of power production from coal over the entire planning time frame is considerably lower in the perfect foresight model. Similar to the CEM runs of Group 1, the highest RES-E generation share is reached by the perfect foresight model. However, differences between the model runs are more pronounced for the CEMs of Group 2. The share of power generation from RES-E over the entire planning time frame is 58% in the perfect foresight model.

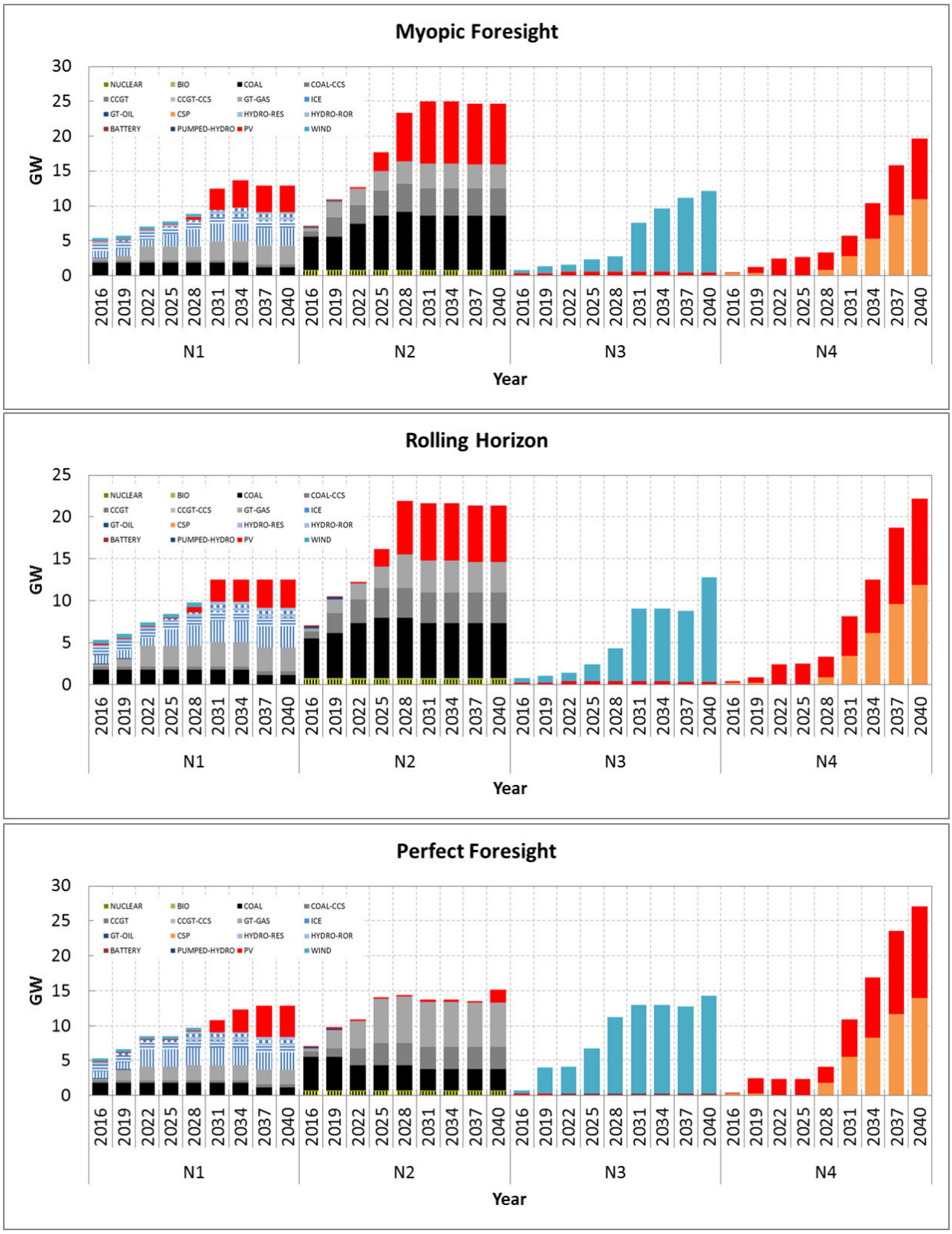

Figure 49: Spatial distribution of cumulative installed gross capacity by foresight approach (Group 2)

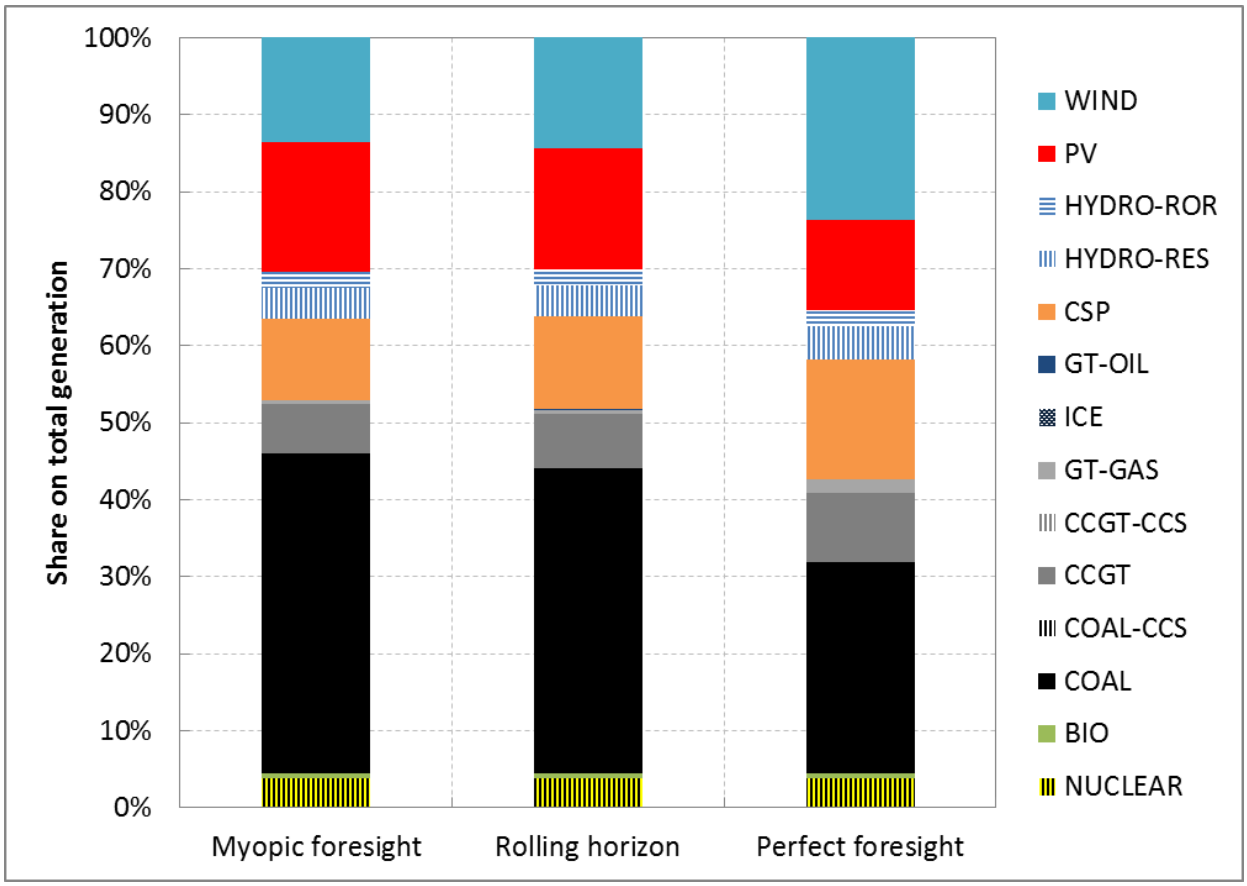

Figure 50: Composition of total power supply for the planning time frame (Group 2)

For the myopic foresight and rolling horizon model, the RES-E share on total power generation over the planning time frame is only 48% and 49% respectively. Until the end of the planning time frame in 2040, the RES-E share is increased from 16% in 2016 to 82% in the perfect foresight model. In the myopic foresight and the rolling horizon model only 74% and 76% of the electricity is generated by RES-E respectively in 2040.

Figure 52 shows the average supply costs of the power system over the planning time frame for the three CEM runs of Group 2. The development of average supply costs is very similar for the myopic foresight and rolling horizon model. The development is characterized by a decrease until 2022 due to large investments in coal generators with low generation costs at the time of installation. However, from 2025 until 2034 when CO_2 emission prices are suddenly introduced and increase strongly, average supply costs of the myopic foresight and rolling horizon model increase sharply. After 2034, due to the large-scale deployment of cheap RES-E average supply costs of the power system decreases again despite a further increase of fossil fuel and CO_2

prices. From 2031, the rolling horizon model has slightly lower average supply costs than the myopic foresight model. Until 2028, the average supply costs of the perfect foresight model are considerably higher compared to the other two CEMs, mainly caused by the early investments in RES-E instead of large investments in coal generators. The abdication of investments in coal power plants and the preponed investments in RES-E pays of in the second half of the planning time frame. The sudden introduction of CO_2 prices in 2025 and the strong increase of them between 2028 and 2034 do not affect the generation costs of the asset fleet as much as the asset fleets of the myopic foresight and rolling horizon model due to higher generation shares of RES-E and gas-fired generators. Hence, average supply costs between 2025 and 2034 increase considerably less sharply in the perfect foresight model. In 2031, average supply costs of the perfect foresight model are already similar to the average supply costs of the other two CEMs and afterwards significantly lower. In 2040, the perfect foresight model has average supply costs of only 79.2 USD/MWh, which is a difference of 3.1 USD/MWh and 2.3 USD/MWh to the myopic foresight (82.3 USD/MWh) and rolling horizon model (81.6 USD/MWh) respectively.

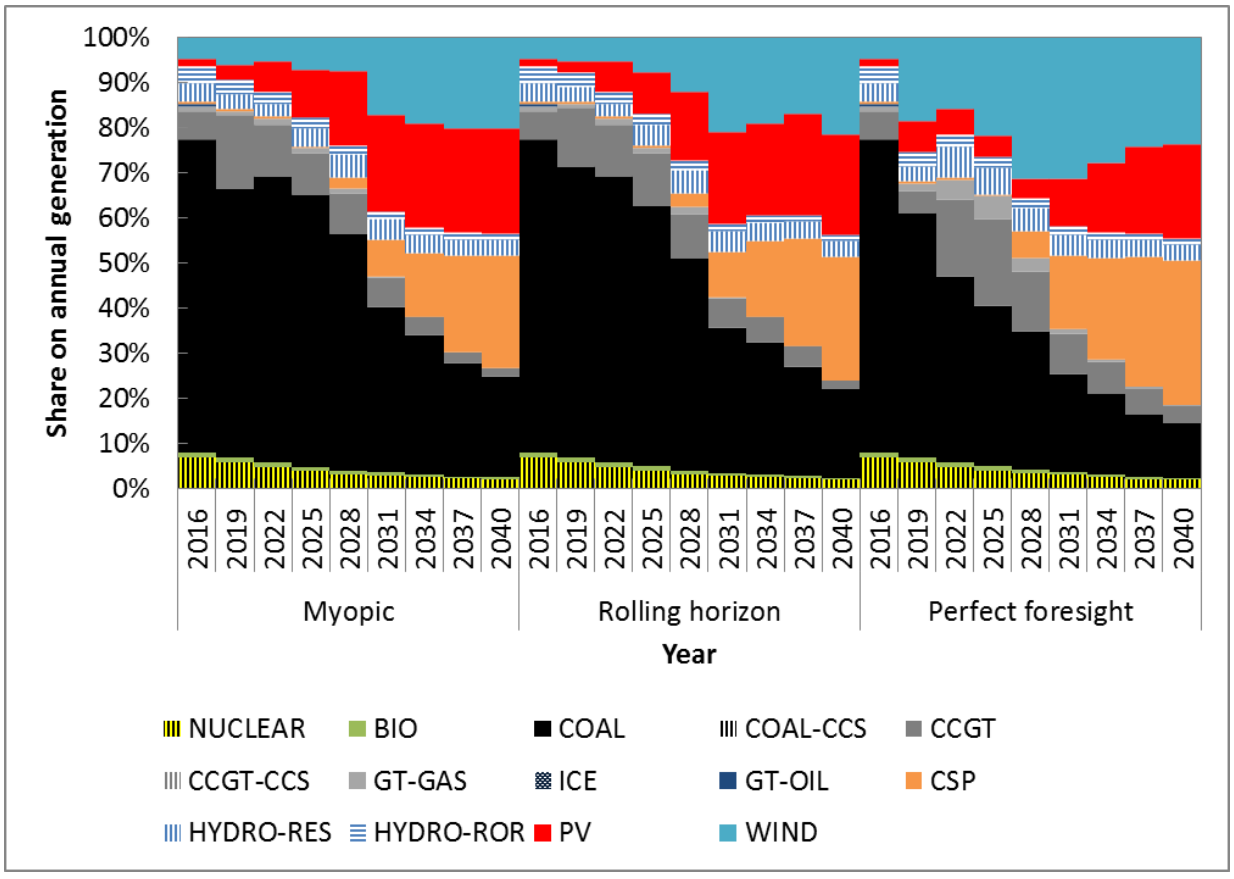

Figure 51: Composition of power supply by milestone year (Group 2)

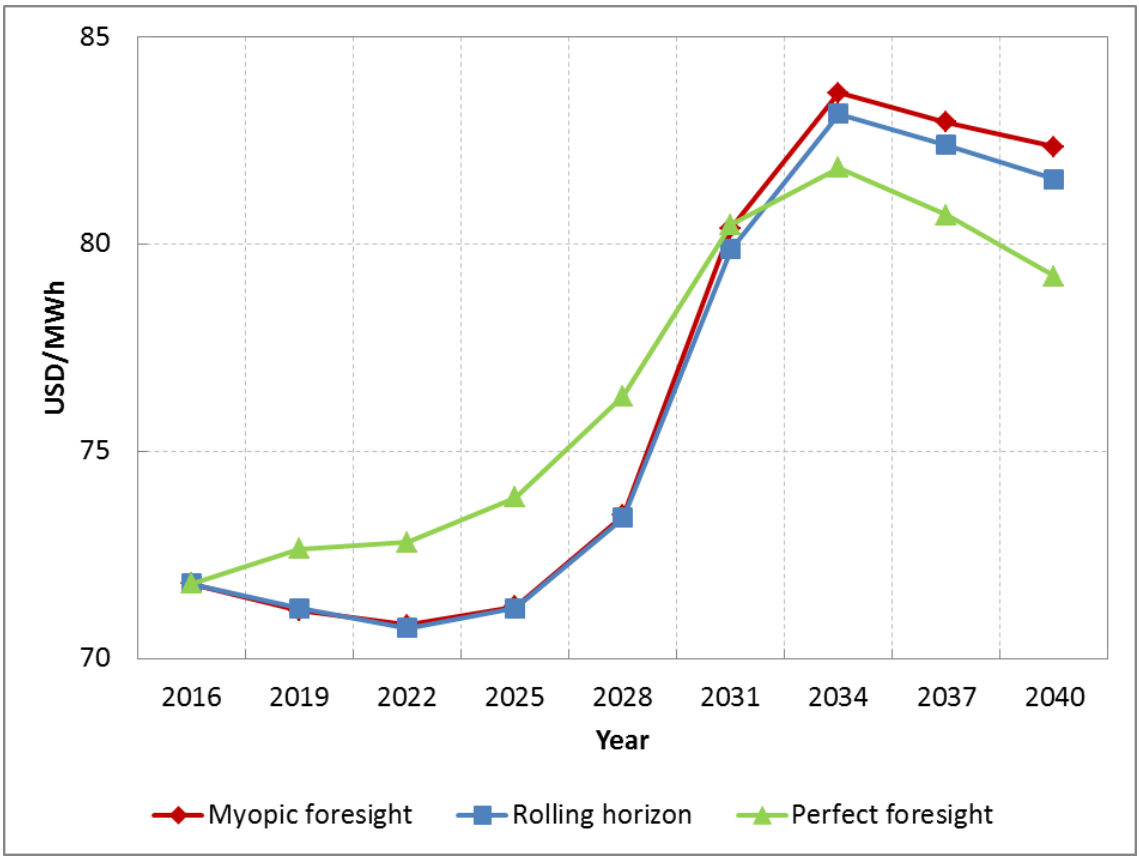

Figure 52: Average supply costs over the planning time frame by foresight approach (Group 2)

Table 18 presents the total system costs (NPV) to meet electricity demand and reliability standards over the planning time frame as well as computing time to solve the capacity expansion optimization problem formulated in the three CEM runs of Group 2. The difference between the total system costs is about twice as much as in the CEM runs of Group 1. Compared to the myopic foresight model, the total system cost of the rolling horizon and perfect foresight model is 0.75% and 2.4% lower respectively. The difference for the CEMs runs of Group 1 is only 0.39% (rolling horizon) and 1.23% (perfect foresight). Computing time of the rolling horizon model is 35% higher than for the myopic foresight model. The computing time of the perfect foresight model is more than three times higher than computing time of the myopic foresight model.

Table 18: Total system costs and computing time by foresight approach (Group 2)

	Myopic foresight	Rolling horizon	Perfect foresight
Total system costs (NPV)	100%	99.25%	97.60%
Computing time	100% 381 sec.	135% 515 sec.	311% 1185 sec.

5.2.5 Summary and discussion

The analysis has shown that the applied foresight approach has a significant impact on results for capacity expansion optimization but also on computational effort. For the parameter set of Group 1, computing time for the perfect foresight model was about 4 times higher than for the single-year myopic foresight model. For the parameter set of Group 2, the perfect foresight model required about three times more computing time than the single-year myopic foresight model. Computing time for the multi-annual rolling horizon model was about 8% (Group 1) and 35% (Group 2) respectively higher than for the single-year myopic foresight model.

Results of the CEM runs of Group 1 showed that if input parameters change continuously over the planning time frame results for the myopic foresight, rolling horizon, and perfect foresight model differ only moderately in terms of total system costs. The solution computed by the perfect foresight model was 0.39% and 1.23% cheaper than the solution determined by the rolling horizon and myopic foresight model respectively.

However, when results are analyzed in detail, several differences can be observed in terms of technology choice (which?), siting (where?), and timing (when?) of new capacity. For example, most CSP units are installed by the perfect foresight model. In contrast to the myopic and rolling horizon model, the perfect foresight model is able to fully consider the advantage of CSP to provide dispatchable and firm capacity at stable generation costs over the planning time frame. Therefore, the CEM increases CSP and decreases CCGT capacity compared to the myopic and rolling horizon model. CCGT represent also firm and dispatchable capacity but cannot provide stable generation costs over the period of study because of increasing fuel and CO_2 prices.

As demonstrated by the CEM runs of Group 2, differences between the foresight approaches are significantly higher if some of the input parameters change suddenly at one point of the planning time frame (e.g. in this analysis CO_2 prices). These findings are in line with results presented in [92], [94]. The solution computed by the perfect foresight model of Group 2 was 0.75% and 2.4% cheaper than the solutions determined by the rolling horizon and myopic foresight model of Group 2 respectively. The larger the foresight the higher is the capability of the CEM to react on future occurrences already in advance and adapt investment decisions accordingly. The myopic foresight model of Group 2 invests in a large number of coal units in

the first half of the planning time frame when CO_2 emissions are on a very low level. In contrast, the perfect foresight model foresees strongly increasing CO_2 prices in the second half of the study period and avoids investments in coal generators completely. Instead, investments in RES-E are preponed to reduce CO_2 emission of the system. Due to its limited foresight, the myopic foresight model misses this opportunity, which leads to higher total system costs.

All foresight approaches have their justification and the suitability depends on the objective of the analysis. In the case an optimal expansion pathway for a power system under a given set of input parameters is the aim of the analysis, the perfect foresight approach is the most suitable approach due to its capability to identify the intertemporal global optimum over the planning time frame [93]. Derived results represent the optimal allocation of resource usage and can be interpreted as the upper limit of the performance of the system.

In the case the study aims to investigate the consequences of unpredictable events for the power system, such as a sudden increase of CO_2 prices or the introduction of any political target (e.g. nuclear phase-out), the myopic foresight approach may better represent the real-life behavior and the evolutionary nature of power systems [94], [95]. However, using the myopic foresight approach changes the character of the optimization model towards a simulation model and results cannot be interpreted anymore as the global optimum to meet demand, reliability standards, and defined targets for the system over the planning time frame.

The rolling horizon approach offers a compromise between the perfect foresight and the myopic foresight approach in terms of computing time but also in terms of the frame conditions of real-life decision makers. Both, a perfect foresight and a single-year myopic foresight, do not reflect the frame conditions of decision makers realistically. In reality future developments of e.g. technology and fuel costs are characterized by uncertainties that increase with the length of the planning time frame. Real-life decision makers do not have perfect information about these developments. However, assuming decision makers have no information at all about future developments is also unrealistic and underestimates strategic planning capabilities significantly. Therefore, the multi-annual rolling horizon approach can be an appropriate approach especially for utilities that want to identify economic efficient investment options under a more conservative assumption than perfect foresight.

5.3 Impact of applied system-operational detail

5.3.1 Hypothesis

Long-term CEMs with multi-annual planning time frames have typically a reduced system-operational detail compared to PCMs due to computational constraints. To keep CEMs manageable, the temporal resolution is reduced from the hourly or sub-hourly ideal to a limited number of representative annual dispatch periods. Furthermore, UCCs of thermal generators are neglected as this would increase complexity of the optimization problem significantly. Historically, long-term CEMs used the integral balance method for capacity expansion optimization, as this approach causes low computational effort and is highly suitable for power systems dominated by conventional thermal power plants whose performance is affected only marginally by fluctuating external influences such as the weather [96]. However, recently it's becoming clear that using the integral balance method is inappropriate for capacity expansion planning with VRE because the value of energy at its time of the delivery and the flexibility effect caused by a large-scale deployment of VRE cannot be considered.

To overcome the limitations of the integral balance method, REMix-CEM applies the semi-dynamic balance method for a better representation of the short-term dynamics of demand and supply of the power system, for which importance increases with the large-scale deployment of VRE. The semi-dynamic balance method uses representative days with chronological dispatch periods to capture seasonal and diurnal variability of load and RE resource availability. This enables REMix-CEM to consider the value of energy at its time of the delivery for the various investment options on the one hand and to capture the flexibility effect caused by VRE on the other hand. The flexibility effect can be considered during capacity expansion optimization by applying UCCs, which limit the flexibility of thermal generators to follow the chronological (residual) load. However, the method for assigning values of RE resource availability to the considered dispatch periods of the CEM is an area of active research and considering UCCs of thermal generators during capacity expansion optimization comes at high computational costs. Therefore, this section aims to investigate two important issues for long-term capacity expansion planning with VRE:

I) The impact of the applied method to assign values for RE resource availability to the dispatch periods of the CEM on model results.

II) The impact of considering UCCs of thermal generators, and hence the flexibility effect, during capacity expansion planning on model results and computational effort.

5.3.2 Methodology

The fictitious power system described in Section 5.1 is used for the analysis. Four CEM runs are executed, each with a common set of input data. Similar to the case study of the previous section, variability of system load over the year is represented by one working and one weekend day per month with hourly dispatch periods. Seasonal and diurnal variability of RE resources is described by one daily resource profile per month. The only difference between the CEM runs is the applied method for assigning values of RE resource availability to the dispatch periods and the way how UCCs of thermal generators are considered.

Figure 53 presents the flow diagram of the analysis. In a first step, the least-cost expansion plans computed in the four CEM runs are compared to evaluate the impact of the applied approach in the respective CEM on investment decisions. In addition, the required computing time to solve the optimization problem formulated in the respective CEM is compared. In a second step, the accuracy of each capacity expansion modelling approach in approximating system operation is validated by performing a detailed production cost analysis for the proposed asset fleet of the last year of the planning time frame (year 2040). For this purpose, the developed optimization model of this work is used as detailed production cost model (REMix-PCM). For production cost modelling the dynamic balance method with an hourly resolution (8760 annual dispatch periods) and the full set of UCCs for conventional thermal generators is applied. Hence, REMix-PCM applies a significant higher system-operational detail and results can be used to benchmark the capability of the respective CEM to approximate system operation accurately during capacity expansion optimization. Results for system operation calculated by the detailed PCM are compared with results determined by the corresponding less detailed CEM. Values that describe the operation of the system comprise annual average supply costs of the system, annual system OPEX, technology-specific generation shares, CO_2 emissions of the system, and curtailment of VRE electricity production.

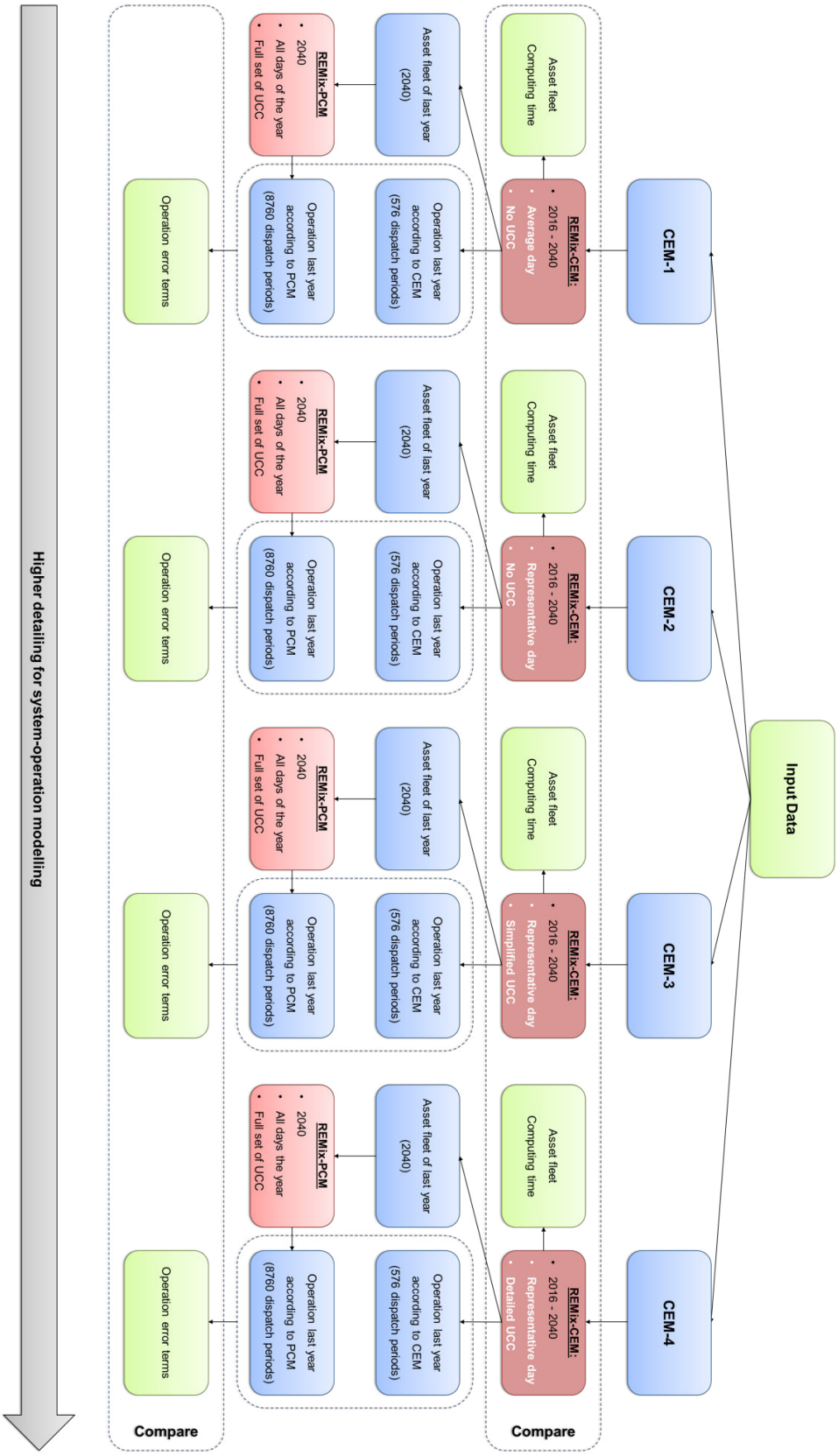

Figure 53: Approach for analyzing the impact of the applied system-operational detail on results of capacity expansion optimization

If not stated otherwise, differences in these values between each pair of CEM and UCM are expressed by a system operation error term, which is calculated according to equation (65).

$$ErrorTerm = \left(\frac{Results^{PCM}}{Results^{CEM}} - 1\right) \cdot 100\% \quad (65)$$

As already mentioned, the methodology for assigning values of RE resource availability to a limited number of dispatch periods that are used for capacity expansion optimization is an area of active research. The assigned values should characterize seasonal and diurnal RE resource variability within the year as accurate as possible. The most commonly applied method is the average day method, often also called integral method [97]. The average day method uses average values for RE resource availability of all data points of a period (e.g. a month) that corresponds to that dispatch period. The advantage of the average day method is its ease of use and that the method ensures that technology-specific annual energy yields are approximated accurately. However, the disadvantage is that the fluctuating nature of RE resources is underestimated considerably as high and low values are averaged.

Another method for assigning values of RE resource availability to the dispatch periods of a CEM is the selection of a set of “real” historical representative days or weeks [102]. The advantage of the so-called representative day method is a better representation of the short-term variability of RE resources because high and low values are not averaged. The drawback of the method is the difficult selection of a set of days (or weeks) that represent technology-specific annual energy yields as well as seasonal and diurnal variability accurately, while considering regional and technology-specific balancing effects. No consistent criterion exist to select representative days or to assess the validity of the assumption that is used for the selection [104].

All four CEM runs of the analysis apply the average day method for assigning values of system load to the dispatch periods considered. Due to the typically high regular seasonal, daily and diurnal variation of the load, the average day method provides a good representation of the real annual hourly load curve. In order to assign values of RE resource availability to the dispatch period, CEM-1 applies the average day method. CEM-2, CEM-3 and CEM-4 use the representative day method. As there is no established criterion for selecting representative days

for RE resource availability, a straight forward approach is applied in this case study. For each RES-E technology, the day of each month for which the daily energy yield of the respective technology is closest to the monthly average is selected as representative day. Afterwards, the selected daily time-series are scaled to meet the technology-specific annual energy yield. Technology-specific representative days are determined at each model node. Figure 54 compares the normalized diurnal time-series for potential wind power generation (hourly capacity factors) at node N1 according to the average day method and the representative day method for each season of the year. Variability of potential wind power generation is significantly higher for the representative day method than for the average day method, because extreme values are not averaged.

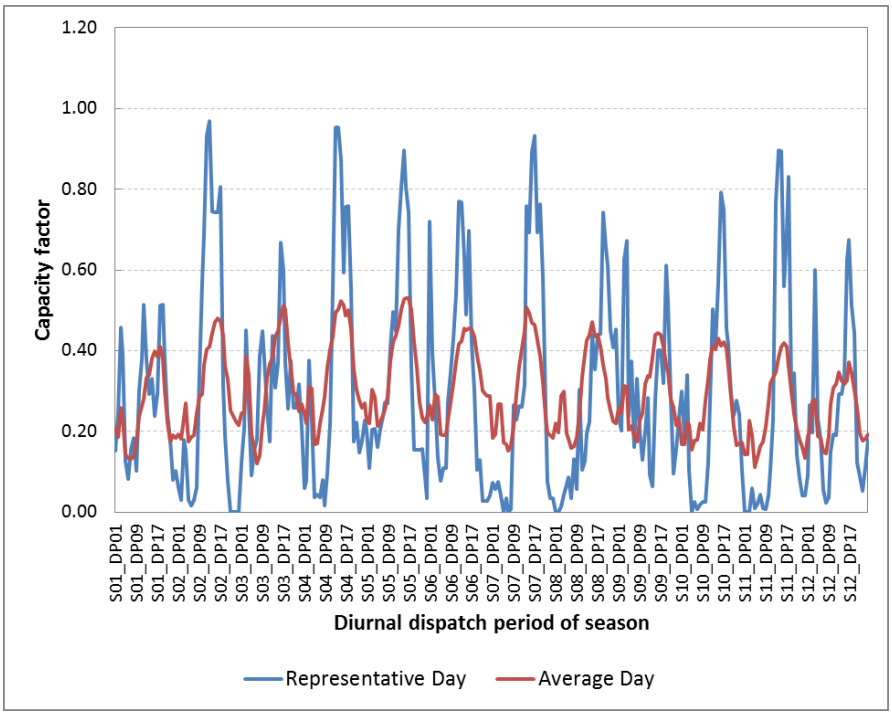

Figure 54: Comparison of average day and representative day method. Daily wind power generation profiles for each month of the year at model node N1 according to the average day and the representative day method.

UCCs of thermal generators are considered only by CEM-3 and CEM-4. Hence, only in these CEM runs the flexibility effect caused by a large-scale integration of VRE can be captured. CEM-3 considers UCCs in in a simplified way by modelling only unit start-up and ramping costs during capacity expansion optimization. Furthermore, a linear relaxation for the integer variables that describe the commitment status of each unit is applied. The linear relaxation of integer variables promises a large computing time reduction as the number of integer variables of the

optimization problem is reduced significantly. This speed-up strategy is sometimes applied for unit commitment optimization problems with long planning schedules that exceed the typical daily or weekly planning horizon in order to keep models manageable. An example is given e.g. in [98]. However, due to the linear relaxation, unrealistic situations, such as e.g. a half unit start-up can occur, while optimizing capacity expansion for the power system. CEM-4 considers UCCs in detail during capacity expansion optimization. Besides start-up and ramping costs, also minimum generation levels and part-load efficiencies of thermal generators are modelled. In addition, no linear relaxation for integer variables describing the unit commitment status is applied in CEM-4. Values describing the flexibility of existing and candidate thermal generators (start-up and ramping costs, minimum generation level, etc.) are presented in the Appendix. The model setup for the four CEM runs is summarized in Table 19. A rolling horizon foresight is applied for all CEM runs and CO_2 prices are assumed to be introduced suddenly after 2025 (see Figure 33 Group 2, Section 5.2.2).

Table 19: Model setup for the different CEMs of case study 2

	CEM-1	CEM-2	CEM-3	CEM-4
Planning horizon	2016 - 2040			
Milestone years	2016, 2019, 2022, …, 2040			
# Milestone years	9			
Foresight approach	Rolling horizon			
# Optimization periods	3 (2016 - 2025, 2025 - 2031, 2031 - 2040)			
# Seasons	12 (each month of the year)			
# Days per season	2 (1 working and 1 weekend day)			
# Daily dispatch periods	24			
# Total annual dispatch periods	576			
CO_2 prices	Sudden introduction after 2025 (see Figure 33, Group 2 at Section 5.2.2)			
Method for assigning load values to dispatch periods	Average day method	Average day method	Average day method	Average day method
Method for assigning values of RE resource availability to dispatch periods	Average day method	Representative day method	Representative day method	Representative day method
Considered unit commitment constraints	• None	• None	• Start-up and ramping costs • Linear relaxation	• Start-up costs • Ramping costs • Min. load level • Part-load efficiency

5.3.3 Comparison of investment decisions

Figure 55 presents the total installed generation capacity over the planning time frame by CEM run. The cumulative installed generation capacity and capacity expansion by milestone year for each CEM run is shown in Figure 56 and Figure 57 respectively. Several differences can be observed between the CEM runs:

The by far most wind power capacity is installed by CEM-1, which applies the average day method for assigning values of RE resource availability to the dispatch periods. In total, 23.5 GW of wind power is installed over the planning time frame. In CEM-2, CEM-3, and CEM-4, which all apply the representative day method, only 13.2 GW, 14.6 GW, and 14.3 GW of wind power capacity is installed respectively. As a consequence of large wind power installations, CEM-1 installs also the most GT generators (11.55 GW). The investments in GT generators in CEM-1 are about twice as much as in CEM-2, CEM-3 and CEM-4, which all install about 6 GW of new GT capacities. The large-scale wind power deployment in CEM-1 reduce potential power generation of mid-merit and base load generators, which in turn makes investment in such technologies economically inefficient (persistent utilization effect). Instead, very flexible GT generators with low investment costs are installed. The main purpose of the GT generators is the provision of firm and flexible reserve capacity to back-up power generation from VRE.

CEM-1 installs not only the most wind power capacity over the planning time frame but also the most total VRE capacity. The share of VRE on total capacity expansion is about 60% in CEM-1. In contrast, VRE represents only 56% of capacity expansion in CEM-2. The difference in VRE installations between CEM-1 and CEM-2 indicates that the average day method assumes a considerably higher value of energy at its time of the delivery for VRE generators than the representative day method. This increases competiveness from a system perspective significantly, which in turn leads to the larger VRE capacity expansion. Compared to CEM-2, the share of VRE on overall capacity expansion is further decreased in CEM-3 and CEM-4 to about 54.5%. As the only difference between CEM-2 and CEM-3/CEM-4 is that the latter CEMs consider UCCs of thermal generators, the lower VRE installations are caused by the flexibility effect. The flexibility effect causes additional integration costs for VRE (balancing costs), which reduce VRE deployment in CEM-3 and CEM-4.

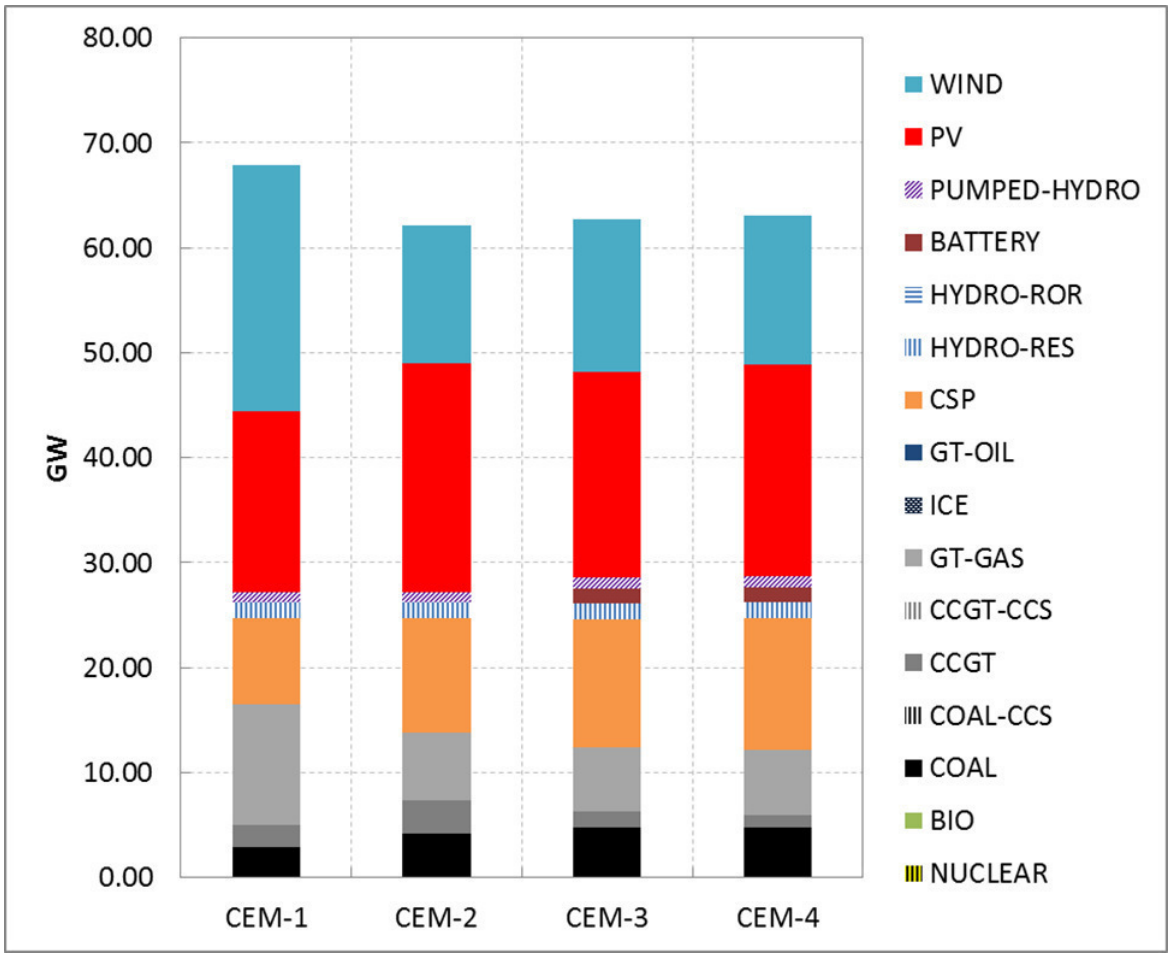

Figure 55: Total added gross capacity over the planning time frame by CEM run

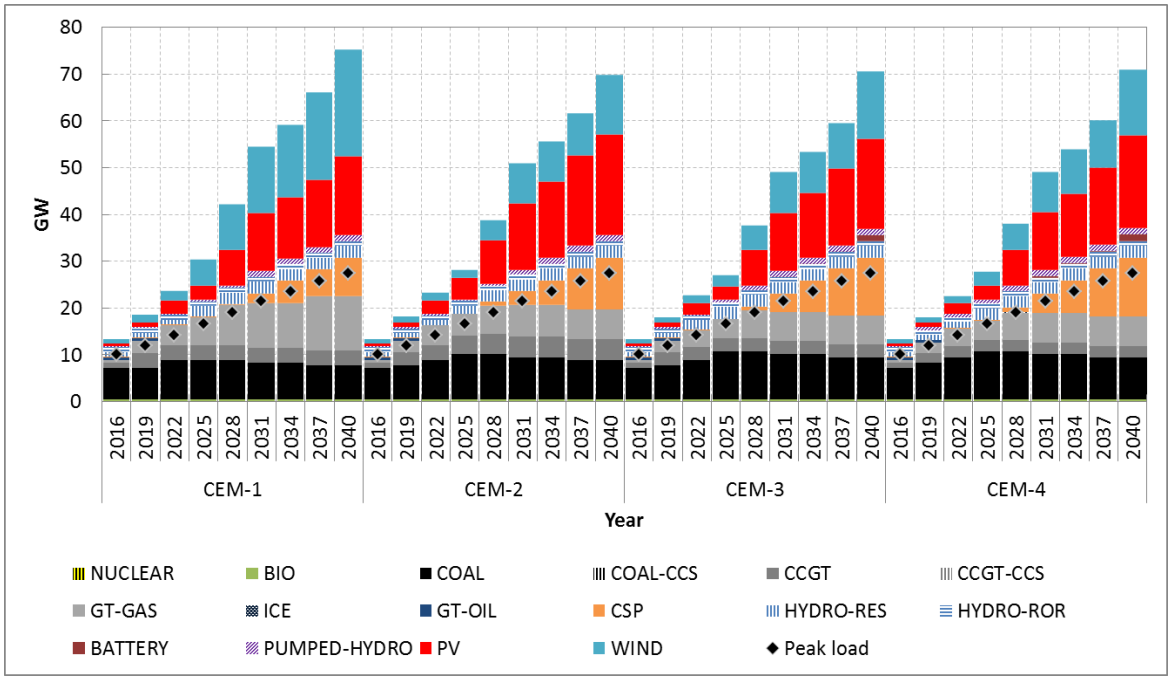

Figure 56: Cumulative installed gross capacity by CEM run

Another observation is that Lithium-ion batteries are only part of the least-cost expansion plan in CEM-3 and CEM-4. Lithium-ion batteries increase the flexibility of the system and therefore reduce balancing costs of thermal generators. The higher value for system flexibility in CEM-3 and CEM-4 is also indicated by earlier investments in pumped-hydro generators (see Figure 57). For example, CEM-4 deploys already 50% (0.5 GW) of the entire remaining pumped-hydro potential in 2019 and installs the remaining 50% in 2028. In contrast, no investments in pumped-hydro units are executed in the same time frame by CEM-2, which has however almost the same VRE deployment until 2028.

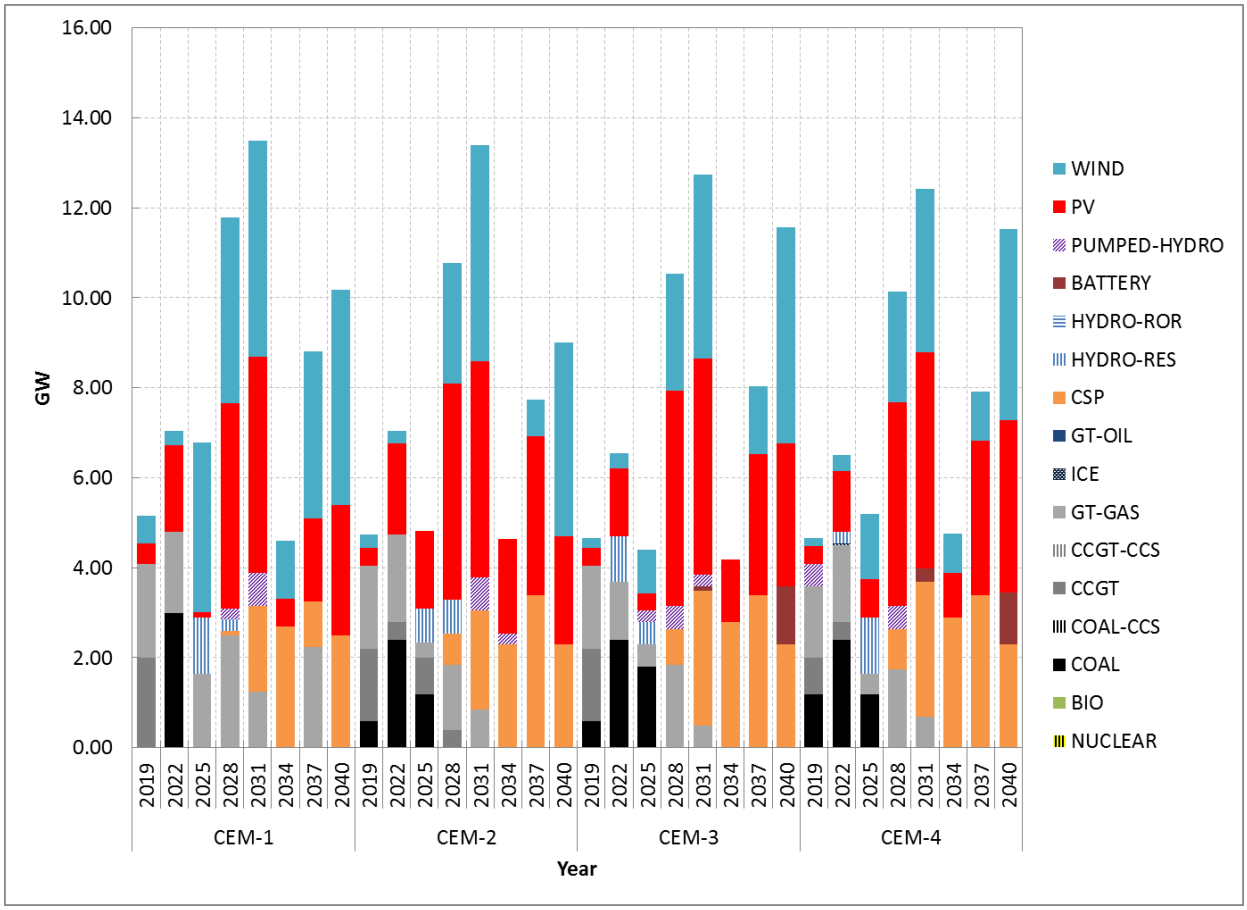

Figure 57: Added generation and storage capacity in each milestone year by CEM run

Figure 58 illustrates the effect of considering the flexibility effect directly during capacity expansion optimization. The left hand side of the figure shows the system dispatch aggregated by technology for a weekend day in September 2019 according to CEM-2. The right hand side of the figure does the same for the least-cost asset fleet determined in CEM-4. It can be clearly observed that CEM-2 does not consider UCCs of thermal generators while CEM-4 does. CCGT

generators are shut-down completely at 3 am and brought online again already one hour later in CEM-2. This is possible because no start-ups costs and minimum offline times are considered (see Figure 58 a). In contrast, shut-downs and start-ups of CCGT generators are avoided by CEM-4 between 3 am and 4 am, because this would cause additional costs for the system. Instead of shutting down the CCGT generator fleet completely, the installed pumped-hydro units are utilized to store produced electricity by the CCGTs for later use during peak load hours. In addition, extensive ramping and part-load operation of online CCGT generators is avoided in CEM-4, as this would also cause additional costs for the system. This is achieved by a higher utilization of pumped-storage hydro facilities (see Figure 58 b). The high value of system flexibility increases competiveness of pumped-hydro facilities in CEM-4, which in turn leads to earlier investments in this flexibility option.

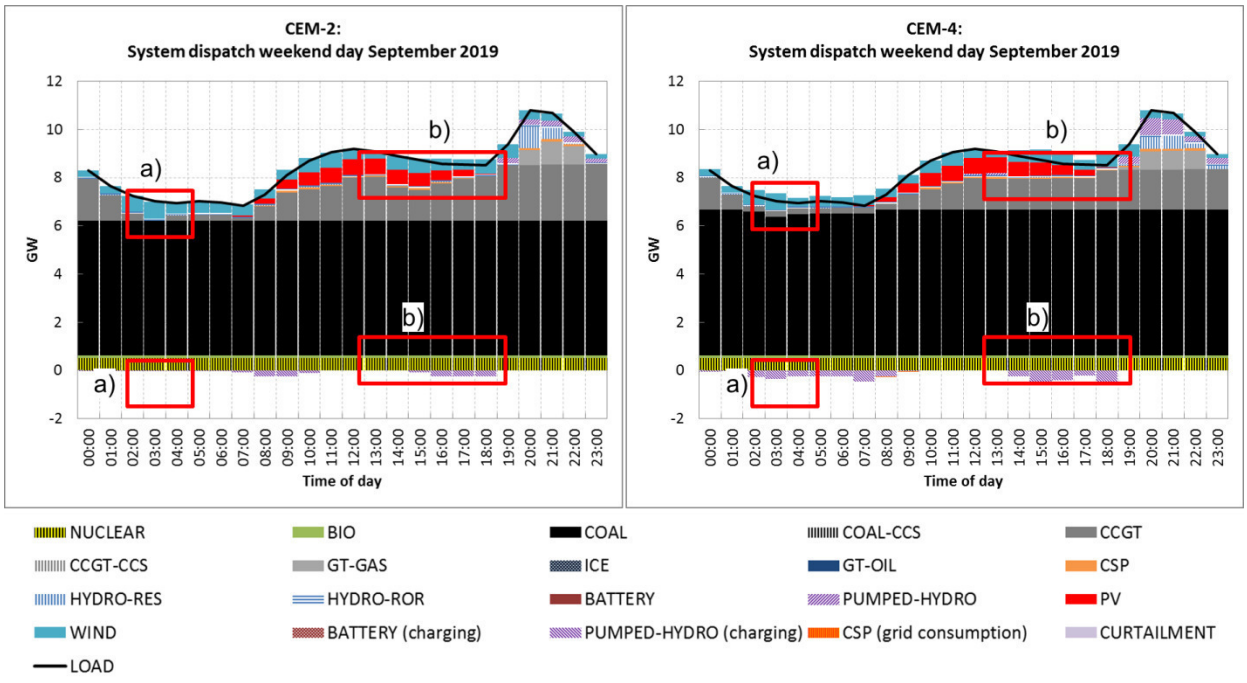

Figure 58: System dispatch of a weekend day in September 2019 according to CEM-2 and CEM-4.

Another difference between investment decisions of the CEMs is the gradual increase of CSP installations from CEM-1 to CEM-4. In total, CSP generators with a capacity of 8.2 GW are installed by CEM-1. In contrast, CEM-4 installs 12.5 GW of CSP, which is an increase of about 52%. The difference between CEM-1 and the other CEMs can be explained by the higher investments in wind power (and overall VRE capacity), which rather favors investments in peak load generators, such as GT power plants, instead of mid-merit generators like CSP (persistent

utilization effect). However, also from CEM-2 to CEM-4, CSP capacity is increased continuously from 10.9 GW (CEM-2) to 12.3 GW (CEM-3) and 12.5 GW (CEM-4). The difference between CEM-2 and CEM-3/CEM-4 can again be traced back on the flexibility effect, as this is the only difference between the three CEMs. Therefore, competiveness of CSP is considerably higher when the flexibility effect is taken into account in capacity expansion planning. To some extent this is caused by the general reduced competiveness of VRE compared to dispatchable generation technologies when integration costs (balancing costs) of VRE are considered. However, the main reason for the larger CSP capacity expansion in CEM-3 and CEM-4 is the higher capability of CSP, compared to other dispatchable mid-merit generation technologies like CCGT, to integrate VRE (especially PV) into the power system. CEM-2 installs 4.4 GW of CCGT generators whereas CEM-3 and CEM-4 install CCGT generators with a total capacity of only 2.8 GW and 2.4 GW respectively. In CEM-3 and CEM-4, the firm and dispatchable CCGT capacity installed in CEM-2, is mainly replaced by firm and dispatchable CSP capacity.

The excellent capability of CSP generators to support VRE integration is highlighted in Figure 59, which shows the system dispatch of a working day in July 2040 according to CEM-4. CSP generators stop power production completely during times of high PV production and consume instead electricity from the grid to cover the auxiliaries required to operate the solar field and the thermal energy storage system to store solar energy for later use after sunset (Figure 58 a). As system load is increased during times of high PV production through electricity consumption of CSP generators, the described operation mode of CSP generators helps to integrated additional PV into the system. This capability, together with good start-up and part-load operation characteristics, makes the CSP technology ideal for integrating PV into the power system. The dispatch schedule of CSP generators shown in Figure 59 has also the advantage that dry-cooled power blocks of CSP generators are operated during lower ambient temperatures (between evening and early morning), which leads to higher efficiencies of the Rankine-Cycle. A higher efficiency at lower ambient temperatures is also the reason why pumped-hydro and batteries systems are discharged first in the afternoon (5 - 6 pm) before CSP generators are dispatched completely (Figure 59 b).

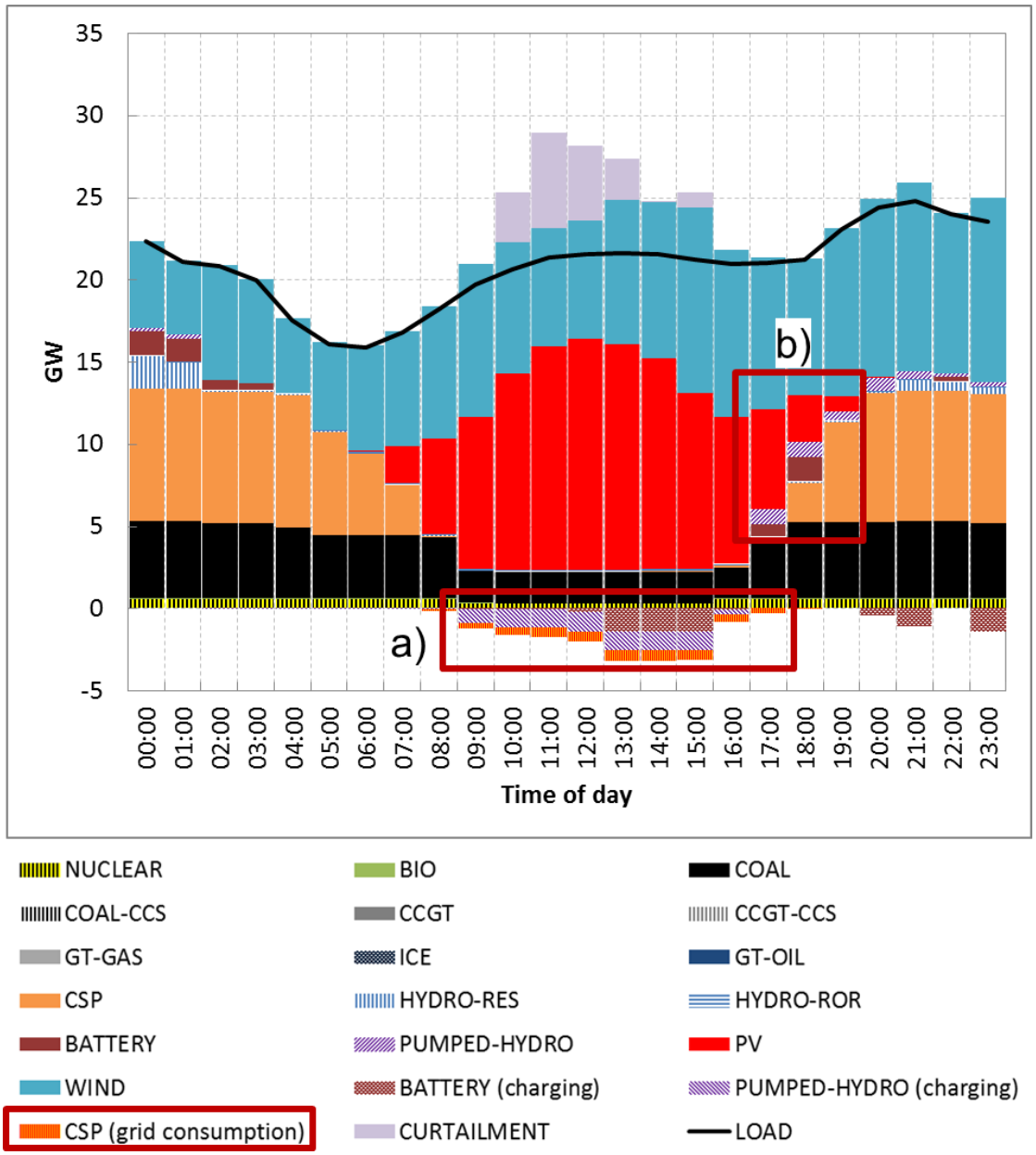

Figure 59: System dispatch for a working day in July 2040 according to CEM-4

The development of the average supply costs of the power system over the planning time frame for the four CEM runs is shown in Figure 60. In 2016, average supply costs of the CEMs are very similar. CEM-1 and CEM-2 have with 71.7 USD/MWh and 71.8 USD/MWh respectively almost identical average supply costs. The average supply costs of CEM-3 and CEM-4 in 2016 are with 72.3 USD/MWh and 72.5 USD/MWh respectively slightly higher. As in 2016 all CEMs have the same asset fleet (first investments possible in 2019), the difference between CEM-1/CEM-2 and CEM-3/CEM-4 results from the flexibility effect that is considered in the later models. Average supply costs are kept relatively constant until 2028 in all CEMs and increase strongly until 2034

due to the introduction of CO_2 prices (see Figure 33, Group 2). After 2034, average supply costs are reduced again due to the large-scale integration of cheap RES-E technologies that have walked down the learning curve considerably until then, and therefore overcompensate further increasing fossil fuel and CO_2 prices. The difference in average supply costs between the CEM runs remains almost constant until 2028 and increases aftwerwards significantly. In 2040, the final year of the planning time frame, the maximum spread in average supply costs between the CEMs is about 6.5%. CEM-1 has with 79.0 USD/MWh the lowest average supply costs in 2040. The least-cost asset fleet determined by CEM-2 leads to average supply costs of 82.3 USD/MWh in the final year of the planning time frame. Similar to the beginning of the planning time frame, average supply costs of CEM-3 and CEM-4 are with 83.8 USD/MWh and 84.1 USD/MWh respectively close together in 2040. Compared to CEM-1 and CEM-2, average supply costs of the system determined by CEM-3 and CEM-4 are about 6.5% and 2.1% higher respectively in 2040.

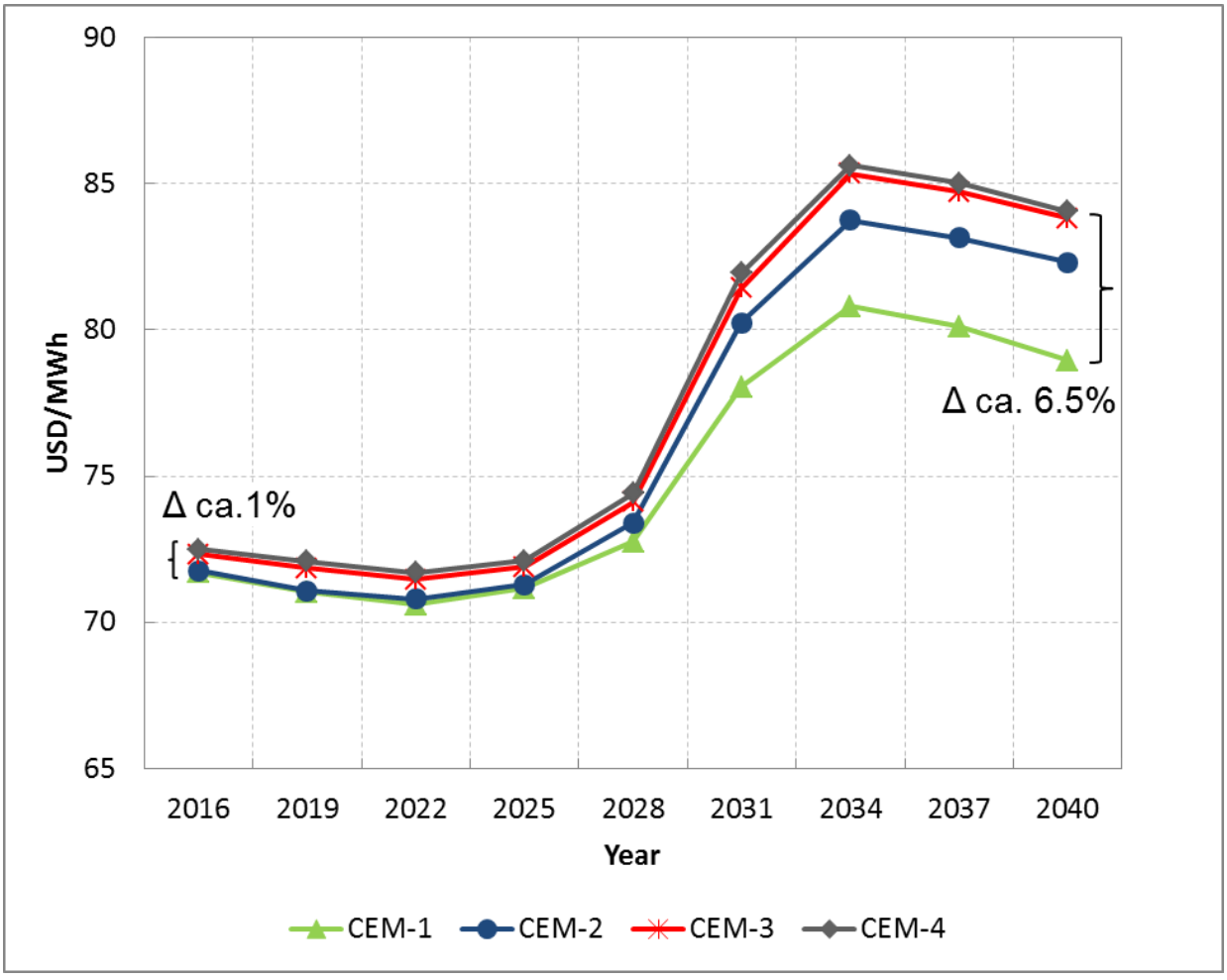

Figure 60: Development of average supply costs over the planning time frame by CEM run

Table 20 presents the computing time to solve the optimization problem formulated in the four CEM runs. CEM-1 and CEM-2 required almost the same computing time. This could be expected as the two CEMs differ only in the applied method for assigning values for RE resource availability to the dispatch periods. The consideration of start-up and ramping costs in CEM-3 increased computing time considerably. Compared to CEM-1 and CEM-2 computing time of CEM-3 was about twice as much, even a linear relaxation for integer variables that define the commitment status of thermal generators was applied. However, the by far highest computing time was required to solve the optimization problem formulated in CEM-4, where UCCs of thermal generators are considered in detail. Compared to CEM-1/CEM-2 and CEM-3 computing time of CEM-4 was about 16 and eight times higher respectively. The high computational effort of CEM-4 is caused by the large number of integer variables that are required to describe the discrete commitment status of each existing and candidate thermal generator in each dispatch period of the optimization problem.

Table 20: Comparison of computing time between CEMs

CEM-1	CEM-2	CEM-3	CEM-4
100%	103%	205%	1641%
715 sec.	735 sec.	1467 sec.	11742 sec.

5.3.4 Comparison of model accuracy regarding system-operational detail

After describing the differences between the applied CEMs regarding investment decisions and required computing time, the question remains which of the four CEMs is truly more accurate and describes operational behavior of the system with highest precision during capacity expansion optimization. To answer this question, a full year production cost optimization with hourly resolution was executed for the asset fleet suggested by each CEM for the final year of the planning time frame (2040) applying REMix-PCM. The full set of UCCs for thermal generators (minimum online- and offline times, minimum generation level, start-up costs, part-load efficiency, and ramping costs) is applied for the annual production cost modelling. Hence, together with the higher temporal resolution (8760 vs 572 dispatch periods), the PCM applies a significant higher system-operational detail than the respective CEM. Results of the more detailed PCM serve as benchmark for evaluating the accuracy of the respective CEM.

Table 21 compares the total annual system costs and resulting average supply costs of the system in 2040 for each pair of CEM and PCM. Total system costs and hence also the average supply costs are considerably underestimated by CEM-1. According to CEM-1 average supply costs of the system are 79 USD/MWh in 2040. For the same asset fleet, the detailed PCM computes average supply costs of 90 USD/MW, which is a difference of 11 USD/MWh. This difference results in a system costs error term of about 14%. Also the CEM-2, CEM-3, and CEM-4 underestimate the annual system costs in 2040. However, the system costs error term of CEM-2 is only 6% and therefore significantly lower compared to CEM-1. The error terms of CEM-3 and CEM-4 are even reduced to 4.5% and 4.2% respectively. This indicates that CEM-3 and CEM-4 are considerably more accurate than CEM-1 and CEM-2 in capturing system-operation details during capacity expansion optimization.

Table 21: Total annual system costs and average supply costs in 2040 for each pair of CEM and PCM

		CEM-1	CEM-2	CEM-3	CEM-4
Total annual system costs					
REMix-CEM	[billion USD]	13.89	13.95	14.21	14.29
REMix-PCM	[billion USD]	15.22	14.81	14.81	14.87
Average supply costs					
REMix-CEM	[USD/MWh]	79.0	82.3	83.8	84.1
REMix-PCM	[USD/MWh]	90.0	87.6	87.6	87.6
System costs error term	**[%]**	**13.7**	**6.1**	**4.2**	**4.1**

Since system CAPEX are identical for each pair of CEM and PCM (same asset fleet), the difference between CEM and PCM in total annual system costs results from the different annual OPEX of the asset fleet. As shown in Table 22, CEM-1 underestimates the OPEX of the system in 2040 significantly. This is indicated by the high error term of 36%. The OPEX error term of CEM-2 is with about 15% considerably lower. With 10.6% and 10.0% respectively, CEM-3 and CEM-4 have the lowest OPEX error term of the four CEMs. Hence, CEM-3 and CEM-4 have the highest accuracy in approximating the OPEX of the suggested asset fleet during capacity expansion optimization. The relatively high inaccuracy of all CEMs in terms of OPEX estimation has only a limited impact on the average supply costs in 2040 because system OPEX represents less than 50% of total annual system costs. This cost structure is common for RES-E dominated systems.

Table 22: Comparison of total system OPEX in 2040 for each pair of CEM and PCM

		CEM-1	CEM-2	CEM-3	CEM-4
Annual OPEX					
REMix-CEM	[billion USD]	5.14	5.96	5.79	5.84
REMix-PCM	[billion USD]	7.01	6.83	6.40	6.44
Specific OPEX					
REMix-CEM	[USD/MWh]	30.4	35.3	34.2	34.1
REMix-PCM	[USD/MWh]	41.4	40.4	37.8	37.5
OPEX error term	**[%]**	**36.4**	**14.6**	**10.6**	**10.0**

The difference in system OPEX between CEM and PCM results from a different utilization of single elements of the asset fleet in the respective model. Figure 61 compares the technology-specific generation shares calculated by the CEMs and their corresponding PCM. The differences in technology-specific generation shares and the overall generation error term[13] are presented in Table 23. It can be observed that CEM-1 overestimates VRE power generation significantly (mainly wind power) and underestimates likewise power generation especially of mid-merit and peak load generators. The share of VRE on annual power generation is reduced by 9.3% points in the PCM due to considerably larger wind power curtailments. For CEM-2, CEM-3, and CEM-4, differences in generation shares between PCM and CEM are less pronounced. The share of VRE on annual supply is reduced by about 3.5%-points in all three PCMs compared to their corresponding CEM. VRE power production is mainly substituted by mid-merit generators (CCGT, CSP) but also partially by peaking and base load units. The high VRE curtailment leads to a generation error term of about 10% for CEM-1. The generation error-terms for the asset fleets of CEM-2, CEM-3, and CEM-4 are considerably lower (4.3%, 3.4% and 3.7% respectively) due to the significantly better approximation of the system operation during capacity expansion optimization.

[13] Definition generation error term: $ErrorTerm = \sum_g \frac{|GenerationShare_g^{CEM} - GenerationShare_g^{PCM}|}{2}$

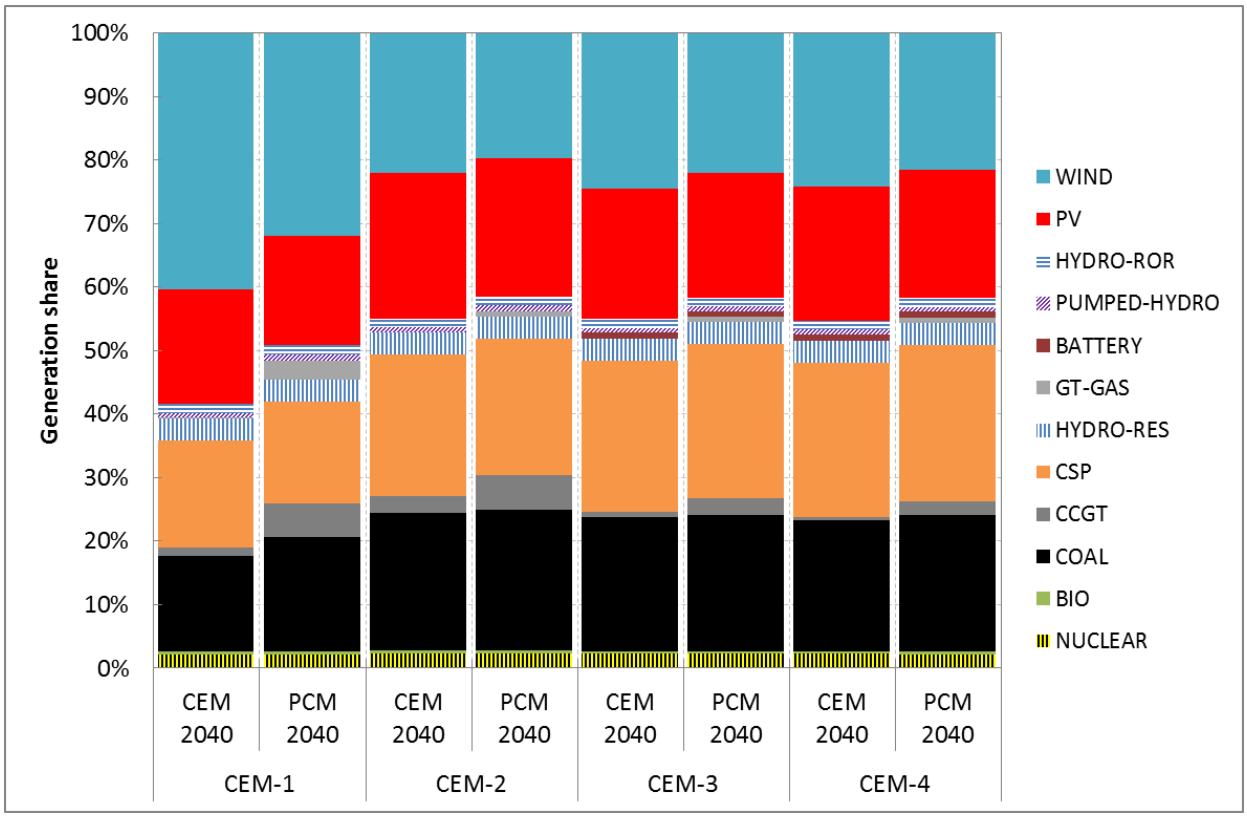

Figure 61: Comparison of generation shares in 2040 for each pair of CEM and PCM

Table 23: Difference (Δ) in generation shares between each pair of CEM and PCM and overall generation error term in 2040

Generator type		CEM-1	CEM-2	CEM-3	CEM-4
Base load	[%]	+3.0	+0.5	+0.4	+0.7
Mid merit	[%]	+3.1	+2.0	+2.2	+2.1
Peak load	[%]	+3.2	+1.0	+0.8	+0.7
VRE	[%]	-9.3	-3.4	-3.4	-3.5
PV	[%]	-0.9	-1.1	-0.9	-0.8
WIND	[%]	-8.4	-2.3	-2.5	-2.7
Generation error term	**[%]**	**10.2**	**4.3**	**3.4**	**3.7**

Base load: NUCLEAR, COAL, BIOMASS
Mid merit: CCGT, CSP
Peak load: GT, HYDRO-RES, PUMPED-HYDRO, BATTERY
VRE: PV, WIND, HYDRO-ROR
$\Delta GenerationShare_g = GenerationShare_g^{PCM} - GenerationShare_g^{CEM}$

The difference in technology-specific generation shares between the CEMs and their corresponding PCM leads also to different CO_2 emissions of the asset fleet. CEM-1 underestimates CO_2 emissions of the power system in 2040 by 42% due to the significant overestimation of VRE uptake and consequently underestimation of power generation of fossil

fuel fired thermal generators. The CO_2 emission error terms of CEM-2, CEM-3, and CEM-4 are with 10.7%, 9.4% and 8.6% respectively comparably low.

Table 24: Total CO_2 emissions of the system in 2040 for each pair of CEM and PCM

		CEM-1	CEM-2	CEM-3	CEM-4
REMix-CEM	[million tons]	26.7	38.5	36.8	36.8
REMix-PCM	[million tons]	37.8	42.7	40.3	39.9
CO_2 emission error term	**[%]**	**41.8**	**10.7**	**9.4**	**8.6**

The analysis for the year 2040 has shown that CEM-1 is not an adequate modelling approach for long-term capacity expansion planning with VRE. System costs and CO_2 emissions of the suggested asset fleet are underestimated significantly by CEM-1, whereas VRE uptake is overestimated. The wrong representation of especially wind power variability by the average day method applied in CEM-1 is the main driver for the high inaccuracy of CEM-1 because the fluctuating nature of wind resources is underestimated significantly. This results in a wrong consideration of the value of energy at its time of the delivery for wind power generators and its impact on the residual system. The disregard of UCCs of thermal generators increases the inaccuracy of CEM-1 additionally.

CEM-2 uses the representative day method instead of the average day method to assign values of RE resource availability to the dispatch periods of the CEM. The analysis above has shown that the accuracy of CEM-2 is significantly higher than the accuracy of CEM-1, which indicates the higher suitability of the representative day method for capacity expansion planning with VRE. This findings are in line with results presented by [102]. However, in most criterions used for comparing the accuracy of the respective CEMs, CEM-2 performed worse than CEM-3 and CEM-4. The latter CEMs apply additionally to the representative day method also UCCs of thermal generators to capture the flexibility effect during capacity expansion optimization with VRE.

For CEM-4, the highest modelling detail has been applied during capacity expansion optimization by considering UCCs of thermal generators in detail. The analysis has shown that the high modelling detail leads to the highest model accuracy in approximating system operation during capacity expansion optimization. However, the disadvantage of CEM-4 is that

the high accuracy of the CEM comes at very high computational cost. Computing time of CEM-4 is more than 16 times higher than computing time of CEM-2. The high computing time makes the modelling approach relatively unmanageable for capacity expansion planning as high computing time constraints the number of parameter variations and sensitivity analyses. Such an analysis is however important to check robustness of results.

CEM-3 represents in terms of model accuracy and computing time a promising compromise. For all criterions used for comparison the accuracy of CEM-3 is almost as high as the accuracy of CEM-4 but computing time is about eight times less. The linear relaxation of integer variables that define the unit commitment status of thermal generators reduces the computational effort dramatically without biasing results for system operation significantly. This indicates that the simplified representation of UCCs is a suitable approach to take into account the flexibility effect during capacity expansion optimization while keeping computational effort manageable.

Detailed comparison of CEM-2 and CEM-3:

The analysis presented above pointed out that CEM-3 is the most suitable approach for capacity expansion optimization with VRE due to the good trade-off between model accuracy and computing time. However, also the modelling approach of CEM-2 should not be disregarded due to the considerably lower computing time (50%) and partially only moderately lower accuracy in approximating system operation during capacity expansion optimization. To finally evaluate which of the two modelling approaches offers the best trade-off between model accuracy and computational effort, the similar analysis that has been executed for the final year (2040) is performed for each milestone year of the planning time frame. The analysis will show if the observed difference in model accuracy between CEM-2 and CEM-3 increases or decreases when the entire planning time frame is considered and therefore the higher computational effort of CEM-3 is justified or not.

Table 25 shows the development of the system costs error term over the planning time frame for CEM-2 and CEM-3. The system costs error term of CEM-2 increases from 1.5% in 2016 to 2.8% until 2028. In the same time frame installed VRE capacity increases from 10% to about 70% of the system peak load (see Figure 62).

Table 25: Annual total system costs error terms over the planning time frame of CEM-2 and CEM-3

	2016	2022	2028	2034	2040	Average	Δ 2040	Δ 2016 - 2040
CEM-2	1.5%	2.1%	2.8%	4.2%	6.4%	3.4%	30%	41%
CEM-3	0.7%	1.0%	1.1%	3.0%	4.5%	2.0%		

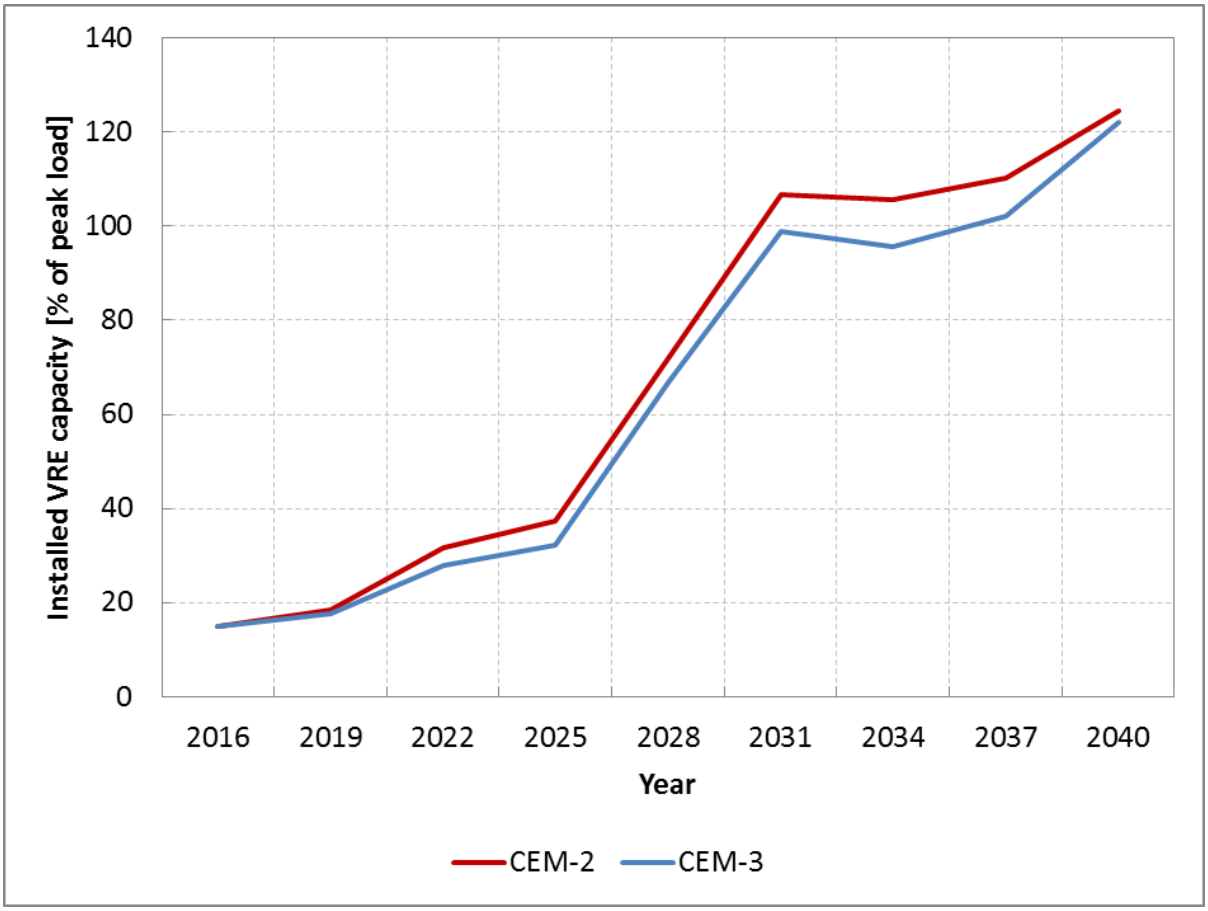

Figure 62: Development of installed VRE capacity at CEM-2 and CEM-3

After 2028, when installed VRE capacity increases further to 100% of the peak load and above, the system costs error term increases sharply and reach 6.4% at the end of the planning time frame. The average system costs error term for the whole planning time frame is 3.4% for CEM-2. CEM-3 has a significantly lower system costs error term in all milestone years of the planning time frame. For the total planning time frame he average system costs error term of CEM-3 is 2%, meaning that the accuracy of CEM-3 compared to CEM-2 increases significantly when all milestone years are considered. Whereas the difference between system costs error terms in

2040 is 30% the difference increases to 41% for the entire planning time frame. Especially until 2028, the error term of CEM-3 remains almost constant on a very low level (between 0.7% and 1.1%). However, when installed VRE capacity increases to more than 100% of the annual peak load, also the annual system cost error term of CEM-3 increases and reaches 4.5% in 2040.

Table 26 presents the development of the system OPEX error term over the planning time frame for CEM-2 and CEM-3. The average OPEX error term for the entire planning time frame is significantly lower than for the last year for both CEMs. The average OPEX error term of CEM-2 and CEM-3 is 7.2% and 4.3% respectively compared to 14.6% and 10.6% respectively for the last year. The advantage of CEM-3 over CEM-2 is increased significantly when the entire planning time frame is used for evaluating the accuracy of the model (40% vs 28%).

Table 26: Annual total system OPEX error terms over the planning time frame of CEM-2 and CEM-3

	2016	2022	2028	2034	2040	Average	Δ 2040	Δ 2016 - 2040
CEM-2	2.1%	3.1%	4.7%	8.0%	14.6%	7.2%	28%	40%
CEM-3	0.8%	1.3%	1.8%	5.1%	10.6%	4.3%		

Figure 63 shows the technology-specific generation shares over the planning time frame according to the CEM and PCM for both CEM approaches. In the first half of the planning time frame until 2028, technology-specific generation shares are very similar in the respective CEM and its corresponding PCM for both capacity expansion modelling approaches. The major difference between CEM and PCM is the higher utilization of peak and mid-merit generators (GT, CCGT and CSP) and a simultaneously lower utilization of base-load generators (coal). In the second half of the planning time frame the difference between CEM and PCM increases for CEM-2 and CEM-3 significantly, mainly due to the overestimation of possible VRE uptake in the respective CEM. The generation share error term for CEM-2 and CEM-3 is presented in Table 27.[14] As long installed VRE capacity is well below 100% of the annual peak load (until 2028), the generation share error term is very low for both CEMs (≤ 1%). With increasing VRE deployment this changes significantly. Until 2040, the error term of CEM-2 and CEM-3 increases

[14] Definition of generation share error term: $ErrorTerm = \sum_g \frac{|GenerationShare_g^{CEM} - GenerationShare_g^{PCM}|}{2}$

to 4.3% and 3.4% respectively. For the entire planning time frame, the average generation share error term is 2.1% and 1.6% for CEM-2 and CEM-3 respectively.

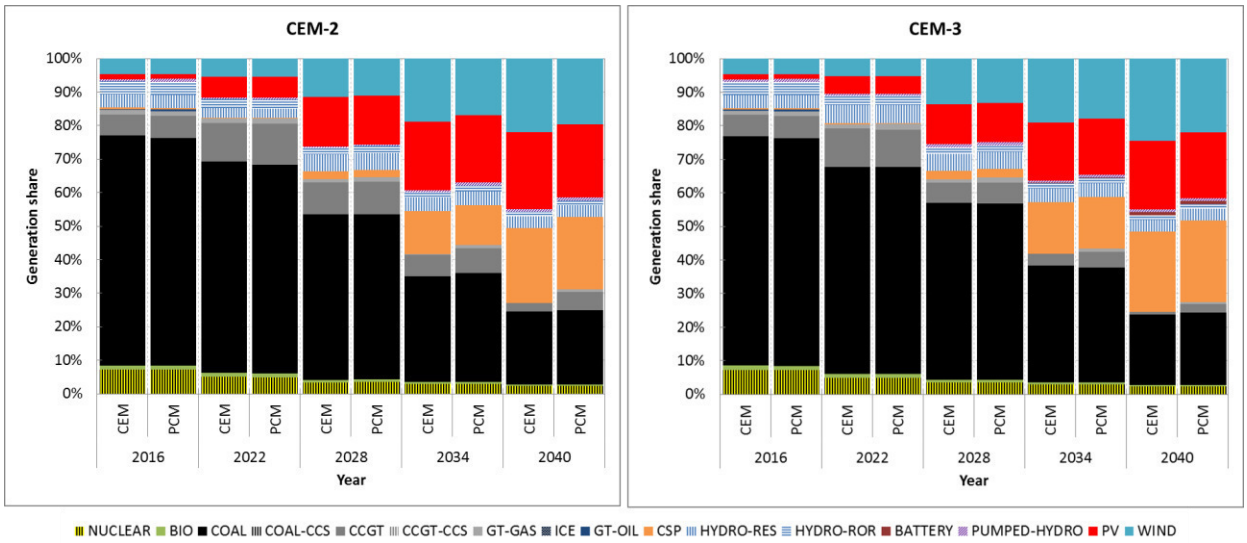

Figure 63: Technology specific generation shares by modelling approach

Table 27: Generation error terms over the planning time frame of CEM-2 and CEM-3

	2016	2022	2028	2034	2040	Average	Δ 2040	Δ 2016 - 2040
CEM-2	0.9%	1.0%	0.9%	3.0%	4.3%	2.1%	20%	22%
CEM-3	0.5%	0.6%	0.9%	2.2%	3.4%	1.6%		

The CO_2 emission error term over the planning time frame for CEM-2 and CEM-3 is shown in Table 28. For the CO_2 emission error term the same situation as for the other indicators can be observed. Until 2028, the error terms are relatively low but increase afterwards significantly for both CEMs. However, accuracy of CEM-3 regarding CO_2 emissions is considerable higher than accuracy of CEM-2. The average CO_2 emission error term for the planning time-frame of CEM-2 and CEM-3 is 3.8% and 2.0 % respectively. Hence, the accuracy of CEM-3 regarding assumed CO_2 emissions of the proposed asset fleet is significantly higher when the entire planning time frame is used for evaluation instead of solely the final year of the study.

Table 28: CO_2 emission error terms over the planning time frame for CEM-2 and CEM-3

	2016	2022	2028	2034	2040	Average	Δ 2040	Δ 2016 - 2040
CEM-2	0.2%	0.3%	0.6%	6.5%	10.7%	3.8%	13%	48%
CEM-3	0.0%	0.3%	0.3%	2.3%	9.4%	2.0%		

The comparison between CEM-2 and CEM-3 over the entire planning time frame has shown that the higher computing time of CEM-3 is justified by the significantly higher model accuracy. In all categories used for comparing the accuracy of the models, the advantage of CEM-3 over CEM-2 increases considerably when the entire planning time frame is used for evaluating the accuracy of the models.

In fact, CEM-3 has a very high accuracy in approximating system operation of the proposed least-cost asset fleet over the planning time frame. The simplified consideration of UCCs of thermal generators through a linear relaxation for integer variables that describe the unit commitment status of thermal generators and the consideration of only start-up and ramping costs ensures already a detailed representation of the flexibility effect during capacity expansion optimization. Especially as long as installed VRE capacity is lower than 70% of the annual peak load (until the year 2028 in this case study), the system operation is approximated with very high accuracy. Whereas the various error terms of CEM-2 increases already considerably when installed VRE capacity increases from 10% of the peak load in 2016 to about 70% in 2028, the different error terms of CEM-3 remain almost constant on a very low level for these VRE deployment levels.

However, after 2028 when VRE capacity increases further to 100% of annual system peak load and above, error terms of CEM-3 also increase considerably. This is caused mainly by an inaccurate representation of the seasonal and diurnal temporal RE resource availability in the CEM. Even though the representative day method provides a significant improvement compared to the average day method, extreme weather situations during a year, such as longer periods of wind calms, extremely short-term RE resource fluctuations, or periods of very high simultaneous solar and wind availability are not considered. Until the installed VRE capacity is well below 100% this lack of the representative day method has a relatively low impact as proven by the low operation error terms of CEM-3 until 2028. However, when VRE capacity increases further and enters the base load segment the impact starts to increase significantly. To overcome these limitations further research is required for a better representation of seasonal a diurnal resource availability of wind and solar technologies by a limited number of intra-annual dispatch periods during long-term capacity expansion optimization.

5.3.5 Summary and discussion

The case study about the influence of applied system-operational detail on results for capacity expansion optimization has highlighted two important issues for capacity expansion planning with VRE. On the one hand, it was shown that the average day method is inappropriate for assigning values of RE resource availability to dispatch periods of a CEM because the variability of VRE (especially wind power) is underestimated considerably. This leads to non-optimal asset fleets with significantly higher generation costs and CO_2 emissions than initially assumed by the CEM. The seasonal and diurnal fluctuation of RE resources can be better captured by the representative day method. The method allows for a better representation of the value of energy at its time of the delivery and the impact of VRE on the residual system operation.

On the other hand it was demonstrated that the flexibility effect should be considered during long-term capacity expansion planning because otherwise the flexibility requirements of the system, due to a large-scale deployment of VRE, are underestimated. In the case the flexibility effect is considered, competiveness of flexible dispatchable generation (GT, CSP) and storage technologies (pumped-storage, batteries) increases while competiveness of less flexible dispatchable generators and VRE decreases. However, it was also demonstrated that considering the flexibility effect during capacity expansion optimization by modelling UCCs of thermal generators in detail, comes at very high computational cost. A linear relaxation for integer variables that describe the unit commitment status of each generator can reduce computational effort dramatically while it biases results only marginally.

It was shown that system operation can be approximated very accurately in REMix-CEM when the representative day method is applied and the flexibility effect is considered. However, it was also shown that for very high VRE capacity shares (≥ 100% of annual peak load), the accuracy of approximating system operation is reduced considerably even if the representative day method is applied and the flexibility effect is considered. This is mainly driven by the fact that extreme weather situations are not considered by the representative days, which were selected in a straight forward approach in this case study. Future research should focus on improving the representation of seasonal and diurnal RE resource availability, including extreme weather situations, during long-term capacity expansion modelling.

6 Using REMix-CEM for a science-based consulting of national energy system planning authorities in collaboration with international cooperation institutions

The optimization model developed during this PhD-thesis is used by DLR-SYS mainly for a science-based consulting of national energy system planning authorities (EPAs) of developing countries in the field of strategic power system capacity expansion planning and integration of RES-E. Typically, the consulting process is carried out in close collaboration with international cooperation institutions (ICIs), such as the World Bank or Deutsche Gesellschaft für International Zusammenarbeit (GIZ). ICIs are well connected in developing economies and typically have own local offices and staff in the countries. Therefore, ICIs can act as link between a scientific advisor (SA), such as DLR-SYS, and the local EPA. This link does not only ease data access but does also help to setup an iterative advisory process between the foreign SA and the local EPA. Project examples of this science-based consultancy by DLR-SYS in collaboration with ICIs are e.g. the "MOREMix" project (in collaboration with GIZ) and the "Renewable Energy Strategy for Botswana" project (in collaboration with the World Bank) [99], [100], [127]. In the former project, REMix-CEM was used to support the Ministry of Energy, Mines, Water and Environment (MEMEE) of Morocco in defining a long-term strategy ("Lead Scenario") for the power sector to meet strongly growing electricity demand until 2050 in a reliable, affordable, and environmental friendly way. In the latter project, results derived from REMix-CEM were used as basis for the definition of a RES-E integration strategy and the development of a RES-E investment roadmap until the year 2030. The investment roadmap is used by the Ministry of Minerals, Energy and Water Resources (MMEWR) of Botswana to tender RES-E projects, which shall be developed by independent power producers (IPPs). Results of the projects cannot be presented in this thesis because of secrecy clauses that are currently in place.

As for any other foreign SA, for DLR-SYS access to data that describes the actual status quo of the power system accurately is a prerequisite for a meaningful and reliable advisory process. However, getting access to relevant data for power system modelling in developing countries can be very challenging and time-consuming for the foreign SA, and sometimes it is even impossible without any local support. One reason for that is that stakeholders of the national

power sector often classify specific requested input data (e.g. techno-economic data for single power plants) as highly sensitive data, which prevent them from sharing it with scientists of foreign countries. Another reason is the lack of understanding of the importance of specific input data for a meaningful model-based capacity expansion planning with VRE from part of the national EPA (e.g. chronological load data with high spatial and temporal resolution). In many cases, EPAs of developing countries are not fully aware of the challenges of power system planning with VRE and how these challenges can be captured within a model-based analysis for capacity expansion planning. Removing these barriers between the foreign SA on the one side and the local EPA on the other side is often impossible without an extensive face-to-face contact. The local staff of ICIs can act here as intermediary whereby barriers can be reduced and access to sensitive data can be accelerated considerably.

An iterative process between the foreign SA and the local EPA is crucial for a successful consulting service because this ensures a common understanding about project targets, the consideration of the most recent developments in the country (e.g. newly defined political targets or finalized investment decisions during the project duration), and achieving a high project commitment and acceptance of results by all project stakeholders. In addition an iterative process leads to capacity building in both directions. The local staff of ICIs is the key for an iterative and participative advisory process because it can organize major project workshops efficiently but more importantly it can undertake daily coordination work with the EPA and the SA, which is of high importance for a successful consulting service.

REMix-CEM is often applied by DLR-SYS to support national EPAs of developing countries in defining a Lead Scenario for the power system. Within this process, in a first step a large number of REMix-CEM runs are conducted with the aim to do an extensive scenario and sensitivity analysis for possible future expansion pathways for the power system under the least-cost criterion (see Figure 64). This modelling work has the aim to provide the national EPA with a broad view about possible strategies to meet future electricity demand and to highlight the consequences of certain political targets (e.g. RES-E quotas) and assumptions for input parameters (e.g. fossil fuel or CO_2 prices) on results for capacity expansion optimization. Within an iterative process between DLR-SYS and the EPA (moderated by the ICI), the lessons-learned

from the extensive modelling work are used to narrow down step-by-step the large number of possible scenarios to meet future electricity demand to a limited number of “Main Scenarios”, which are investigated in more detail. During this process, several guide rails (user-constraints) are introduced into REMix-CEM to identify the least-cost capacity expansion pathway for the power system that not only ensures the defined reliability standards to meet future electricity demand but also the various strategic targets of the national EPA (planning imperatives). After the detailed analysis of the Main Scenarios and the consequences of certain planning imperatives, a final story line for the Lead Scenario is formulated. This story line includes all finally defined strategic planning imperatives of the national EPA and the final set of input parameters for the optimization model which was agreed upon within the iterative process. In a last step, REMix-CEM is used to calculate the least-cost capacity expansion plan to meet future electricity demand over the planning time frame under the story line of the Lead Scenario. The Lead Scenario is used by the EPA as basis for the formulation of a detailed strategy for the future development of the power system (targets, implementation strategy, financing options, grid codes, etc.). Detailed preparation of this strategy and frequent updates are rather done without DLR-SYS but with support from the ICI and the private sector.

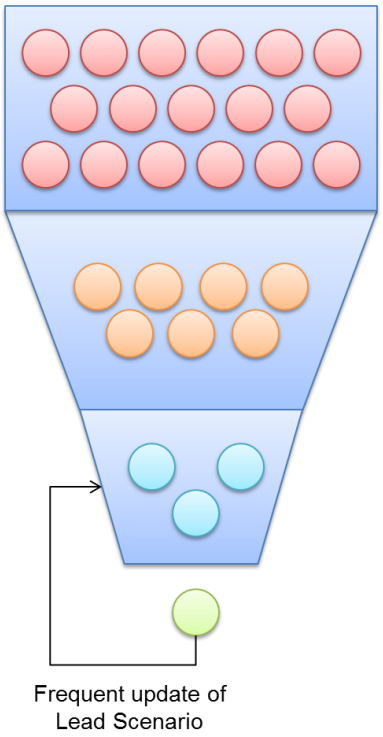

1) Providing a broad View

- Large number of story lines
- All possible investment options included (technology open analysis)
- Large number of sensitivity analyses for input parameters

→ **Outcome: Definition of story lines for Main Scenarios**

2) Elaboration of selected Main Scenarios

- Solution space restriction by introducing guide rails (user-constraints)
- Only relevant investment options included
- Limited number of story lines and sensitivity analyses

→ **Outcome: Definition of story line for Lead Scenario**

3) Detailed elaboration of Lead Scenario

- Solution space further restricted by updating guide rails
- Sensitivity analysis for final story line

→ **Outcome: Least-cost expansion plan for Lead Scenario**

Figure 64: Approach for developing a Lead Scenario for a power system using REMix-CEM

Figure 65 presents the typically applied project flow of DLR-SYS (SA), when REMix-CEM is used to support national EPAs of developing countries in the process of determining a Lead Scenario for the power system. The advisory process has an iterative character and is executed in close collaboration with an ICI. The ICI initiate the project by setting up a Kick-Off Workshop where the advisory requirements and project targets are discussed in detail. Furthermore, a detailed introduction into REMix-CEM is provided by DLR-SYS to provide the EPA with profound knowledge about the capabilities of the optimization model. After this workshop, the EPA is able to concretize its advisory requirements due to a better understanding of the applied model. Based on that, DLR-SYS can adapt REMix-CEM according to the project requirements.

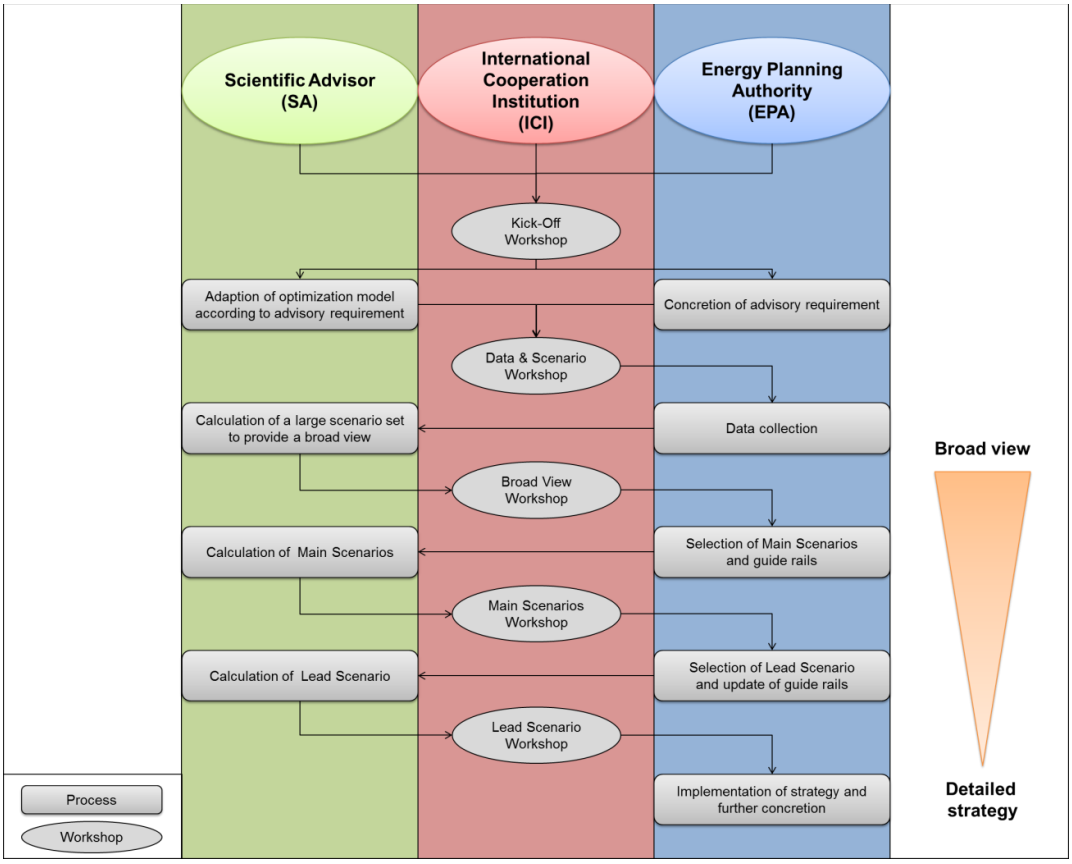

Figure 65: Process flow of the applied iterative advisory process

Afterwards, a Data & Scenario Workshop is organized by the ICI which has the aim to define data requirements for the optimization model and to determine a large set of scenarios and sensitivities that should be calculated by REMix-CEM to provide a broad view on possible expansion pathways for the power system and its consequences in terms of costs, GHG emissions, energy independency, and other important issues for a strategic system planning.

Subsequently to the Data & Scenario Workshop, the EPA collects the relevant data (supported by the ICI and SA) and provides it as input for REMix-CEM. Based on the provided input data, REMix-CEM is used to calculate a large number of possible least-cost capacity expansion pathways for the power system under various political story lines and various assumptions for input parameters. This provides a broad view on possible expansion pathways for the power system and the consequences of certain assumptions. The results of this extensive scenario analysis are presented at a Broad View Workshop. The results of the extensive modelling work enable the EPA to narrow down potential scenarios to meet electricity demand in the future to a limited number of Main Scenarios.

At this stage of the project several guide rails (user-constraints) are implemented in REMix-CEM to identify solutions for least-cost capacity expansion optimization that are compatible with the defined story lines of the Main Scenarios. To check robustness of results, several sensitivity analyses are conducted for the Main Scenarios. After finishing the modelling work, results are presented at a Main Scenario Workshop, which again is organized by the ICI.

After analyzing the results of the Main Scenarios, the EPA defines a story line for the Lead Scenario. This story line considers all strategic planning imperatives of the EPA for the future design of the power system. As in this project stage further guide rails are introduced into REMix-CEM to ensure that the calculated least-cost expansion plans meet the strategic targets of the EPA, the character of the optimization model is shifted more and more towards a simulation model (reduced solution space). The definition of the guide rails is again an iterative process between the EPA and the SA, moderated by the ICI.

After agreeing on the final set of guide rails and input parameters, REMix-CEM is used to optimize the least-cost capacity expansion plan for the power system under the story line of the Lead Scenario. Results are presented and discussed in detail at a Lead Scenario Workshop. This workshop marks the end of the iterative science-based advisory process. Based on the results for the Lead Scenario, the EPA may define its final strategy to meet future electricity demand and concretize the necessary actions to implement the strategy.

7 Conclusions and future research requirements

This PhD thesis extended the REMix energy system modelling framework with the capacity expansion optimization model REMix-CEM. The developed optimization model bridges the gap between traditional long-term capacity expansion planning and short-term power system production cost models for a concerted capacity expansion planning with VRE.

In REMix-CEM, capacity expansion optimization can be conducted under the assumption of a single-year myopic, a multi-annual rolling horizon, and a perfect foresight over the planning time frame. It was shown that the model foresight has a significant impact on results when some of the model input parameters change suddenly at a certain point of the planning time frame. The influence is less pronounced when input parameters change monotonously. Only the perfect foresight and partially the multi-annual rolling horizon foresight enable the model to anticipate future occurrences in advance and adjust investment decisions accordingly. These foresight approaches are also necessary to consider the utilization effect caused by a large-scale deployment of VRE during capacity expansion optimization. Without considering the utilization effect, the computed least-cost expansion plan might contain stranded investments especially in conventional thermal power plants. The analysis also highlighted that competiveness of RES-E increases with the length of the model foresight, because the advantage of RES-E to provide electricity at stable costs over the lifetime is considered and valued.

However, the larger the applied foresight of the model the higher is the computational effort. In addition, a large model foresight with perfect information might overestimate the capability to foresee future developments and therefore does not realistically represent the frame conditions of real-life decision makers. Hence, the suitability of the applied foresight approach depends on the purpose of the study and the acceptable computational effort.

The perfect foresight approach is especially suitable for policy makers to identify economically efficient transition pathways towards a sustainable electricity supply, because results represent the intertemporal global optimum for the planning time frame to meet electricity demand, reliability standards, and transition targets with lowest costs. Results can be used as basis for a policy design that enables the evolution of the system towards this ideal world.

The single-year myopic foresight approach is suitable to investigate the consequences of unpredictable events for the power system (e.g. sudden introduction of CO_2 prices), because the characteristic of the model is shifted towards a simulation model. A short model foresight might better represent the evolutionary nature of the power system. However, computed results cannot be interpreted anymore as the global optimum for the planning time frame.

The multi-annual rolling horizon approach offers a compromise between the perfect foresight and the single-year myopic foresight approach in terms of the model capability to anticipate future occurrences and in terms of computational effort. The approach is an appropriate approach especially for utilities that aim to identify economic efficient investment options under a more conservative assumption than perfect foresight over the entire planning horizon.

Long-term capacity expansion optimization with REMix-CEM is typically based on a limited number of representative dispatch periods in order to keep computational effort manageable. This work demonstrated that the average day method is inappropriate to assign values for RE resource availability to the considered dispatch periods. By averaging values for temporal RE resource availability the method underestimates the variability of VRE, especially of wind power, significantly. This overestimates the value of VRE from a system perspective considerably and underestimates flexibility requirements for the system caused by a large-scale integration of VRE. As a consequence, non-optimal investment decisions are made by the optimization model and putative least-cost power systems have higher generation costs and CO_2 emissions than initially expected during capacity expansion optimization.

The representative day method, which uses “real” historical days instead of synthetic average days, models the seasonal and diurnal variability of RE resources more precisely. This allows a more accurate consideration of the value of energy at its time of the delivery and flexibility requirements of the system within capacity expansion optimization. Nevertheless, this work also highlighted that for high VRE shares the accuracy of the representative day method starts to decrease because extreme situations are also not captured by this method. Future research is required to improve the temporal representation of VRE generation during capacity expansion modelling. Such research can set-up on work presented in [101–104].

This work showed that the flexibility effect and related costs caused by a large-scale integration of VRE can have a significant impact on investment decisions and should therefore be considered within long-term capacity expansion optimization. Neglecting the flexibility effect underestimates significantly the flexibility requirements of the power system. This leads to an overestimation of VRE competiveness from a system perspective and a simultaneous underestimation of the competiveness of and the need for flexible power generation and energy storage technologies.

The flexibility effect can be considered during capacity expansion optimization by modelling unit commitment constraints of thermal generators. As modelling unit commitment constraints requires a large number of integer decision variables, this comes typically at very high computational cost. However, this work demonstrated that the flexibility effect can be considered already accurately during capacity expansion optimization with comparably low additional computational effort, when only start-up and ramping costs are considered and a linear relaxation for integer unit commitment decision variables is applied.

The focus of this work was not to investigate the competiveness of a certain technology. However, this work indicates that CSP can play a major role for the transition towards a sustainable electricity supply for power systems with high solar resource potentials. CSP represents firm and flexible generation capacity with stable generation costs over the lifetime. In addition, due to its technical characteristics, CSP is highly suitable to support the integration of VRE (especially of PV). This makes CSP a very attractive investment option from a least-cost system perspective for countries with excellent solar resource potentials.

The excellent capabilities of CSP to integrate PV has led to the development of CSP-PV hybrid concepts which combine the advantages of both technologies [132]. Hybrid power plants that are composed of a PV system, Lithium-ion batteries, and a conventional thermal generator might become an economic efficient complement in the medium-term, due to expected further cost reduction of PV and promising recent price reductions of Lithium-ion batteries [105], [106].

However, within the analysis of this work it could also be observed that, based on the applied cost assumptions, CSP is only competitive from a least-cost system perspective in the medium-

to long-term. Yet, this is a chicken-and-egg problem because assumed future cost reductions can only be achieved through technology learning. This however requires the installation of units. Applying de-risking measures could increase competiveness of CSP in the short-term. This could ensure the achievement of the required future cost reduction [107], [108].

Results from a least-cost optimization model like REMix-CEM must be interpreted carefully. The outcome of the model must be taken rather as what-if-analysis than as prediction of the future. In addition, it must be kept in mind that the simple application of an optimization model will in most cases not lead to a balanced scenario for the power system that meets all strategic targets of a national planning authority. Hence, when DLR-SYS applies REMix-CEM to support national planning authorities of developing and emerging countries to develop a balanced "lead scenario" for the power system, the model is applied in an iterative way. Planning imperatives formulated by the national planning authority during the advisory process, such as e.g. GHG mitigation, diversification of supply, or consistent technology-specific growth rates, are incorporated step-by-step into the optimization model to narrow down the solution space. This process is typically supported by international cooperation institutions.

This work leaves spaces for future research and enhancements of the REMix modelling framework. The method for selecting a limited number of typical days to represent temporal variability of RE resources within capacity expansion optimization should be improved. Furthermore, stochastic optimization procedures could be introduced to identify robust least-cost capacity expansion pathways that consider the uncertainty of input parameters. In this context, new solution methods to speed up computing times should be developed and implemented. Here, the Benders' Decomposition algorithm is a promising option [109], [110]. Subsequent research should also focus on the transformation of the modelling framework from a single-criterion to a multi-criteria optimization model. This would allow identifying solutions that are not only driven by the least-cost criterion but also by other criteria like e.g. environmental aspects. The Energy-Water-Nexus is a huge challenge [111–113]. The modelling framework could be enhanced for co-optimizing capacity expansion of the energy and water sector in detail. Such an integrated resource planning could identify possible benefits from sector-coupling and help to develop sustainable strategies to solve the Energy-Water-Nexus.

Bibliography

[1] UNFCCC, “Paris Agreement.” United Nations Framework Convention on Climate Change (UNFCCC), http://unfccc.int/paris_agreement/items/9485.php (accessed 6 December 2016), 2016.

[2] IPCC, “Climate Change 2014: Mitigation of Climate Change, Working Group III Contribution to the Fifth Assessment Report of the Intergovernmantal Panel on Climate Change,” Cambridge University Press, 2014.

[3] L. Hirth, “The benefits of flexibility: The value of wind energy with hydropower,” *Applied Energy*, vol. 181, pp. 210–223, 2016.

[4] F. Trieb, “Integration erneuerbarer Energie bei hohen Anteilen an der Stromversorgung.,” *Energiewirtschaftliche Tagesfragen*, vol. 63:7, pp. 28–32, 2013.

[5] C. Breyer, D. Bogdanov, K. Komoto, T. Ehara, J. Song, and N. Enebish, “North-East Asian Super Grid: Renewable energy mix and economics,” *Japanese Journal of Applied Physics*, vol. 54, no. 8S1, p. 08KJ01, 2015.

[6] IRENA, “Estimating the Renewable Energy Potential in Africa - A GIS-based approach (Working Paper),” International Renewable Energy Agency, 2014.

[7] M. G. Pereira, C. F. Camacho, M. A. V. Freitas, and N. F. da Silva, “The renewable energy market in Brazil: Current status and potential,” *Renewable and Sustainable Energy Reviews*, vol. 16, no. 6, pp. 3786–3802, 2012.

[8] F. Trieb, C. Schillings, S. Kronshage, P. Viebahn, M. Kabariti, D. K.M., A. Bennouna, H. El Nokraschy, S. Hassan, L. G. Yussef, T. Hasni, N. El Bassam, and H. Satoguina, “Concentrating Solar Power for the Mediterranian Region: MED-CSP,” German Aersopace Center (DLR), 2005.

[9] K. Ummel, “Concentrating Solar Power in China and India: A Spatial Analysis of Technical Potential and the Cost of Deployment,” Center for Global Development, Jul. 2010.

[10] P. Gauché, “Spatial-temporal model to evaluate the system potential of concentrating solar power towers in South Africa,” Faculty of Engineering at Stellenbosch University, 2016.

[11] C. G. Heaps, “Long-range Energy Alternatives Planning (LEAP) system,” Stockholm Environment Institute, Somerville, MA, USA, 2016.

[12] IAEA, “Wien Automatic System Planning (WASP) Package - A Computer code for Power Generating System Expansion Planning, Version WASP-IV, User’s Manual,” International Atomic Energy Agency (IAEA), 2001.

[13] L. Schrattenholzer, “The Energy Supply Model MESSAGE,” IIASA, Dec. 1981.

[14] H. Seifi and M. Sepasian, “Power System Planning, Basic Principles,” in *Electric Power System Planning*, Springer Berlin Heidelberg, 2011, pp. 1–14.

[15] K.-K. Cao, “Analyse langfristiger Ausbauszenarien des deutschen und europäischen Stromübertragungsnetzes und deren Rolle im zukünftigen Energiesystem (working titel of ongoing PhD thesis),” Universität Stuttgart, 2017.

[16] F. Cebulla, “Perspectives of electricity storages with respect to the integration of high shares of renewable energies into the German supply structure (working titel of ongoing PhD thesis),” Universität Stuttgart, 2017.

[17] D. Stetter, “Enhancement of the REMix energy system model: Global renewable energy potentials, optimized power plant siting and scenario validation,” Universität Stuttgart, 2014.

[18] A. M. Foley, B. P. Ó. Gallachóir, J. Hur, R. Baldick, and E. J. McKeogh, “A strategic review of electricity systems models,” *Energy*, vol. 35, no. 12, pp. 4522–4530, 2010.

[19] M. Moechtar, T. C. Cheng, and L. Hu, “Transient stability of power system - a survey,” in *WESCON/’95. Conference record. ’Microelectronics Communications Technology Producing Quality Products Mobile and Portable Power Emerging Technologies*, 1995, pp. 166–171.

[20] B. Chowdhury and S. Rahman, “A review of recent advances in economic dispatch,” *IEEE Transactions on Power Systems*, vol. 5, no. 4, pp. 1248–1259, Nov. 1990.
[21] Z. Qiu, G. Deconinck, and R. Belmans, “A literature survey of Optimal Power Flow problems in the electricity market context,” in *Power Systems Conference and Exposition, 2009. PSCE ’09. IEEE/PES*, 2009, pp. 1–6.
[22] N. P. Padhy, “Unit commitment-a bibliographical survey,” *IEEE Transactions on Power Systems*, vol. 19, no. 2, pp. 1196–1205, May 2004.
[23] D. Chattopadhyay, “A practical maintenance scheduling program mathematical model and case study,” *IEEE Transactions on Power Systems*, vol. 13, no. 4, pp. 1475–1480, Nov. 1998.
[24] N. Nabona, J. Castro, and J. A. Gonzalez, “Optimum long-term hydrothermal coordination with fuel limits,” *IEEE Transactions on Power Systems*, vol. 10, no. 2, pp. 1054–1062, May 1995.
[25] P. Denholm, J. Jorgenson, M. Hummon, T. Jenkin, and D. Palchak, “The Value of Energy Storage for Grid Applications,” National Renewable Energy Laboritory (NREL), NREL/TP-6A20-58465, May 2013.
[26] J. Jorgenson, P. Denholm, M. Mehos, and C. Turchi, “Estimating the Performance and Economic Value of Multiple Concentrating Solar Power Technologies in a Production Cost Model,” National Renewable Energy Laboratory (NREL), TP-6A20-58645, Dec. 2013.
[27] J. P. Deane, G. Drayton, and B. P. Ó. Gallachóir, “The impact of sub-hourly modelling in power systems with significant levels of renewable generation,” *Applied Energy*, vol. 113, pp. 152–158, 2014.
[28] N. V. Beeck, “Classification of Energy Models.,” Tilburg University, Faculty of Economics and Business Administration, 1999.
[29] G. Latorre, R. D. Cruz, J. M. Areiza, and A. Villegas, “Classification of publications and models on transmission expansion planning,” *IEEE Transactions on Power Systems*, vol. 18, no. 2, pp. 938–946, May 2003.
[30] D. Möst and W. Fichtner, *Energiesystemanalyse*. Universitätsverlag Karlsruhe, 2009, pp. 11–31.
[31] B. S. Palmintier, “Incorporating operational flexibility into electric generation planning: impacts and methods for system design and policy analysis,” Massachusetts Institute of Technology, 2013.
[32] P. Donohoo-Vallett, M. Milligan, and B. Frew, “Capricious Cables: Understanding the Limitations and Context of Transmission Expansion Planning Models,” *The Electricity Journal*, vol. 28, no. 9, pp. 85–99, 2015.
[33] V. Krishnan, J. Ho, B. F. Hobbs, A. L. Liu, J. D. McCalley, M. Shahidehpour, and Q. P. Zheng, “Co-optimization of electricity transmission and generation resources for planning and policy analysis: review of concepts and modeling approaches,” *Energy Systems*, pp. 1–36, 2015.
[34] R. Jones, “Diversity Benefit for Solar and Wind with Increasing Market Penetration. System Capacity Value,” in *Presentation at the Intersolar 2012 Conference*.
[35] REN21, “Renewables 2016, Global Status Report,” Renweable Energy Policy Network for the 21st century, 2016.
[36] IRENA, “Renewable Power Generation Costs in 2014,” International Renewable Energy Agency (IRENA), 2015.
[37] WB, “Bringing Variable Renewable Energy up to Scale - Options for Grid Integration Using Natural Gas and Energy Storage,” The World Bank (WB)- Energy Sector Management Assistance Program (ESMAP), 2015.
[38] J. P. M. Sijm, “Cost and revenue related impacts of integrating electricity from variable renewable energy into the power system - A review of recent literature.” ECN, May-2014.
[39] IEA, “The Power of Transformation,” International Energy Agency (IEA), 2014.

[40] M. Nicolosi, “The Economics of Renewable Electricity Market Integration. An Empirical and Model-Based Analysis of Regulatory Frameworks and their Impacts on the Power Market,” Universität Köln, 2012.

[41] D. Lew, G. Brinkman, E. Ibanez, A. Florita, M. Heaney, B.-M. Hodge, M. Hummon, G. Stark, J. King, S. A. Lefton, N. Kumar, D. Agan, G. Jordan, and S. Venkataraman, “The Western Wind and Solar Integration Study Phase 2,” National Renewable energy Laboratory (NREL), NREL/TP-5500-55588, Sep. 2013.

[42] H. Holttinen, J. Kiviluoma, A. Robitaille, N. Cutululis, A. Orths, F. van Hulle, I. Pineda, B. Lange, M. O’Malley, J. Dillon, E. Carline, C. Vergine, J. Kondoh, M. Gibescu, J. Tande, A. Stanqueiro, E. Gomez, L. Söder, J. Smith, M. Milligan, and D. Lew, “Design and operation of power systems with large amounts of wind power - Final summary report, IEA WIND Task 25, Phase two 2009–2011,” Technical Research Centre of Finland (VTT), 2013.

[43] H. Holttinen, P. Meibom, A. Orths, B. Lange, M. O’Malley, J. O. Tande, A. Estanqueiro, E. Gomez, L. Söder, G. Strbac, J. C. Smith, and F. van Hulle, “Impacts of large amounts of wind power on design and operation of power systems, results of IEA collaboration,” *Wind Energy*, vol. 14, no. 2, pp. 179–192, 2011.

[44] L. Hirth, “Market value of solar power: Is photovoltaics cost-competitive?,” *Renewable Power Generation, IET*, vol. 9, no. 1, pp. 37–45, 2015.

[45] S. Lu, M. Warwick, N. Samaan, J. Fuller, D. Meng, R. Diao, F. Chassin, T. Nguyen, Y. Zhang, C. Jin, and B. Vyakaranam, “Duke Energy Photovoltaic Integration Study: Carolinas Service Areas,” Pacific Northwest National Laboratory, Mar. 2014.

[46] J. Wu, A. Botterud, A. Mills, Z. Zhou, B.-M. Hodge, and M. Heaney, “Integrating solar PV (photovoltaics) in utility system operations: Analytical framework and Arizona case study,” *Energy*, vol. 85, pp. 1–9, 2015.

[47] L. Hirth, F. Ueckerdt, and O. Edenhofer, “Integration costs revisited: An economic framework for wind and solar variability,” *Renewable Energy*, vol. 74, pp. 925–939, 2015.

[48] A. S. Malik and C. Kuba, “Power Generation Expansion Planning Including Large Scale Wind Integration: A Case Study of Oman,” *Journal of Wind Energy*, vol. 2013, p. 7, 2013.

[49] NEA, “Nuclear Energy and Renewables System Effects in Low-carbon Electricity Systems,” Nuclear Energy Agency (NEA), 2012.

[50] J. P. Deane, A. Chiodi, M. Gargiulo, and B. P. Ó. Gallachóir, “Soft-linking of a power systems model to an energy systems model,” *Energy*, vol. 42, no. 1, pp. 303–312, 2012.

[51] A. Pina, C. Silva, and P. Ferrão, “High-resolution modeling framework for planning electricity systems with high penetration of renewables,” *Applied Energy*, vol. 112, pp. 215–223, 2013.

[52] J. Rosen, I. Tietze-Stöckinger, and O. Rentz, “Model-based analysis of effects from large-scale wind power production,” *Energy*, vol. 32, no. 4, pp. 575–583, 2007.

[53] S. Ludig, M. Haller, E. Schmid, and N. Bauer, “Fluctuating renewables in a long-term climate change mitigation strategy,” *Energy*, vol. 36, no. 11, pp. 6674–6685, 2011.

[54] A. Pina, C. Silva, and P. Ferrão, “Modeling hourly electricity dynamics for policy making in long-term scenarios,” *Energy Policy*, vol. 39, no. 9, pp. 4692–4702, 2011.

[55] C. I. Nweke, F. Leanez, G. R. Drayton, and M. Kolhe, “Benefits of chronological optimization in capacity planning for electricity markets,” in *Power System Technology (POWERCON), 2012 IEEE International Conference*, 2012, pp. 1–6.

[56] M. Welsch, P. Deane, M. Howells, B. Ó. Gallachóir, F. Rogan, M. Bazilian, and H.-H. Rogner, “Incorporating flexibility requirements into long-term energy system models - A case study on high levels of renewable electricity penetration in Ireland,” *Applied Energy*, vol. 135, pp. 600–615, 2014.

[57] P. Sullivan, K. Eurek, and R. Margolis, “Advanced Methods for Incorporating Solar Energy Technologies into Electric Sector Capacity-Expansion Models: Literature Review and Analysis,” National Renewable Energy Laboritory (NREL), NREL/TP-6A20-61185, Jul. 2014.

[58] J. Johnston, A. Mileva, and J. H. Nelson, “SWITCH-WECC Data, Assumptions, and Model Formulation,” Energy Resource Group, University of California, Berkeley, Oct. 2013.

[59] B. Brand, A. B. Stambouli, and D. Zejli, “The value of dispatchability of CSP plants in the electricity systems of Morocco and Algeria,” *Energy Policy*, vol. 47, pp. 321–331, 2012.

[60] T. Fichter, F. Trieb, and M. Moser, “Optimized Integration of Renewable Energy Technologies Into Jordan’s Power Plant Portfolio,” *Heat Transfer Engineering*, vol. 35, no. 3, pp. 281–301, 2014.

[61] T. Fichter, F. Trieb, M. Moser, and J. Kern, “Optimized Integration of Renewable Energies into Existing Power Plant Portfolios,” *Energy Procedia*, vol. 49, pp. 1858–1868, 2014.

[62] T. Fichter, R. Soria, A. Szklo, R. Schaeffer, and A. F. P. Lucena, “Assessing the potential role of concentrated solar power (CSP) for the northeast power system of Brazil using a detailed power system model,” *Energy*, vol. 121, pp. 695–715, 2017.

[63] V. Krishnan and J. D. McCalley, “Building Foresight in Long-Term Infrastructure Planning Using End-Effect Mitigation Models,” *Systems Journal, IEEE*, vol. PP, no. 99, pp. 1–12, 2015.

[64] R. Soria, A. F. P. Lucena, J. Tomaschek, T. Fichter, T. Haasz, A. Szklo, R. Schaeffer, P. Rochedo, U. Fahl, and J. Kern, “Modelling concentrated solar power (CSP) in the Brazilian energy system: A soft-linked model coupling approach,” *Energy*, vol. 116, Part 1, pp. 265–280, 2016.

[65] F. Cebulla and T. Fichter, “Merit order or unit-commitment: How does thermal power plant modeling affect storage demand in energy system models?,” *Renewable Energy*, vol. 105, pp. 117–132, 2017.

[66] M. Moser, F. Trieb, T. Fichter, J. Kern, H. Maier, and P. Schicktanz, “Techno-economic Analysis of Enhanced Dry Cooling for CSP,” *Energy Procedia*, vol. 49, pp. 1177–1186, 2014.

[67] H. C. Gils, “Balancing of Intermittent Renewable Power Generation by Demand Response and Thermal Energy Storage,” Universität Stuttgart, 2015.

[68] H. C. Gils, Y. Scholz, T. Pregger, D. L. de Tena, and D. Heide, “Integrated modelling of variable renewable energy-based power supply in Europe,” *Energy*, vol. 123, pp. 173–188, 2017.

[69] D. L. de Tena, “Large Scale Renewable Power Integration with Electric Vehicles,” Universität Stuttgart, 2014.

[70] Y. Scholz, “Renewable energy based electricity supply at low costs: development of the REMix model and application for Europe,” Universität Stuttgart, 2012.

[71] ENTSO-E, “Scenario Outlook And Adequacy Forecast 2013-2030,” European Network of Transmission System Operators for Electricity (ENTSO-E), Apr. 2013.

[72] A. S. Brouwer, M. van den Broek, A. Seebregts, and A. Faaij, “Impacts of large-scale Intermittent Renewable Energy Sources on electricity systems, and how these can be modeled,” *Renewable and Sustainable Energy Reviews*, vol. 33, no. 0, pp. 443–466, 2014.

[73] R. Doherty, H. Outhred, and M. O’Malley, “Establishing the role that wind generation may have in future generation portfolios,” *Power Systems, IEEE Transactions on*, vol. 21, no. 3, pp. 1415–1422, Aug. 2006.

[74] S. H. Madaeni, R. Sioshansi, and P. Denholm, “Comparing Capacity Value Estimation Techniques for Photovoltaic Solar Power,” *IEEE Journal of Photovoltaics*, vol. 3, no. 1, pp. 407–415, Jan. 2013.

[75] D. Pudjianto, P. Djapic, J. Dragovic, and G. Strbac, “Grid Integration Cost of PhotoVoltaic Power Generation - Direct Costs Analysis related to Grid Impacts of Photovoltaics,” Imperial College London, 2013.

[76] B. Sirgin, P. Sullivan, E. Ibanenz, and R. Margolis, “Representation of Solar Capacity Value in the ReEDS Capacity Expansion Model,” National Renewable energy Laboratory (NREL), NREL/TP-6A20-61182, Mar. 2014.

[77] B. Palmintier and M. Webster, “Impact of unit commitment constraints on generation expansion planning with renewables,” in *Power and Energy Society General Meeting, 2011 IEEE*, 2011, pp. 1–7.
[78] D. Rajan and S. Takriti, “Minimum up/down polytopes of the unit commitment problem with start-up costs.,” IBM Research Report RC23628, 2005.
[79] G. Morales-Espana, J. M. Latorre, and A. Ramos, “Tight and Compact MILP Formulation for the Thermal Unit Commitment Problem,” *Power Systems, IEEE Transactions on*, vol. 28, no. 4, pp. 4897–4908, Nov. 2013.
[80] J. M. Arroyo and A. J. Conejo, “Optimal response of a thermal unit to an electricity spot market,” *Power Systems, IEEE Transactions on*, vol. 15, no. 3, pp. 1098–1104, Aug. 2000.
[81] J. Ostrowski, M. F. Anjos, and A. Vannelli, “Tight Mixed Integer Linear Programming Formulations for the Unit Commitment Problem,” *Power Systems, IEEE Transactions on*, vol. 27, no. 1, pp. 39–46, Feb. 2012.
[82] M. Carróin and J. M. Arroyo, “A computationally efficient mixed-integer linear formulation for the thermal unit commitment problem,” *Power Systems, IEEE Transactions on*, vol. 21, no. 3, pp. 1371–1378, 2006.
[83] F. R. P. Arrieta and E. E. S. Lora, “Influence of ambient temperature on combined-cycle power-plant performance,” *Applied Energy*, vol. 80, no. 3, pp. 261–272, 2005.
[84] A. D. Sa and S. A. Zubaidy, “Gas turbine performance at varying ambient temperature,” *Applied Thermal Engineering*, vol. 31, no. 14–15, pp. 2735–2739, 2011.
[85] H. Zhai and E. S. Rubin, “Performance and cost of wet and dry cooling systems for pulverized coal power plants with and without carbon capture and storage,” *Energy Policy*, vol. 38, no. 10, pp. 5653–5660, 2010.
[86] P. Denholm, Y.-H. Wan, M. Hummon, and M. Mehos, “An Analysis of Concentrating Solar Power with Thermal Energy Storage in a California 33% Renewable Scenario,” National Renewable Energy Laboratory (NREL), NREL/TP-6A20-58186, Mar. 2013.
[87] F. Trieb, T. Fichter, and M. Moser, “Concentrating solar power in a sustainable future electricity mix,” *Sustainability Science*, vol. 9, no. 1, pp. 47–60, 2014.
[88] M. Moser, “Combined electricity and water production based on solar energy,” Universität Stuttgart, 2015.
[89] P. Seljom and A. Tomasgard, “Short-term uncertainty in long-term energy system models - A case study of wind power in Denmark,” *Energy Economics*, vol. 49, no. Supplement C, pp. 157–167, 2015.
[90] A. Tuohy, P. Meibom, E. Denny, and M. O’Malley, “Benefits of Stochastic Scheduling for Power Systems with Significant Installed Wind Power,” in *Proceedings of the 10th International Conference on Probablistic Methods Applied to Power Systems*, 2008, pp. 1–7.
[91] W. Usher and N. Strachan, “Critical mid-term uncertainties in long-term decarbonisation pathways,” *Energy Policy*, vol. 41, no. Supplement C, pp. 433–444, 2012.
[92] M. Babiker, A. Gurgel, S. Paltsev, and J. Reilly, “Forward-looking versus recursive-dynamic modeling in climate policy analysis: A comparison,” *Economic Modelling*, vol. 26, no. 6, pp. 1341–1354, 2009.
[93] V. Krey, “Vergleich kurz- und langfristig ausgerichteter Optimierungsansätze mit einem multi-regionalen Energiesystemmodell unter Berücksichtigung stochastischer Parameter,” Ruhr-Universität Bochum, 2006.
[94] S. Babrowski, T. Heffels, P. Jochem, and W. Fichtner, “Reducing computing time of energy system models by a myopic approach,” *Energy Systems*, vol. 5, no. 1, pp. 65–83, 2014.
[95] I. Keppo and M. Strubegger, “Short term decisions for long term problems - The effect of foresight on model based energy systems analysis,” *Energy*, vol. 35, no. 5, pp. 2033–2042, 2010.

[96] S. Pfenninger, A. Hawkes, and J. Keirstead, “Energy systems modeling for twenty-first century energy challenges,” *Renewable and Sustainable Energy Reviews*, vol. 33, pp. 74–86, 2014.
[97] G. Haydt, V. Leal, A. Pina, and C. A. Silva, “The relevance of the energy resource dynamics in the mid/long-term energy planning models,” *Renewable Energy*, vol. 36, no. 11, pp. 3068–3074, 2011.
[98] A. Ceselli, A. Gelmini, G. Righini, and A. Taverna, “Mathematical Programming bounds for Large-Scale Unit Commitment Problems in Medium-Term Energy System Simulations,” in *4th Student Conference on Operational Research*, 2014, vol. 37, pp. 63–75.
[99] DLR, “MOREMix project.” Project conducted for the Ministry of Energy, Mines, Water and Environment (MEMEE) of Morocco on behalf of GIZ, http://www.dlr.de/tt/en/desktopdefault.aspx/tabid-2885/4422_read-43923/ (accessed 10 December 2016).
[100] J. Kern, T. Fichter, M. Moser, F. Trieb, F. Seidel, K. Heising, and P. Lempp, “MOREMix - Power sector optimization for Morocco,” *AIP Conference Proceeding*, vol. 1734, no. 1, May 2016.
[101] P. Nahmmacher, E. Schmid, L. Hirth, and B. Knopf, “Carpe diem: A novel approach to select representative days for long-term power system modeling,” *Energy*, vol. 112, pp. 430–442, 2016.
[102] K. Poncelet, E. Delarue, D. Six, J. Duerinck, and W. D’haeseleer, “Impact of the level of temporal and operational detail in energy-system planning models,” *Applied Energy*, vol. 162, pp. 631–643, 2016.
[103] K. Poncelet, H. Höschle, E. Delarue, and W. D’haeseleer, “Selecting representative days for investment planning models,” *KU Leuven, Division of applied mechanics and energy conversion,*, vol. Working paper EN2015–10, 2015.
[104] F. J. de Sisternes and M. D. Webster, “Optimal selection of sample weeks for approximating the net load in generation planning problems,” *Massachusetts Institute of Technology (MIT) Engineering Systems Division (ESD)*, no. ESD-WP-2013–03, Mar. 2013.
[105] S. Afanasyeva, C. Breyer, and M. Engelhard, “Impact of Battery Cost on the Economics of Hybrid Photovoltaic Power Plants,” *Energy Procedia*, vol. 99, pp. 157–173, 2016.
[106] C. Cader, P. Bertheau, P. Blechinger, H. Huyskens, and C. Breyer, “Global cost advantages of autonomous solarr-battery-diesel systems compared to diesel-only systems,” *Energy for Sustainable Development*, vol. 31, pp. 14–23, 2016.
[107] F. Trieb, H. Müller-Steinhagen, and Jürgen Kern, “Financing concentrating solar power in the Middle East and North Africa - Subsidy or investment?,” *Energy Policy*, vol. 39, no. 1, pp. 307–317, 2011.
[108] O. Waissbein, Y. Glemarec, H. Bayraktar, and T. S. Schmidt, “Derisking Renewable Energy Investment - A Framework to Support Policymakers in Selecting Public Instruments to Promote Renewable Energy Investment in Developing Countries,” United Nation Development Programme (UNDP), 2013.
[109] J. Linderoth and S. Wright, “Decomposition Algorithms for Stochastic Programming on a Computational Grid,” *Computational Optimization and Applications*, vol. 24, no. 2, pp. 207–250, 2003.
[110] C. Skar, G. Doorman, and A. Tomasgard, “Large-scale power system planning using enhanced Benders decomposition,” in *2014 Power Systems Computation Conference*, 2014, pp. 1–7.
[111] IEA, “World Energy Outlook 2012,” OECD Publishing, 2012.
[112] IRENA, “Renewable Energy in the Water, Energy & Food Nexus,” International Renewable Energy Agency (IRENA), 2015.
[113] A. Siddiqi and L. D. Anadon, “The water-energy nexus in Middle East and North Africa,” *Energy Policy*, vol. 39, no. 8, pp. 4529–4540, 2011.
[114] IEA, “Biomass for Heat and Power, Energy Technology Systems Analysis Program (ETSAP), Technology Brief E05,” International Energy Agency (IEA), May 2010.

[115] International Energy Agency (IEA), “Nuclear Power, Energy Technology Systems Analysis Program (ETSAP), Technology Brief E03,” International Energy Agency IEA, Apr. 2010.
[116] IEA, “World Energy Outlook 2015,” OECD Publishing, 2015.
[117] IPCC, “2006 IPCC Guidelines for National Greenhouse Gas Inventories – Chapter 2: Stationary Combustion,” Intergovernmental Panel on Climate Change IPCC, 2006.
[118] IRENA, “Biomass for Power Generation - Renewable Energy Technoogies: Cost Analysis Series Volume 1: Power Sector, Issue 1/5,” International Renewable Energy Authority (IRENA), Jun. 2012.
[119] IEA, “World Energy Outlook 2014,” OECD Publishing, 2014.
[120] A. S. Brouwer, M. van den Broek, A. Seebregts, and A. Faaij, “Operational flexibility and economics of power plants in future low-carbon power systems,” *Applied Energy*, vol. 156, pp. 107–128, 2015.
[121] IEA, “Technology Roadmap - Solar Photovoltaic Energy - 2014,” International Energy Agency (IEA), 2014.
[122] IRENA, “Renewable Energy Technologies: Cost Analysis Series, Volume 1: Power Sector Issue 5/5 Wind Power,” International Renewable Energy Agency (IRENA), 2012.
[123] IRENA, “The Power to Change: Solar and Wind Cost Reduction Potential to 2025,” International Renewable Energy Agency, Jun. 2016.
[124] P. Konstantin, “Praxisbuch Energiewirtschaft: Energieumwandlung, -transport und -beschaffung im liberalisierten Markt,” Springer, 2009.
[125] IEA, “Technology Roadmap - Solar Thermal Electricity - 2014,” International Energy Agency (IEA), 2014.
[126] N. Kumar, P. Besuner, S. Lefton, and D. Agan, “Power Plant Cycling Costs,” NREL, Intertek APTECH, Jul. 2012.
[127] DLR, “Renewable Energy Strategy for Botswana.” Project conducted for the Ministry of Minerals, Energy and Water Resources (MMEWR) of Botswanathe on behalf of the World Bank, http://www.dlr.de/tt/en/desktopdefault.aspx/tabid-2885/4422_read-45668/ (accessed 10 December 2016).
[128] A. Moser, N. Rotering, and A. Schäfer, “Unterstützung der Energiewende in Deutschland durch einen Pumpspeicherausbau – Potentiale zur Verbesserung der Wirtschaftlichkeit und der Versorgungssicherheit. Wissenschaftliche Studie im Auftrag der Voith Hydro GmbH & Co. KG,” Institut für Elektrische Anlagen und Energiewirtschaft, RWTH Aachen, Apr. 2014.
[129] IRENA, “Renewable Energy Technologies: Cost Analysis Series, Volume 1: Power Sector Issue 3/5 Hydropower,” International Renewable Energy Agency (IRENA), 2012.
[130] BV, “Cost and Performance Data for Power Generation Technologies - Prepared for the National Renewable Energy Laboratory,” Black & Veatch, 2012.
[131] C. Kost, “Renewable energy in North Africa: Modeling of future electricity scenarios and the impact on manufacturing and employment,” Technischen Universität Dresden, Fakultät Wirtschaftswissenschaften, 2015.
[132] S. Giuliano, M. Puppe, H. Schenk, T. Hirsch, M. Moser, T. Fichter, J. Kern, F. Trieb, M. Engelhard, S. Hurler, A. Weigand, D. Brakemeier, J. Kretschmann, U. Haller, R. Klingler, C. Breyer, and S. Afanasyeva, “THERMVOLT - Systemvergleich von solarthermischen und photovoltaischen Kraftwerken für die Versorgungssicherheit, Schlussbericht,” Deutsches Zentrum für Luft- und Raumfahrt e.V. (DLR), Fichtner GmbH, M&W GmbH, Lappeenranta University of Technology (LTU) on behalf of the Federal Minstry for Economic Affairs and Energy (BMWi), 2016.

Appendix

A1: Characteristics of fictitious power system

Table 29: Existing generation capacity [GW] by model node in 2016

	N1	N2	N3	N4	Total
NUCLEAR	0	0.6	0	0	**0.6**
BIO	0	0.15	0	0	**0.15**
COAL	1.8	4.8	0	0	**6.6**
CCGT	0.4	0.8	0	0	**1.2**
GT-GAS	0.2	0.4	0	0	**0.6**
GT-OIL	0.1	0.2	0.15	0.15	**0.6**
CSP	0	0	0	0.1	**0.1**
HYDRO-RES	1.0	0	0	0	**1.0**
HYDRO-ROR	1.0	0	0	0	**1.0**
BATTERY	0	0	0	0	**0**
PUMPED-HYDRO	0.25	0	0	0	**0.25**
PV	0.1	0.1	0.1	0.2	**0.5**
WIND	0.5	0	0.5	0	**1.0**
Total	5.35	7.05	0.75	0.45	**13.6**

Table 30: Existing generation capacity [GW] by milestone year aggregated by technology

	2016	2019	2022	2025	2028	2031	2034	2037	2040
NUCLEAR	0.6	0.6	0.6	0.6	0.6	0.6	0.6	0.6	0.6
BIO	0.15	0.15	0.15	0.15	0.15	0.15	0.15	0.15	0.15
COAL	6.6	6.6	6.6	5.4	5.4	5.4	5.4	4.2	4.2
CCGT	1.2	1.2	1.2	1.2	1.2	1.2	1.2	1.2	0
GT-GAS	0.6	0.6	0.4	0.4	0.4	0.2	0.2	0	0
GT-OIL	0.6	0.6	0	0	0	0	0	0	0
CSP	0.1	0.1	0.1	0.1	0.1	0.1	0.1	0.1	0.1
HYDRO-RES	1.0	1.0	1.0	1.0	1.0	1.0	1.0	1.0	1.0
HYDRO-ROR	1.0	1.0	1.0	1.0	1.0	1.0	1.0	1.0	1.0
PUMPED-HYDRO	0.25	0.25	0.25	0.25	0.25	0.25	0.25	0.25	0.25
PV	0.5	0.5	0.5	0.5	0.5	0.5	0.5	0	0
WIND	1.0	1.0	1.0	1.0	1.0	0.5	0.5	0	0
Total	**13.6**	**13.6**	**12.8**	**11.6**	**11.6**	**10.9**	**10.9**	**8.5**	**7.3**

Table 31: Fuel price development over planning time frame [USD/MWh_{th}]
Fossil fuel prices aligned to the "New Energy Policy" scenario of IEA [116]**. Biomass and nuclear fuel prices also from IEA** [114], [115]**.**

Year	Oil	Natural gas	Coal	Nuclear	Biomass
2016	34.4	30.7	10.0	10.0	5.0
2019	45.4	27.6	11.2	10.0	5.0
2022	53.2	28.9	11.7	10.0	5.0
2025	59.3	32.4	12.0	10.0	5.0
2028	65.3	35.9	12.3	10.0	5.0
2031	70.3	38.6	12.6	10.0	5.0
2034	73.1	39.8	12.8	10.0	5.0
2037	75.9	41.1	13.0	10.0	5.0
2040	78.6	42.3	13.3	10.0	5.0

Table 32: CO_2 price development over planning time frame [USD/t]
aligned to assumed CO_2 prices in China in 2040 according to the New Policy scenario of the IEA [116]

Year	Group 1	Group2
2016	0	0
2019	5	0
2022	9	0
2025	14	0
2028	18	3
2031	23	20
2034	28	32
2037	32	36
2040	37	37

Table 33: CO_2 content of fuel [117]

Fuel	tCO_2/MWh_{th}
Oil	0.275
Natural gas	0.202
Coal	0.346

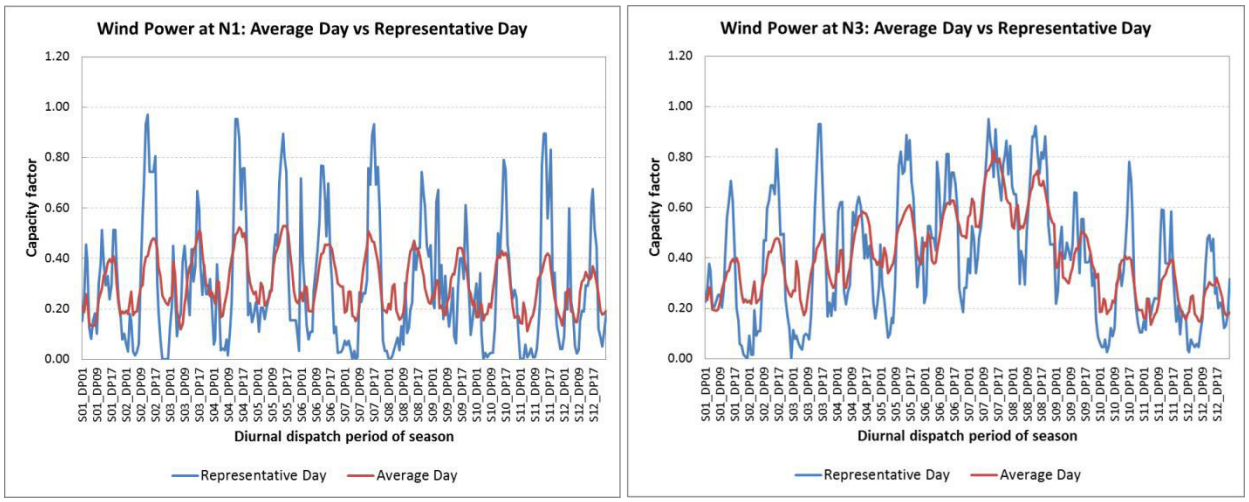

Figure 66: Comparison of daily wind power generation profiles according to average day and representative day method at model node N1 (left) and N3 (right)

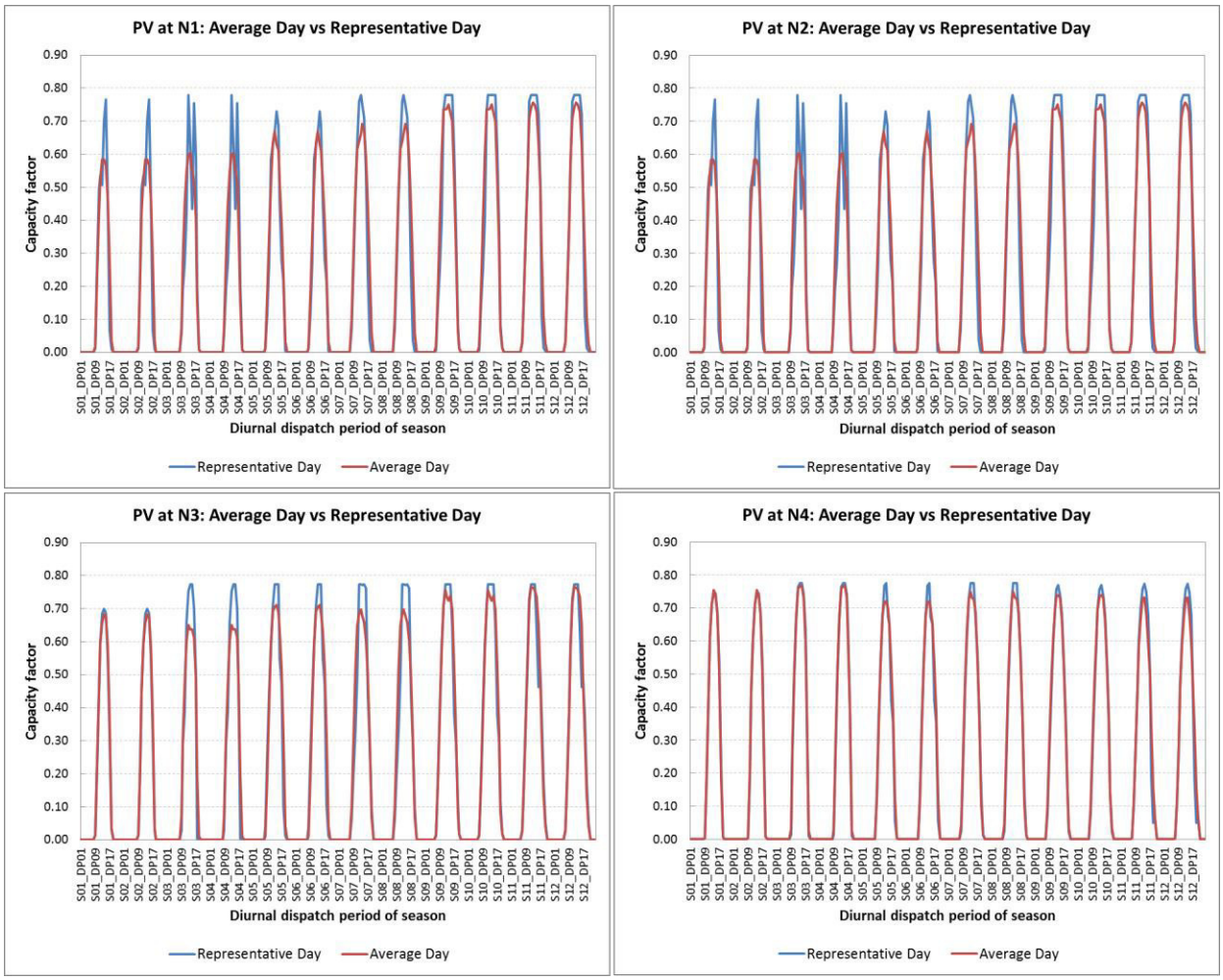

Figure 67: Comparison of daily PV generation profiles according to average day and representative day method at model node N1 (left-top), N2 (right-top), N3 (left-bottom), and N4 (right bottom)

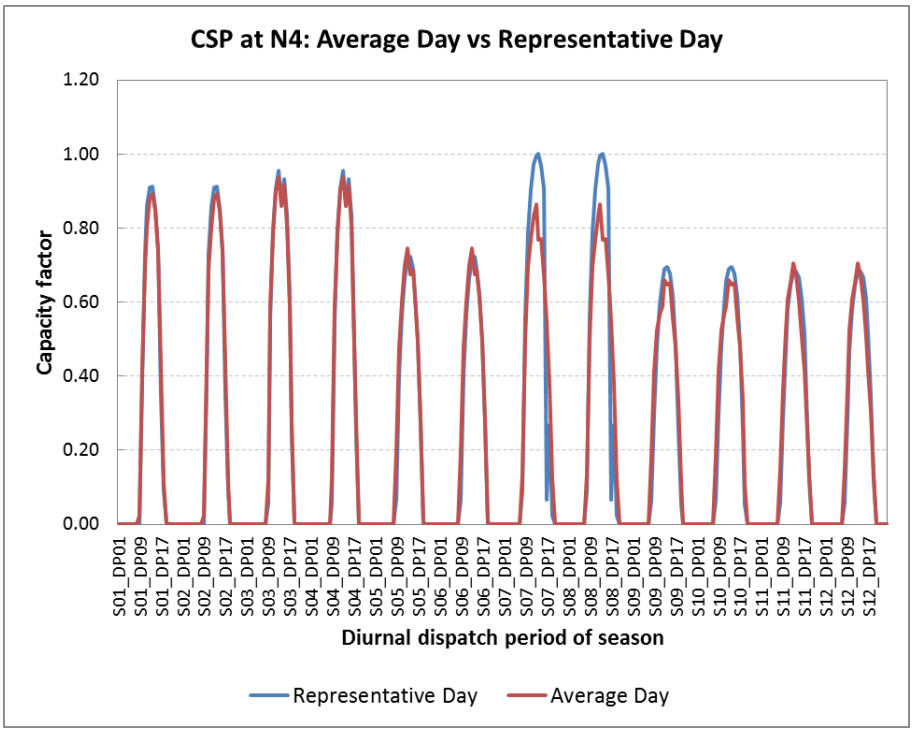

Figure 68: Comparison of daily CSP solar field generation profiles according to average day and representative day method at model node N4

Table 34: Assumed technology-specific capacity credits

Technology	Capacity credit [%] (incl. technically forced outage rate)
NUCLEAR	96
COAL	94
CCGT	96
OCGT	97
ICE	97
BIO	91
CSP	94 (related to capacity of back-up burner)
PUMPED-HYDRO	0 (only for operating reserve)
BATTERY	0 (only for operating reserve)
HYDRO-RES	95
HYDRO-ROR	Time-dependent
PV	Time-dependent
WIND	Time-dependent

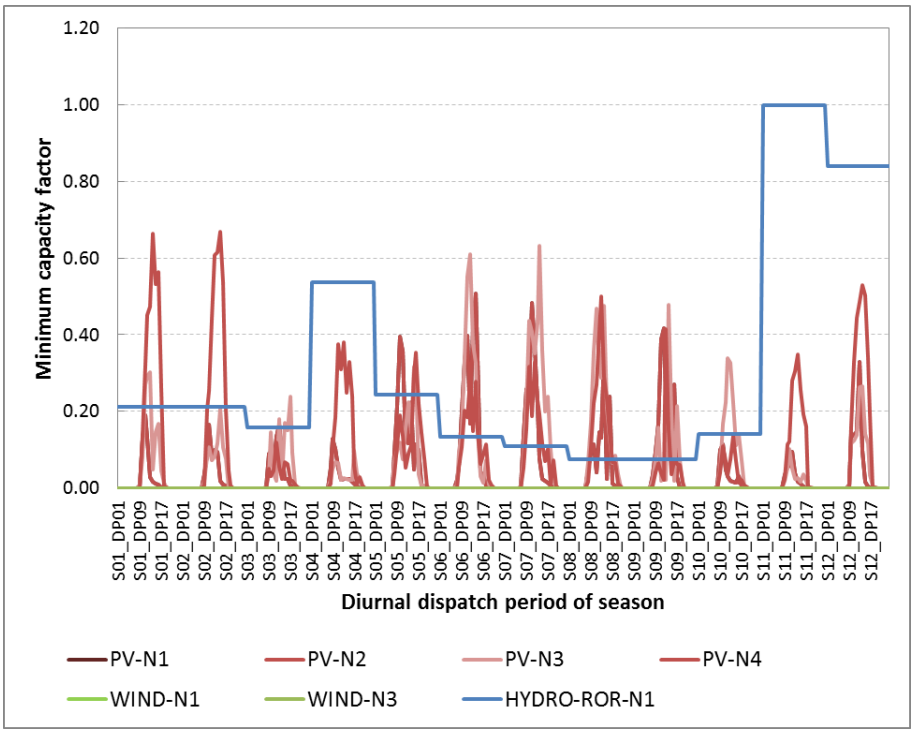

Figure 69: Time-dependent capacity credits of VRE generators (= minimum capacity factor for dispatch period, without technically forced outage rate)

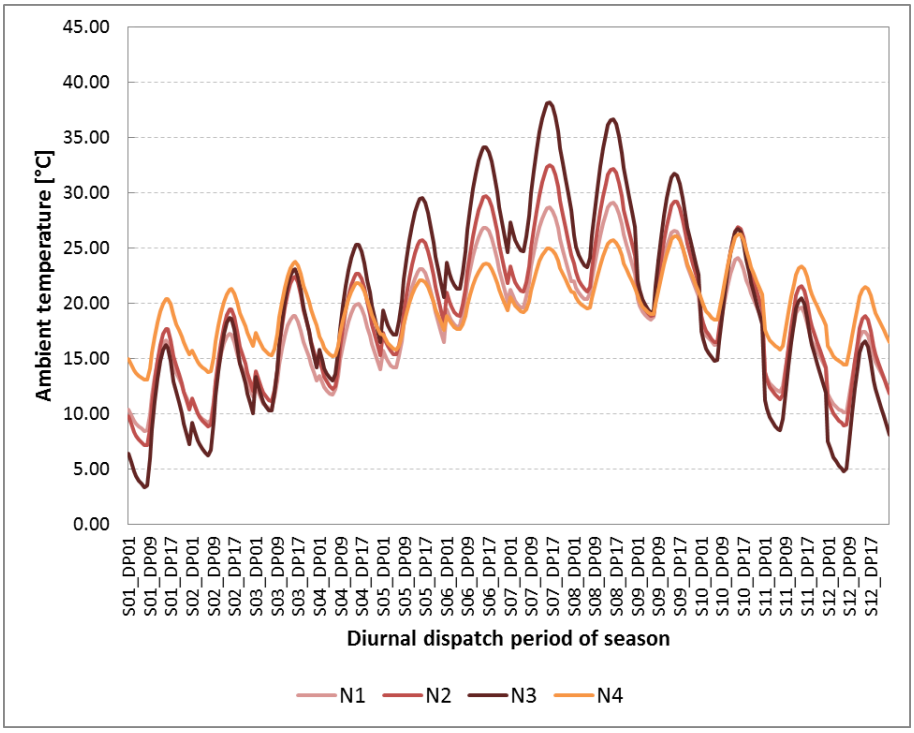

Figure 70: Ambient temperature at considered annual dispatch periods by model node

A2: Major techno-economic parameters of existing and candidate units

Table 35: Techno-economic parameters of existing VRE and hydro power units

Generator type	Capacity of single unit	Number of units	Fix O&M costs	Variable O&M costs	Maintenance outage rate	Forced outage rate
	[MW]	[-]	[kUSD/MW]	[kUSD/MWh]	[%]	[%]
PV	100	5	17	0	2.0	0.0
WIND	100	10	23	0.0075	0.6	5.0
HYDRO-ROR	250	4	35	0	1.9	5.0
HYDRO-RES (500 Flh reservoir)	250	4	35	0	1.9	5.0
References/notes	Own assumption	Own assumption	[123], [129], [132]	[123], [129], [132]	[130]	[130]

Table 36: Techno-economic parameters of existing thermal generators I

Generator type	Capacity of single unit	Number of units	Fix O&M costs	Start-up costs	Ramping costs	Maintenance outage rate	Forced outage rate
	[MW]	[-]	[kUSD/MW]	[kUSD/MW]	[kUSD/MW]	[%]	[%]
NUCLEAR	600	1	124	0.08	0.0026	6.0	4.0
COAL	600	11	62	0.08	0.0026	10.0	6.0
CCGT	400	3	27	0.07	0.0014	6.0	4.0
GT	50	24	22	0.03	0.0019	5.0	3.0
BIO	150	1	172	0.18	0.0042	7.6	9.0
CSP (10h TES)	100	1	124	0.00	0.0013	0.0	6.0
Reference	Own assumption	Own assumption	[118], [119], [132]	[126], [132], warm start values, biomass = small coal	[126], CSP = gas-fired steam power plants, biomass = small coal	[130]	[130]

Table 37: Techno-economic parameters of existing thermal generators II

Generator type	Efficiency (gross, LHV) at max. load [%]	Efficiency (gross, LHV) at min. load [%]	Total auxiliaries [%]	Minimum output [MW]	Fuel use start-up [MWh_{th}/MW]	Minimum online time [h]	Minimum offline time [h]	Maximum ramp rate [%/min]
NUCLEAR	33.0	30.7	4.5	300.0	5.00	24	24	5.0
COAL	34.0	31.6	7.5	240.0	5.00	24	24	2.0
CCGT	57.0	51.3	1.5	252.0	0.06	4	2	4.0
GT	37.0	30.1	1.0	27.5	0.05	1	1	10.0
BIO	35.0	32.6	14.0	60.0	1.95	8	8	2.0
CSP (10h TES)	42.5	34.4	9.8	20.0	1.18	1	1	8.0
References/notes	[119], [132], IEA values for Africa, coal units subcritical	Based on [120], [132], own assumptions	[124], [132], For biomass same values as for small coal	[130], [132]	[126], [132], warm start values, nuclear = large coal, biomass = small coal	Based on [120], [132]	Based on [120], [132]	Based on [120], [130], [132]

Table 38: Major techno-economic parameters of candidate supercritical coal power plants I (unit size 600 MW)

Year of commissioning	Investment costs [kUSD/MW]	Fix O&M costs [%]	Start-up costs [kUSD/MW]	Ramping costs [kUSD/MW]	Construction time [years]	Economic lifetime [years]	Maintenance outage rate [%]	Forced outage rate [%]
2019	1765	3.5	0.08	0.0026	3.0	35	10	6
2022	1765	3.5	0.08	0.0026	3.0	35	10	6
2025	1765	3.5	0.08	0.0026	3.0	35	10	6
2028	1765	3.5	0.08	0.0026	3.0	35	10	6
2031	1765	3.5	0.08	0.0026	3.0	35	10	6
2034	1765	3.5	0.08	0.0026	3.0	35	10	6
2037	1765	3.5	0.08	0.0026	3.0	35	10	6
2040	1765	3.5	0.08	0.0026	3.0	35	10	6
References/notes	[119], IEA values for Africa	[119]	[126]	[126]	[124]	[124]	[130]	[130]

Table 39: Major techno-economic parameters of candidate supercritical coal power plants II (unit size 600 MW)

Year of commissioning	Efficiency* (gross, LHV) at max. load [%]	Efficiency (gross, LHV) at min. load [%]	Total auxiliaries [%]	Minimum output [MW]	Fuel use start-up [MWh_{th}/MW]	Minimum online time [h]	Minimum offline time [h]	Maximum ramp rate [%/min]
2019	39.0	36.3	7.5	240	5.00	6	6	2.0
2022	39.0	36.3	7.5	240	5.00	6	6	2.0
2025	39.0	36.3	7.5	240	5.00	6	6	3.0
2028	39.0	36.3	7.5	240	5.00	6	6	3.0
2031	39.0	36.3	7.5	240	5.00	6	6	3.0
2034	39.0	36.3	7.5	240	5.00	4	4	4.5
2037	39.0	36.3	7.5	240	5.00	4	4	4.5
2040	39.0	36.3	7.5	240	5.00	4	4	4.5
References/notes	[119], IEA values for Africa	Based on [120]	[124]	[130]	[126]	[120]	[120]	[120]

*Best-in-class ultra-supercritical coal power plants can achieve an efficiency of up to 49% until 2040 (investment costs 2450 - 2900 USD/kW) [119].

Table 40: Major techno-economic parameters of candidate coal power plants with CCS I (unit size 600 MW)

Year of commissioning	Investment costs [kUSD/MW]	Fix O&M costs [%]	Start-up costs [kUSD/MW]	Ramping costs [kUSD/MW]	Construction time [years]	Economic lifetime [years]	Maintenance outage rate [%]	Forced outage rate [%]
2019	3180	3.5	0.08	0.0026	3.0	35	10	6
2022	3180	3.5	0.08	0.0026	3.0	35	10	6
2025	2880	3.5	0.08	0.0026	3.0	35	10	6
2028	2880	3.5	0.08	0.0026	3.0	35	10	6
2031	2880	3.5	0.08	0.0026	3.0	35	10	6
2034	2580	3.5	0.08	0.0026	3.0	35	10	6
2037	2580	3.5	0.08	0.0026	3.0	35	10	6
2040	2580	3.5	0.08	0.0026	3.0	35	10	6
References/notes	[119], IEA values for Africa	[119]	[126]	[126]	[124]	[124]	[130]	[130]

Table 41: Major techno-economic parameters of candidate coal power plants with CCS II (unit size 600 MW)

Year of commissioning	Efficiency (gross, LHV) at max. load [%]	Efficiency (gross, LHV) at min. load [%]	Total auxiliaries [%]	Minimum output [MW]	Fuel use start-up [MWh_{th}/MW]	Minimum online time [h]	Minimum offline time [h]	Maximum ramp rate [%/min]
2019	30.0	27.9	7.5	240	5	8	8	2.0
2022	30.0	27.9	7.5	240	5	8	8	2.0
2025	30.0	27.9	7.5	240	5	6	6	3.0
2028	30.0	27.9	7.5	240	5	6	6	3.0
2031	30.0	27.9	7.5	240	5	6	6	3.0
2034	31.0	27.9	7.5	240	5	4	4	4.5
2037	31.0	27.9	7.5	240	5	4	4	4.5
2040	31.0	27.9	7.5	240	5	4	4	4.5
References/notes	[119], IEA values for Africa	Based on [120],	[124]	[130]	[126]	[120]	[120]	[120]

Table 42: Major techno-economic parameters of candidate CCGT power plants I (unit size 400 MW)

Year of commissioning	Investment costs [kUSD/MW]	Fix O&M costs [%]	Start-up costs [kUSD/MW]	Ramping costs [kUSD/MW]	Construction time [years]	Economic lifetime [years]	Maintenance outage rate [%]	Forced outage rate [%]
2019	775	3.5	0.07	0.0014	2.0	25	6	4
2022	775	3.5	0.07	0.0014	2.0	25	6	4
2025	775	3.5	0.07	0.0014	2.0	25	6	4
2028	775	3.5	0.07	0.0014	2.0	25	6	4
2031	775	3.5	0.07	0.0014	2.0	25	6	4
2034	775	3.5	0.07	0.0014	2.0	25	6	4
2037	775	3.5	0.07	0.0014	2.0	25	6	4
2040	775	3.5	0.07	0.0014	2.0	25	6	4
References/notes	[119], IEA values for Africa	[119]	[126]	[126]	[124]	[124]	[130]	[130]

Table 43: Major techno-economic parameters of candidate CCGT power plants II (unit size 400 MW)

Year of commissioning	Efficiency (gross, LHV) at max. load [%]	Efficiency (gross, LHV) at min. load [%]	Total auxiliaries [%]	Minimum output [MW]	Fuel use start-up [MWh_{th}/MW]	Minimum online time [h]	Minimum offline time [h]	Maximum ramp rate [%/min]
2019	59.0	53.1	1.5	252	0.06	4	2	4
2022	59.0	53.1	1.5	252	0.06	4	2	4
2025	60.0	54.0	1.5	252	0.06	4	2	6
2028	60.0	54.0	1.5	252	0.06	4	2	6
2031	60.0	54.0	1.5	252	0.06	4	2	6
2034	62.0	55.8	1.5	252	0.06	4	2	8
2037	62.0	55.8	1.5	252	0.06	4	2	8
2040	62.0	55.8	1.5	252	0.06	4	2	8
References/notes	[119], IEA values for Africa	Based on [132]	[132]	[132]	[126]	[132]	[132]	[120], [132]

Table 44: Major techno-economic parameters of candidate CCGT power plants with CCS I (unit size 400 MW)

Year of commissioning	Investment costs [kUSD/MW]	Fix O&M costs [%]	Start-up costs [kUSD/MW]	Ramping costs [kUSD/MW]	Construction time [years]	Economic lifetime [years]	Maintenance outage rate [%]	Forced outage rate [%]
2019	1390	3.5	0.07	0.0014	2.0	25	6	4
2022	1390	3.5	0.07	0.0014	2.0	25	6	4
2025	1300	3.5	0.07	0.0014	2.0	25	6	4
2028	1300	3.5	0.07	0.0014	2.0	25	6	4
2031	1300	3.5	0.07	0.0014	2.0	25	6	4
2034	1205	3.5	0.07	0.0014	2.0	25	6	4
2037	1205	3.5	0.07	0.0014	2.0	25	6	4
2040	1205	3.5	0.07	0.0014	2.0	25	6	4
References/notes	[119], IEA values for Africa	[119]	[126]	[126]	[124]	[124]	[130]	[130]

Table 45: Major techno-economic parameters of candidate CCGT power plants with CCS II (unit size 400 MW)

Year of commissioning	Efficiency (gross, LHV) at max. load [%]	Efficiency (gross, LHV) at min. load [%]	Total auxiliaries [%]	Minimum output [MW]	Fuel use start-up [MWh_{th}/MW]	Minimum online time [h]	Minimum offline time [h]	Maximum ramp rate [%/min]
2019	51.0	45.9	1.5	252	0.06	4	2	4
2022	51.0	45.9	1.5	252	0.06	4	2	4
2025	53.0	47.7	1.5	252	0.06	4	2	6
2028	53.0	47.7	1.5	252	0.06	4	2	6
2031	53.0	47.7	1.5	252	0.06	4	2	6
2034	55.0	49.5	1.5	252	0.06	4	2	8
2037	55.0	49.5	1.5	252	0.06	4	2	8
2040	55.0	49.5	1.5	252	0.06	4	2	8
References/notes	[119], IEA values for Africa	Based on [132]	[132]	[132]	[126]	[132]	[132]	[120], [132]

Table 46: Major techno-economic parameters of candidate nuclear power plants I (unit size 600 MW)

Year of commissioning	Investment costs [USD/kW]	Fix O&M costs [%]	Start-up costs [kUSD/MW]	Ramping costs [kUSD/MW]	Construction time [years]	Economic lifetime [years]	Maintenance outage rate [%]	Forced outage rate [%]
2019	4415	3.5	0.08	0.0026	5.0	50	6	4
2022	4415	3.5	0.08	0.0026	5.0	50	6	4
2025	4415	3.5	0.08	0.0026	5.0	50	6	4
2028	4415	3.5	0.08	0.0026	5.0	50	6	4
2031	4415	3.5	0.08	0.0026	5.0	50	6	4
2034	4415	3.5	0.08	0.0026	5.0	50	6	4
2037	4415	3.5	0.08	0.0026	5.0	50	6	4
2040	4415	3.5	0.08	0.0026	5.0	50	6	4
References/notes	[119], IEA values for Africa	[119]	Based on [126], = large coal	Based on [126], = large coal	[124]	[124]	[130]	[130]

Table 47: Major techno-economic parameters of candidate nuclear power plants II (unit size 600 MW)

Year of commissioning	Efficiency (gross, LHV) at max. load [%]	Efficiency (gross, LHV) at min. load [%]	Total auxiliaries [%]	Minimum output [MW]	Fuel use start-up [MWh_{th}/MW]	Minimum online time [h]	Minimum offline time [h]	Maximum ramp rate [%/min]
2019	33.0	30.7	4.5	300	5.0	24	24	5
2022	33.0	30.7	4.5	300	5.0	24	24	5
2025	33.0	30.7	4.5	300	5.0	24	24	5
2028	33.0	30.7	4.5	300	5.0	24	24	5
2031	33.0	30.7	4.5	300	5.0	24	24	5
2034	33.0	30.7	4.5	300	5.0	24	24	5
2037	33.0	30.7	4.5	300	5.0	24	24	5
2040	33.0	30.7	4.5	300	5.0	24	24	5
References/notes	[119], IEA values for Africa	Based on [120]	[124]	[130]	Based on [126], = large coal	Own assumption	Own assumption	[130]

Table 48: Major techno-economic parameters of candidate GT power plants I (unit size 50 MW)

Year of commissioning	Investment costs [kUSD/MW]	Fix O&M costs [%]	Start-up costs [kUSD/MW]	Ramping costs [kUSD/MW]	Construction time [years]	Economic lifetime [years]	Maintenance outage rate [%]	Forced outage rate [%]
2019	440	5.0	0.03	0.0019	1.0	25	5	3
2022	440	5.0	0.03	0.0019	1.0	25	5	3
2025	440	5.0	0.03	0.0019	1.0	25	5	3
2028	440	5.0	0.03	0.0019	1.0	25	5	3
2031	440	5.0	0.03	0.0019	1.0	25	5	3
2034	440	5.0	0.03	0.0019	1.0	25	5	3
2037	440	5.0	0.03	0.0019	1.0	25	5	3
2040	440	5.0	0.03	0.0019	1.0	25	5	3
References/notes	[119], IEA values for Africa	[119]	[126]	[126]	[124]	[124]	[130]	[130]

Table 49: Major techno-economic parameters of candidate GT power plants II (unit size 50 MW)

Year of commissioning	Efficiency (gross, LHV) at max. load [%]	Efficiency (gross, LHV) at min. load [%]	Total auxiliaries [%]	Minimum output [MW]	Fuel use start-up [MWh_{th}/MW]	Minimum online time [h]	Minimum offline time [h]	Maximum ramp rate [%/min]
2019	38.0	30.9	1.0	27.5	0.05	1	1	10.0
2022	38.0	30.9	1.0	27.5	0.05	1	1	10.0
2025	39.5	32.2	1.0	27.5	0.05	1	1	12.5
2028	39.5	32.2	1.0	27.5	0.05	1	1	12.5
2031	39.5	32.2	1.0	27.5	0.05	1	1	12.5
2034	41.0	33.4	1.0	27.5	0.05	1	1	15.0
2037	41.0	33.4	1.0	27.5	0.05	1	1	15.0
2040	41.0	33.4	1.0	27.5	0.05	1	1	15.0
References/notes	[119], IEA values for Africa	Based on [132]	[132]	[132]	[126]	[132]	[132]	[120], [132]

Table 50: Major techno-economic parameters of candidate ICE power plants I (unit size 50 MW)

Year of commissioning	Investment costs [kUSD/MW]	Fix O&M costs [%]	Start-up costs [kUSD/MW]	Ramping costs [kUSD/MW]	Construction time [years]	Economic lifetime [years]	Maintenance outage rate [%]	Forced outage rate [%]
2019	980	1.8	0.015	0.0010	1.0	25	5	3
2022	980	1.8	0.015	0.0010	1.0	25	5	3
2025	940	1.8	0.015	0.0010	1.0	25	5	3
2028	940	1.8	0.015	0.0010	1.0	25	5	3
2031	940	1.8	0.015	0.0010	1.0	25	5	3
2034	900	1.8	0.015	0.0010	1.0	25	5	3
2037	900	1.8	0.015	0.0010	1.0	25	5	3
2040	900	1.8	0.015	0.0010	1.0	25	5	3
References/notes	[132]	[132]	Based on [126], = 50% of GT	Based on [126], = 50% of GT	Based on [124], = GT	Based on [124], = GT	Based on [130], = GT	Based on [130], = GT

Table 51: Major techno-economic parameters of candidate ICE power plants II (unit size 50 MW)

Year of commissioning	Efficiency (gross, LHV) at max. load [%]	Efficiency (gross, LHV) at min. load [%]	Total auxiliaries [%]	Minimum output [%]	Fuel use start-up [MWh_{th}/MW]	Minimum online time [h]	Minimum offline time [h]	Maximum ramp rate [%/min]
2019	44.0	42.9	2.5	5	0	1	1	8.0
2022	44.0	42.9	2.5	5	0	1	1	8.0
2025	44.5	43.4	2.5	5	0	1	1	9.0
2028	44.5	43.4	2.5	5	0	1	1	9.0
2031	44.5	43.4	2.5	5	0	1	1	9.0
2034	45.0	43.9	2.5	5	0	1	1	10.0
2037	45.0	43.9	2.5	5	0	1	1	10.0
2040	45.0	43.9	2.5	5	0	1	1	10.0
References/notes	[132]	[132]	[132]	[132]	[132]	[132]	[132]	[132]

Table 52: Techno-economic parameters of candidate biomass power plants I (unit size 150 MW)

Year of commissioning	Investment costs [kUSD/MW]	Fix O&M costs [%]	Start-up costs [kUSD/MW]	Ramping costs [kUSD/MW]	Construction time [years]	Economic lifetime [years]	Maintenance outage rate [%]	Forced outage rate [%]
2019	4300	4.0	0.18	0.0042	3.0	25	7.6	9.0
2022	4300	4.0	0.18	0.0042	3.0	25	7.6	9.0
2025	4300	4.0	0.18	0.0042	3.0	25	7.6	9.0
2028	4300	4.0	0.18	0.0042	3.0	25	7.6	9.0
2031	4300	4.0	0.18	0.0042	3.0	25	7.6	9.0
2034	4300	4.0	0.18	0.0042	3.0	25	7.6	9.0
2037	4300	4.0	0.18	0.0042	3.0	25	7.6	9.0
2040	4300	4.0	0.18	0.0042	3.0	25	7.6	9.0
References/notes	[130]	[118]	Based on [126], = small coal	Based on [126], = small coal	[130]	[124]	[130]	[130]

Table 53: Techno-economic parameters of candidate biomass power plants II (unit size 150 MW)

Year of commissioning	Efficiency (gross, LHV) at max. load [%]	Efficiency (gross, LHV) at min. load [%]	Total auxiliaries [%]	Minimum output [MW]	Fuel use start-up [MWh_{th}/MW]	Minimum online time [h]	Minimum offline time [h]	Maximum ramp rate [%/min]
2019	35.0	32.6	14	60	5	8	8	2.0
2022	35.0	32.6	14	60	5	8	8	2.0
2025	35.0	32.6	14	60	5	8	8	2.0
2028	35.0	32.6	14	60	5	8	8	2.0
2031	35.0	32.6	14	60	5	8	8	2.0
2034	35.0	32.6	14	60	5	8	8	2.0
2037	35.0	32.6	14	60	5	8	8	2.0
2040	35.0	32.6	14	60	5	8	8	2.0
References/notes	[119], IEA values for Africa	Based on [120], own assumption	Based on [124], = small coal	Based on [130], = coal	Based on [126], = small coal	Based on [120], own assumption	Based on [120], own assumption	Based on [120], own assumption

Table 54: Techno-economic parameters of candidate reservoir hydro power plants (unit size 250 MW, 500 Flh reservoir size)

Year of commissioning	Investment costs [kUSD/MW]	Fix O&M costs [%]	Variable O&M costs [%]	Construction time [years]	Economic lifetime [years]	Maintenance outage rate [%]	Forced outage rate [%]
2019	1750	2.0	0	2.0	50	1.9	5
2022	1750	2.0	0	2.0	50	1.9	5
2025	1750	2.0	0	2.0	50	1.9	5
2028	1750	2.0	0	2.0	50	1.9	5
2031	1750	2.0	0	2.0	50	1.9	5
2034	1750	2.0	0	2.0	50	1.9	5
2037	1750	2.0	0	2.0	50	1.9	5
2040	1750	2.0	0	2.0	50	1.9	5
References/notes	[129], IEA values for Africa	[129]	In fix O&M costs included	[130]	[129]	[130]	[130]

Table 55: Techno-economic parameters of candidate utility-scale PV (unit size min. 100 MW)

Year of commissioning	Investment costs	Fix O&M costs	Variable O&M costs	Construction time	Economic lifetime	Maintenance outage rate	Forced outage rate
	[kUSD/MW]	[%]	[%]	[years]	[years]	[%]	[%]
2019	945	1.5	0	1.0	20	2.0	0
2022	840	1.5	0	1.0	20	2.0	0
2025	770	1.5	0	1.0	20	2.0	0
2028	695	1.5	0	1.0	20	2.0	0
2031	640	1.5	0	1.0	20	2.0	0
2034	620	1.5	0	1.0	20	2.0	0
2037	605	1.5	0	1.0	20	2.0	0
2040	590	1.5	0	1.0	20	2.0	0
References/notes	Based on [121], [132]	[132]	In fix O&M costs included	[130]	[124]	[130]	[130]

Table 56: Techno-economic parameters of candidate onshore wind power (unit size min. 100 MW)

Year of commissioning	Investment costs	Fix O&M costs	Variable O&M costs	Construction time	Economic lifetime	Maintenance outage rate	Forced outage rate
	[kUSD/MW]	[%]	[kUSD/MWh]	[years]	[years]	[%]	[%]
2019	1505	1.5	0.0075	1.0	20	0.6	5.0
2022	1450	1.5	0.0075	1.0	20	0.6	5.0
2025	1400	1.5	0.0075	1.0	20	0.6	5.0
2028	1380	1.5	0.0075	1.0	20	0.6	5.0
2031	1360	1.5	0.0075	1.0	20	0.6	5.0
2034	1335	1.5	0.0075	1.0	20	0.6	5.0
2037	1315	1.5	0.0075	1.0	20	0.6	5.0
2040	1295	1.5	0.0075	1.0	20	0.6	5.0
References/notes	Based on [122], [123]	[123]	[123]	[130]	[124]	[130]	[130]

Table 57: Techno-economic parameters of candidate CSP reference plant I (Solar Tower, 100 MW, SM 2, TES 10h, back-up burner 30%)

Year of commissioning	Investment costs	Fix O&M costs	Start-up costs	Ramping costs	Construction time	Economic lifetime	Maintenance outage rate	Forced outage rate
	[kUSD/MW]	[%]	[kUSD/MW]	[kUSD/MW]	[years]	[years]	[%]	[%]
2019	4305	2.5	0	0.0013	2.0	30	0	6
2022	4050	2.5	0	0.0013	2.0	30	0	6
2025	3740	2.5	0	0.0013	2.0	30	0	6
2028	3450	2.5	0	0.0013	2.0	30	0	6
2031	3365	2.5	0	0.0013	2.0	30	0	6
2034	3290	2.5	0	0.0013	2.0	30	0	6
2037	3220	2.5	0	0.0013	2.0	30	0	6
2040	3150	2.5	0	0.0013	2.0	30	0	6
References/notes	Based on [125], [132]	[132]	No additional cost as designed for daily cycling	Based on [126], = gas-fired steam power plants	[130]	Based on financing experts involved in [127]	[130]	[130]

Table 58: Techno-economic parameters of candidate CSP reference plant II (Solar Tower, 100 MW, SM 2, TES 10h, back-up burner 30%)

Year of commissioning	Efficiency (gross, LHV) at max. load	Efficiency (gross, LHV) at min. load	Auxiliaries power block	Auxiliaries solar field	Minimum output	Fuel use start-up	Minimum online time	Minimum offline time	Maximum ramp rate
	[%]	[%]	[MW]	[MW]	[MW]	[MWh_{th}/MW]	[h]	[h]	[%/min]
2019	42.5	34.4	5.0	4.8	20	1.18	1	1	8.0
2022	42.5	34.4	5.0	4.8	20	1.18	1	1	8.0
2025	42.5	34.4	5.0	4.8	20	1.18	1	1	8.0
2028	42.5	34.4	5.0	4.8	20	1.18	1	1	8.0
2031	42.5	34.4	5.0	4.8	20	1.18	1	1	8.0
2034	42.5	34.4	5.0	4..8	20	1.18	1	1	8.0
2037	42.5	34.4	5.0	4.8	20	1.18	1	1	8.0
2040	42.5	34.4	5.0	4.8	20	1.18	1	1	8.0
References/notes	[132]	[132]	[132]	[132]	[132]	[132]	[132]	[132]	[132]

Table 59: Techno-economic parameters of candidate pumped-storage hydro power plants (unit size 250 MW)

Year of commissioning	Investment costs - Converter	Investment costs - Storage	Fix O&M costs	Construction time	Economic lifetime	Maintenance outage rate	Forced outage rate	Round-trip efficiency
	[kUSD/MW]	[kUSD/MWh]	[%]	[years]	[years]	[%]	[%]	[%]
2019	600	25	2.0	2.5	50	3.8	3.0	80
2022	600	25	2.0	2.5	50	3.8	3.0	80
2025	600	25	2.0	2.5	50	3.8	3.0	80
2028	600	25	2.0	2.5	50	3.8	3.0	80
2031	600	25	2.0	2.5	50	3.8	3.0	80
2034	600	25	2.0	2.5	50	3.8	3.0	80
2037	600	25	2.0	2.5	50	3.8	3.0	80
2040	600	25	2.0	2.5	50	3.8	3	80
References/notes	Based on [128], aligned to recent projects in Africa	Based on [128], aligned to recent projects in Africa	[129]	[130]	[129]	[130]	[130]	[130]

Table 60: Techno-economic parameters of candidate Lithium-ion batteries (unit size min. 50 MW)

Year of commissioning	Investment costs - Converter	Investment costs - Storage	Fix O&M costs	Construction time	Economic lifetime	Maintenance outage rate	Forced outage rate	Round-trip efficiency
	[kUSD/MW]	[kUSD/MWh]	[%]	[years]	[years]	[%]	[%]	[%]
2019	175	350	2.5	0.5	15	0.55	2.0	93
2022	145	295	2.5	0.5	20	0.55	2.0	93
2025	125	250	2.5	0.5	20	0.55	2.0	93
2028	105	205	2.5	0.5	20	0.55	2.0	94
2031	89	172	2.5	0.5	20	0.55	2.0	94
2034	83	163	2.5	0.5	20	0.55	2.0	94
2037	77	154	2.5	0.5	20	0.55	2.0	94
2040	73	145	2.5	0.5	20	0.55	2.0	94
References/notes	Until 2030 [132], after 2030: 2.5% reduction p.a.	Until 2030 [132], after 2030: 2.5% reduction p.a.	[132]	[130]	[132]	[130]	[130]	[132]

Table 61: Techno-economic parameters of candidate transmission lines ([131] and own assumptions)

Voltage level	[kV]	400
NTC	[MW]	600
Investment costs	[kUSD/(MW km)]	0.785
Construction time	[years]	1.0
Economic lifetime	[years]	50
Losses	[%/100km]	0.8

Table 62: Coefficients for piecewise linear approach for impact of ambient temperature on power generation

Ambient temperature [°C]	**≤ 5**		**5 - ≤ 15**		**15 - ≤ 25**		**25 - ≤ 35**		**> 35**		**References/notes**
	$tc^{p,01}$	$tc^{p,02}$	$tc^{p,03}$	$tc^{p,04}$	$tc^{p,05}$	$tc^{p,06}$	$tc^{p,07}$	$tc^{p,08}$	$tc^{p,09}$	$tc^{p,10}$	
NUCLEAR	0	1	0	1	0	0	0	0	0	0	Wet cooling
COAL	0	1	0	1	1	1	1	1	1	1	Wet cooling
CCGT	-0.003	1.060	-0.004	1.060	-0.006	1.090	-0.008	1.130	-0.008	1.140	[132]
OCGT	-0.005	1.072	-0.005	1.072	-0.005	1.072	-0.005	1.072	-0.005	1.072	[132]
ICE	0	1	0	1	0	0	0	0	-0.007	1.230	[132]
BIO	0	1	0	1	1	1	1	1	1	1	Wet cooling
CSP	-0.0002	1.0438	-0.00025	1.0436	-0.003	1.085	-0.00415	1.114	-0.0041	1.114	[132]

Table 63: Coefficients for piecewise linear approach for impact of ambient temperature on efficiency

Ambient temperature [°C]	**≤ 5**		**5 - ≤ 15**		**15 - ≤ 25**		**25 - ≤ 35**		**> 35**		**References/notes**
	$tc^{\eta,01}$	$tc^{\eta,02}$	$tc^{\eta,03}$	$tc^{\eta,04}$	$tc^{\eta,05}$	$tc^{\eta,06}$	$tc^{\eta,07}$	$tc^{\eta,08}$	$tc^{\eta,09}$	$tc^{\eta,10}$	
NUCLEAR	0	1	0	1	0	0	0	0	0	0	Wet cooling
COAL	0	1	0	1	1	1	1	1	1	1	Wet cooling
CCGT	0.0017	0.9973	-0.00001	1.0108	-0.001	1.0243	-0.0013	1.0311	-0.0013	1.0313	[132]
OCGT	-0.0002	1.0057	-0.00055	1.0074	-0.001	1.0156	-0.0013	1.0215	-0.0017	1.0340	[132]
ICE	0	1	0	1	0	0	-0.0005	1.0125	-0.0005	1.0125	[132]
BIO	0	1	0	1	1	1	1	1	1	1	Wet cooling
CSP	-0.0002	1.0438	-0.00025	1.0436	-0.003	1.085	-0.00415	1.114	-0.0041	1.114	[132]

A3: Major results of case study 1 (model foresight)

Table 64: Capacity addition [GW] according to myopic foresight approach (Group 1)

Year	NUCLEAR	BIO	COAL	COAL-CCS	CCGT	CCGT-CCS	GT-GAS	ICE	GT-OIL	CSP	HYDRO-RES	HYDRO-ROR	BATTERY	PUMPED-HYDRO	PV	WIND
2019	0.00	0.00	0.00	0.00	1.60	0.00	2.45	0.00	0.00	0.00	0.00	0.00	0.00	0.00	1.13	0.69
2022	0.00	0.00	0.00	0.00	2.00	0.00	1.30	0.00	0.00	0.00	1.50	0.00	0.00	0.00	4.80	0.98
2025	0.00	0.00	0.00	0.00	2.00	0.00	1.20	0.00	0.00	0.00	0.00	0.00	0.00	0.00	4.62	1.74
2028	0.00	0.00	0.00	0.00	0.00	0.00	0.95	0.00	0.00	1.40	0.00	0.00	0.00	0.75	3.39	1.60
2031	0.00	0.00	0.00	0.00	0.00	0.00	0.00	0.00	0.00	3.50	0.00	0.00	0.00	0.25	3.46	1.10
2034	0.00	0.00	0.00	0.00	0.00	0.00	0.00	0.00	0.00	2.80	0.00	0.00	0.00	0.00	1.82	1.56
2037	0.00	0.00	0.00	0.00	0.00	0.00	0.00	0.00	0.00	3.40	0.00	0.00	0.00	0.00	1.41	2.41
2040	0.00	0.00	0.00	0.00	0.00	0.00	0.00	0.00	0.00	2.40	0.00	0.00	0.00	0.00	2.40	2.10

Table 65: Capacity addition [GW] according to rolling horizon approach (Group 1)

Year	NUCLEAR	BIO	COAL	COAL-CCS	CCGT	CCGT-CCS	GT-GAS	ICE	GT-OIL	CSP	HYDRO-RES	HYDRO-ROR	BATTERY	PUMPED-HYDRO	PV	WIND
2019	0.00	0.00	0.00	0.00	2.00	0.00	2.15	0.00	0.00	0.00	0.00	0.00	0.00	0.00	0.70	0.53
2022	0.00	0.00	0.00	0.00	1.60	0.00	1.55	0.00	0.00	0.00	1.50	0.00	0.00	0.00	4.80	1.15
2025	0.00	0.00	0.00	0.00	0.80	0.00	2.25	0.00	0.00	0.00	0.00	0.00	0.00	0.00	0.92	4.80
2028	0.00	0.00	0.00	0.00	0.00	0.00	0.70	0.00	0.00	1.60	0.00	0.00	0.00	1.00	4.80	1.06
2031	0.00	0.00	0.00	0.00	0.00	0.00	0.00	0.00	0.00	3.60	0.00	0.00	0.00	0.00	4.14	0.66
2034	0.00	0.00	0.00	0.00	0.00	0.00	0.00	0.00	0.00	2.90	0.00	0.00	0.00	0.00	0.78	0.00
2037	0.00	0.00	0.00	0.00	0.00	0.00	0.00	0.00	0.00	3.40	0.00	0.00	0.00	0.00	3.58	0.27
2040	0.00	0.00	0.00	0.00	0.00	0.00	0.00	0.00	0.00	2.30	0.00	0.00	0.00	0.00	2.23	3.81

Table 66: Capacity addition [GW] according to perfect foresight approach (Group 1)

Year	NUCLEAR	BIO	COAL	COAL-CCS	CCGT	CCGT-CCS	GT-GAS	ICE	GT-OIL	CSP	HYDRO-RES	HYDRO-ROR	BATTERY	PUMPED-HYDRO	PV	WIND
2019	0.00	0.00	0.00	0.00	0.40	0.00	3.75	0.00	0.00	0.00	0.00	0.00	0.00	0.00	2.45	4.01
2022	0.00	0.00	0.00	0.00	1.20	0.00	1.95	0.00	0.00	0.00	1.50	0.00	0.35	0.00	0.00	0.00
2025	0.00	0.00	0.00	0.00	0.80	0.00	2.50	0.00	0.00	0.00	0.00	0.00	0.00	0.00	0.00	4.03
2028	0.00	0.00	0.00	0.00	0.00	0.00	0.15	0.00	0.00	2.10	0.00	0.00	0.00	1.00	0.34	3.07
2031	0.00	0.00	0.00	0.00	0.00	0.00	0.00	0.00	0.00	3.70	0.00	0.00	0.00	0.00	4.80	0.45
2034	0.00	0.00	0.00	0.00	0.00	0.00	0.00	0.00	0.00	2.80	0.00	0.00	0.00	0.00	4.80	0.00
2037	0.00	0.00	0.00	0.00	0.00	0.00	0.00	0.00	0.00	3.40	0.00	0.00	0.00	0.00	4.80	1.03
2040	0.00	0.00	0.00	0.00	0.00	0.00	0.00	0.00	0.00	2.30	0.00	0.00	0.00	0.00	4.80	4.80

Table 67: Cumulative installed gross capacity [GW] according to myopic foresight approach (Group 1)

Year	NUCLEAR	BIO	COAL	COAL-CCS	CCGT	CCGT-CCS	GT-GAS	ICE	GT-OIL	CSP	HYDRO-RES	HYDRO-ROR	BATTERY	PUMPED-HYDRO	PV	WIND
2016	0.60	0.15	6.60	0.00	1.20	0.00	0.60	0.00	0.60	0.10	1.00	1.00	0.00	0.25	0.50	1.00
2019	0.60	0.15	6.60	0.00	2.80	0.00	3.05	0.00	0.60	0.10	1.00	1.00	0.00	0.25	1.63	1.69
2022	0.60	0.15	5.40	0.00	4.80	0.00	4.15	0.00	0.00	0.10	2.50	1.00	0.00	0.25	6.43	2.66
2025	0.60	0.15	5.40	0.00	6.80	0.00	5.35	0.00	0.00	0.10	2.50	1.00	0.00	0.25	11.1	4.41
2028	0.60	0.15	5.40	0.00	6.80	0.00	6.30	0.00	0.00	1.50	2.50	1.00	0.00	1.00	14.4	6.01
2031	0.60	0.15	4.80	0.00	6.80	0.00	6.10	0.00	0.00	5.00	2.50	1.00	0.00	1.25	17.9	6.61
2034	0.60	0.15	4.80	0.00	6.80	0.00	6.10	0.00	0.00	7.80	2.50	1.00	0.00	1.25	19.7	8.17
2037	0.60	0.15	4.20	0.00	6.80	0.00	5.90	0.00	0.00	11.2	2.50	1.00	0.00	1.25	20.6	10.1
2040	0.60	0.15	4.20	0.00	6.80	0.00	5.90	0.00	0.00	13.6	2.50	1.00	0.00	1.25	21.9	11.5

Table 68: Cumulative installed gross capacity [GW] according to rolling horizon approach (Group 1)

Year	NUCLEAR	BIO	COAL	COAL-CCS	CCGT	CCGT-CCS	GT-GAS	ICE	GT-OIL	CSP	HYDRO-RES	HYDRO-ROR	BATTERY	PUMPED-HYDRO	PV	WIND
2016	0.60	0.15	6.60	0.00	1.20	0.00	0.60	0.00	0.60	0.10	1.00	1.00	0.00	0.25	0.50	1.00
2019	0.60	0.15	6.60	0.00	3.20	0.00	2.75	0.00	0.60	0.10	1.00	1.00	0.00	0.25	1.20	1.53
2022	0.60	0.15	5.40	0.00	4.80	0.00	4.10	0.00	0.00	0.10	2.50	1.00	0.00	0.25	6.00	2.68
2025	0.60	0.15	5.40	0.00	5.60	0.00	6.35	0.00	0.00	0.10	2.50	1.00	0.00	0.25	6.92	7.48
2028	0.60	0.15	5.40	0.00	5.60	0.00	7.05	0.00	0.00	1.70	2.50	1.00	0.00	1.25	11.7	8.54
2031	0.60	0.15	4.80	0.00	5.60	0.00	6.85	0.00	0.00	5.30	2.50	1.00	0.00	1.25	15.9	8.71
2034	0.60	0.15	4.80	0.00	5.60	0.00	6.85	0.00	0.00	8.20	2.50	1.00	0.00	1.25	16.6	8.71
2037	0.60	0.15	4.20	0.00	5.60	0.00	6.65	0.00	0.00	11.6	2.50	1.00	0.00	1.25	19.7	8.48
2040	0.60	0.15	4.20	0.00	5.60	0.00	6.65	0.00	0.00	13.0	2.50	1.00	0.00	1.25	21.3	11.8

Table 69: Cumulative installed gross capacity [GW] according to perfect foresight approach (Group 1)

Year	NUCLEAR	BIO	COAL	COAL-CCS	CCGT	CCGT-CCS	GT-GAS	ICE	GT-OIL	CSP	HYDRO-RES	HYDRO-ROR	BATTERY	PUMPED-HYDRO	PV	WIND
2016	0.60	0.15	6.60	0.00	1.20	0.00	0.60	0.00	0.60	0.10	1.00	1.00	0.00	0.25	0.50	1.00
2019	0.60	0.15	6.60	0.00	1.60	0.00	4.35	0.00	0.60	0.10	1.00	1.00	0.00	0.25	2.95	5.01
2022	0.60	0.15	5.40	0.00	2.80	0.00	6.10	0.00	0.00	0.10	2.50	1.00	0.35	0.25	2.95	5.01
2025	0.60	0.15	5.40	0.00	3.60	0.00	8.60	0.00	0.00	0.10	2.50	1.00	0.35	0.25	2.95	9.03
2028	0.60	0.15	5.40	0.00	3.60	0.00	8.75	0.00	0.00	2.20	2.50	1.00	0.35	1.25	3.28	12.1
2031	0.60	0.15	4.80	0.00	3.60	0.00	8.55	0.00	0.00	5.90	2.50	1.00	0.35	1.25	8.08	12.1
2034	0.60	0.15	4.80	0.00	3.60	0.00	8.55	0.00	0.00	8.70	2.50	1.00	0.35	1.25	12.9	12.1
2037	0.60	0.15	4.20	0.00	3.60	0.00	8.35	0.00	0.00	12.1	2.50	1.00	0.35	1.25	17.2	12.6
2040	0.60	0.15	4.20	0.00	3.60	0.00	8.35	0.00	0.00	14.4	2.50	1.00	0.35	1.25	19.5	13.4

Table 70: NTC addition [GW] according to myopic foresight approach (Group 1)

Year	N1 - N2	N1 - N4	N2 - N3	N2 - N4	N3 - N4
2019	0.0	0.0	0.0	0.0	0.0
2022	0.0	0.6	0.6	0.0	0.0
2025	0.0	0.0	1.2	0.0	0.0
2028	0.0	0.0	0.6	0.0	0.6
2031	0.0	0.0	0.6	1.8	0.0
2034	0.0	0.6	0.6	1.8	0.6
2037	0.0	0.6	1.2	0.6	0.0
2040	0.0	0.6	0.6	1.2	0.6

Table 71: NTC addition [GW] according to rolling horizon approach (Group 1)

Year	N1 - N2	N1 - N4	N2 - N3	N2 - N4	N3 - N4
2019	0.0	0.6	0.0	0.0	0.0
2022	0.0	0.0	0.6	0.0	0.0
2025	0.0	0.0	3.6	0.0	0.0
2028	0.0	0.0	0.0	0.0	0.6
2031	0.0	0.0	0.0	2.4	0.6
2034	0.0	0.6	0.0	1.2	0.0
2037	0.0	0.6	0.0	1.8	0.0
2040	0.0	0.6	1.8	1.2	0.0

Table 72: NTC addition [GW] according to perfect foresight approach (Group 1)

Year	N1 - N2	N1 - N4	N2 - N3	N2 - N4	N3 - N4
2019	0.0	0.6	2.4	0.0	0.0
2022	0.0	0.0	0.0	0.0	0.0
2025	0.0	0.0	3.0	0.0	0.0
2028	0.0	0.6	1.2	0.0	0.6
2031	0.0	0.6	0.0	2.4	0.6
2034	0.0	0.0	0.0	1.8	0.0
2037	0.0	0.6	0.0	1.8	0.0
2040	0.0	0.6	0.0	0.6	0.6

Table 73: Cumulative installed NTC [GW] according to myopic foresight approach (Group 1)

Year	N1 - N2	N1 - N4	N2 - N3	N2 - N4	N3 - N4
2016	1.8	0	0.6	0.6	0
2019	1.8	0	0.6	0.6	0
2022	1.8	0.6	1.2	0.6	0
2025	1.8	0.6	2.4	0.6	0
2028	1.8	0.6	3	0.6	0.6
2031	1.8	0.6	3.6	2.4	0.6
2034	1.8	1.2	4.2	4.2	1.2
2037	1.8	1.8	5.4	4.8	1.2
2040	1.8	2.4	6	6	1.8

Table 74: Cumulative installed NTC [GW] according to rolling horizon approach (Group 1)

Year	N1 - N2	N1 - N4	N2 - N3	N2 - N4	N3 - N4
2016	1.8	0	0.6	0.6	0
2019	1.8	0.6	0.6	0.6	0
2022	1.8	0.6	1.2	0.6	0
2025	1.8	0.6	4.8	0.6	0
2028	1.8	0.6	4.8	0.6	0.6
2031	1.8	0.6	4.8	3	1.2
2034	1.8	1.2	4.8	4.2	1.2
2037	1.8	1.8	4.8	6	1.2
2040	1.8	2.4	6.6	7.2	1.2

Table 75: Cumulative installed NTC [GW] according to perfect foresight approach (Group 1)

Year	N1 - N2	N1 - N4	N2 - N3	N2 - N4	N3 - N4
2016	1.8	0	0.6	0.6	0
2019	1.8	0.6	3	0.6	0
2022	1.8	0.6	3	0.6	0
2025	1.8	0.6	6	0.6	0
2028	1.8	1.2	7.2	0.6	0.6
2031	1.8	1.8	7.2	3	1.2
2034	1.8	1.8	7.2	4.8	1.2
2037	1.8	2.4	7.2	6.6	1.2
2040	1.8	3	7.2	7.2	1.8

Table 76: Capacity addition [GW] according to myopic foresight approach (Group 2)

Year	NUCLEAR	BIO	COAL	COAL-CCS	CCGT	CCGT-CCS	GT-GAS	ICE	GT-OIL	CSP	HYDRO-RES	HYDRO-ROR	BATTERY	PUMPED-HYDRO	PV	WIND
2019	0.00	0.00	0.00	0.00	2.00	0.00	2.10	0.00	0.00	0.00	0.00	0.00	0.00	0.00	0.74	0.49
2022	0.00	0.00	3.00	0.00	0.00	0.00	1.75	0.00	0.00	0.00	0.00	0.00	0.00	0.00	1.84	0.00
2025	0.00	0.00	1.20	0.00	0.80	0.00	0.45	0.00	0.00	0.00	0.75	0.00	0.00	0.00	2.70	0.84
2028	0.00	0.00	0.60	0.00	0.40	0.00	0.40	0.00	0.00	0.60	0.75	0.00	0.00	0.00	4.80	0.41
2031	0.00	0.00	0.00	0.00	0.00	0.00	1.30	0.00	0.00	2.00	0.00	0.00	0.00	0.75	4.80	4.80
2034	0.00	0.00	0.00	0.00	0.00	0.00	0.00	0.00	0.00	2.50	0.00	0.00	0.00	0.25	3.12	2.08
2037	0.00	0.00	0.00	0.00	0.00	0.00	0.00	0.00	0.00	3.40	0.00	0.00	0.00	0.00	2.17	2.11
2040	0.00	0.00	0.00	0.00	0.00	0.00	0.00	0.00	0.00	2.30	0.00	0.00	0.00	0.00	2.30	1.51

Table 77: Capacity addition [GW] according to rolling horizon approach (Group 2)

Year	NUCLEAR	BIO	COAL	COAL-CCS	CCGT	CCGT-CCS	GT-GAS	ICE	GT-OIL	CSP	HYDRO-RES	HYDRO-ROR	BATTERY	PUMPED-HYDRO	PV	WIND
2019	0.00	0.00	0.60	0.00	1.60	0.00	1.95	0.00	0.00	0.00	0.00	0.00	0.00	0.00	0.45	0.30
2022	0.00	0.00	2.40	0.00	0.40	0.00	1.95	0.00	0.00	0.00	0.00	0.00	0.00	0.00	2.09	0.23
2025	0.00	0.00	0.60	0.00	0.80	0.00	0.60	0.00	0.00	0.00	1.00	0.00	0.00	0.00	2.03	0.98
2028	0.00	0.00	0.00	0.00	0.00	0.00	1.50	0.00	0.00	0.80	0.50	0.00	0.00	0.25	4.80	1.89
2031	0.00	0.00	0.00	0.00	0.00	0.00	0.55	0.00	0.00	2.50	0.00	0.00	0.00	0.75	4.80	4.76
2034	0.00	0.00	0.00	0.00	0.00	0.00	0.00	0.00	0.00	2.80	0.00	0.00	0.00	0.00	1.57	0.00
2037	0.00	0.00	0.00	0.00	0.00	0.00	0.00	0.00	0.00	3.40	0.00	0.00	0.00	0.00	3.83	0.32
2040	0.00	0.00	0.00	0.00	0.00	0.00	0.00	0.00	0.00	2.30	0.00	0.00	0.00	0.00	1.60	4.29

Table 78: Capacity addition [GW] according to perfect foresight approach (Group 2)

Year	NUCLEAR	BIO	COAL	COAL-CCS	CCGT	CCGT-CCS	GT-GAS	ICE	GT-OIL	CSP	HYDRO-RES	HYDRO-ROR	BATTERY	PUMPED-HYDRO	PV	WIND
2019	0.00	0.00	0.00	0.00	0.40	0.00	3.55	0.00	0.00	0.00	0.00	0.00	0.00	0.00	2.12	3.29
2022	0.00	0.00	0.00	0.00	1.20	0.00	1.95	0.00	0.00	0.00	1.50	0.00	0.25	0.00	0.00	0.00
2025	0.00	0.00	0.00	0.00	0.80	0.00	2.35	0.00	0.00	0.00	0.00	0.00	0.00	0.00	0.00	2.55
2028	0.00	0.00	0.00	0.00	0.00	0.00	0.50	0.00	0.00	1.70	0.00	0.00	0.00	1.00	0.10	4.50
2031	0.00	0.00	0.00	0.00	0.00	0.00	0.00	0.00	0.00	3.70	0.00	0.00	0.00	0.00	4.80	1.81
2034	0.00	0.00	0.00	0.00	0.00	0.00	0.00	0.00	0.00	2.80	0.00	0.00	0.00	0.00	4.80	0.00
2037	0.00	0.00	0.00	0.00	0.00	0.00	0.00	0.00	0.00	3.40	0.00	0.00	0.00	0.00	4.80	0.33
2040	0.00	0.00	0.00	0.00	0.00	0.00	0.00	0.00	0.00	2.30	0.00	0.00	0.00	0.00	4.80	4.80

Table 79: Cumulative installed gross capacity [GW] according to myopic foresight approach (Group 2)

Year	NUCLEAR	BIO	COAL	COAL-CCS	CCGT	CCGT-CCS	GT-GAS	ICE	GT-OIL	CSP	HYDRO-RES	HYDRO-ROR	BATTERY	PUMPED-HYDRO	PV	WIND
2016	0.60	0.15	6.60	0.00	1.20	0.00	0.60	0.00	0.60	0.10	1.00	1.00	0.00	0.25	0.50	1.00
2019	0.60	0.15	6.60	0.00	3.20	0.00	2.70	0.00	0.60	0.10	1.00	1.00	0.00	0.25	1.24	1.49
2022	0.60	0.15	8.40	0.00	3.20	0.00	4.25	0.00	0.00	0.10	1.00	1.00	0.00	0.25	3.08	1.49
2025	0.60	0.15	9.60	0.00	4.00	0.00	4.70	0.00	0.00	0.10	1.75	1.00	0.00	0.25	5.78	2.33
2028	0.60	0.15	10.2	0.00	4.40	0.00	5.10	0.00	0.00	0.70	2.50	1.00	0.00	0.25	10.6	2.74
2031	0.60	0.15	9.60	0.00	4.40	0.00	6.20	0.00	0.00	2.70	2.50	1.00	0.00	1.00	15.4	7.04
2034	0.60	0.15	9.60	0.00	4.40	0.00	6.20	0.00	0.00	5.20	2.50	1.00	0.00	1.25	18.5	9.12
2037	0.60	0.15	9.00	0.00	4.40	0.00	6.00	0.00	0.00	8.60	2.50	1.00	0.00	1.25	20.2	10.7
2040	0.60	0.15	9.00	0.00	4.40	0.00	6.00	0.00	0.00	10.9	2.50	1.00	0.00	1.25	21.7	11.8

Table 80: Cumulative installed gross capacity [GW] according to rolling horizon approach (Group 2)

Year	NUCLEAR	BIO	COAL	COAL-CCS	CCGT	CCGT-CCS	GT-GAS	ICE	GT-OIL	CSP	HYDRO-RES	HYDRO-ROR	BATTERY	PUMPED-HYDRO	PV	WIND
2016	0.60	0.15	6.60	0.00	1.20	0.00	0.60	0.00	0.60	0.10	1.00	1.00	0.00	0.25	0.50	1.00
2019	0.60	0.15	7.20	0.00	2.80	0.00	2.55	0.00	0.60	0.10	1.00	1.00	0.00	0.25	0.95	1.30
2022	0.60	0.15	8.40	0.00	3.20	0.00	4.30	0.00	0.00	0.10	1.00	1.00	0.00	0.25	3.04	1.53
2025	0.60	0.15	9.00	0.00	4.00	0.00	4.90	0.00	0.00	0.10	2.00	1.00	0.00	0.25	5.06	2.51
2028	0.60	0.15	9.00	0.00	4.00	0.00	6.40	0.00	0.00	0.90	2.50	1.00	0.00	0.50	9.86	4.40
2031	0.60	0.15	8.40	0.00	4.00	0.00	6.75	0.00	0.00	3.40	2.50	1.00	0.00	1.25	14.7	8.66
2034	0.60	0.15	8.40	0.00	4.00	0.00	6.75	0.00	0.00	6.20	2.50	1.00	0.00	1.25	16.2	8.66
2037	0.60	0.15	7.80	0.00	4.00	0.00	6.55	0.00	0.00	9.60	2.50	1.00	0.00	1.25	19.6	8.48
2040	0.60	0.15	7.80	0.00	4.00	0.00	6.55	0.00	0.00	11.9	2.50	1.00	0.00	1.25	20.7	12.5

Table 81: Cumulative installed gross capacity [GW] according to perfect foresight approach (Group 2)

Year	NUCLEAR	BIO	COAL	COAL-CCS	CCGT	CCGT-CCS	GT-GAS	ICE	GT-OIL	CSP	HYDRO-RES	HYDRO-ROR	BATTERY	PUMPED-HYDRO	PV	WIND
2016	0.60	0.15	6.60	0.00	1.20	0.00	0.60	0.00	0.60	0.10	1.00	1.00	0.00	0.25	0.50	1.00
2019	0.60	0.15	6.60	0.00	1.60	0.00	4.15	0.00	0.60	0.10	1.00	1.00	0.00	0.25	2.62	4.29
2022	0.60	0.15	5.40	0.00	2.80	0.00	5.90	0.00	0.00	0.10	2.50	1.00	0.25	0.25	2.62	4.29
2025	0.60	0.15	5.40	0.00	3.60	0.00	8.25	0.00	0.00	0.10	2.50	1.00	0.25	0.25	2.62	6.85
2028	0.60	0.15	5.40	0.00	3.60	0.00	8.75	0.00	0.00	1.80	2.50	1.00	0.25	1.25	2.72	11.4
2031	0.60	0.15	4.80	0.00	3.60	0.00	8.55	0.00	0.00	5.50	2.50	1.00	0.25	1.25	7.52	12.7
2034	0.60	0.15	4.80	0.00	3.60	0.00	8.55	0.00	0.00	8.30	2.50	1.00	0.25	1.25	12.3	12.7
2037	0.60	0.15	4.20	0.00	3.60	0.00	8.35	0.00	0.00	11.7	2.50	1.00	0.25	1.25	16.6	12.5
2040	0.60	0.15	4.20	0.00	3.60	0.00	8.35	0.00	0.00	14.0	2.50	1.00	0.25	1.25	19.3	14.0

Table 82: NTC addition [GW] according to myopic foresight approach (Group 2)

Year	N1 - N2	N1 - N4	N2 - N3	N2 - N4	N3 - N4
2019	0.0	0.0	0.0	0.0	0.0
2022	0.0	0.6	0.0	0.0	0.0
2025	0.0	0.0	0.6	0.0	0.0
2028	0.0	0.0	0.0	0.0	0.0
2031	0.0	0.0	3.0	0.6	0.6
2034	0.0	0.6	1.2	1.2	0.0
2037	0.0	0.6	0.6	1.2	0.6
2040	0.0	0.6	0.6	1.2	0.0

Table 83: NTC addition [GW] according to rolling horizon approach (Group 2)

Year	N1 - N2	N1 - N4	N2 - N3	N2 - N4	N3 - N4
2019	0.0	0.6	0.0	0.0	0.0
2022	0.0	0.0	0.0	0.0	0.0
2025	0.0	0.0	0.6	0.0	0.0
2028	0.0	0.0	1.2	0.0	0.0
2031	0.0	0.6	3.0	1.2	0.6
2034	0.0	0.0	0.0	1.8	0.0
2037	0.0	0.6	0.0	1.8	0.0
2040	0.0	0.6	1.8	0.6	0.6

Table 84: NTC addition [GW] according to perfect foresight approach (Group 2)

Year	N1 - N2	N1 - N4	N2 - N3	N2 - N4	N3 - N4
2019	0.0	0.6	1.8	0.0	0.0
2022	0.0	0.0	0.0	0.0	0.0
2025	0.0	0.0	1.8	0.0	0.0
2028	0.0	0.0	3.0	0.0	0.6
2031	0.0	0.6	0.0	2.4	1.2
2034	0.0	0.0	0.0	1.8	0.0
2037	0.0	0.6	0.0	1.8	0.0
2040	0.0	0.6	0.0	0.6	0.6

Table 85: Cumulative installed NTC [GW] according to myopic foresight approach (Group 2)

Year	N1 - N2	N1 - N4	N2 - N3	N2 - N4	N3 - N4
2016	1.8	0	0.6	0.6	0
2019	1.8	0	0.6	0.6	0
2022	1.8	0.6	0.6	0.6	0
2025	1.8	0.6	1.2	0.6	0
2028	1.8	0.6	1.2	0.6	0
2031	1.8	0.6	4.2	1.2	0.6
2034	1.8	1.2	5.4	2.4	0.6
2037	1.8	1.8	6	3.6	1.2
2040	1.8	2.4	6.6	4.8	1.2

Table 86: Cumulative installed NTC [GW] according to rolling horizon approach (Group 2)

Year	N1 - N2	N1 - N4	N2 - N3	N2 - N4	N3 - N4
2016	1.8	0	0.6	0.6	0
2019	1.8	0.6	0.6	0.6	0
2022	1.8	0.6	0.6	0.6	0
2025	1.8	0.6	1.2	0.6	0
2028	1.8	0.6	2.4	0.6	0
2031	1.8	1.2	5.4	1.8	0.6
2034	1.8	1.2	5.4	3.6	0.6
2037	1.8	1.8	5.4	5.4	0.6
2040	1.8	2.4	7.2	6	1.2

Table 87: Cumulative installed NTC [GW] according to perfect foresight approach (Group 2)

Year	N1 - N2	N1 - N4	N2 - N3	N2 - N4	N3 - N4
2016	1.8	0	0.6	0.6	0
2019	1.8	0.6	2.4	0.6	0
2022	1.8	0.6	2.4	0.6	0
2025	1.8	0.6	4.2	0.6	0
2028	1.8	0.6	7.2	0.6	0.6
2031	1.8	1.2	7.2	3	1.8
2034	1.8	1.2	7.2	4.8	1.8
2037	1.8	1.8	7.2	6.6	1.8
2040	1.8	2.4	7.2	7.2	2.4

A4: Major results of case study 2 (system-operational detail)

Table 88: Capacity addition [GW] according to CEM-1 (average day method & no UCC)

Year	NUCLEAR	BIO	COAL	COAL-CCS	CCGT	CCGT-CCS	GT-GAS	ICE	GT-OIL	CSP	HYDRO-RES	HYDRO-ROR	BATTERY	PUMPED-HYDRO	PV	WIND
2019	0.00	0.00	0.00	0.00	2.00	0.00	2.10	0.00	0.00	0.00	0.00	0.00	0.00	0.00	0.45	0.62
2022	0.00	0.00	3.00	0.00	0.00	0.00	1.80	0.00	0.00	0.00	0.00	0.00	0.00	0.00	1.93	0.32
2025	0.00	0.00	0.00	0.00	0.00	0.00	1.65	0.00	0.00	0.00	1.25	0.00	0.00	0.00	0.12	3.77
2028	0.00	0.00	0.00	0.00	0.00	0.00	2.50	0.00	0.00	0.10	0.25	0.00	0.00	0.25	4.56	4.14
2031	0.00	0.00	0.00	0.00	0.00	0.00	1.25	0.00	0.00	1.90	0.00	0.00	0.00	0.75	4.80	4.80
2034	0.00	0.00	0.00	0.00	0.00	0.00	0.00	0.00	0.00	2.70	0.00	0.00	0.00	0.00	0.61	1.29
2037	0.00	0.00	0.00	0.00	0.00	0.00	2.25	0.00	0.00	1.00	0.00	0.00	0.00	0.00	1.85	3.71
2040	0.00	0.00	0.00	0.00	0.00	0.00	0.00	0.00	0.00	2.50	0.00	0.00	0.00	0.00	2.89	4.80

Table 89: Capacity addition [GW] according to CEM-2 (representative day method & no UCC)

Year	NUCLEAR	BIO	COAL	COAL-CCS	CCGT	CCGT-CCS	GT-GAS	ICE	GT-OIL	CSP	HYDRO-RES	HYDRO-ROR	BATTERY	PUMPED-HYDRO	PV	WIND
2019	0.00	0.00	0.60	0.00	1.60	0.00	1.85	0.00	0.00	0.00	0.00	0.00	0.00	0.00	0.40	0.31
2022	0.00	0.00	2.40	0.00	0.40	0.00	1.95	0.00	0.00	0.00	0.00	0.00	0.00	0.00	2.02	0.27
2025	0.00	0.00	1.20	0.00	0.80	0.00	0.35	0.00	0.00	0.00	0.75	0.00	0.00	0.00	1.73	0.00
2028	0.00	0.00	0.00	0.00	0.40	0.00	1.45	0.00	0.00	0.70	0.75	0.00	0.00	0.00	4.80	2.69
2031	0.00	0.00	0.00	0.00	0.00	0.00	0.85	0.00	0.00	2.20	0.00	0.00	0.00	0.75	4.80	4.80
2034	0.00	0.00	0.00	0.00	0.00	0.00	0.00	0.00	0.00	2.30	0.00	0.00	0.00	0.25	2.10	0.00
2037	0.00	0.00	0.00	0.00	0.00	0.00	0.00	0.00	0.00	3.40	0.00	0.00	0.00	0.00	3.53	0.80
2040	0.00	0.00	0.00	0.00	0.00	0.00	0.00	0.00	0.00	2.30	0.00	0.00	0.00	0.00	2.41	4.30

Table 90: Capacity addition [GW] according to CEM-3 (representative day method & simplified UCC)

Year	NUCLEAR	BIO	COAL	COAL-CCS	CCGT	CCGT-CCS	GT-GAS	ICE	GT-OIL	CSP	HYDRO-RES	HYDRO-ROR	BATTERY	PUMPED-HYDRO	PV	WIND
2019	0.00	0.00	0.60	0.00	1.60	0.00	1.85	0.00	0.00	0.00	0.00	0.00	0.00	0.00	0.41	0.22
2022	0.00	0.00	2.40	0.00	0.00	0.00	1.30	0.00	0.00	0.00	1.00	0.00	0.00	0.00	1.52	0.34
2025	0.00	0.00	1.80	0.00	0.00	0.00	0.50	0.00	0.00	0.00	0.50	0.00	0.00	0.25	0.39	0.97
2028	0.00	0.00	0.00	0.00	0.00	0.00	1.85	0.00	0.00	0.80	0.00	0.00	0.00	0.50	4.80	2.60
2031	0.00	0.00	0.00	0.00	0.00	0.00	0.50	0.00	0.00	3.00	0.00	0.00	0.10	0.25	4.80	4.10
2034	0.00	0.00	0.00	0.00	0.00	0.00	0.00	0.00	0.00	2.80	0.00	0.00	0.00	0.00	1.40	0.00
2037	0.00	0.00	0.00	0.00	0.00	0.00	0.00	0.00	0.00	3.40	0.00	0.00	0.00	0.00	3.13	1.51
2040	0.00	0.00	0.00	0.00	0.00	0.00	0.00	0.00	0.00	2.30	0.00	0.00	1.30	0.00	3.17	4.80

Table 91: Capacity addition [GW] according to CEM-4 (representative day method & detailed UCC)

Year	NUCLEAR	BIO	COAL	COAL-CCS	CCGT	CCGT-CCS	GT-GAS	ICE	GT-OIL	CSP	HYDRO-RES	HYDRO-ROR	BATTERY	PUMPED-HYDRO	PV	WIND
2019	0.00	0.00	1.20	0.00	0.80	0.00	1.60	0.00	0.00	0.00	0.00	0.00	0.00	0.50	0.38	0.18
2022	0.00	0.00	2.40	0.00	0.40	0.00	1.70	0.05	0.00	0.00	0.25	0.00	0.00	0.00	1.35	0.37
2025	0.00	0.00	1.20	0.00	0.00	0.00	0.45	0.00	0.00	0.00	1.25	0.00	0.00	0.00	0.85	1.45
2028	0.00	0.00	0.00	0.00	0.00	0.00	1.75	0.00	0.00	0.90	0.00	0.00	0.00	0.50	4.53	2.46
2031	0.00	0.00	0.00	0.00	0.00	0.00	0.70	0.00	0.00	3.00	0.00	0.00	0.30	0.00	4.80	3.63
2034	0.00	0.00	0.00	0.00	0.00	0.00	0.00	0.00	0.00	2.90	0.00	0.00	0.00	0.00	1.00	0.87
2037	0.00	0.00	0.00	0.00	0.00	0.00	0.00	0.00	0.00	3.40	0.00	0.00	0.00	0.00	3.44	1.08
2040	0.00	0.00	0.00	0.00	0.00	0.00	0.00	0.00	0.00	2.30	0.00	0.00	1.15	0.00	3.84	4.23

Table 92: Cumulative installed capacity [GW] according to CEM-1 (average day method & no UCC)

Year	NUCLEAR	BIO	COAL	COAL-CCS	CCGT	CCGT-CCS	GT-GAS	ICE	GT-OIL	CSP	HYDRO-RES	HYDRO-ROR	BATTERY	PUMPED-HYDRO	PV	WIND
2016	0.60	0.15	6.60	0.00	1.20	0.00	0.60	0.00	0.60	0.10	1.00	1.00	0.00	0.25	0.50	1.00
2019	0.60	0.15	6.60	0.00	3.20	0.00	2.70	0.00	0.60	0.10	1.00	1.00	0.00	0.25	0.95	1.62
2022	0.60	0.15	8.40	0.00	3.20	0.00	4.30	0.00	0.00	0.10	1.00	1.00	0.00	0.25	2.88	1.94
2025	0.60	0.15	8.40	0.00	3.20	0.00	5.95	0.00	0.00	0.10	2.25	1.00	0.00	0.25	2.99	5.71
2028	0.60	0.15	8.40	0.00	3.20	0.00	8.45	0.00	0.00	0.20	2.50	1.00	0.00	0.50	7.55	9.85
2031	0.60	0.15	7.80	0.00	3.20	0.00	9.50	0.00	0.00	2.10	2.50	1.00	0.00	1.25	12.4	14.2
2034	0.60	0.15	7.80	0.00	3.20	0.00	9.50	0.00	0.00	4.80	2.50	1.00	0.00	1.25	13.0	15.4
2037	0.60	0.15	7.20	0.00	3.20	0.00	11.6	0.00	0.00	5.80	2.50	1.00	0.00	1.25	14.3	18.7
2040	0.60	0.15	7.20	0.00	3.20	0.00	11.6	0.00	0.00	8.30	2.50	1.00	0.00	1.25	16.8	22.8

Table 93: Cumulative installed capacity [GW] according to CEM-2 (representative day method & no UCC)

Year	NUCLEAR	BIO	COAL	COAL-CCS	CCGT	CCGT-CCS	GT-GAS	ICE	GT-OIL	CSP	HYDRO-RES	HYDRO-ROR	BATTERY	PUMPED-HYDRO	PV	WIND
2016	0.60	0.15	6.60	0.00	1.20	0.00	0.60	0.00	0.60	0.10	1.00	1.00	0.00	0.25	0.50	1.00
2019	0.60	0.15	7.20	0.00	2.80	0.00	2.45	0.00	0.60	0.10	1.00	1.00	0.00	0.25	0.90	1.31
2022	0.60	0.15	8.40	0.00	3.20	0.00	4.20	0.00	0.00	0.10	1.00	1.00	0.00	0.25	2.92	1.58
2025	0.60	0.15	9.60	0.00	4.00	0.00	4.55	0.00	0.00	0.10	1.75	1.00	0.00	0.25	4.65	1.58
2028	0.60	0.15	9.60	0.00	4.40	0.00	6.00	0.00	0.00	0.80	2.50	1.00	0.00	0.25	9.45	4.27
2031	0.60	0.15	9.00	0.00	4.40	0.00	6.65	0.00	0.00	3.00	2.50	1.00	0.00	1.00	14.3	8.57
2034	0.60	0.15	9.00	0.00	4.40	0.00	6.65	0.00	0.00	5.30	2.50	1.00	0.00	1.25	16.4	8.57
2037	0.60	0.15	8.40	0.00	4.40	0.00	6.45	0.00	0.00	8.70	2.50	1.00	0.00	1.25	19.4	8.87
2040	0.60	0.15	8.40	0.00	4.40	0.00	6.45	0.00	0.00	11.0	2.50	1.00	0.00	1.25	21.4	12.9

Table 94: Cumulative installed capacity [GW] according to CEM-3 (representative day method & simplified UCC)

Year	NUCLEAR	BIO	COAL	COAL-CCS	CCGT	CCGT-CCS	GT-GAS	ICE	GT-OIL	CSP	HYDRO-RES	HYDRO-ROR	BATTERY	PUMPED-HYDRO	PV	WIND
2016	0.60	0.15	6.60	0.00	1.20	0.00	0.60	0.00	0.60	0.10	1.00	1.00	0.00	0.25	0.50	1.00
2019	0.60	0.15	7.20	0.00	2.80	0.00	2.45	0.00	0.60	0.10	1.00	1.00	0.00	0.25	0.91	1.22
2022	0.60	0.15	8.40	0.00	2.80	0.00	3.55	0.00	0.00	0.10	2.00	1.00	0.00	0.25	2.42	1.56
2025	0.60	0.15	10.2	0.00	2.80	0.00	4.05	0.00	0.00	0.10	2.50	1.00	0.00	0.50	2.82	2.53
2028	0.60	0.15	10.2	0.00	2.80	0.00	5.90	0.00	0.00	0.90	2.50	1.00	0.00	1.00	7.62	5.13
2031	0.60	0.15	9.60	0.00	2.80	0.00	6.20	0.00	0.00	3.90	2.50	1.00	0.10	1.25	12.4	8.73
2034	0.60	0.15	9.60	0.00	2.80	0.00	6.20	0.00	0.00	6.70	2.50	1.00	0.10	1.25	13.8	8.73
2037	0.60	0.15	9.00	0.00	2.80	0.00	6.00	0.00	0.00	10.1	2.50	1.00	0.10	1.25	16.4	9.75
2040	0.60	0.15	9.00	0.00	2.80	0.00	6.00	0.00	0.00	12.4	2.50	1.00	1.40	1.25	19.2	14.3

Table 95: Cumulative installed capacity [GW] according to CEM-4 (representative day method & detailed UCC)

Year	NUCLEAR	BIO	COAL	COAL-CCS	CCGT	CCGT-CCS	GT-GAS	ICE	GT-OIL	CSP	HYDRO-RES	HYDRO-ROR	BATTERY	PUMPED-HYDRO	PV	WIND
2016	0.60	0.15	6.60	0.00	1.20	0.00	0.60	0.00	0.60	0.10	1.00	1.00	0.00	0.25	0.50	1.00
2019	0.60	0.15	7.80	0.00	2.00	0.00	2.20	0.00	0.60	0.10	1.00	1.00	0.00	0.75	0.88	1.18
2022	0.60	0.15	9.00	0.00	2.40	0.00	3.70	0.05	0.00	0.10	1.25	1.00	0.00	0.75	2.23	1.55
2025	0.60	0.15	10.2	0.00	2.40	0.00	4.15	0.05	0.00	0.10	2.50	1.00	0.00	0.75	3.07	3.01
2028	0.60	0.15	10.2	0.00	2.40	0.00	5.90	0.05	0.00	1.00	2.50	1.00	0.00	1.25	7.60	5.47
2031	0.60	0.15	9.60	0.00	2.40	0.00	6.40	0.05	0.00	4.00	2.50	1.00	0.30	1.25	12.4	8.60
2034	0.60	0.15	9.60	0.00	2.40	0.00	6.40	0.05	0.00	6.90	2.50	1.00	0.30	1.25	13.4	9.47
2037	0.60	0.15	9.00	0.00	2.40	0.00	6.20	0.05	0.00	10.3	2.50	1.00	0.30	1.25	16.3	10.1
2040	0.60	0.15	9.00	0.00	2.40	0.00	6.20	0.05	0.00	12.6	2.50	1.00	1.45	1.25	19.8	14.1

Table 96: Annual power generation [TWh] according to CEM-1 (average day method & no UCC)

Year	NUCLEAR	BIO	COAL	COAL-CCS	CCGT	CCGT-CCS	GT-GAS	ICE	GT-OIL	CSP	HYDRO-RES	HYDRO-ROR	BATTERY	PUMPED-HYDRO	PV	WIND
2016	4.5	0.7	42.7	0.0	4.0	0.0	0.8	0.0	0.2	0.3	2.4	2.4	0.0	0.4	0.9	2.9
2019	4.5	0.9	44.0	0.0	12.3	0.0	0.6	0.0	0.0	0.3	2.4	2.4	0.0	0.2	1.8	4.9
2022	4.5	0.9	55.6	0.0	9.5	0.0	0.9	0.0	0.0	0.3	2.4	2.4	0.0	0.4	5.5	6.0
2025	4.4	0.9	55.1	0.0	9.2	0.0	0.9	0.0	0.0	0.3	5.5	2.4	0.0	0.4	5.7	18.4
2028	4.0	0.9	49.9	0.0	7.2	0.0	1.2	0.0	0.0	0.6	6.1	2.4	0.0	0.8	14.0	32.0
2031	4.2	0.8	38.5	0.0	4.9	0.0	0.5	0.0	0.0	7.4	6.1	2.4	0.0	1.3	22.9	45.6
2034	4.3	0.9	37.8	0.0	4.1	0.0	0.3	0.0	0.0	17.0	6.1	2.4	0.0	0.8	24.0	50.2
2037	4.2	0.8	34.1	0.0	4.8	0.0	0.6	0.0	0.0	20.5	6.1	2.4	0.0	1.0	26.6	59.8
2040	3.9	0.7	26.0	0.0	2.2	0.0	0.1	0.0	0.0	29.3	6.1	2.4	0.0	1.3	31.3	69.7

Table 97: Annual power generation [TWh] according to CEM-2 (representative day method & no UCC)

Year	NUCLEAR	BIO	COAL	COAL-CCS	CCGT	CCGT-CCS	GT-GAS	ICE	GT-OIL	CSP	HYDRO-RES	HYDRO-ROR	BATTERY	PUMPED-HYDRO	PV	WIND
2016	4.5	0.7	42.7	0.0	3.9	0.0	0.8	0.0	0.2	0.3	2.4	2.4	0.0	0.4	0.9	2.9
2019	4.5	0.9	47.6	0.0	9.8	0.0	0.6	0.0	0.0	0.3	2.4	2.4	0.0	0.3	1.7	3.9
2022	4.5	0.9	55.7	0.0	10.2	0.0	1.2	0.0	0.0	0.3	2.4	2.4	0.0	0.4	5.5	4.8
2025	4.5	0.9	63.7	0.0	12.1	0.0	1.3	0.0	0.0	0.3	4.2	2.4	0.0	0.4	8.7	4.8
2028	4.0	0.9	58.5	0.0	11.2	0.0	1.1	0.0	0.0	2.8	6.1	2.4	0.0	0.5	17.4	13.6
2031	4.2	0.8	46.0	0.0	8.8	0.0	0.3	0.0	0.0	10.6	6.1	2.4	0.0	1.0	26.3	27.6
2034	4.3	0.9	46.6	0.0	9.7	0.0	0.3	0.0	0.0	18.8	6.1	2.4	0.0	0.9	30.3	27.8
2037	4.3	0.9	42.7	0.0	8.8	0.0	0.1	0.0	0.0	30.8	6.1	2.4	0.0	0.8	35.8	28.4
2040	4.0	0.8	37.6	0.0	4.5	0.0	0.0	0.0	0.0	38.9	6.1	2.4	0.0	1.3	39.6	38.2

Table 98: Annual power generation [TWh] according to CEM-3 (representative day method & simplified UCC)

Year	NUCLEAR	BIO	COAL	COAL-CCS	CCGT	CCGT-CCS	GT-GAS	ICE	GT-OIL	CSP	HYDRO-RES	HYDRO-ROR	BATTERY	PUMPED-HYDRO	PV	WIND
2016	4.5	0.8	42.6	0.0	4.0	0.0	0.8	0.0	0.2	0.3	2.4	2.4	0.0	0.5	0.9	2.9
2019	4.5	0.9	46.4	0.0	11.3	0.0	0.7	0.0	0.0	0.3	2.4	2.4	0.0	0.4	1.7	3.6
2022	4.3	0.9	54.6	0.0	10.2	0.0	1.1	0.0	0.0	0.3	4.8	2.4	0.0	0.5	4.6	4.7
2025	4.2	0.9	66.3	0.0	8.7	0.0	1.0	0.0	0.0	0.3	6.1	2.4	0.0	0.7	5.4	7.9
2028	4.1	0.9	63.4	0.0	7.4	0.0	1.2	0.0	0.0	2.9	6.1	2.4	0.0	1.3	14.1	16.4
2031	4.2	0.9	51.3	0.0	4.6	0.0	0.2	0.0	0.0	13.2	6.1	2.4	0.1	1.4	23.0	27.9
2034	4.3	0.9	51.7	0.0	5.2	0.0	0.2	0.0	0.0	22.6	6.1	2.4	0.1	1.0	25.6	28.3
2037	4.2	0.9	47.0	0.0	3.8	0.0	0.1	0.0	0.0	34.1	6.1	2.4	0.1	1.0	30.7	31.0
2040	4.0	0.8	37.0	0.0	1.4	0.0	0.0	0.0	0.0	42.0	6.1	2.4	1.5	1.4	35.9	43.1

Table 99: Annual power generation [TWh] according to CEM-4 (representative day method & detailed UCC)

Year	NUCLEAR	BIO	COAL	COAL-CCS	CCGT	CCGT-CCS	GT-GAS	ICE	GT-OIL	CSP	HYDRO-RES	HYDRO-ROR	BATTERY	PUMPED-HYDRO	PV	WIND
2016	4.4	0.8	42.6	0.0	4.0	0.0	0.8	0.0	0.2	0.3	2.4	2.4	0.0	0.5	0.9	2.9
2019	4.4	0.9	51.0	0.0	7.3	0.0	0.7	0.0	0.0	0.2	2.4	2.4	0.0	0.7	1.7	3.5
2022	4.3	0.9	59.5	0.0	8.0	0.0	1.1	0.0	0.0	0.2	3.0	2.4	0.0	0.9	4.2	4.7
2025	4.2	0.9	66.2	0.0	6.9	0.0	1.1	0.0	0.0	0.2	6.1	2.4	0.0	1.0	5.9	9.5
2028	4.3	0.9	62.9	0.0	6.2	0.0	1.3	0.0	0.0	3.2	6.1	2.4	0.0	1.6	14.2	17.6
2031	4.2	0.9	51.7	0.0	4.0	0.0	0.3	0.0	0.0	13.4	6.1	2.4	0.4	1.4	23.0	27.8
2034	4.3	0.9	50.9	0.0	3.8	0.0	0.2	0.0	0.0	23.2	6.1	2.4	0.4	0.9	24.9	30.7
2037	4.2	0.9	46.2	0.0	3.0	0.0	0.2	0.0	0.0	34.7	6.1	2.4	0.5	1.0	30.6	32.2
2040	4.0	0.8	36.3	0.0	0.9	0.0	0.0	0.0	0.0	42.7	6.1	2.4	1.8	1.4	37.1	42.4

Table 100: Power generation [TWh] of generation fleet in 2040 calculated by REMix-PCM

Model	NUCLEAR	BIO	COAL	COAL-CCS	CCGT	CCGT-CCS	GT-GAS	ICE	GT-OIL	CSP	HYDRO-RES	HYDRO-ROR	BATTERY	PUMPED-HYDRO	PV	WIND
PCM-1	3.8	0.7	31.3	0.0	9.0	0.0	5.1	0.0	0.0	27.8	6.1	2.4	0.0	1.8	29.8	55.2
PCM-2	4.0	0.8	38.4	0.0	9.4	0.0	1.3	0.0	0.0	37.4	6.1	2.4	0.0	1.6	37.7	34.1
PCM-3	4.0	0.8	37.6	0.0	4.5	0.0	1.2	0.0	0.0	42.5	6.1	2.4	1.7	1.3	34.2	38.5
PCM-4	3.9	0.8	37.3	0.0	3.8	0.0	1.4	0.0	0.0	43.2	6.1	2.4	1.7	1.2	35.4	37.4